Master's thesis

NTNU
Norwegian University of Science and Technology
Faculty of Natural Sciences
Department of Chemistry

Lucas Bocquin

Chemoenzymatic synthesis of enantiopure beta blockers (*R*)-sotalol, (*S*)-penbutolol and (*S*)-bisoprolol

Master's thesis in Chemistry
Supervisor: Elisabeth Egholm Jacobsen
June 2022

NTNU
Norwegian University of
Science and Technology

Lucas Bocquin

Chemoenzymatic synthesis of enantiopure beta blockers (*R*)-sotalol, (*S*)-penbutolol and (*S*)-bisoprolol

Master's thesis in Chemistry
Supervisor: Elisabeth Egholm Jacobsen
June 2022

Norwegian University of Science and Technology
Faculty of Natural Sciences
Department of Chemistry

NTNU
Kunnskap for en bedre verden

Preface

This thesis has been performed as a part of the Master of Science in Chemistry (MsCHEM) at the Department of Chemistry at the Norwegian University of Science and Technology. All work was carried out between January 2021 and June 2022, under the supervision of Associate Professor Elisabeth Egholm Jacobsen.

I would like to thank Elisabeth for her professional guidance, her positive mind, her trust in me, and for always being available to answer questions. A special thanks to Susanne Hansen Troøyen for the great company in the laboratory, for all the interesting discussions, and for having unconsciously made me a more organized person. A big thanks to Camille Dejoux for all the agreeable lunches and coffee breaks and the great moments spent in and outside the school. I would also like to thank master students Maja Christensen and Fredrik Bjørnes for the impressive work they did on this project under my supervision in March and April 2022.

Thanks to Mari Rødseth, Raymond Trohjell, Kristoffer Klungseth and Anna Tennfjord for sharing their interesting results during the research group meetings of 2021. Thanks also to Andreea Ftodiev and Mara Badea who joined the Biocatalysis research group for one month in 2021 and who shared with us their interesting projects.

Thanks also to head engineer Roger Aarvik for ordering and providing all the chemicals needed for this project, Julie Asmussen for her assistance with the HPLC instruments, Susana Villa Gonzalez for her help with MS analyses, and Torun Melø for the NMR assistance.

Finally, I would like to kindly thank my friends and family for their continued support during the last two years.

Abstract

Beta blockers are medications used to reduce blood pressure. In commercial beta blockers, the active pharmaceutical ingredient (API) is always a chiral molecule, and is usually present as a racemic mixture. Usually, one enantiomer of the API, called the eutomer, has most of the beta-blocking properties, while the other can be responsible for unwanted side effects. This thesis concerns the chemo-enzymatic synthesis of enantiopure (*R*)-sotalol, (*S*)-penbutolol and (*S*)-bisoprolol, the eutomers of the beta-blockers sotalol, penbutolol and bisoprolol. The aim was to synthesize them and their precursors in an environmentally friendly and efficient way, and with an enantiomeric excess of at least 96%.

All the reaction performed to synthesize (*R*)-sotalol precursor (*R*)-N-(4-(2-chloro-1-hydroxyethyl)phenyl)methanesulfonamide ((*R*)-**5**) and other derivatives, as well as the yields obtained, are shown in Scheme 0.1.1. Compound (*R*)-**5** was synthesized from aniline in three steps with a combined yield of 53%.

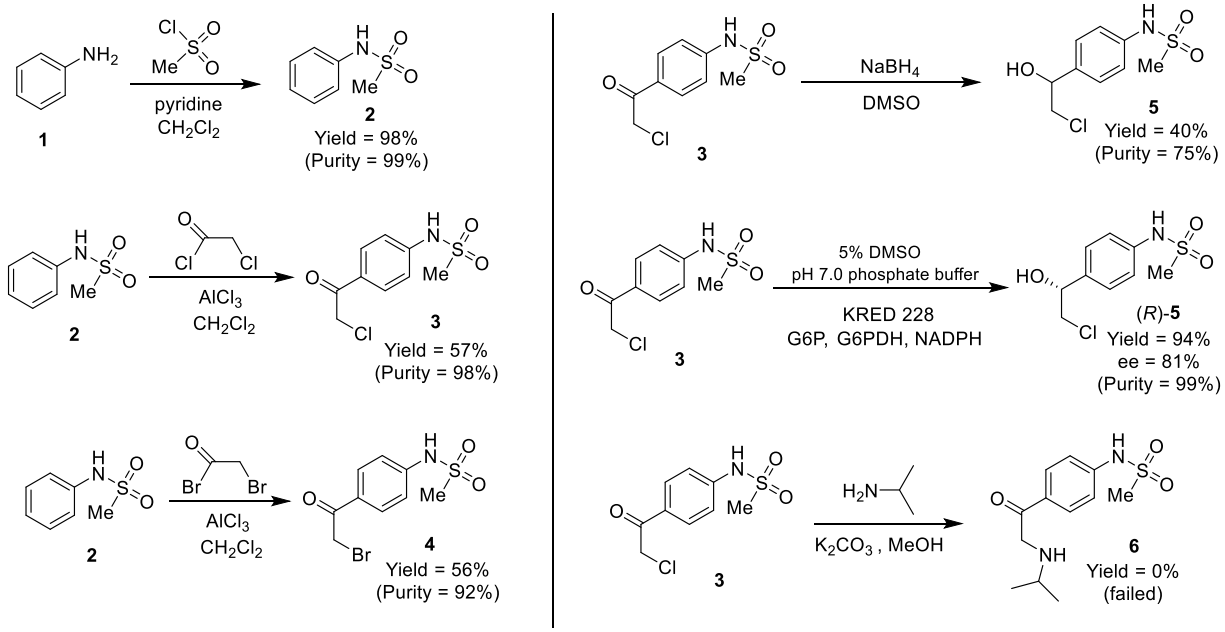

Scheme 0.1.1: Summary of the reactions carried out to synthesize (*R*)-N-(4-(2-chloro-1-hydroxyethyl)phenyl)methanesulfonamide ((*R*)-**5**)

All the reaction performed to synthesize (*S*)-penbutolol ((*S*)-**10**), as well as the yields obtained, are shown in Scheme 0.1.2. (*S*)-Penbutolol hydrochloride ((*S*)-**10*HCl***) was obtained from 2-cyclopentylphenol in five steps with a combined yield of 20%.

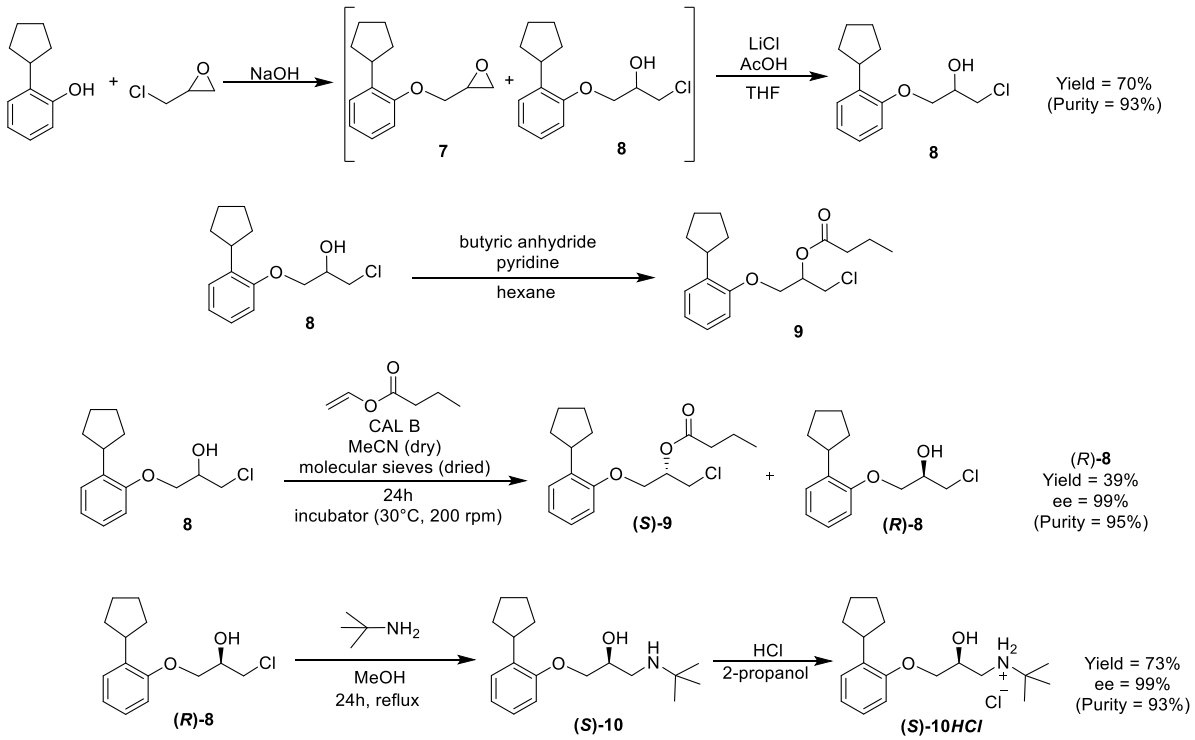

Scheme 0.1.2: Summary of the reactions carried out to synthesize (*S*)-penbutolol.

All the reaction performed to synthesize (*S*)-bisoprolol ((*S*)-**17**), as well as the yields obtained, are shown in Scheme 0.1.3. (*S*)-bisoprolol hemifumarate ((*S*)-**17*salt***) was synthesized from 4-(hydroxymethyl)phenol in six steps with a combined yield of 19%.

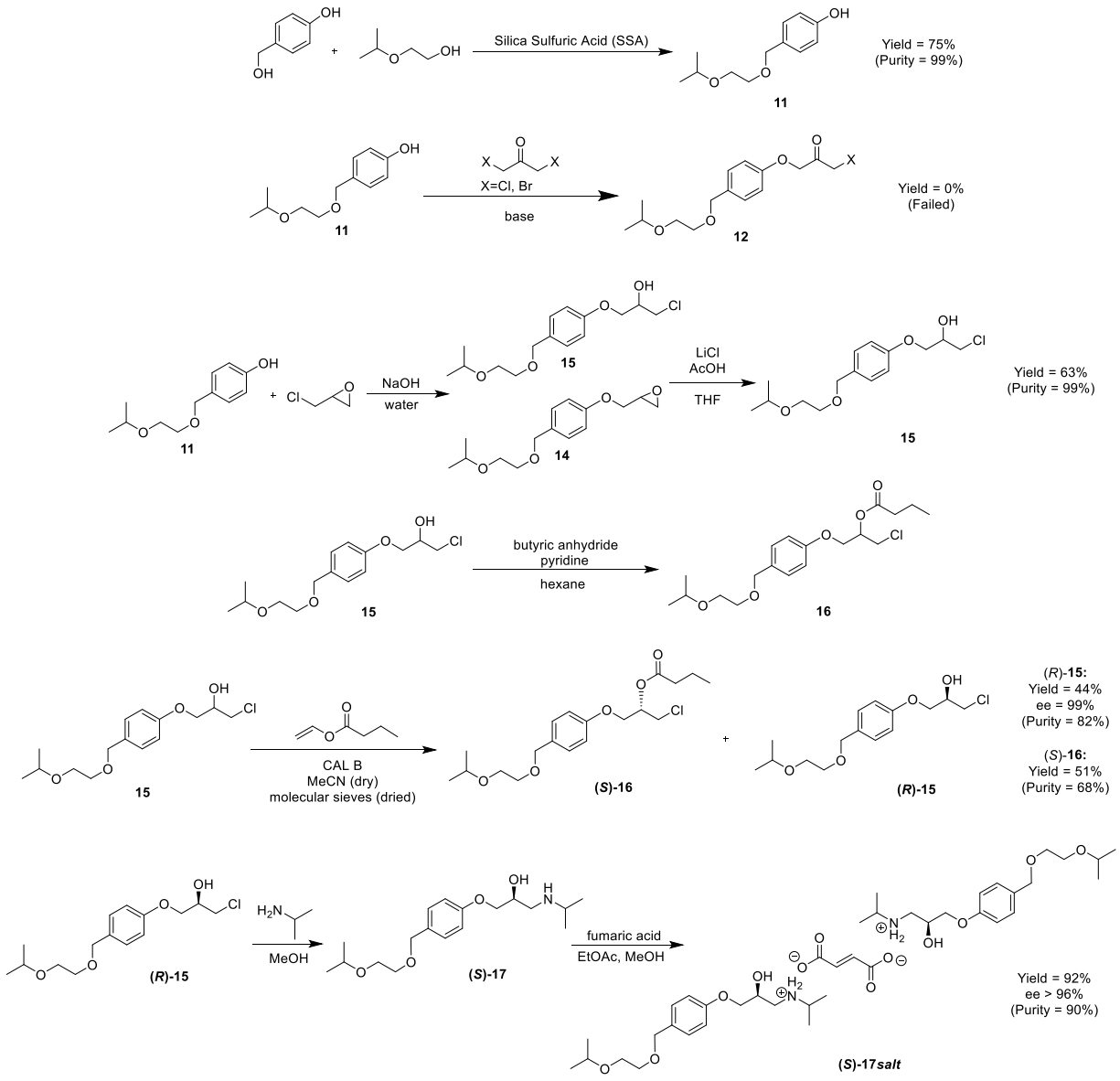

Scheme 0.1.3: Summary of the reactions carried out to synthesize (*S*)-bisoprolol.

Symbols and Abbreviations

API	Active pharmaceutical ingredient
CALB	*Candida Antarctica* Lipase B
COSY	Correlation spectroscopy
d	Doublet
dd	Doublet of doublet
DMSO	Dimethyl sulfoxide
Dist.	Distilled
ee	Enantiomeric excess
ee_S	Enantiomeric excess of the substrate
ee_p	Enantiomeric excess of the product
E	Enantiomeric ratio
G6P	Glucose-6-phosphate
G6PDH	Glucose-6-phosphate dehydrogenase
h	Hours
HMBC	Heteronuclear Multiple Bond Correlation
HPLC	High-Performance Liquid Chromatography
Hz	Hertz
J	Coupling constant
k	Reaction rate constant
KRED	Ketoreductase
LG	Leaving group
m	Multiplet
MS	Mass Spectrometry
NADH	Nicotinamide adenine dinucleotide
NADPH	Nicotinamide adenine dinucleotide phosphate
NMR	Nuclear Magnetic Resonance
ppm	Parts per million
R_f	Retention factor
R_s	Resolution
rpm	Rotations per minute
rt	Room temperature
s	Singlet
SSA	Silica sulfuric acid catalyst
t	Triplet
TLC	Thin Layer Chromatography
t_R	Retention time

List of Synthesized Compounds

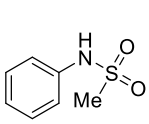

1

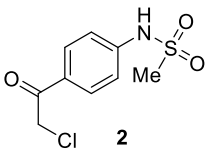

2

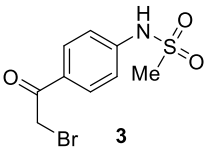

3

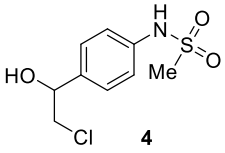

4

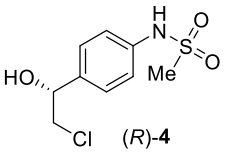

(*R*)-**4**

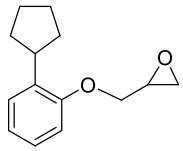

7 (not isolated)

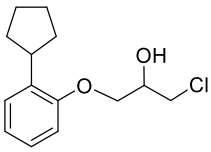

8

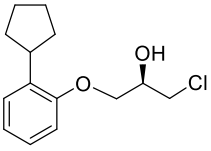

(*R*)-**8**

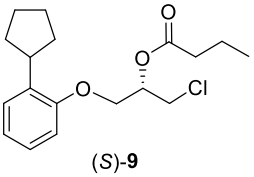

(*S*)-**9**

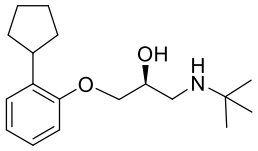

(*R*)-**10**

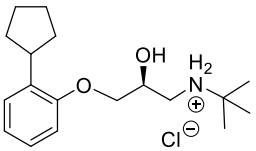

(*R*)-**10*HCl***

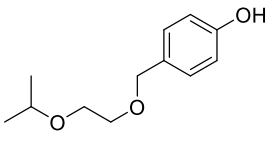

11

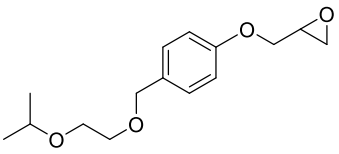

14 (not isolated)

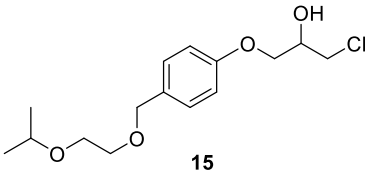

15

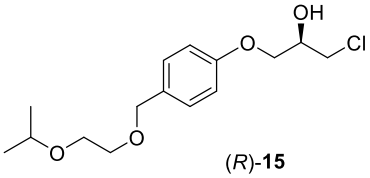

(*R*)-**15**

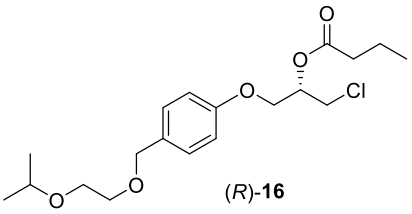

(*R*)-**16**

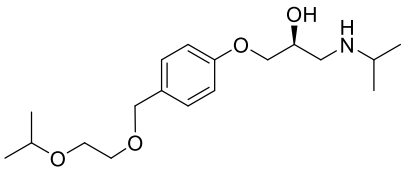

(*S*)-**Bisoprolol** ((*S*)-**17**)

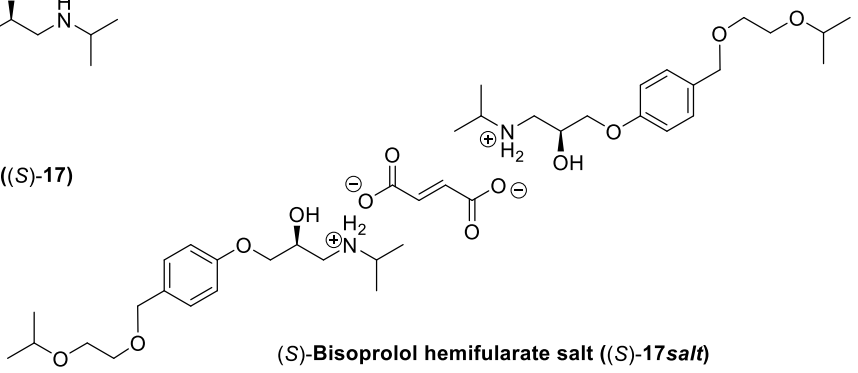

(*S*)-**Bisoprolol hemifularate salt** ((*S*)-**17*salt***)

Table of Contents

1. Introduction

1.1. Aim of the thesis

The main aim of this thesis was to synthesize enantiopure (*R*)-sotalol, (*S*)-penbutolol, and (*S*)-bisoprolol in an efficient and environmentally friendly way, by enzyme-catalyzed reduction of ketones and kinetic resolution of racemic secondary alcohols. Enantiopure beta blockers should be obtained with an enantiomeric excess of at least 96%.

1.2. Enantiopure drugs in the pharmaceutical industry

The active substance in drugs is called the active pharmaceutical ingredient (API). When drugs are mentioned in this thesis, it always refers to their API. More than half of the drugs currently in use are chiral, but the majority of them are sold as a racemic mixture [1]. And even if two enantiomers of a racemic drug have the same 2D chemical structure, most of them exhibit significant differences in biological activities such as pharmacology, toxicology, pharmacokinetics and metabolism. It is common for chiral drugs to have one enantiomer mainly responsible for the desired effect, while the other is useless, or even harmful. For this type of drug, the enantiomer having higher pharmacological activity is called eutomer, while the other one is called distomer [2].

A famous example of this is thalidomide, sold between 1957 and 1961 as a racemic drug and promoted for morning sickness in pregnant women. The *S*-enantiomer of this drug had strong teratogenic effects, and the consumption of this drug led to the death of thousands of children. In this case, prescribing only the *R*-enantiomer is not a solution either, because the molecule rapidly racemizes in the body [3].

Since the late 1990's, more and more chiral drugs that were developed as a racemic mixture are switched to their enantiopure form [4]. The term "chiral switch" was introduced in 1999 by Agranat and Caner to describe this phenomenon [5]. To be marketed as enantiopure, drugs need to have an enantiomeric excess of at least 96%. Ibuprofen was one of the first commercial drugs to undergo such a switch, in 1994. The use of its enantiopure eutomer gave, among others, faster onset of action [6]. Overall, potential advantages of using an enantiopure drug over its racemic mixture include decreased side effects, a faster onset of action, less drug-drug interaction, and the use of a lower dosage for the same effects [4].

A main limitation to the development and commercialization of enantiopure drugs is the increased production cost it goes with [7]. Three main pathways are available for the production of enantiopure drugs. The synthesis can start from an enantiopure starting material, include the use a chiral catalyst to form only one enantiomer, or rely on chiral resolution. The latter method is not ideal, because it means that both enantiomers are synthesized before being separated [4]. The unwanted enantiomer is therefore also isolated, and can result in increased waste. Ideally, the direct synthesis of only one enantiomer is desired.

In some cases, both enantiomers of a chiral drug have similar pharmacological effects, or the slightly superior efficacy of an enantiopure version of a drug is outweighed by the increased production costs. Commercializing enantiopure drugs instead of their racemic mixture is not always done to optimize their pharmaceutical effect. “Chiral switch” can allow pharmaceutical companies to maintain market exclusivity on drugs that would otherwise lose soon their patent protection. Most newly marketed single-enantiomer drugs are not directly compared to their racemic counterpart, suggesting that the switches were mainly done for financial reasons [8].

In the case of beta blockers, however, pharmacological activities of eutomers are usually significantly higher than the ones of their racemic mixtures.

1.3. Beta blockers

Beta-adrenoreceptor antagonists (beta blockers) are an important class of drugs used for decades for the treatment of arterial hypertension, chronic heart failure, coronary artery disease, as well as in the management of anxiety, migraine and glaucoma. Those drugs have proven their efficiency to reduce hospitalization and mortality in patients diagnosed with heart failure [9]. Recently, probable anticancer properties have been discovered and studied, expanding the potential of beta blockers in the pharmaceutical world [10].

They act through the blockade of beta-receptors such as beta1-, beta2- and beta3- receptors [9]. Beta1 receptors are located mainly in the heart and beta2 receptors in bronchial smooth muscle, cardiac myocytes and vascular smooth muscle cells. Epinephrine and norepinephrine are their most important endogenous ligands and they interact with the receptors to, among others, mediate alterations in heart rate [11]. Structures of epinephrine and norepinephrine are shown in Figure 1.3.1.

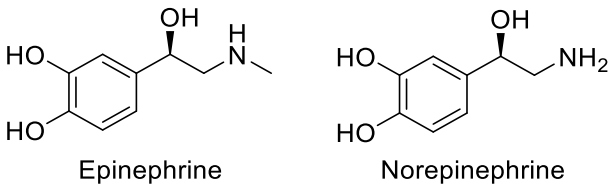

Figure 1.3.1: Structures of epinephrine and norepinephrine

Beta blocking drugs usually have similar structures to the ones of epinephrine and norepinephrine. This explains their affinity with beta receptors.

The effect of such drugs depends on the type of beta-receptors blocked. Some beta blockers, such as bisoprolol, are beta1-selective and result mainly in a decreased heart rate and a reduced heart oxygen requirement. Others, such as sotalol and penbutolol, are non-selective beta blockers, and have in addition to the previously mentioned effects vasodilating effects [9] and negative side effects such as bronchospasm [12]. Due to the negative side effects of beta2-antagonism, selective beta1-antagonism is preferred in most treatments using beta blockers. Most of the clinically approved beta blockers have nevertheless a relatively low beta1-selectivity, and the development and commercialization of more selective beta blockers is therefore needed [12].

Beta blockers contain one or more chiral centers, and the effects of their chirality have been extensively studied. For most of those drugs, one enantiomer has a lot more beta blocking properties than the other. Depending on their structure, beta blockers can be classified as arylaminoethanols or aryloxyaminopropanols (Figure 1.3.2). In both groups, the isomers presenting a negative specific rotation value have the most beta blocking properties. This corresponds to the *R*-enantiomers for the arylaminoethanol group and *S*-enantiomers for the aryloxyaminopropanol group [13].

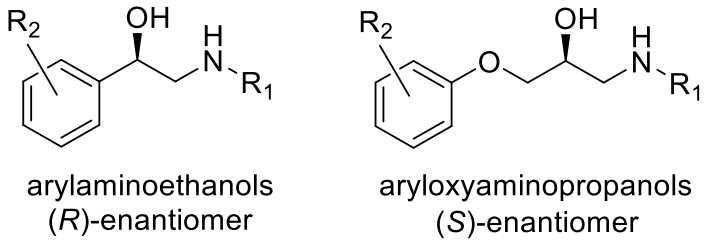

Figure 1.3.2: Structure and stereochemistry of the most beta blocking enantiomers of arylaminoethanols and aryloxyaminopropanols.

Enantiomers can also have a different beta selectivity. This is the case for metoprolol, where the *S*-enantiomer is a beta1-selective beta blocker while the *R*-enantiomer is non-selective [13].

This thesis is focusing on the synthesis of three beta blockers: Sotalol, penbutolol and bisoprolol.

Sotalol is an antiarrhythmic agent used for treatment of highly symptomatic atrial fibrillation/flutter and of life-threatening ventricular arrhythmias. Due to potentially life-threatening side effects, this drug is only prescribed to treat very serious conditions [14]. The *R*-enantiomer of sotalol is 14 to 50 times more efficient at blocking beta-receptors than its racemic form, while the *S*-enantiomer is almost inactive. However, both enantiomers have the same antidysrhythmic activity [13]. The distomer of sotalol has been shown to increase mortality in patients with myocardial infarction [15]. Using only the enantiopure eutomer could therefore limit the apparition of serious side effects in some patients.

(*S*)-Penbutolol is one of the few beta blockers that has been prescribed in its enantiopure form [2]. The *S*-enantiomer of penbutolol is 200 times more active than its *R*-enantiomer, and has other properties, like an antiarrhythmic effect [13]. Moreover, (*R*)-penbutolol has a significant mutagenic activity [16], which explains why this beta blocker is sold as enantiopure. Since most of its syntheses involve the use of hazardous transition metal catalysts, developing a more environmentally friendly and economically viable pathway would be a positive development.

Bisoprolol is a beta blocker considered as safe and effective for the short-term management of hypertension [17]. The drug is one of the ten beta blockers most prescribed in 2017 [18]. The *S*-enantiomer of bisoprolol has about 30 to 80 times greater beta blocking activity than its *R*-enantiomer [19].

Nowadays, most beta blockers are sold in their racemic form [10]. This is due to the fact that asymmetric synthesis and enantiomer separation are quite expensive, and because it is believed that most of the distomers do not exhibit any harmful side effects [20]. However, it is not always the case, and even if most beta blockers distomers do not have serious side effects, they are still considered as unnecessary and potentially harmful [21]. Finding new ways to produce only the eutomer of such drugs in an economically viable way is therefore needed.

1.4. Green chemistry

The field of green chemistry exists since the early 1990s, and is defined as the “design of chemical products and processes to reduce or eliminate the use and generation of hazardous substances.”. In order to achieve this, chemists need to carefully design their synthesis with sustainability in mind [22], and try to follow the twelve principles that were presented by Paul Anastas in 1998. Those principles include waste and accident prevention, the use of catalysts, less hazardous chemicals, safer solvents, and renewable feedstocks [23]. During the past thirty years, the field of green chemistry has grown considerably and filled up scientific journals and

patent literature [24]. Nevertheless, the global economy is still based on unsustainable fossil resources, and as scientists all over the world are sounding the alarm on the necessity of massive actions to limit the terrible consequences of global warming [25], the need for the development of more sustainable chemical processes is self-evident.

As it will be described more in detail in the next part, the use of biocatalysis has a lot of potential for the development of greener chemical synthesis.

1.5. Biocatalysis in organic chemistry

Biocatalysis can be defined as the use of natural substances such as isolated enzymes and whole cells to catalyze chemical transformations of organic compounds. Its field fits well with nine of the twelve green chemistry principles, as shown in Table 1.5.1.

Table 1.5.1: Biocatalysis and the principles of green chemistry [26].

Green chemistry principles	Biocatalysis
Waste prevention	Enables more sustainable routes with significantly reduced waste
Atom economy	Enables more atom and step economic routes
Less hazardous syntheses	Generally low toxicity
Safer solvents and auxiliaries	Usually performed in water or low-toxicity solvents
Energy efficient	Mild conditions often implies energy efficiency
Renewable feedstocks	Enzymes are renewable and can be reused after a reaction
Reduce derivatization	Biocatalysis obviates the need for protection/ deprotection
Catalysis	Enzymes are catalysts
Inherently safer processes	Performed under mild and safe conditions
Real-time analysis for pollution prevention	Can be applicable in biocatalytic processes

Enzymes are often considered expensive, too sensitive, and only working with their natural substrate and in their natural environment. However, those drawbacks are only concerning some enzymes. Cheap, stable enzymes accepting a large variety of substrate do exist, and some enzymes are able to catalyze reactions in organic solvents. Moreover, enzymes are very efficient catalysts, giving rates typically 10^8 times higher than those of the corresponding non-enzymatic reactions. Enzymes are also often highly selective in terms of chemo-, regio-, dia- and enantioselectivity [27]. Thanks to their high selectivity, protection and deprotection steps can be avoided, and compounds can be synthesized in fewer steps.

In this thesis, enzymes are used in key steps of the syntheses for their very high enantioselectivity, in order to either create a new chiral center in an enantiopure way (via enzymatic ketone reduction), or to only transform one enantiomer of a chiral mixture (via kinetic resolution).

1.5.1. Kinetic resolution in irreversible reactions

Because of the enantioselectivity of enzymes, two enantiomers of a racemic substrate usually react at different rates. This will result in an enantiomerically enriched substrate and product when conversion is non-zero and not total. In an ideal situation, the reaction would stop when the enantiomer preferred by the enzymes has been fully transformed, and the unpreferred substrate would be left unreacted, yielding an enantiopure product with a 50% yield and an enantiopure substrate with a 50% yield that can then easily be isolated. From as early as in 1903, scientists took advantage of this process to isolate one enantiomer in racemic mixtures [28]. One big drawback of kinetic resolution is that the enantiopure product (or substrate) can only be obtained with a yield below or equal to 50%. To obtain better yields, special techniques have to be used, such as dynamic resolution. When the substrates rapidly racemize in the reaction mixture, the enzyme never lacks its preferred enantiomer, and a yield of 100% is then possible. However, this technique is only applicable to certain reactions. Other techniques such as repeated resolution can almost always be used, but are very tedious to implement, especially on an industrial scale. The general kinetic and dynamic resolution of the *R*- and *S*- enantiomers of a substrate is illustrated in Figure 1.5.1.

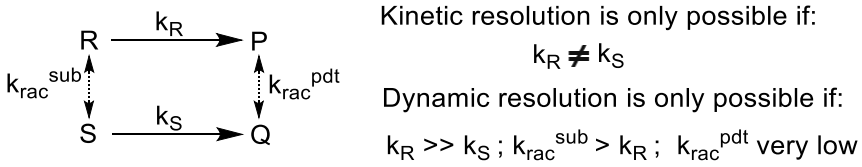

Figure 1.5.1: Kinetic resolution of the (*R*)- and (*S*)- enantiomer of a substrate, written **R** and **S**. They react to form products P and Q with rate constants of k_R and k_S respectively.

The enantioselectivity of an enzyme for a particular kinetic resolution can be characterized by the enantiomeric ratio E. This value will stay constant throughout the reaction. It corresponds to the ratio of the relative second order rate constants of the individual substrates enantiomers A and B, as expressed in the following formula:

$$E = \frac{\nu_A}{\nu_B} = \frac{\left(\frac{k_{cat}}{K_M}\right)_A}{\left(\frac{k_{cat}}{K_M}\right)_B}$$

k_{cat} and K_M are Michaelis-Menten rate constants, and are quite difficult to measure and calculate. Instead of using this formula, the enantiomeric ratio E is often calculated from the reaction conversion and from the enantiomeric excesses of the substrate and the product, which are usually easier to obtain.

The enantiomeric excess (ee) of a chiral substance represents the enantiopurity of a chiral compound. It is expressed in percentage and is defined by the following formula:

$$ee = \left|\frac{(A-B)}{(A+B)}\right| \times \mathbf{100}$$

A and B respectively correspond to the amount of enantiomer A and B in the mixture.

The conversion c of a kinetic resolution reaction in percentage can be calculated directly from the enantiomeric excesses of the product ee_S and of the reactant ee_P by the following formula:

$$c = \frac{ee_S}{ee_S + ee_P} \times \mathbf{100}$$

The E-value is then expressed according to the following formula:

$$E = \frac{\ln\frac{[ee_P \times (1-ee_s)]}{ee_P + ee_S}}{\ln\frac{[ee_P \times (1+ee_s)]}{ee_P + ee_S}}$$

When the conversion is not very low nor very high, the equation above can be approximated by the following formulas:

$$E = \frac{\ln[1 - c \times (1+ee_P)]}{\ln[1 - c \times (1-ee_P)]} \qquad E = \frac{\ln[(1-c) \times (1-ee_S)]}{\ln[(1-c) \times (1+ee_S)]}$$

Other methods exist to calculate the E value, such as ping-pong bi-bi resolutions, which are used by the *E & K calculator* software [29].

An E value between 15 and 30 is regarded as moderate to good. Above 30, it is regarded as excellent. The effect of the E-value on the enantiomeric excesses of the product and the substrate as a function of conversion are given in Figure 1.5.2.

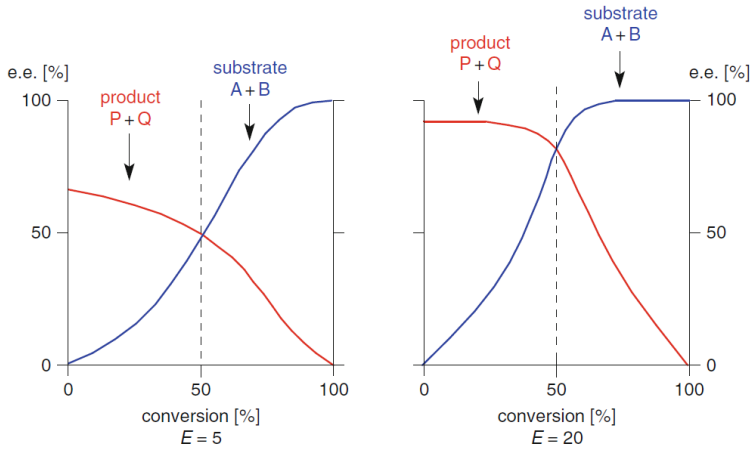

Figure 1.5.2: Effect of the E-value on the enantiomeric excesses of the product and the substrate as a function of conversion [27].

In this thesis, kinetic resolution is used to obtain the substrate with an enantiomeric excess of at least 96%. On the left graph in Figure 1.5.2, we would therefore stop the reaction at around 80% conversion, which means the enantiopure substrate will only be obtained with a maximum yield of 20%. On the other hand, with an E-value of 20 (right graph), the reaction would be stopped at around 60% conversion, and the enantiopure substrate would be obtained with a potential yield of 40%. Therefore, choosing an enzyme allowing a high E-value is important.

1.5.2. Classification of enzymes

Enzyme-catalyzed processes exist for almost every type of organic reactions, and can even allow reactions that are not possible in nonenzymatic chemistry, such as very selective functionalization of inactivated positions in organic molecules.

Depending on the type of reaction they catalyze, enzymes can be classified into six categories, as shown in Table 1.5.2.

Table 1.5.2: Classification of enzymes [27]

Enzyme class	**Reaction type**
Oxidoreductases	Oxidations and reductions
Transferases	Transfer of chemical groups
Hydrolases	Hydrolysis – Formation of esters
Lyases	Addition/elimination of small molecules
Isomerases	Isomerizations
Ligases	Formation/cleavage of C-O, C-S, C-N and C-C bonds

Each of those classes can be divided into subclasses. Lipases, which will be used for the kinetic resolutions, are part of the hydrolases class. Ketoreductases, which will be used for the enzymatic reduction steps, are part of the oxidoreductases class.

1.5.3. Lipases

Lipases are enzymes specialized in the hydrolysis of ester bonds in triglycerides to form fatty acids and glycerol. They play a very important role in biotechnology, for food and oil processing but also for the preparation of chiral intermediates. Contrary to the other types of hydrolases, lipases are only active at an aqueous-lipid interface. This effect is called interfacial activation. What makes them useful in organic chemistry is the fact that they can hydrolyze esters other than glycerides. Depending on the structure and the size of the substrate, different lipases can be used, as shown in Figure 1.5.3.

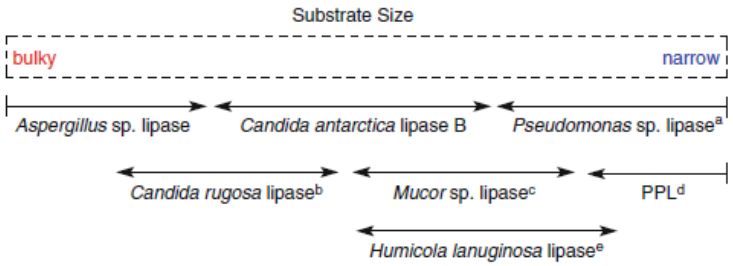

Figure 1.5.3: Steric requirements of several lipases

Lipases catalyze the hydrolysis of ester bonds, and can, under certain conditions, catalyze their formation. This can happen in a non-aqueous environment in the presence of an alcohol and an excess of acyl donor. However, only few enzymes can catalyze reaction in non-aqueous mediums. Among them is *Candida Antarctica* lipase B, a very robust enzyme that can withstand temperatures of more than 50°C, and does not show a pronounced interfacial activation effect. It can also achieve very high enantioselectivity if a well-suited substrate is chosen. In this thesis, kinetic resolution of halohydrin precursors of aryloxyaminopropanols will be performed. The *S*-enantiomer of such molecules fits well the active site of CALB, as shown in Figure 1.5.4. The big difference in size between X and R_2 is what allows CALB to be very enantioselective with this type of substrate.

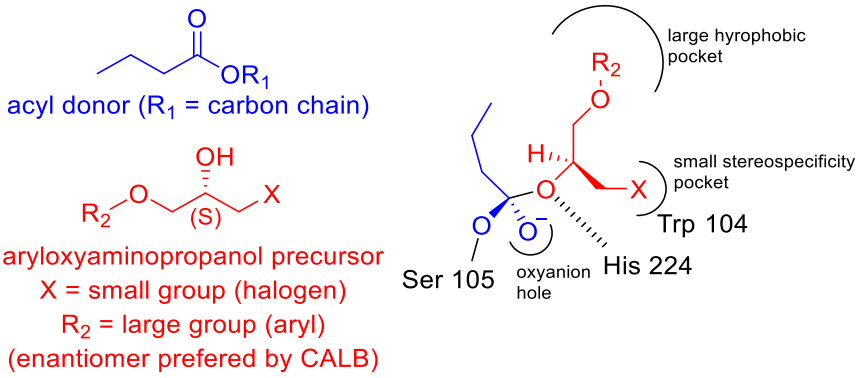

Figure 1.5.4: Suggested model for the CALB catalyzed esterification of the halohydrin precursors of aryloxyaminopropanols. The *S*-enantiomer of such substrates is preferred by CALB [30].

The kinetic resolution of those beta blocker precursors is shown in Scheme 1.5.1.

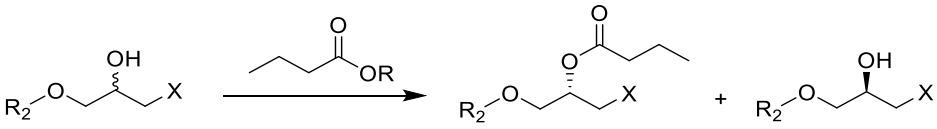

Scheme 1.5.1: Kinetic resolution of the halohydrin precursors of aryloxyaminopropanols. Ideally, only the *S*-enantiomer of such substrates is esterified by CALB. X = halogen; R_2 = aryl group.

The catalytic activity of CALB is mainly due to its active site, composed of a serine-histidine-asparate catalytic triad. The mechanism of CALB catalyzed transesterification of halohydrin precursors of aryloxyaminopropanols is shown in Figure 1.5.5. It is based on the general mechanism proposed by Li *et al.* [31].

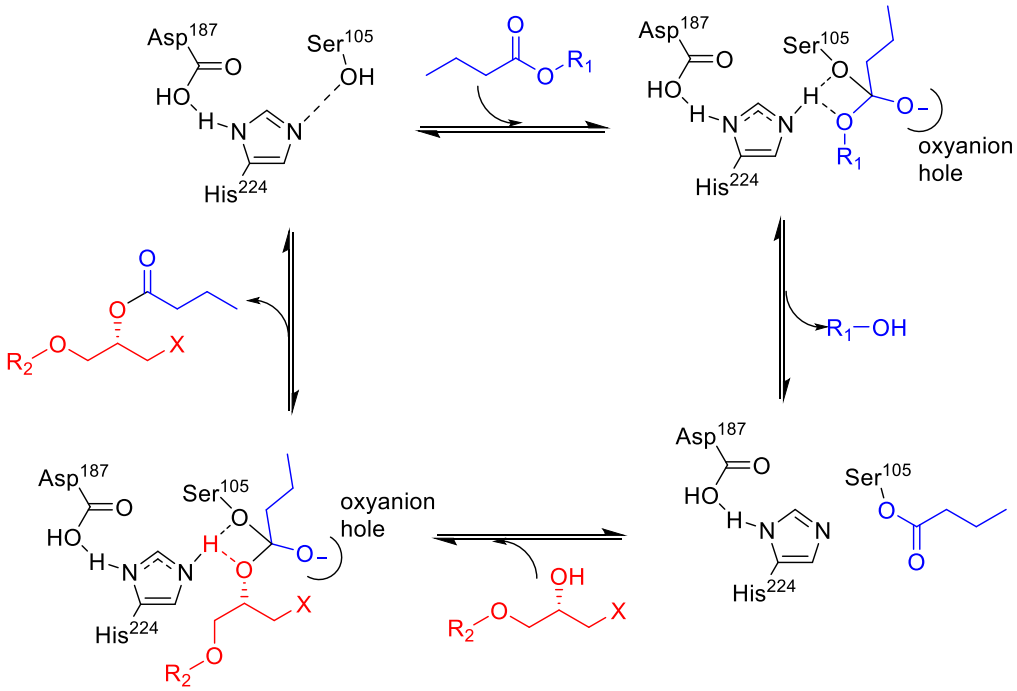

Figure 1.5.5: Catalytic mechanism of CALB for transesterification of halohydrin precursors of aryloxyaminopropanols. R_1 = carbon chain; X = halogen; R_2 = aryl group. Based on Li *et al.* mechanism [31].

For the transesterification to be the only reaction happening, the environment must be anhydrous. Otherwise, CALB would catalyze the hydrolysis of the ester formed, which would decrease the enantiomeric excess of the remaining substrate. CALB would also catalyze the hydrolysis of the acyl donor, yielding butyric acid.

The choice of acyl donor can have an impact on the enzymatic transesterification. The accumulation of R_1-OH in the reaction mixture can lead to the hydrolysis of the ester formed, which would decrease the enantiopurity of the remaining substrate. In this thesis, vinyl butyrate is used as the acyl donor. It is hydrolyzed by CALB to release a vinyl alcohol (R_1-OH) that readily tautomerize to yield acetaldehyde, which evaporates at 20°C. Therefore, the vinyl alcohol can hardly accumulate in the reaction mixture. The enzymatic transesterification can then be considered irreversible if the environment is anhydrous.

1.5.4. Ketoreductases

Ketoreductases are a subgroup of alcohol dehydrogenases, and catalyze hydride transfers, allowing the reduction of ketones to alcohols and the oxidation of alcohols to ketones. In the industry, they are mainly used as an alternative method to conventional chemical reduction. During the reduction of a ketone, a chiral center is created. Two enantiomers can therefore be produced, and ketoreductases can be very selective towards one of them. Enzymes are less used for oxidation reactions, because their high enantioselectivity can then not be taken advantage of. Alcohol oxidation leads indeed to the destruction of a chiral center.

Most alcohol dehydrogenases follow the “Prelog’s Rule” during the reduction of ketones. This rule allows to predict which enantiomer of the alcohol will be mainly formed, as shown in Figure 1.5.6.

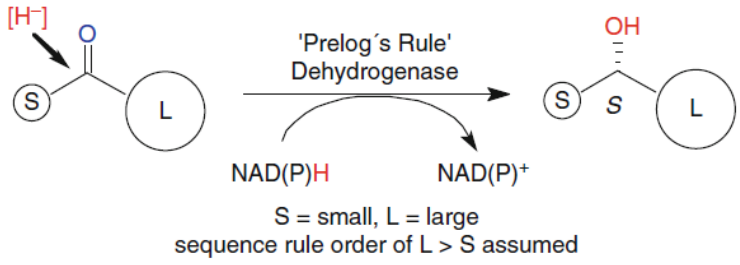

Figure 1.5.6: Enantiomer preferentially formed by alcohol dehydrogenases following the Prelog’s rule [27].

Ketoreductases need the presence of a specific redox cofactor. For most of those enzymes, it is either Nicotinamide adenine dinucleotide NAD(H) or its phosphate NADP(H). Whole cell metabolisms readily regenerate the oxidized or reduced cofactor, so that stoichiometric amounts are not needed. However, without a recycling system, isolated enzymes would need the same

amount of cofactor as of substrate. Isolated enzymes are often preferred to whole cells in the industry because their use limits side reactions and facilitate workups. NAD(H) and NADP(H) being very expensive, using stoichiometric amounts would not be economically viable at an industrial scale. Fortunately, regeneration systems have been developed, reducing the amount of redox cofactor needed to catalytic amounts. In this thesis, a regenerating system using glucose-6-phosphate dehydrogenase is used to regenerate NADPH. This system was first reported by Wong *et al*. in 1981 [32], and is illustrated in Scheme 1.5.2.

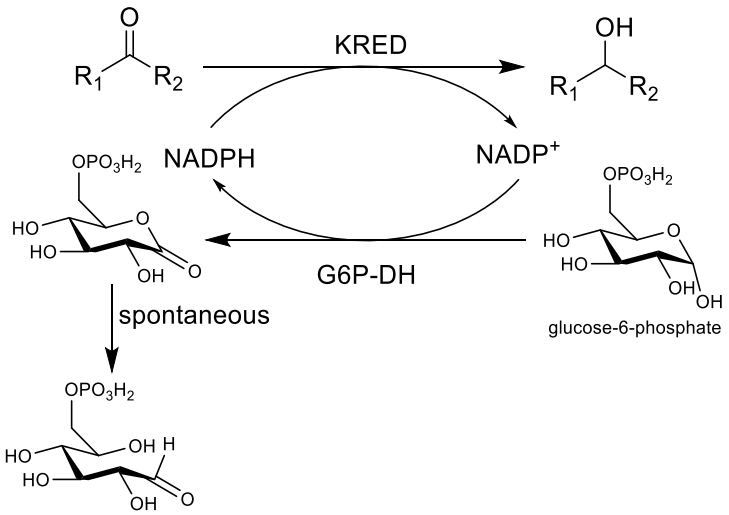

Scheme 1.5.2: Recycling of NADPH using G6P-DH and glucose-6-phosphate.

G6P-DH is relatively cheap in comparison with enzymes used in other NADPH regeneration system such as formate dehydrogenase. Moreover, the 6-phosphoglucolactone formed spontaneously hydrolyzes to the corresponding phosphogluconate, which ensures the irreversibility of the reaction. Drawbacks of this system include the relatively high cost of glucose-6-phosphate, which has to be used in stoichiometric amounts, and the potential difficulty to separate 6-phosphogluconate from the product [33].

The exact mechanism of enzymatic reductions depends on the type of alcohol dehydrogenase used. Most of them contain a zinc atom in their catalytic site that coordinates with the oxygen atom of the ketone substrate. A nucleophilic attack of a hydride coming from the redox cofactor can then happen.

Unlike kinetic resolution, enzymatic reduction does not limit the yield of obtaining an enantiopure alcohol. Therefore, in this thesis, pathways containing enzymatic reductions will be preferred over the ones containing kinetic resolutions.

1.5.5. Optimizing enzyme selectivity

Every catalytic system is composed of three main components: (bio)catalyst, substrate, and medium. Each of those parameters can be adjusted to try to improve an enzymatic reaction.

Testing a reaction using different enzymes could be beneficial, as one could have a better selectivity towards a given substrate. If the equipment is available, enzyme engineering can also allow to optimize the selectivity of an enzyme in a specific reaction. This can be done either through rational protein design, or through directed evolution. Modification of small groups in the enzyme can result in a significant selectivity improvement, as shown in Table 1.5.3.

Table 1.5.3: Selectivity enhancement of Candida rugosa lipase by covalent enzyme modification [27]. [a] Reductive amination of ε-amino groups of lysine. [b] Nitration of tyrosine. [c] Reduction of nitro-tyrosine to amino-tyrosine.

Modification	**Selectivity (*E*)**
None	1.5
Pyridoxal phosphate [a]	2.4
Tetranitromethane [b]	33
Tetranitromethane, then $Na_2S_2O_4$ [c]	37

Modifying the structure of a substrate, for instance by adding or removing protective groups with different sizes and polarity, can lead to a better fit for the enzyme, and to a better selectivity.

Finally, modifying the medium properties, such as its pH, its temperature, and its composition can be a powerful technique to enhance an enzyme selectivity. Adding chiral compounds to a reaction mixture can improve the selectivity of an enzyme by inhibiting the formation of an undesired enantiomer. Changing the pH has an effect on the ionization state of an enzyme, and therefore on its structure and on its selectivity. Changing the temperature has an effect on the thermodynamics of enzymatic reactions, and therefore on the stereopurity of the product obtained. Finally, changing the solvent or cosolvent of a reaction can have a big effect on the selectivity of the enzyme.

The natural medium of most enzymes is water. It is a poor solvent in preparative organic chemistry because most organic compounds are not soluble in it, a lot of side reactions happen because of it, and its removal is tedious. For those reasons among others, solvent systems for enzymatic reactions have been developed. Two of them are used in this thesis: A monophasic

aqueous-organic system for the enzymatic reduction steps and a monophasic organic system for the CALB-catalyzed kinetic resolutions.

A monophasic aqueous-organic system allows the solubilization of lipophilic substrates. The sotalol precursors used in this thesis are not soluble in water, and their enzymatic reduction would not be possible without the addition of an organic solvent. This kind of system can also improve reaction rates and selectivity. Most enzymes are deactivated when more than around 10% of water-miscible organic cosolvent are used, but in some rare cases more than 70% of co-solvent can be used. Water serves as a "molecular lubricant" for enzymes, and increasing the amount of cosolvent can make the enzyme more rigid [27]. It can therefore have a big effect on the enantiomeric excess of the product.

In a monophasic organic system, the enzyme is in suspension in the organic solvent. Water is not present as a solvent, but the structural water, being part of the enzyme structure, is still there. Removal of the structural water of an enzyme by overdrying leads to its deactivation. In this type of system, the catalytic activity is usually lower than in water, but reactions that were not possible before due to the presence of water, such as the esterification of alcohol compounds by lipases, become possible.

1.6. Enantiopurity analysis methods

1.6.1. Chiral HPLC

In order to measure the enantiomeric excess of the products in this thesis, chiral HPLC analyses were performed. Chiral HPLC is a type of HPLC able to separate enantiomers thanks to the presence of an enantiopure compound in the stationary phase.

For the separation of two enantiomers to happen, the two enantiomers must have different affinities with the stationary phase of the column. This is possible if the stationary phase is chiral. To explain this phenomenon, the most popular simple model is the three-point attachment model, suggested by C. E. Dalgliesh in 1952 [34], and illustrated in Figure 1.6.1.

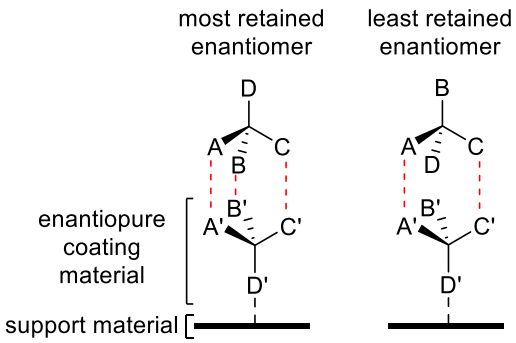

Figure 1.6.1: Three-point attachment model explaining the difference in retention of two enantiomers in chiral HPLC [35]. A, B and C represent groups having a strong affinity with A', B' and C' respectively.

While the most retained enantiomer has three strong interactions A-A', B-B' and C-C', the other enantiomer only has two, and will therefore elute more quickly.

If a suitable chiral coating material is used, two enantiomers of a chiral analyte will therefore elute at a different time, and two peaks will be visible on the obtained chromatogram. In order to measure the enantiomeric excess of the chiral compound analyzed, the following formula can be used:

$$ee = \left|\frac{(A_a - A_b)}{(A_a + A_b)}\right| \times \mathbf{100}$$

A_a and A_b correspond to the area under the peaks corresponding to the elution of two enantiomers a and b.

Each of the enantiomer's peaks must be precisely measured, and therefore separated enough. The resolution factor represents how well two elution peaks can be differentiated, and is defined as follows [36]:

$$R_S = 1.177 \times \left|\frac{{t_R}^a - {t_R}^b}{{b_{0.5}}^a + {b_{0.5}}^b}\right|$$

${t_R}^a$ and ${t_R}^b$ correspond to the elution time of the enantiomers a and b. ${b_{0.5}}^a$ and ${b_{0.5}}^b$ correspond to their peak width at half height. Baseline separation is considered obtained with a retention factor of at least 1.5 [37].

Chiral HPLC analyses were carried out using a Chiralcel OD-H column. This column is composed of cellulose tris(3,5-dimethylphenylcarbamate) coated on 5µm silica-gel. The structure of the coating material is shown in Figure 1.6.2.

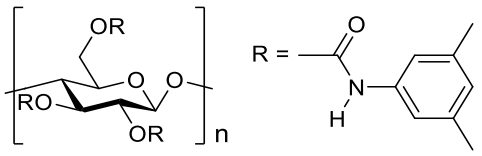

Figure 1.6.2: Structure of cellulose tris(3,5-dimethylphenylcarbamate)

1.6.2. Polarimetry

One particular property of enantioenriched compound is their ability to rotate plane-polarized light. Two enantiomers will moreover rotate it in opposite direction. Those optical rotations can be measured with a polarimeter, and be used to calculate the specific rotation of the analyte:

$$[\alpha]_{\lambda}^{T} = \frac{100 \times \alpha}{c \times l}$$

T is the temperature at which the measure was done (in °C); λ is the wavelength of the polarized light (in nm); α is the observed angle through which the light is rotated (in °); c is the concentration in analyte of the solution (in g/100mL); l is the length of the cell containing the analyte solution (in dm). Usually, λ is equal to 589 nm and is noted D (this wavelength corresponds to the "D line" of a sodium lamp) [38].

At a fixed wavelength, temperature, concentration and cell length, the specific rotation of an enantiomerically enriched chiral analyte can be compared with previously reported data of one of the enantiomers. An identical sign means that the major enantiomer in the analyte is the same as the one previously reported. An opposite sign means that the major enantiomer in the analyte is the opposite enantiomer to the one previously reported.

Comparing the absolute specific rotation of an enantiomerically enriched chiral analyte with the one of the corresponding enantiopure analyte can also be used to know approximately the enantiomeric excess of the analyte, although chiral HPLC is a more accurate method. Slight impurities can distort the results [38], and sometimes the linear relationship between the enantiomeric excess and the optical rotation fails [39].

1.7. Synthesis pathway to enantiopure (*R*)-sotalol, (*S*)-penbutolol and (*S*)-bisoprolol

1.7.1. Synthesis pathway to enantiopure (*R*)-sotalol

Most of the synthesis of enantiopure (*R*)-sotalol previously reported rely on the asymmetric hydrogenation of the ketone in N-(4-(2-chloroacetyl)phenyl)methanesulfonamide and N-(4-(isopropylglycyl)phenyl)methanesulfonamide, as shown in Scheme 1.7.1.

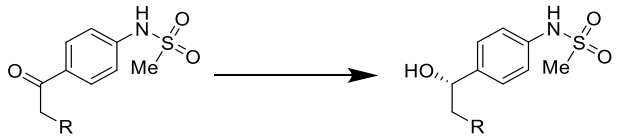

Scheme 1.7.1: Crucial step in most syntheses of (*R*)-sotalol. Starting materials: R = Cl: N-(4-(2-chloroacetyl)phenyl)methanesulfonamide; R = Br: N-(4-(2-bromoacetyl)phenyl)methanesulfonamide; R = NH*i*Pr: N-(4-(isopropylglycyl)phenyl)methanesulfonamide. Products: R = Cl: (*R*)-N-(4-(2-chloro-1-hydroxyethyl)phenyl)methanesulfonamide; R = NH*i*Pr : (*R*)-Sotalol.

Non-enzymatic methods employed include a Noyori asymmetric hydrogenation of N-(4-(isopropylglycyl)phenyl)methanesulfonamide using a ruthenium-BINAP catalyst [40], a Corey-Bakshi-Shibata reduction of N-(4-(2-chloroacetyl)phenyl)methanesulfonamide using the chiral catalyst (*S*)-2-methyl-CBS-oxazaborolidine [41], and a Sharpless asymmetric dihydroxylation of a sotalol precursor in the presence of the chiral ligand DHQ-PHAL [42].

The stereoselective microbial reduction of N-(4-(2-chloroacetyl)phenyl)methanesulfonamide to one of the enantiomers of its reduced derivative was first reported by Patel *et al*. in 1993 [43]. Cell extracts of *H. polymorpha* gave the product with an enantiomeric excess of 99.4%, but while they draw in a scheme the structure of (*R*)-(-)-N-(4-(2-chloro-1-hydroxyethyl)phenyl)methanesulfonamide, they name it (+)-N-(4-(2-chloro-1-hydroxyethyl)phenyl)methanesulfonamide, so the exact enantiomer formed is not known. An enzymatic method to synthesize both enantiomers of sotalol was developed by Kamal *et al*. [44] in 2004. It involved the kinetic resolution of racemic N-(4-(2-chloro-1-hydroxyethyl)phenyl)methanesulfonamide using *Pseudomonas cepacia* lipase. Kapoor *et al*. [45] worked on the enzymatic reduction of N-(4-(2-bromoacetyl)phenyl)methanesulfonamide using ketoreductases, but the enantiomeric excesses of the products obtained were below 70%. They also worked on the hydrolysis of esters of this molecule using the commercial enzyme CRL and *Arthrobecter* sp., which did not give better enantiomeric excesses. They also carried out kinetic resolution of N-(4-(2-bromoacetyl)phenyl)methanesulfonamide catalyzed by PS-C-II, which gave the bromohydrin product with a 99.5% enantiomeric excess. Finally, although they did not work on the whole synthesis of sotalol, Zhu *et al*. reported the synthesis of enantiopure (*R*)-N-(4-(2-chloro-1-hydroxyethyl)phenyl)methanesulfonamide (ee > 99%) by the reduction of N-(4-(2-chloroacetyl)phenyl)methanesulfonamide using the commercial ketoreductase KRED 130 [46].

In this thesis, the synthesis of enantiopure (*R*)-sotalol from aniline is attempted. The key step is the enzymatic reduction of sotalol precursors using commercially available KRED 228 and KRED 238. The rest of the synthesis steps are mostly adapted from the pathway described by Kamal *et al.* [44]. The planned synthesis path is summarized in Scheme 1.7.2.

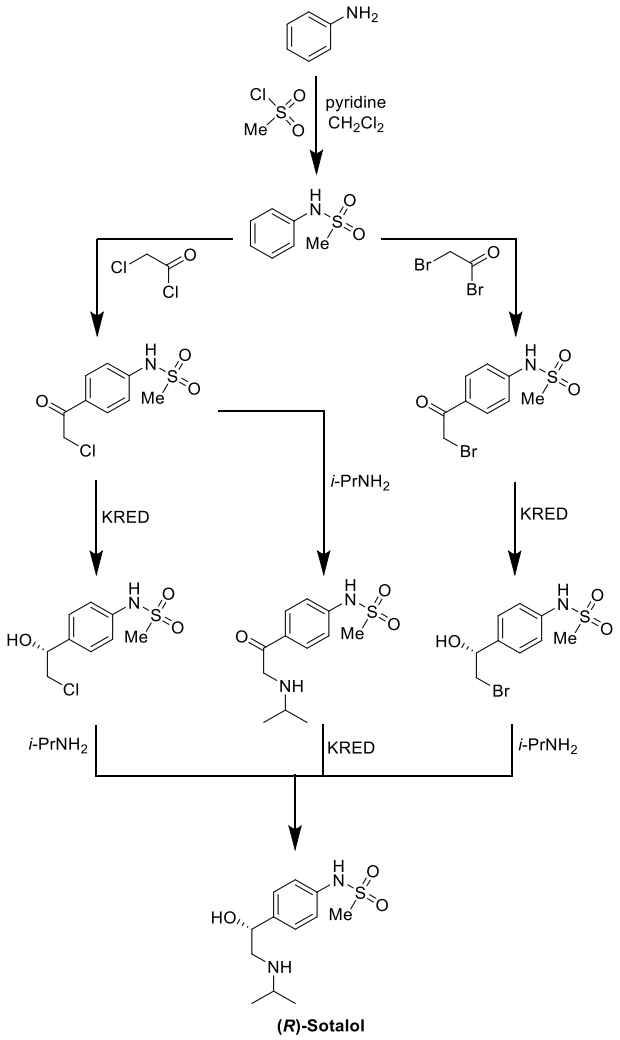

Scheme 1.7.2: Planned synthesis pathway of (*R*)-sotalol.

1.7.2. Synthesis pathway to enantiopure (*S*)-penbutolol

Synthesis of enantiopure (*S*)-penbutolol has been previously performed via enzymatic hydrolysis of acetates using lipases by Hamaguchi *et al.* [47, 48], kinetic resolution using lipase from *Pseudomonas sp.* by Ader *et al.* [49], addition of enantiopure (2*S*)-glycidyl tosylate to a penbutolol precursor by Klunder *et al.* [50], via Sharpless asymmetric dihydroxylation of a precursor of the drug by Phukan *et al.* [51]. Those methods suffer, however, from drawbacks as shown in Table 1.7.1.

Table 1.7.1: Main drawbacks of the previous synthesis of (*S*)-penbutolol

Method	Main drawbacks
Hamaguchi *et al*. [47]	8 steps needed
Ader *et al*. [49]	(*S*)-penbutolol synthesized with only 91% ee
Klunder *et al*. [50]	(*S*)-penbutolol synthesized with only 86% ee
Phukan *et al*. [51]	Use of toxic and expensive catalysts and (*S*)-penbutolol synthesized with a relatively low ee (95%)

In this thesis, the synthesis of (*S*)-penbutolol is composed of only four steps, and uses a nontoxic enzyme (CALB) as the chiral catalyst. The key step is a kinetic resolution, as in the synthesis performed by Ader *et al*., but here the product is obtained with an enantiomeric excess of 99%. The planned synthesis pathway chosen is shown in Scheme 1.7.3, and is adapted from the synthesis pathway used for others aryloxyaminopropanol beta blockers in the Biocatalysis research group [52].

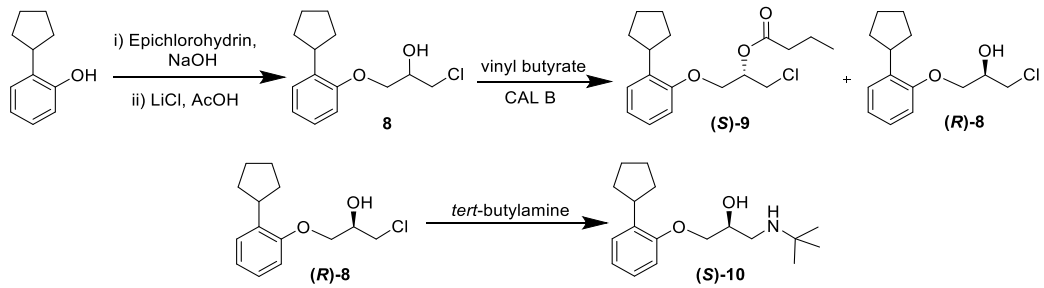

Scheme 1.7.3: Planned synthesis pathway to enantiopure (*S*)-penbutolol

A similar synthesis pathway was attempted by master student Kristoffer Klungseth as part of his master's thesis at NTNU [53], but the (*S*)-penbutolol synthesized was impure and had an enantiomeric excess of 96% only. The main impurity was butyric acid, which was formed during the enzymatic step. Flash chromatography purification did not allow the removal of the impurity. Butyric acid is probably the result of the hydrolysis of vinyl butyrate catalyzed by CALB.

These procedures will therefore be optimized in this thesis in order to obtain better yields, higher enantiomeric excesses, and purer products.

1.7.3. Synthesis pathway to enantiopure (*S*)-bisoprolol

Asymmetric syntheses of (*S*)-bisoprolol have not been reported extensively. Most of the syntheses reported don't involve asymmetric catalysis, and rely on the use of stoichiometric

amounts of commercial enantiopure reactant, such as (*R*)-epichlorohydrin [54], (*R*)-epoxipropanol [55], (*S*)- glycidyl tosilate [56], and (*S*)-glycidyl nosilate [57].

Syntheses relying on biocatalysis have not been reported. The structure of (*S*)-bisoprolol is, however, quite close to the one of (*S*)-penbutolol, and it is plausible that kinetic resolution using CALB would give good results, as it has given good results for the synthesis of numerous enantiopure aryloxyaminopropanol beta blockers in the Biocatalysis research group at NTNU [52, 58]. The pathway using kinetic resolution for the synthesis of (*S*)-bisoprolol chosen in this thesis is very similar to the one chosen for the synthesis of (*S*)-penbutolol, except that an additional step is needed at the beginning to form 4-((2-isopropoxyethoxy)methyl)phenol from 4-(hydroxymethyl)phenol (see Scheme 1.7.4).

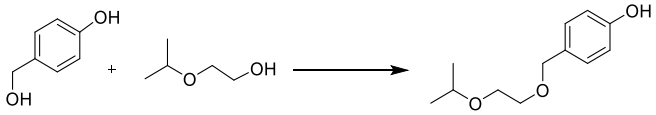

Scheme 1.7.4: Synthesis of 4-((2-isopropoxyethoxy)methyl)phenol from 4-(hydroxymethyl)phenol and 2-isopropoxyethan-1-ol.

The synthesis of 4-((2-isopropoxyethoxy)methyl)phenol has been previously performed using sulfuric acid [59], ion exchange resins [60], and silica sulfuric acid, an acid catalyst [61]. The use of sulfuric acid usually leads to the formation of a significant amount of impurities in this reaction [61]. The use of an exchange resin has already been tried by master student Pål Bøckmann [62], and did not give good results. Therefore, this synthesis step is performed using silica sulfuric acid in this thesis.

Another synthesis pathway using ketoreductases will also be attempted. As explained in the biocatalysis part, kinetic resolution limits the yield to 50% in most of the cases, while with enzymatic reduction a yield of 100% is theoretically possible. Moreover, no additional step would be needed in comparison with the pathway using kinetic resolution. The pathway using ketoreductases would therefore be preferred. It relies, however, on the synthesis of 1-chloro-3-(4-((2-isopropoxyethoxy)methyl)phenoxy)propan-2-one or its bromine equivalent from 4-((2-isopropoxyethoxy)methyl)phenol (see Scheme 1.7.5), which has not been reported previously.

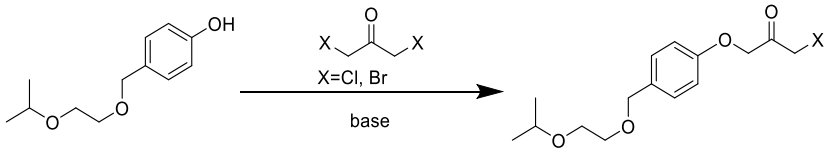

Scheme 1.7.5: Synthesis of 1-chloro-3-(4-((2-isopropoxyethoxy)methyl)phenoxy)propan-2-one and 1-bromo-3-(4-((2-isopropoxyethoxy)methyl)phenoxy)propan-2-one from 4-((2-isopropoxyethoxy)methyl)phenol.

Similar reactions have been reported, as shown in Scheme 1.7.6. Most of the procedures tried in this thesis to synthesize 1-chloro-3-(4-((2-isopropoxyethoxy)methyl)phenoxy)propan-2-one and its bromine equivalent are adapted from the ones described in those articles. Reaction 4 from Scheme 1.7.6 is especially promising, because the pKa of their starting material (naphthalen-1-ol) is quite close to the one of 4-((2-isopropoxyethoxy)methyl)phenol.

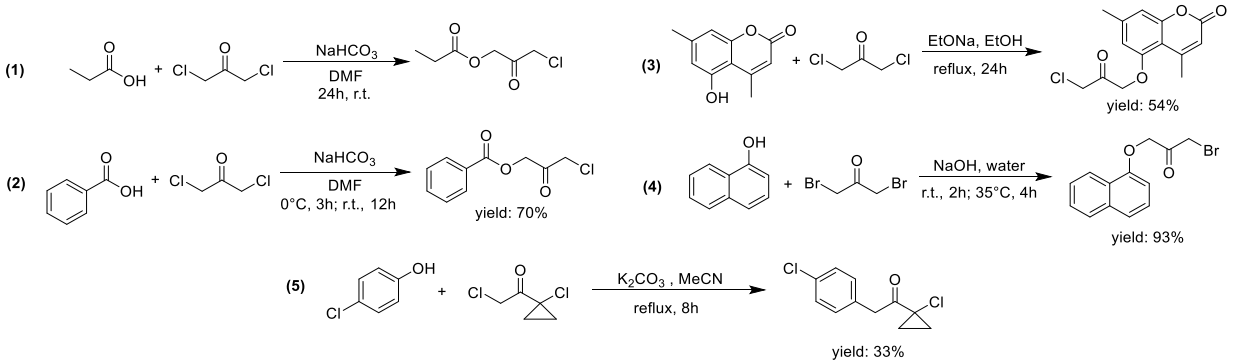

Scheme 1.7.6: Reactions that include the addition of 1,3-dibromopropan-2-one or similar compounds on alcohols ((1) by Sibley et al. [63]; (2) by Kubo et al. [64] ; (3) by Hassan et al. [65]; (4) by Ying Zhou [66];(5) by Stroech et al. [67].

The planned synthesis pathways of (*S*)-bisoprolol are presented in Scheme 1.7.7. The left pathway contains an enzymatic reduction step while the right one includes a kinetic resolution using *Candida antarctica* Lipase B (CALB).

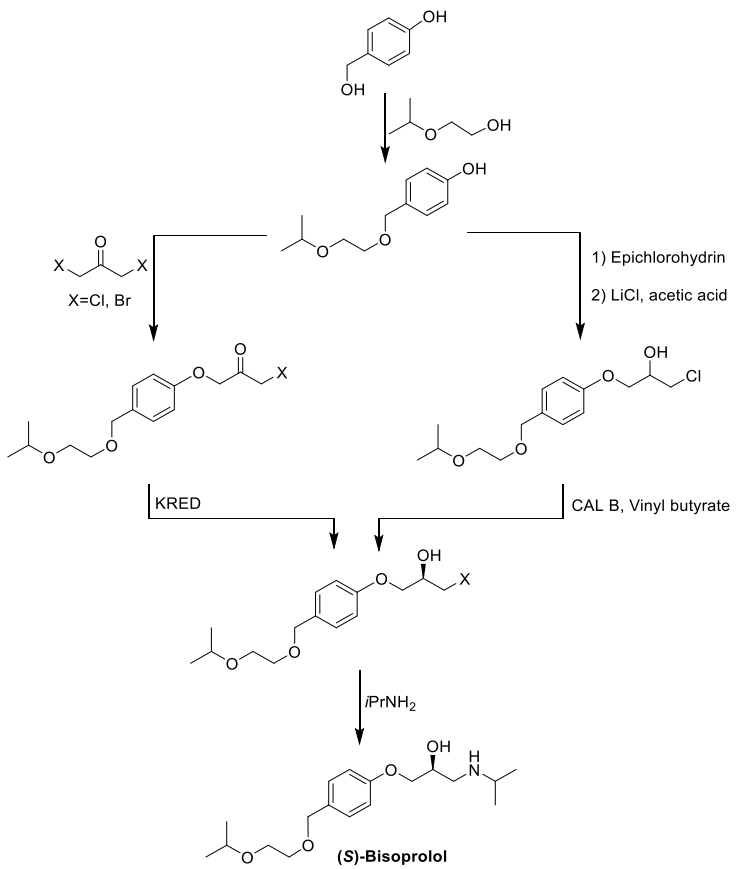

Scheme 1.7.7: Planned synthesis pathways of (*S*)-bisoprolol.

1.8. Theoretical organic chemistry

1.8.1. Nucleophilic substitution reactions

Nucleophilic substitution reactions are very common in organic chemistry. They correspond to substitution reactions where a nucleophile attacks a molecule and replaces one of its functional groups. Those reactions can be divided in two types: S_N1 and S_N2.

S_N1 have a mechanism consisting of two steps, the rate-determining step (formation of the carbocation) being unimolecular. First, a functional group leaves a molecule, leading to the formation of a carbocation intermediate. Then, a nucleophile attacks the carbocation. The mechanism is shown in Scheme 1.8.1. S_N1 reactions are favored when the carbon skeleton of a molecule allows the formation of a relatively stable carbocation intermediate. The rate of the reaction does not depend on the concentration and the strength of the nucleophile. A polar solvent also favors an S_N1 mechanism, mainly because it stabilizes the carbocation intermediate.

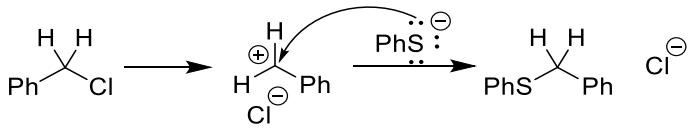

Scheme 1.8.1: Mechanism of an S_N1 reaction.

S_N2 are bimolecular reactions. The nucleophile attack and the leaving of a functional group happen at the same time. The mechanism is shown in Scheme 1.8.2. Here, the rate of the reaction depends on the concentration and the strength of the nucleophile. A non-polar solvent favors an S_N2 mechanism, mainly because it makes the nucleophile anion more reactive. In a protic solvent, the order of nucleophilicity for halogens is as follows: $I^- > Br^- > Cl^- > F^-$.

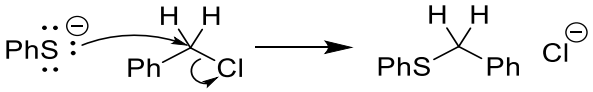

Scheme 1.8.2: Mechanism of an S_N2 reaction.

A better leaving group leads to a faster reaction for both reaction types. For halogens, the reaction rate order is as follows: R-I > R-Br > R-Cl > R-F.

1.8.2. Ring opening of epoxides

Ring opening of epoxides can be either base catalyzed or acid catalyzed.

Base catalyzed opening happens when a strong nucleophile is used. The mechanism of a base-catalyzed ring opening is given in Scheme 1.8.3.

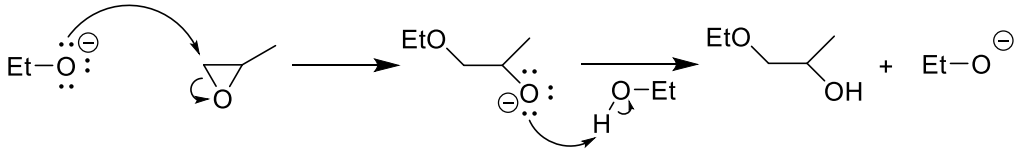

Scheme 1.8.3: Mechanism of a base-catalyzed epoxide opening

This is an S_N2 type mechanism, and the nucleophile will primarily attack the least hindered carbon atom.

Acid catalyzed opening happens when a strong nucleophile is used. The mechanism of a base-catalyzed ring opening is given in Scheme 1.8.3.

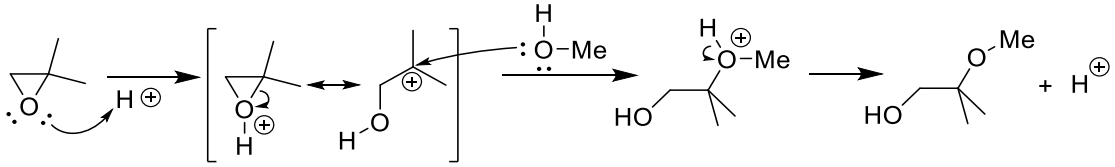

Scheme 1.8.4: Mechanism of an acid-catalyzed epoxide opening

In Scheme 1.8.3, the mechanism is closer to an S_N1 than to an S_N2, and the protonated epoxide resembles a carbocation, as the positive charge is distributed between the most substituted carbon and the oxygen. In acid catalyzed epoxide opening, the nucleophile will often attack the least hindered carbon atom [68] but this will depend on the strength of the nucleophile, and on the stability of the carbocation mesomere intermediate. For instance, during the opening of propylene oxide with hydrogen bromide in water, an acid-catalyzed epoxide opening, the least hindered carbon is mainly attacked, as shown in Scheme 1.8.5. This could be explained by the fact that the bromide anion is a stronger nucleophile than methanol, and because the most hindered carbon here is only a tertiary carbon, so that a carbocation intermediate would not be very stable.

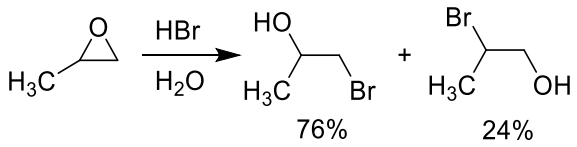

Scheme 1.8.5: Opening of propylene oxide with hydrogen bromide in water [69].

In this thesis, opening of epoxides of aryloxyaminopropanol precursors are done via acid catalysis using either hydrogen chloride or lithium chloride and acetic acid. When using lithium chloride and acetic acid, the epoxide can be activated either by a proton from the acid or by a lithium cation, as shown in Scheme 1.8.6.

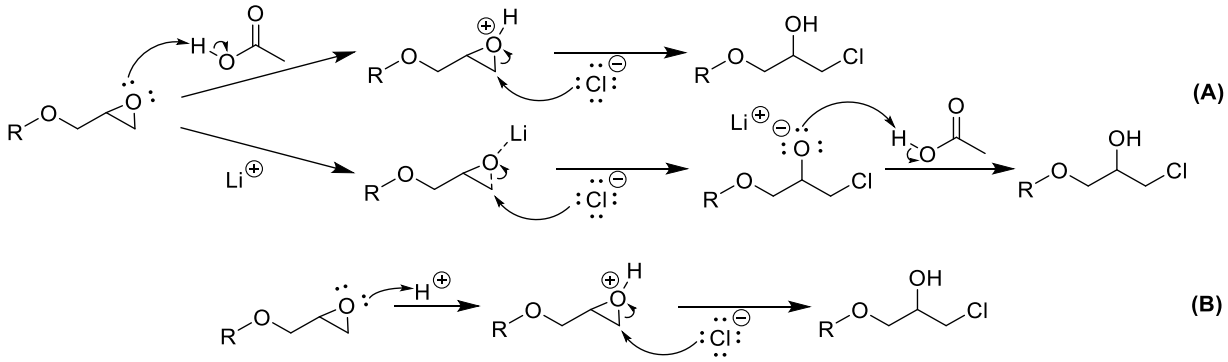

Scheme 1.8.6: Mechanism for the opening of epoxides of aryloxyaminopropanol precursors using lithium chloride and acetic acid (**A**) or hydrogen chloride (**B**). R = aryl group.

Chlorine mainly attacks the least hindered carbon when concentrated hydrochloric acid or lithium chloride and acetic acid are used [52, 58], signifying that a carbocation intermediate is not likely to form, and that the main mechanism is S_N2-like.

The use of a dilute hydrochloric acid solution could be seen as a greener option than the use of lithium chloride and acetic acid, or than the use of concentrated hydrochloric acid. This would indeed optimize the atom economy of the reaction, as little to no waste would be produced. It

could, however, lead to the addition of chlorine on the most substituted carbon, and to obtaining an undesired product. This is because reducing the concentration of nucleophile reduces the rate of S_N2-like reactions, and does not affect the yield of S_N1-like reactions.

1.8.3. Secondary amine synthesis via amine alkylation

Amine alkylation describes the reaction between a primary or secondary amine and a halogenated compound. Usually, secondary amine formation via this method is not possible, because the secondary amine produced is more nucleophile than the primary amine starting material. The reaction continues then to form a tertiary amine, as shown in Scheme 1.8.7 [38].

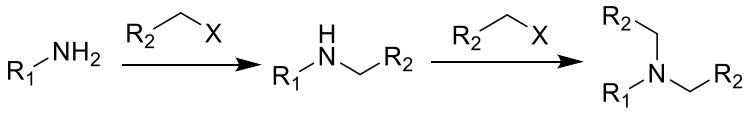

Scheme 1.8.7: Alkylation of a primary amine. The mechanism consists of two S_N2 steps.

In this thesis, the alkylating agent is an aryloxyaminopropanol precursor, and the amine is either isopropyl amine or *tert*-butyl amine. This type of reaction has been performed before, and the main product obtained was a secondary amine, as shown in Scheme 1.8.8.

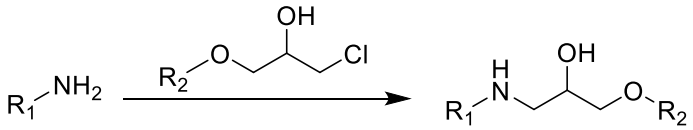

Scheme 1.8.8: Alkylation of a primary amine with an aryloxyaminopropanol precursor. R_1 = *i*-Pr or *tert*-butyl. R_2 = aryl group.

This can be explained for two main reasons. First, both the alkylating agent and the amine are quite bulky. A second alkylation is therefore less likely to happen due to steric hindrance. Second, the alkylating agent contains inductive electron-withdrawing groups, which reduce the reactivity of the amine formed [38].

1.8.4. Friedel-Crafts acylation

Friedel-Crafts acylation is a type of reaction in which an acyl chloride or anhydride reacts with an electron-rich aromatic compound to form an aromatic ketone. The reaction is catalyzed by aluminum chloride, and stoichiometric amounts have to be used, because it complexes with the ketone product. Adding water in the reaction mixture stops the reaction and allows to obtain the desired product. The general mechanism of the reaction is shown in Scheme 1.8.9.

Polyacylation are usually not happening, because the product is less reactive than the starting material, due to the presence of the electron-withdrawing acyl group.

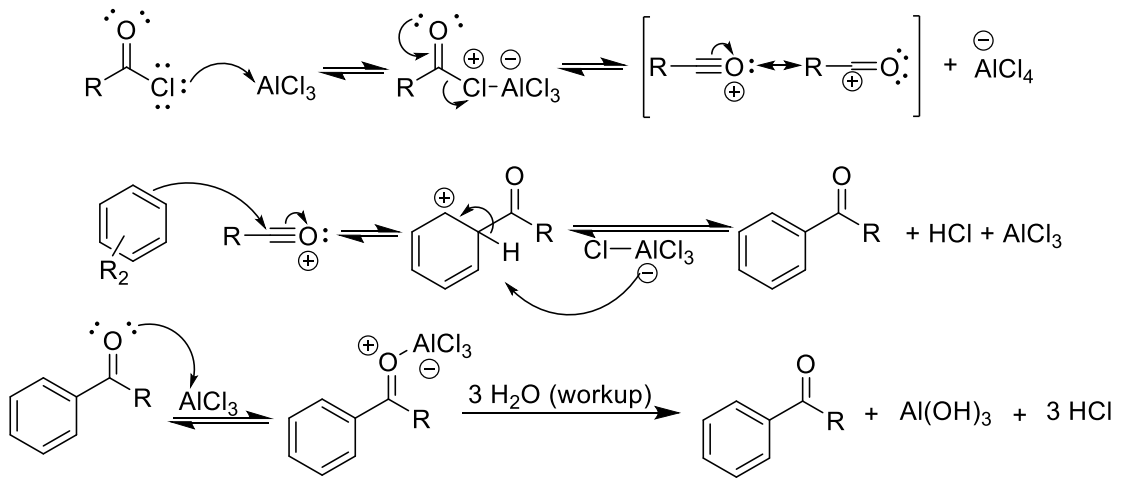

Scheme 1.8.9: Friedel-Crafts acylation mechanism [68].

This reaction requires the aromatic reactant to be electron-rich. The presence of powerful electron-withdrawing groups on the ring such as amines usually gives poor yield [68].

In this thesis, Friedel-Crafts acylation is used in order to form N-(4-(2-chloroacetyl)phenyl)methanesulfonamide, as shown in Scheme 1.8.10.

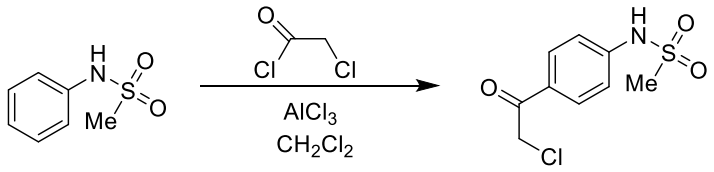

Scheme 1.8.10: Synthesis of N-(4-(2-chloroacetyl)phenyl)methanesulfonamide from N-phenylmethanesulfonamide and 2-chloroacetyl chloride

Although the sulfonamide group attached to the aromatic ring in the starting material N-phenylmethanesulfonamide has an electron withdrawing inductive effect, its contribution to the electron density of the benzene ring through resonance enables the Friedel–Crafts Acylation to happen. This contribution is illustrated in Scheme 1.8.11. For this reaction, Kamal *et al.* [44] obtained a yield of 75%.

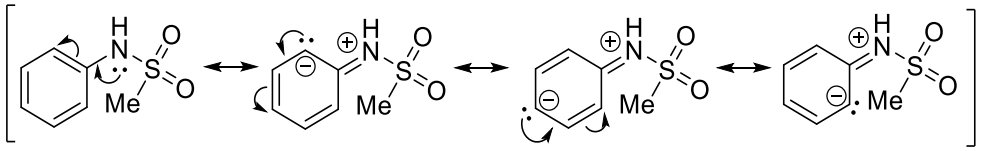

Scheme 1.8.11: Main resonance structures of N-phenylmethanesulfonamide.

The sulfonamide group is an ortho-para director, but the main reaction is an ortho addition, because the para regions are sterically hindered.

1.8.5. Asymmetric ether formation

The most common way of synthesizing asymmetric ether is via the Williamson ether synthesis, shown in Scheme 1.8.12. The mechanism is the one of a typical S_N2 reaction [68].

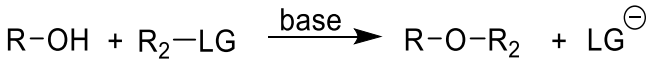

Scheme 1.8.12: General Williamson ether synthesis. LG = Leaving group; usually a halogen.

In this thesis, 4-((2-isopropoxyethoxy)methyl)phenol has to be formed, and its retrosynthesis via a Williamson ether synthesis is shown in Scheme 1.8.13.

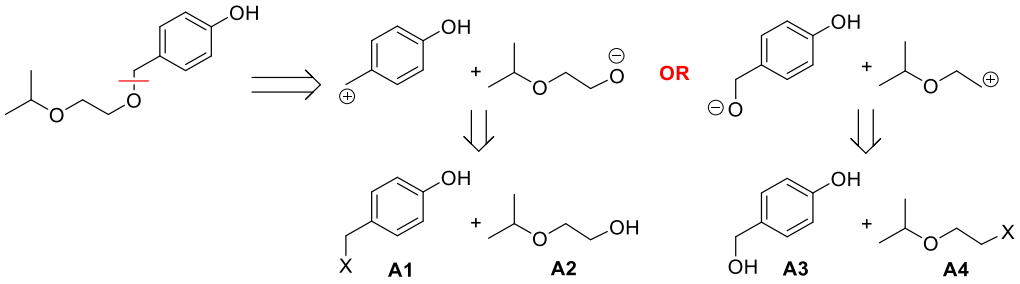

Scheme 1.8.13: Retrosynthesis of 4-((2-isopropoxyethoxy)methyl)phenol via a Williamson ether synthesis. X = halogen.

Reactants **A2** and **A3** are commercially available, but halogenated compounds **A1** and **A4** are not. They could be synthesized as an additional step, but instead, 4-((2-isopropoxyethoxy)methyl)phenol could be synthesized directly from alcohols **A2** and **A3** via intermolecular dehydration of alcohols, as illustrated in Scheme 1.8.14.

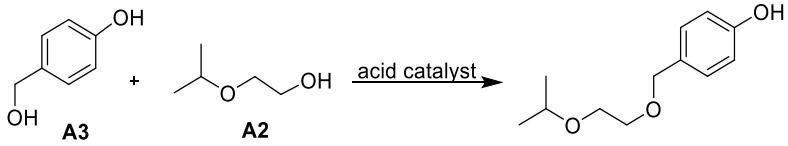

Scheme 1.8.14: Synthesis of 4-((2-isopropoxyethoxy)methyl)phenol from **A2** and **A3** via intermolecular dehydration of alcohols.

Intermolecular dehydration of alcohols is usually not recommended for the synthesis of unsymmetrical ethers, because it could lead to the formation of dimers [68]. A general mechanism for this type of reaction is given in Scheme 1.8.15. The unsymmetrical ether R_1OR_2 is only one of the three products possible.

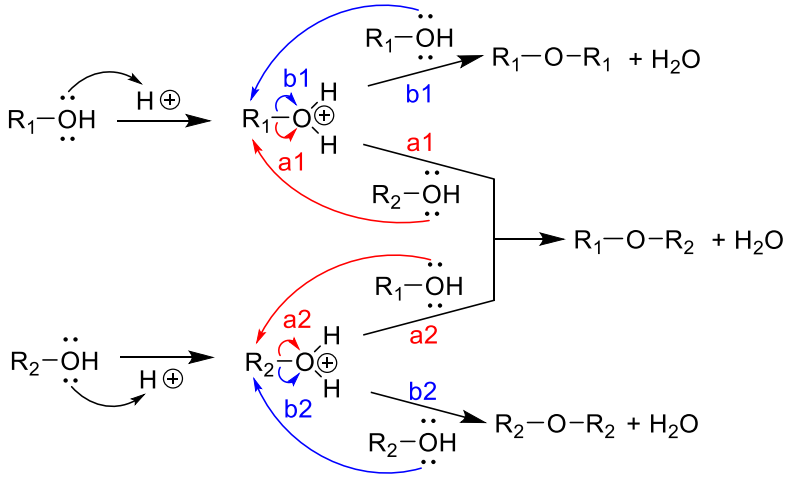

Scheme 1.8.15: Mechanism for the synthesis of esters via intermolecular dehydration of two different alcohols.

The reaction conditions employed during the synthesis of 4-((2-isopropoxyethoxy)methyl)phenol are however allowing the formation of the desired unsymmetrical ether to be dominant, as explained in the results and discussion part.

2 Results and Discussion

2.1 Synthesis of enantiopure (*R*)-sotalol precursors

The aim of this part is to synthesize enantiopure (*R*)-sotalol precursors in an environmentally friendly and efficient way.

2.1.1 Synthesis of N-phenylmethanesulfonamide (1)

N-Phenylmethanesulfonamide (**1**) was synthesized from aniline and methane sulfonyl chloride, as shown in Scheme 2.1.1. The procedure was adapted from the one described by Lis *et al.* [70].

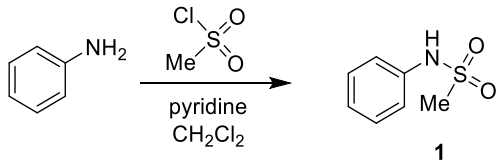

Scheme 2.1.1: Synthesis of N-phenylmethanesulfonamide (**1**) from aniline and methane sulfonyl chloride.

The reaction is exothermic, and the addition of methane sulfonyl chloride needs to be done dropwise and at 0°C. One attempt was done at room temperature, the solution boiled after the first drops of methane sulfonyl chloride reached the reaction mixture, and the final product was more colored than in the other attempts, indicating the presence of more impurities.

Methanesulfonyl chloride reacts vigorously with water to form, among others, methane sulfonic acid, so the reaction should be done under inert atmosphere, with dry dichloromethane and dry pyridine. The reaction is also releasing gas, among other hydrogen chloride, and a needle to evacuate the pressure during the addition is not sufficient. In one attempt, the addition was done completely under inert atmosphere, and the flask was linked to an oil bubbler via a needle and a tube. The septum popped due to an overpressure. Therefore, in the later attempts, the flask was only flushed with nitrogen during the addition of methane sulfonyl chloride, and linked to an oil bubbler afterwards to keep it under inert atmosphere.

When methane sulfonyl chloride is added to the mixture of aniline and pyridine in dichloromethane, the solution immediately turns yellow, and then red. The color does not come from the formation of the desired product. Since methane sulfonyl chloride leads to the formation of colored byproducts even when added under nitrogen and at 0°C, 1.1 equivalents were used. The formation of colored byproduct will be discussed in the next part.

The reaction mixture was stirred overnight. Following the reaction by TLC was tried, but due to the very close R_f values of the starting material and the product with all the eluents tested, it was hard to be sure all the starting material had been consumed.

2.1.1.1 Reaction mechanism for the synthesis of N-phenylmethanesulfonamide (1) from aniline and methane sulfonyl chloride

The mechanisms of similar reactions have been studied by J. F. King [71]. It was proven by isotope labeling that methane sulfonyl chloride in the presence of a tertiary amine base leads to the formation of a very reactive intermediate: sulfene. The proposed mechanism of the synthesis of N-phenylmethanesulfonamide (**1**) from aniline and methane sulfonyl chloride is shown in Scheme 2.1.2.

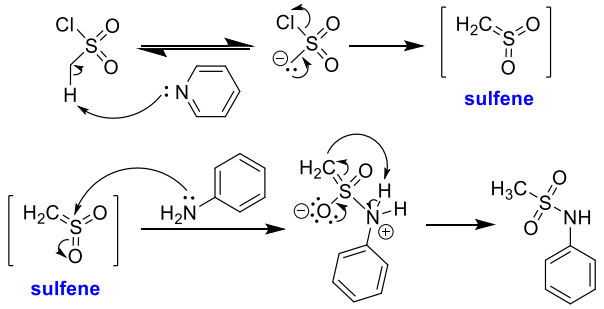

Scheme 2.1.2: Reaction mechanism suggested for the synthesis of N-phenylmethanesulfonamide (**1**) from aniline and methane sulfonyl chloride.

The formation of the very reactive sulfene intermediate explains the exothermic nature of the reaction, and the formation of byproducts. It also explains why water should not be present in the reaction mixture. Water will indeed attack the sulfene intermediate to form methane sulfonic acid, as shown in Scheme 2.1.3.

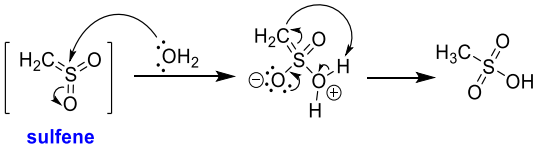

Scheme 2.1.3: Reaction mechanism for the reaction of sulfene with water.

2.1.1.2 Work-up and purification of the crude product

To remove the remaining pyridine and its protonated form, the reaction mixture was concentrated under reduced pressure. This is done to prevent the loss of product when the reaction mixture is washed with water. Pyridine is soluble in water, and the desired product might be soluble in pyridine.

The reddish oil obtained is then dissolved in dichloromethane and washed with water. The organic layer stays orange/reddish, and the aqueous phase becomes slightly yellow. The organic layer is then dried over magnesium sulfate. Some of the red color stays on the magnesium sulfate, even when washed with dichloromethane.

A TLC (6 n-pentane/4 ethyl acetate) of the organic layer shows three compounds. Two of them are colored, and are labeled compounds **I1** and **I2**, with respective R_f of 0 and 0.14. They are probably polar sulfonyl impurities. The obtained product is not very soluble in ethyl acetate, which would make column chromatography purification hard with this eluent. First, triturations in different solvents were attempted to try to get rid of the colored impurities. Petroleum ether didn't dissolve any colored compound, while ethyl acetate could dissolve some of it, but also partly dissolved the desired product. Dichloromethane dissolved most of the desired compound.

The reaction mixture dissolved in a large amount of ethyl acetate was passed through silica. Impurity **I1** was mainly retained by the silica, as shown by a TLC analysis of the filtrate, but the solution remained colored afterwards, mostly because of the presence of impurity **I2**.

To facilitate the following of the reaction by TLC and to find a good eluent for column chromatography, several eluent systems were tested. However, R_f of the starting material and the desired product were always very close. Retention factors of product **1**, aniline and impurity **I2** in all the eluent systems tested are shown in Table 2.1.1.

Table 2.1.1: Retention factors obtained by TLC analysis of product 1, aniline and impurity I2 with several eluent systems.

Eluent	**Mixing ratio**	**Rf of product 1**	**Rf of aniline**	**Rf of impurity I2**
n-pentane:ethyl acetate	6:4	0.56	0.51	0.14
dichloromethane:ethyl acetate	7:3	0.69	0.69	0.24
n-pentane:tetrahydrofuran	6:4	0.65	0.65	0.46
dichloromethane:tetrahydrofuran	8:2	0.88	0.80	0.29
n-pentane:propan-2-ol	9:1	0.40	0.46	0.29
dichloromethane:propan-2-ol	9.1:0.9	0.58	0.61	0.44
dichloromethane:methanol	8.5:1.5	0.75	0.81	0.67
dichloromethane:diethyl ether	8:2	0.59	0.59	-

Recrystallizations from different solvents were attempted, including petroleum ether, ethyl acetate, water, and toluene. Petroleum ether did not dissolve anything, even under reflux.

Recrystallization from boiling ethyl acetate gave very pure crystals, but a bad yield. Boiling water gave better results, although the procedure was tedious. During the first attempts, an oil formed at the bottom instead of crystals. White crystals were eventually obtained by breaking the oil and reheating the solution each time the oil formed, seeding the solution when it was cooling down, and scratching the walls of the flask with a glass rod. This procedure gave a yield of 87%, while the recrystallization in ethyl acetate only gave a yield of 34%. Recrystallization in toluene was the easiest to perform, and gave a product with a very high purity the form of big translucid crystals, with a yield of 73%. This yield could potentially be improved by using less toluene during the recrystallization.

On another batch, another purification technique was tried. It was noticed that during the workup, magnesium sulfate became bright red even after being washed with dichloromethane. The colored impurity present in the crude mixture is probably a sulfate-related compound, which explains its affinity with the magnesium sulfate. After being washed with distilled water, the orange crude product dissolved in dichloromethane was therefore washed with a saturated solution of magnesium sulfate. The organic layer changed color to become yellow, as well as the aqueous layer. When separated, the organic layer turned orange again, but the color was less intense. It was washed two more times with a saturated solution of magnesium sulfate, and the organic layer was then only slightly yellow. After drying the organic layer over magnesium sulfate, the solution was completely uncolored. Solvent removal gave compound **1** as a white powder with a very high yield (98%) and purity (99%, ^{1}H-NMR). This means that the desired product did not have any affinity with the saturated magnesium sulfate aqueous solution, while the colored impurities did. This purification method is a lot simpler and less time consuming than column chromatography or recrystallization.

2.1.1.3 Characterization of N-phenylmethanesulfonamide (1)

Characterization of compound **1** was carried out by NMR spectroscopy, with deuterated dimethyl sulfoxide as solvent. Compound **1** with numbered carbon atoms is shown in Figure 2.1.1, and assignment of chemical shifts are given in Table 2.1.2.

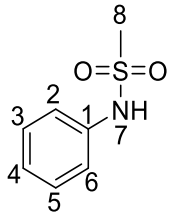

Figure 2.1.1: Compound **1** with numbered carbon and nitrogen atoms. Assignment of chemical shifts are given in Table 2.1.2, and all spectra are given in the appendix (Part 6.1.1).

Table 2.1.2: Characterization of compound **1** given ^{1}H-, ^{13}C-, H,H-COSY, HSQC- and HMBC-NMR (600 MHz, CDCl3), see the appendix (Part 6.1.1).

Numbered atom	**^{1}H-NMR [ppm] (mult., int., ^{3}J)**	**^{13}C-NMR [ppm]**	**COSY**	**HMBC**
1	-	138.86	-	2,3,5,6
2	7.25 – 7.18 (m, 2H)	120.26	3,5	1,3,4,5,6
3	7.37 – 7.30 (m, 2H)	129.76	2,4,6	1,2,5,6
4	7.13 – 7.06 (m, 1H)	124.31	3,5	2,3,5,6
5	7.37 – 7.30 (m, 2H)	129.76	2,4,6	1,2,3,6
6	7.25 – 7.18 (m, 2H)	120.26	3,5	1,2,3,4,5
7	9.72 (s, 1H)	-	-	2,6
8	2.98 (s, 3H)	39.64	-	-

2.1.2 Synthesis of N-(4-(2-chloroacetyl)phenyl)methanesulfonamide (2)

N-(4-(2-Chloroacetyl)phenyl)methanesulfonamide (**2**) was synthesized from N-phenylmethanesulfonamide (**1**) and 2-chloroacetyl chloride by adapting the procedure described by Lis *et al.* [72].

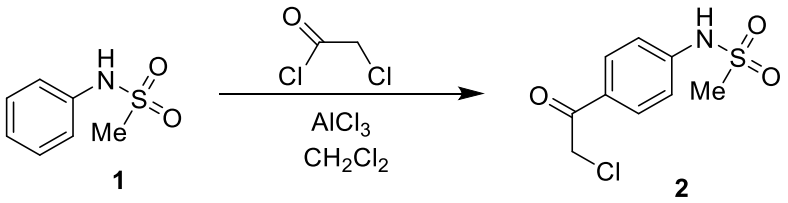

Scheme 2.1.4: Synthesis of N-(4-(2-chloroacetyl)phenyl)methanesulfonamide (**2**) from N-phenylmethanesulfonamide (**1**) and 2-chloroacetyl chloride

Anhydrous aluminum chloride and 2-chloroacetyl chloride are moisture sensitive, so the reaction was performed under inert atmosphere, and with a dry solvent. The reaction is very exothermic, and addition of 2-chloroacetyl chloride was performed dropwise and at 0 °C. HCl gas is released during the reaction, so the flask should always be linked to an oil bubbler to

avoid overpressure. Aluminium chloride is a catalyst, but large quantities have to be used because it forms a complex with the product, as shown in Scheme 2.1.6 and as explained in the introduction. Two equivalents of 2-chloroacetyl chloride are used to try to maximize the conversion of compound **1** to product **2**.

Pouring the reaction mixture into water at the end is necessary to destroy the ketone-aluminum complex and obtain compound **2**, which will precipitate (see Scheme 2.1.6). Using an acidic aqueous mixture is useful to get rid of the aluminum catalyst. The aluminum chloride present at the end of the reaction is indeed forming aluminum hydroxide in the presence of water at a neutral pH. Aluminum hydroxide is completely insoluble in water, and would precipitate with the desired product. In a hydrochloric acid aqueous solution, aluminum chloride will be dissolved into the aqueous phase. Excesses of 2-chloroacetyl chloride react with water to form water-soluble chloroacetic acid and hydrochloric acid. The precipitate obtained after pouring the reaction mixture into acidic water is therefore mainly composed of product **2**. The product obtained was colored, so a purification step was performed.

At room temperature, compound **2** is not soluble in n-pentane, dichloromethane, methanol, ethyl acetate, acetonitrile, toluene, 2-propanol, ethanol and water. It is slightly soluble in tetrahydrofuran and acetone, and soluble in dimethyl sulfoxide. This makes its purification difficult. Heating the product in different solvents was attempted to find a potential solvent for recrystallization. The product was soluble in boiling methanol, so this solvent was chosen for the purification.

Recrystallization from boiling methanol gave the desired product with a yield of 57% with an 98% purity (^{1}H-NMR). Traces of methanol (2%, ^{1}H-NMR) were present even after drying the crystals under vacuum overnight. The crystals obtained were slightly orange, while pure N-(4-(2-chloroacetyl)phenyl)methanesulfonamide (**2**) is a white solid. An impurity was therefore responsible of the color, but it was not present in significant amounts for it to be visible on the ^{1}H-NMR spectrum.

2.1.2.1 Reaction mechanism for the synthesis of compound 2 from compound 1 and 2-chloroacetyl chloride

This reaction is a Friedel–Crafts acylation. Main resonance structures of compound **1** are shown in Scheme 1.8.11. The mechanism of the reaction shown in Scheme 2.1.6 is based on the Friedel–Crafts Acylation mechanism proposed by Solomons *et al.* (p. 686-687) [68]. A very

reactive acylium ion is formed from 2-chloroacetyl chloride and aluminum chloride, which explains the exothermic nature of the reaction.

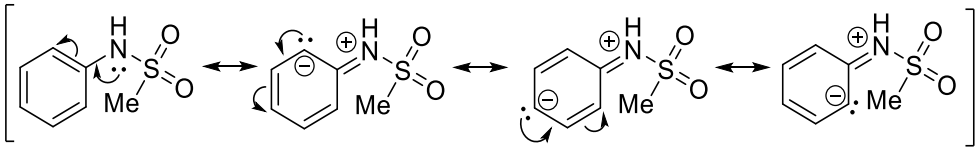

Scheme 2.1.5: Main resonance structures of compound **1**.

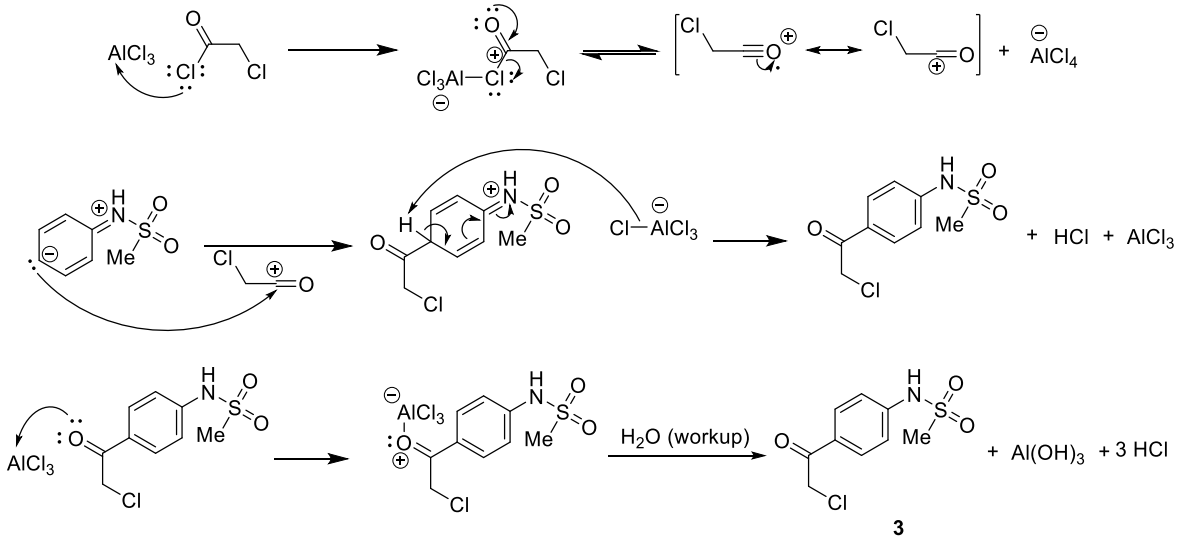

Scheme 2.1.6: Reaction mechanism for the synthesis of N-(4-(2-chloroacetyl)phenyl)methanesulfonamide (**2**) from N-phenylmethanesulfonamide (**1**) and 2-chloroacetyl chloride [68].

2.1.2.2 Synthesis of N-(4-(2-bromoacetyl)phenyl)methanesulfonamide (3)

The synthesis of N-(4-(2-bromoacetyl)phenyl)methanesulfonamide (**3**) was performed using the same procedure, only replacing 2-chloroacetyl chloride with 2-bromoacetyl bromide, as shown in Scheme 2.1.7. Bromine is a better leaving group than chlorine, and this reaction could lead to a better yield. Also, bromine is bigger than chlorine, and N-(4-(2-bromoacetyl)phenyl)methanesulfonamide (**3**) could be a better substrate than compound **2** for the enzymatic reduction discussed in Section 2.1.4.

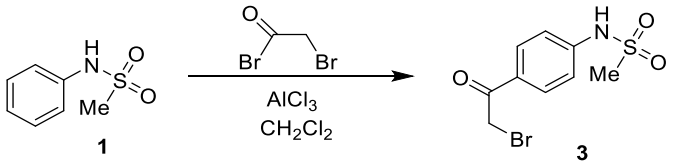

Scheme 2.1.7: Synthesis of N-(4-(2-bromoacetyl)phenyl)methanesulfonamide (**3**) from N-phenylmethanesulfonamide (**1**) and 2-bromoacetyl bromide

This reaction was performed by master student Fredrik Bjørnes under my supervision as part of a course project. N-(4-(2-Bromoacetyl)phenyl)methanesulfonamide (**3**) was obtained with a

yield of 58% and a purity of around 80% (^{1}H-NMR). The main impurity present is an unisolated byproduct containing an aromatic ring with two groups of equivalent protons. It is believed to be the compound shown in Figure 2.1.2, and potentially formed via a Friedel-Craft alkylation where the aromatic ring attacks the carbon of 2-bromoacetyl bromide bearing a bromine and a hydrogen instead of attacking the acyl bromide group.

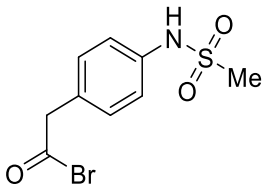

Figure 2.1.2: Structure of a potential byproduct during the synthesis of compound **3** from N-phenylmethanesulfonamide (**1**) and 2-bromoacetyl bromide.

This kind of byproduct was not present in product **2**.

2.1.2.3 Characterization of N-(4-(2-chloroacetyl)phenyl)methanesulfonamide (2) and N-(4-(2-bromoacetyl)phenyl)methanesulfonamide (3)

Characterization of compounds **2** and **3** were carried out by NMR spectroscopy, with deuterated dimethyl sulfoxide as solvent. Compounds **2** and **3** with numbered carbon atoms are shown in Figure 2.1.3, and assignment of chemical shifts are given in Table 2.1.3.

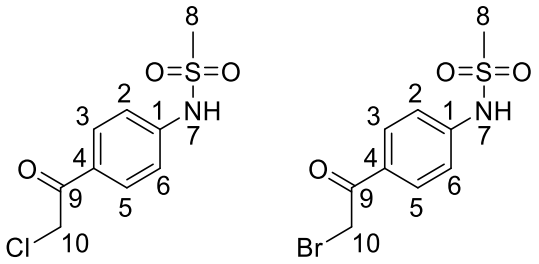

Figure 2.1.3: Compounds **2** and **3** with numbered carbon and nitrogen atoms. Assignment of chemical shifts are given in Table 2.1.3 for compound **2** and in Table 2.1.4 for compound **3**. All spectra are given in the appendix (Part 6.1.2 and 5.1.3).

Table 2.1.3: Characterization of product **2** given ^{1}H-, ^{13}C-, H,H-COSY, HSQC- and HMBC-NMR (600 MHz, CDCl3), see the appendix (Part 6.1.2).

Numbered atom	^{1}H-NMR [ppm] (mult., int., ^{3}J)	^{13}C-NMR [ppm]	COSY	HMBC
1	-	144.10	-	-
2	7.50 – 7.06 (m, 2H)	117.92	3,5	1,3,5,6,9
3	8.16 – 7.77 (m, 2H)	130.70	2,6	1,2,5,6,9
4	-	129.34	-	-
5	8.16 – 7.77 (m, 2H)	130.70	2,6	1,2,3,6,9
6	7.50 – 7.06 (m, 2H)	117.92	3,5	1,2,3,5,9
7	10.44 (s, 1H)	-	-	2,6
8	3.14 (s, 3H)	40.49	-	-
9	-	190.64	-	-
10	5.13 (s, 2H)	47.76	-	9

Table 2.1.4: Characterization of compound **3** given ^{1}H-, ^{13}C-, H,H-COSY, HSQC- and HMBC-NMR (600 MHz, CDCl3), see the appendix (Part 6.1.3).

Numbered atom	^{1}H-NMR [ppm] (mult., int., ^{3}J)	^{13}C-NMR [ppm]	COSY	HMBC
1	-	144.12	-	-
2	7.32 – 7.28 (m, 2H)	117.89	3,5	1,3,5,6
3	8.01 – 7.97 (m, 2H)	131.13	2,6	1,2,5,6,9
4	-	128.98	-	-
5	8.01 – 7.97 (m, 2H)	131.13	2,6	1,2,3,6,9
6	7.32 – 7.28 (m, 2H)	117.89	3,5	1,2,3,5
7	10.44 (s, 1H)	-	-	2,6
8	3.14 (s, 3H)	40.53	-	-
9	-	190.82	-	-
10	4.85 (s, 2H)	34.14	-	9

2.1.3 Reduction of N-(4-(2-chloroacetyl)phenyl)methanesulfonamide (2) using sodium borohydride

Reduction of N-(4-(2-chloroacetyl)phenyl)methanesulfonamide (**2**) with sodium borohydride was performed in order to obtain racemic N-(4-(2-chloro-1-hydroxyethyl)phenyl)methanesulfonamide (**4**) and determine the retention times of its *R*- and *S*-enantiomers on chiral HPLC. The procedure was adapted from the one described by Kamal

et al. [44], by replacing diisopropyl ether with dimethyl sulfoxide and by removing alumina (acting as a support material), because those compounds were not available.

Sodium borohydride is usually used in a protic solvent, but the use of wet or dry aprotic solvents like dimethyl sulfoxide is also possible [73, 74], although it could slow down the reaction [75]. The reaction has been carried out in dimethyl sulfoxide as shown in Scheme 2.1.8, because reactant **2** is not soluble in all the protic solvents tested.

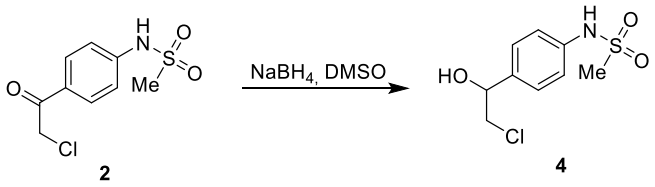

Scheme 2.1.8: Chemical reduction of N-(4-(2-chloroacetyl)phenyl)methanesulfonamide (**2**) to N-(4-(2-chloro-1-hydroxyethyl)phenyl)methanesulfonamide (**4**)

The reaction was followed by TLC (n-pentane:ethyl acetate 6:4), and full conversion was observed after 4 days. The speed of the reaction could potentially be increased if some water was added to the dimethyl sulfoxide. Since this reaction is not an actual part of the synthesis of enantiopure sotalol, and is only needed for analytical purposes, the procedure was not further optimized.

In an aprotic solvent, sodium borohydride and the ketone react to form a tetraalkoxyborate salt instead of a free alcohol [73], as shown in Scheme 2.1.9. To yield alcohol **4**, ice-cold water followed by a dilute HCl solution was added at the end of the reaction. The acidic solution was added slowly to the reaction mixture, because unreacted sodium borohydride is quite violently hydrolyzed by the acid and releases hydrogen gas.

Several extractions with ethyl acetate were then performed in order to recover the product from the aqueous phase. Since compound **4** is very soluble in dimethyl sulfoxide, it is very likely that some of it was lost in the aqueous phase.

Two compounds were observed on the TLC plate at the end of the reaction, none of them having the Rf of the starting material **2**. The obtained product was purified by column chromatography (n-pentane:ethyl acetate 6:4) to give compound **4** with a yield of 40% and a purity of 75% (^{1}H-NMR).

2.1.3.1 Reaction mechanism for the chemical reduction of compound 2

The reaction mechanism shown in Scheme 2.1.9 was based on the ketone reduction mechanism proposed by Kayser *et al*. [73]. Due to steric hindrance, it is likely that the reaction stops at the stage of di- or trialhoxyborates. For this reason, and to accelerate the reaction, sodium borohydride was introduced in excess.

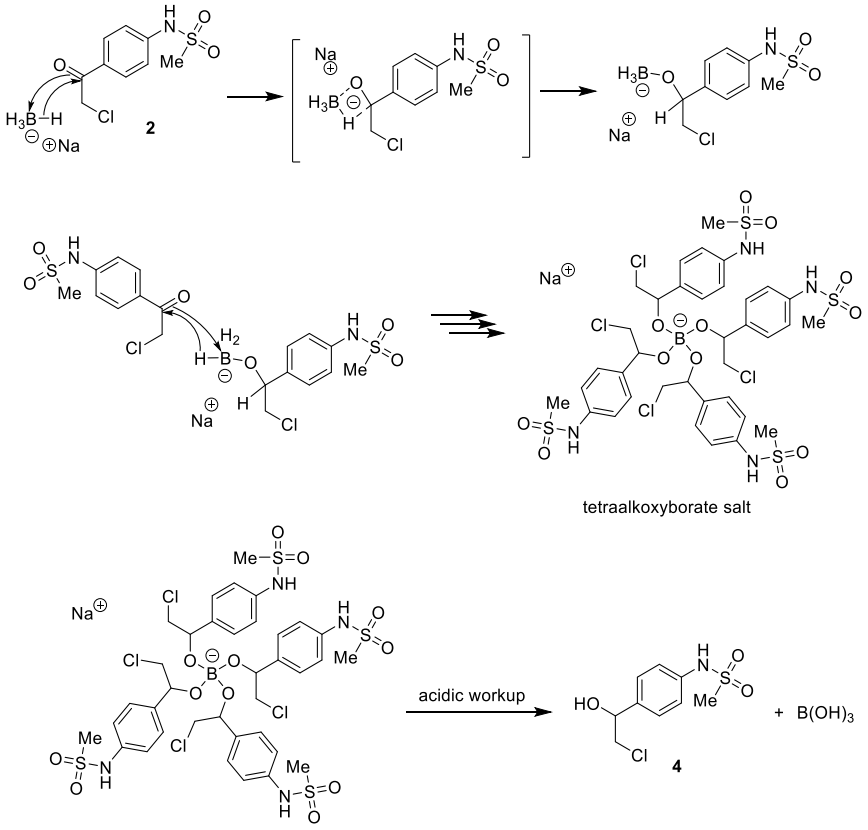

Scheme 2.1.9: Reaction mechanism for the chemical reduction of N-(4-(2-chloroacetyl)phenyl)methanesulfonamide (**2**) to N-(4-(2-chloro-1-hydroxyethyl)phenyl)methanesulfonamide (**4**)

2.1.3.2 Characterization of compound 4

Characterization of compound **4** was carried out by NMR spectroscopy, with deuterated dimethyl sulfoxide as solvent. N-(4-(2-Chloro-1-hydroxyethyl)phenyl)methanesulfonamide (**4**) with numbered carbon atoms is shown in Figure 2.1.4, and assignment of chemical shifts are given in Table 2.1.5.

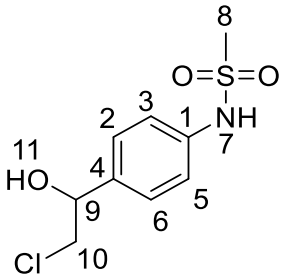

Figure 2.1.4: Compound **4** with numbered carbon and nitrogen atoms. Assignment of chemical shifts are given in Table 2.1.3, and all spectra are given in the appendix (Part 6.1.4).

Table 2.1.5: Characterization of compound **4** given ^{1}H-, ^{13}C-, H,H-COSY, HSQC- and HMBC-NMR (600 MHz, CDCl3), see the appendix (Part 6.1.4).

Numbered atom	**^{1}H-NMR [ppm] (mult., int., ^{3}J)**	**^{13}C-NMR [ppm]**	**COSY**	**HMBC**
1	-	137.74	-	-
2	7.41 – 7.31 (m, 2H)	127.30	3,5,6	1,3,4,5,6,9
3	7.22 – 7.13 (m, 2H)	119.49	2,5,6	1,2,4,5,6
4	-	137.57	-	-
5	7.22 – 7.13 (m, 2H)	119.49	2,3,6	1,2,3,4,6
6	7.41 – 7.31 (m, 2H)	127.30	2,3,5	1,2,3,4,5,9
7	9.72 (s, 1H)	-	-	-
8	2.97 (s, 3H)	40.04	-	-
9	4.73 (dt, *J* = 6.9, 4.6 Hz, 1H)	71.93	10,11	4,6,10,11
10	3.79 – 3.58 (m, 2H)	50.19	9	4,9
11	5.75 (d, *J* = 4.7 Hz, 1H)	-	9	4,9,10

2.1.3.3 Determination of the retention times of the (*R*)- and (*S*)-enantiomers of compound 4 on chiral HPLC

Separation of the enantiomers of compound **4** was obtained by using a Chiralcel OD-H column, a mobile phase composition of hexane (90%) and 2-propanol (10%) as the eluent, and a flow of 1 mL/min. As shown in Figure 2.1.5, the retention times obtained are t_R((*S*)-**4**) = 50.51 min and t_R((*R*)-**4**) = 63.51 min. As expected, two peaks having the same area are visible on the chromatogram. Attribution of each of the peaks to one particular enantiomer will be discussed in the next section.

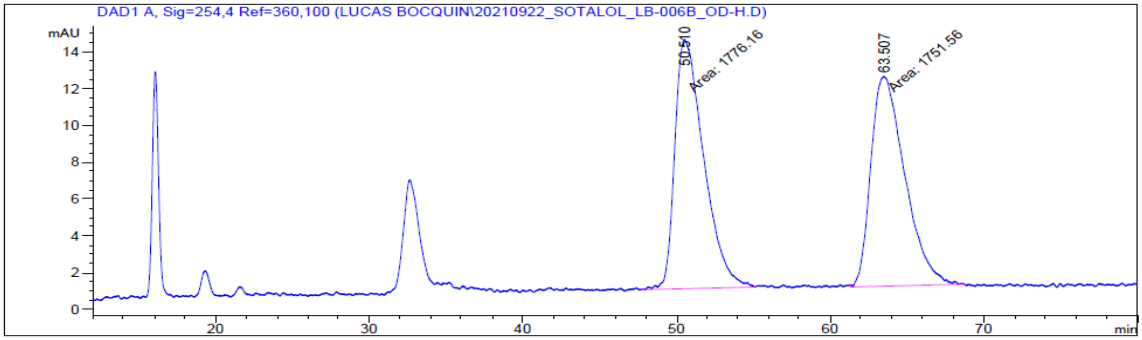

Figure 2.1.5: Chiral HPLC chromatogram of chlorohydrin **4**. The analysis was performed on a Chiralcel OD-H column with hexane and 2-propanol (90:10) as eluent and 1 mL/min flow. The retention times obtained are t_R((*S*)-**4**) = 50.51 min and t_R((*R*)-**4**) = 63.51 min. R_S ((R)/(S)-**4**) = 3.45.

Good separation could be achieved in less time using more 2-propanol in the isocratic eluent mixture. However, an impurity with a similar retention time as the two enantiomers was formed during the enzymatic reduction of compound **2**. The HPLC method was therefore adapted to avoid any overlap with this impurity. This will be discussed into more details in the next part.

2.1.4 Enzymatic reduction of N-(4-(2-chloroacetyl)phenyl)methanesulfonamide (2) and N-(4-(2-bromoacetyl)phenyl)methanesulfonamide (3)

Enzymatic reduction of **2** using KRED 228 was carried out by adapting the procedure described by Blindheim *et al*. [76]. The reaction is shown in Scheme 2.1.10.

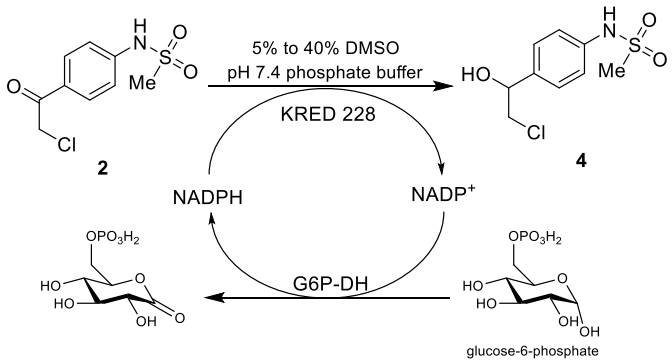

Scheme 2.1.10: Enzymatic reduction of N-(4-(2-chloroacetyl)phenyl)methanesulfonamide (**2**) to N-(4-(2-chloro-1-hydroxyethyl)phenyl)methanesulfonamide (**4**)

The KRED 228-catalyzed reduction of **2** was first tried in an aqueous environment containing 5% dimethyl sulfoxide. Substrate **2** was dissolved into the dimethyl sulfoxide, and was then added to a phosphate buffer containing all the enzymes and cosubstrates. Some of the starting material **2** precipitates when added to the aqueous mixture. It was first thought it could be a problem limiting the conversion of the reaction, but it was not the case. It turned out to be very

practical, because the reaction mixture turned less and less cloudy when conversion increased. This is because compound **4** is more soluble in dimethyl sulfoxide and water than substrate **2**. At the end of the reaction, the mixture was not cloudy anymore. Therefore, it could be known only by the appearance of the solution if the reaction was approximately complete or not. Compound (*R*)-**4** was obtained as a white solid with a yield of 94% and a purity of 99% (^{1}H-NMR). Measurement of the enantiomeric excess will be described in the next part.

2.1.4.1 Measurement of the enantiomeric excess of the product 4 obtained

The obtained chlorohydrin **4** was analyzed by chiral HPLC using a mobile phase composition of hexane (90%) and 2-propanol (10%), and the resulting chromatogram is shown in Figure 2.1.6. An enantiomeric excess of 76% was calculated from the area under the peaks corresponding to the two enantiomers.

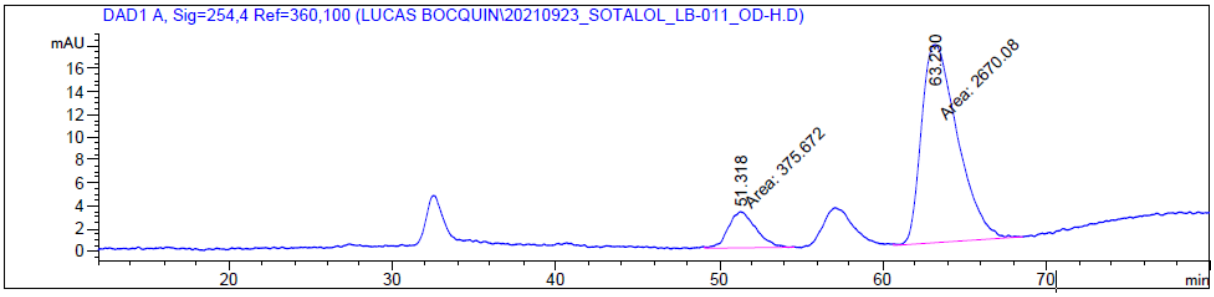

Figure 2.1.6: Chiral HPLC of chlorohydrin **4**. The analysis was performed on a Chiralcel OD-H column with hexane and 2-propanol (90:10) as eluent and 1 mL/min flow, and with a detection wavelength of 254.4 nm. The retention times obtained are t_R((*S*)-**4**) = 50.32 min and t_R((*R*)-**4**) = 63.23 min.

A peak is visible in the middle of the two enantiomer peaks. This comes from an unidentified impurity that could be, for instance, a part of the enzyme that got deactivated. This impurity has unfortunately the same retention time on TLC than the desired product **4**, and it has not been possible to remove it from the reaction mixture. The chiral HPLC method was therefore adapted so that the impurity peak does not overlap with the peaks of the enantiomers. Another impurity is eluting at around 33 min. It was also observable in the reaction mixture of the chemical reduction, and it is believed to come from either trace amounts of the starting material, or an impurity already present in the starting material. It is surprising to see that this impurity was still there after the column chromatography performed on the racemic product **4**. Those two impurities were, however, not visible on the NMR spectra.

Another impurity could exactly overlap with one of the enantiomer peaks and therefore not be visible on the chromatogram. The measured enantiomeric excess would then be distorted. For

this reason, the DAD wavelength was changed to see if the measured enantiomeric excess would stay the same. Different compounds can indeed have different wavelengths for their maximum of absorption. The chromatogram obtained for a detection wavelength of 280.8 nm is shown in Figure 2.1.7. The area under the impurity peak eluting at 57 min is a lot bigger, while the enantiomeric excess of the desired product remains constant. It is therefore likely that no impurity is overlapping with one of the enantiomers peaks.

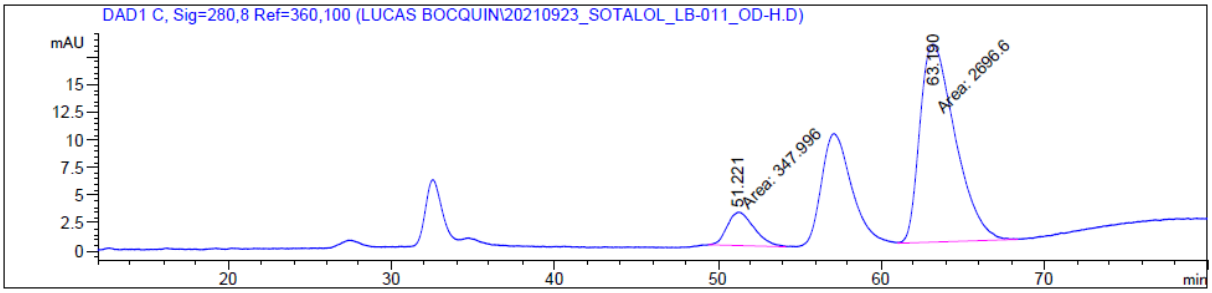

Figure 2.1.7: Chiral HPLC of chlorohydrin **4**. The analysis was performed on a Chiralcel OD-H column with hexane and 2-propanol (90:10) as eluent and 1 mL/min flow, and with a detection wavelength of 280.8 nm. The retention times obtained are t_R((*S*)-**4**) = 51.22 min and t_R((*R*)-**4**) = 63.19 min.

2.1.4.2 Measurement of the specific rotation of the product

Specific rotation of (R)-N-(4-(2-chloro-1-hydroxyethyl)phenyl)methanesulfonamide (**(R)-4**) has been previously measured by Kamal *et al.* [44] for an enantiomeric excess of 90%. They obtained a specific rotation of $[\alpha]_D^{25} - 19.09$ (c 1.03, EtOH). Specific rotation of the enzymatic product **4** obtained in this thesis was measured in the same conditions, and a value of $[\alpha]_D^{25} - 17.50$ (c 1.03, EtOH) was obtained. This means that KRED 228 forms preferentially the (*R*)-**4**, which is a direct precursor of (*R*)-sotalol.

2.1.4.3 Attempts made to improve the enantiomeric excess of the chlorohydrin 4 obtained after enzymatic reduction

As discussed in the introduction, drugs marketed as enantiopure need to have an enantiomeric excess of at least 96%. The enantiomeric excess of 76% obtained previously is therefore not good enough.

Several parameters can be changed in order to improve the enantiomeric excess while keeping the same enzyme and substrate. Although changing the pH could have a small effect, it was decided to focus rather on the temperature and the amount of cosolvent. Since the only tested solvent capable of dissolving compound **2** at room temperature is dimethyl sulfoxide, changing the nature of the cosolvent was not attempted. As discussed in the introduction, changing the

amount of cosolvent can change the rigidity of the enzyme, potentially increasing the enantiomeric excess of the product.

Other attempts with different amount of dimethyl sulfoxide at 38 °C and at 25 °C were therefore carried out. The results at 38 °C are presented in Table 2.1.6. When the amount of DMSO was higher than 25%, the starting material **2** was still present in significant amounts in the reaction mixture after 24 hours, and the exact enantiomeric excesses of compound **4** obtained were only approximately calculated, because the peak of compound **2** partly overlapped with the peak of one of the enantiomers of compound **4** on the chromatograms.

Table 2.1.6: Effect of the amount of dimethyl sulfoxide on conversion and enantiomeric excess of the product **4** (at 38°C with KRED 228). Conversions were calculated via ^{1}H NMR analysis of the crude products. Enantiomeric excesses were calculated via chiral HPLC analysis.

Volume of DMSO (mL)	**Volume of buffer (mL)**	**Conversion after 24h (%)**	**Enantiomeric excess of the product (%)**
0.25	**5**	**>99**	**70**
0.5	**5**	**>99**	**76**
1	**5**	**98**	**56**
1.5	**5**	**98**	**28**
2	**5**	**83**	**< 40**
3	**5**	**26**	**< 70**

To obtain higher enantiomeric excesses, another option is to try different ketoreductases. Zhu *et al*. [46] claim to obtain respectively (*R*)-**4** and (*S*)-**4** with enantiomeric excesses of more than 99% using ketoreductases named KRED130 and KRED113. Reduction using those enzymes was therefore tried in order to confirm the results obtained in this article. A reaction using KRED 238, another ketoreductase available in the laboratory, was also performed. Reaction conditions were slightly different from the ones used by Zhu *et al*. [46] for KRED 130 and KRED 113. The differences are described in Table 2.1.7.

Table 2.1.7: Reaction conditions for the enzymatic reduction of **2** using KRED130 and KRED113

Reaction conditions	**Zhu *et al*. article [46]**	**This work**
Temperature	25°C	38°C
NADPH recycling system	G6-DH / G6	G6P-DH / G6P
pH of phosphate buffer	7.0	7.4
Reaction time	Overnight	24h
Amount of cosolvent	5%	5%

Unfortunately, this led to no conversion (^{1}H-NMR) for KRED 130, 113, and 238, while in the same conditions, conversion of 100% was achieved with KRED 228. This is surprising, because Zhu *et al*. [46] obtained a conversion of 89% with KRED 130, and 96% with KRED 113. This difference could be due to the difference in the reaction conditions. It is not likely that the NADPH recycling system is responsible, because it does not intervene directly in the reaction between the enzyme and the substrate. A pH difference of 0.4 is not likely to have such an effect on the conversion. The temperature, which is 13 degrees higher than in the procedure used by Zhu *et al.*, could, however, lead to the deactivation of the enzyme. This would be surprising, because 38 °C is a quite standard temperature for enzymatic reactions.

The reaction was therefore performed once more at 25 °C, using KRED 130 and KRED 228. The mixtures were stirred overnight. While KRED 228 gave a complete conversion (^{1}H NMR) and an enantiomeric excess of 81% (chiral HPLC), KRED 130 gave no conversion at all. It is believed that the KRED 130 that was used for those experiments was deactivated, because the results obtained as a part of this thesis were not corresponding to the ones reported by Zhu *et al*. [46].

Because an enantiomeric excess of 96% was not achieved after the enzymatic reduction, it was decided not to perform the synthesis of sotalol from alcohol **4**.

2.1.4.1 Enzymatic reduction of N-(4-(2-bromoacetyl)phenyl)methanesulfonamide (3)

The enzymatic reduction of compound **3** was attempted by using the same conditions as the ones giving the best conversion and enantiomeric excess for the reduction of compound **2**. The conditions of the reaction are described in Scheme 2.1.11.

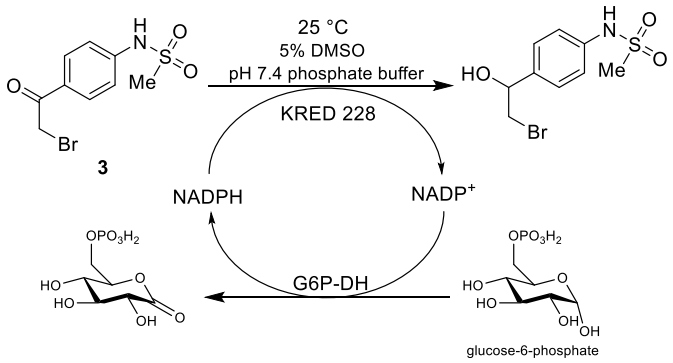

Scheme 2.1.11: Enzymatic reduction of N-(4-(2-bromoacetyl)phenyl)methanesulfonamide (**3**) to N-(4-(2-bromo-1-hydroxyethyl)phenyl)methanesulfonamide

Unfortunately, after 48 hours of reaction in the incubator at 25 °C, most of the starting material had not reacted. This could be directly seen because the starting material was in suspension in the medium. A ^{1}H-NMR analysis revealed that the solid obtained was composed of the starting material (36%), a non-desired byproduct (22%), the impurity already present in the starting material (see **Part 2.1.2.2**) (4%), and numerous other small byproducts (28%). Due to the low conversion obtained when using compound **3** as a substrate for KRED 228, this synthesis pathway was not further investigated. It is believed that the brominated substrate fits less the active site of KRED 228 than its chlorinated homolog. This could be due to the bigger size of the bromine atom.

2.1.5 Synthesis of N-(4-(isopropylglycyl)phenyl)methanesulfonamide from N-(4-(2-chloroacetyl)phenyl)methanesulfonamide (5)

In order to improve the enantiomeric excess of the product, another possibility is to try other substrates to enzymatically reduce, such as compound **5**. The procedure used in this thesis was based on the procedure used for a similar reaction by Anna Lifen Tennfjord [77].

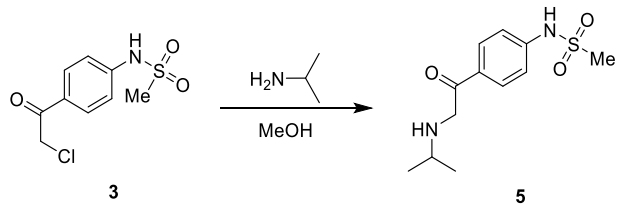

Scheme 2.1.12: Synthesis of N-(4-(isopropylglycyl)phenyl)methanesulfonamide from N-(4-(2-chloroacetyl)phenyl)methanesulfonamide

The reaction was first performed under reflux for one day, but the solution turned orange, and after workup the product was very impure. The ^{1}H-NMR analysis did not show the presence of the desired product.

The reaction was then performed at room temperature for 18 hours, and by using potassium carbonate as a base, following the procedure described by Kamal *et al.* [44] for the amine alkylation of chlorohydrin **4**. Since the starting material is very similar, it was believed the desired product could be obtained with a good yield. However, the main product obtained was not compound **5**. After ^{1}H-, ^{13}C-, COSY-, HSQC- and HMBC-NMR analysis of the product, it was hypothesized that the main product formed was byproduct **M** (38% of the mixture (^{1}H-NMR)), shown in Figure 2.1.8.

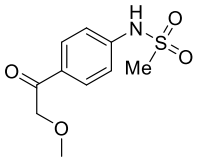

Figure 2.1.8: Structure of byproduct **M**.

The other compounds present in the mixture include the starting material **3** (10%) and numerous unknown impurities containing aromatic protons. The isopropyl group of compound **5** should give a doublet integrating for six protons before two ppm. A small doublet is visible at 1.05 ppm, but it is quite small. If compound **5** has been formed, it composes less than 3% of the mixture.

This is quite surprising that this amine alkylation reaction works well on chlorohydrin **4**, as reported by Kamal *et al.*, but not on its ketone derivative **5**. The ketone is therefore probably involved in the mechanism of this reaction. A mechanism that could explain the formation of byproduct **M** is suggested in Scheme 2.1.13.

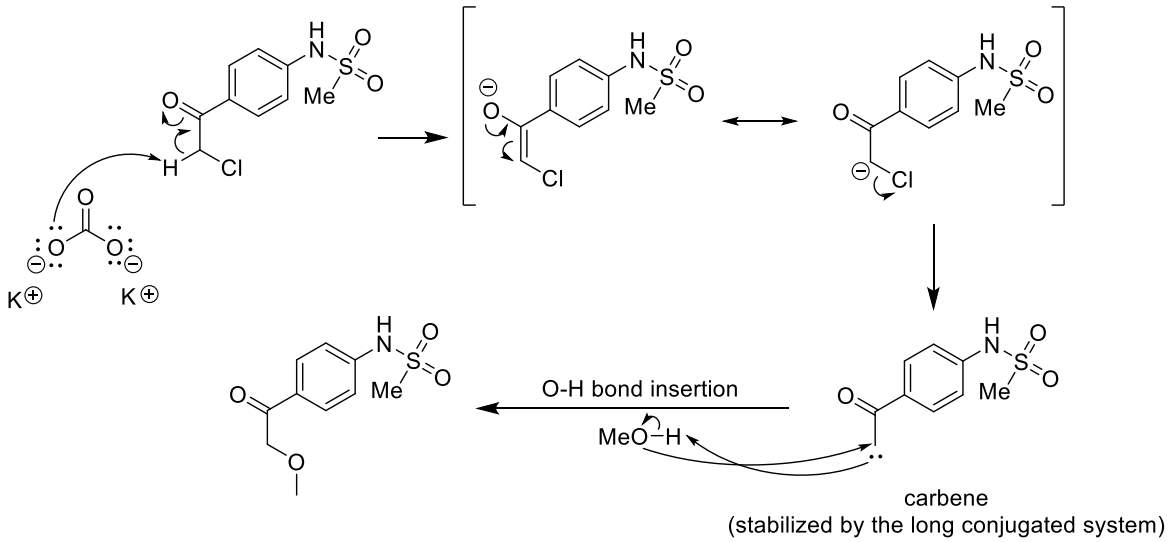

Scheme 2.1.13: Suggested mechanism for the formation of byproduct **M**.

The alpha hydrogen of the ketone is quite acidic, due to the presence of the chlorine as well as the ketone. This makes the enol formation easier. The fact that numerous impurities are present in the reaction mixture could indicate that a very reactive transition molecule is formed, such as a carbene. It has been reported by Montero *et al.* [78] that carbene can be formed when α-aromatic α'-haloketones are in a basic environment. Methanol is sometimes used to trap carbenes to form methyl ethers, as reported by Kapur *et al.* [79]. In the mechanism shown in Scheme 2.1.13, the carbene reacts in a concerted mechanism with methanol. This is because the carbene formed is most probably in its singlet state, as it has been shown that whereas those carbenes prefer O-H bond insertions over C-H bond insertions when they react with methanol, triplet state carbenes prefer C-H bond insertions [80].

A simpler mechanism that could explain the formation of byproduct **M** is the addition of methanol or methanolate on the carbon bearing the chlorine, in an S_N2 mechanism. However, methanol is not a very good nucleophile, and methanolate would require the presence of a strong base to be formed. Moreover, it would not explain why this addition does not happen significatively when the reaction is performed on the chlorohydrin under the same conditions.

Byproduct **M** was not isolated properly because it was decided to focus on the synthesis of penbutolol, but characterization by NMR was still carried out. Byproduct **M** with numbered carbon atoms is shown in Figure 2.1.9, and assignment of chemical shifts are given in Table 2.1.8. The presence of byproduct **M** in the mixture was also confirmed by mass spectrometry analysis, as shown in Figure 6.1.26 in the appendix.

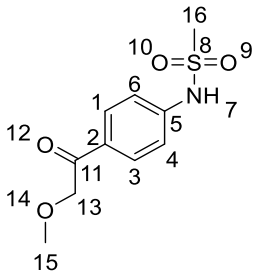

Figure 2.1.9: Compound **M** with numbered carbon and nitrogen atoms. Assignment of chemical shifts are given in Table 2.1.8, and all spectra are given in the appendix (Part 6.1.5).

Table 2.1.8: Characterization of compound **M** given ^{1}H-, ^{13}C-, H,H-COSY, HSQC- and HMBC-NMR (600 MHz, CDCl3), see the appendix (Part 6.1.4).

Numbered atom	**^{1}H-NMR [ppm] (mult., int., ^{3}J)**	**^{13}C-NMR [ppm]**	**COSY**	**HMBC**
1	7.92 – 7.87 (m, 2H)	129.94	3,4,6	2,3,4,5,6,11
2	-	130.70	-	-
3	7.92 – 7.87 (m, 2H)	129.94	1,4,6	1,2,4,5,6,11
4	7.30 – 7.28 (m, 2H)	118.00	1,3,6	1,3,5,6
5	-	143.71	-	-
6	7.30 – 7.28 (m, 2H)	118.00	1,3,4	1,3,5,6
7	-	-	-	-
11	-	195.61	-	-
13	4.71 (s, 2H)	74.86	-	15,11
15	3.35 (s, 3H)	58.95	-	13
16	3.11 (s, 3H)	40.38	-	-

2.2 Synthesis of enantiopure (*S*)-penbutolol ((*S*)-10)

The aim of this part was to synthesize enantiopure (*S*)-penbutolol ((*S*)-**10**) in an environmentally friendly and efficient way.

2.2.1 Synthesis of 1-chloro-3-(2-cyclopentylphenoxy)propan-2-ol

1-Chloro-3-(2-cyclopentylphenoxy)propan-2-ol (**8**) was synthesized from 2-cyclopentylphenol and epichlorohydrin adapting the procedure described by previous master candidate Kristoffer Klungseth [53]. In order to optimize the yield, epoxide **7** and chlorohydrin **8** were not separated by flash chromatography, and lithium chloride and acetic acid were added directly to the mixture of compounds **7** and **8**, as shown in Scheme 2.2.1.

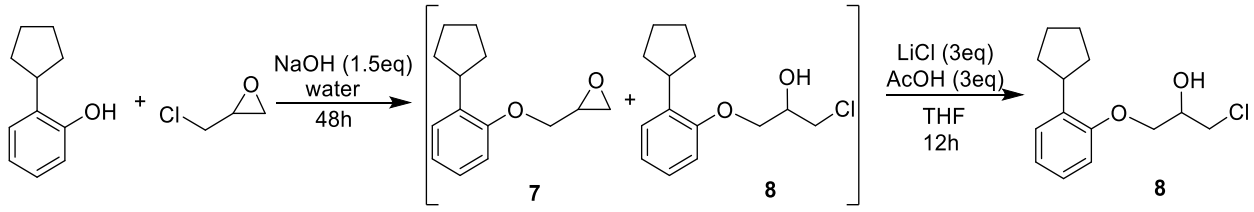

Scheme 2.2.1: Synthesis of 1-chloro-3-(2-cyclopentylphenoxy)propan-2-ol (**8**) from 2-cyclopentylphenol and epichlorohydrin.

In order to deprotonate the 2-cyclopentylphenol before the addition of epichlorohydrin, and to minimize the formation of byproducts, 2-cyclopentylphenol was added to the sodium hydroxide aqueous solution and mixed for around five minutes before epichlorohydrin was added. Epichlorohydrin has been shown to react with sodium hydroxide to form products such as 3-chloropropane-1,2-diol, oxiran-2-ylmethanol and propane-1,2,3-triol [52]. These potential byproducts are shown in Figure 2.2.1. The order of addition of the reactants could help to limit their formation.

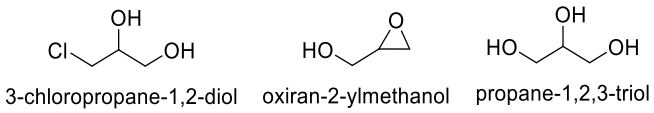

Figure 2.2.1: Potential byproducts formed from the reaction of epichlorohydrin with hydroxide.

When epichlorohydrin was added, the solution turns pale green/yellow, and the color does not change significantly after that. In comparison, Kristoffer Klungseth obtained a dark green mixture immediately after adding all the reagents, and observed a pale-yellow mixture the day after. This difference in color could be linked to the change in the order of addition of the reactants, and to the formation of colored byproducts (chlorohydrin **8** being colorless).

Ethyl acetate was added and the reaction mixture was washed with distilled water to remove the excesses of epichlorohydrin and sodium hydroxide. ^{1}H-NMR analysis of the mixture revealed the presence of around 13% of 2-cyclopentylphenol, 36% of the epoxide **7** and 39% of chlorohydrin **8**. Other impurities, that are believed to be mostly composed of dimer **D** shown in Scheme 2.2.2, make up the rest of the mixture (around 12%).

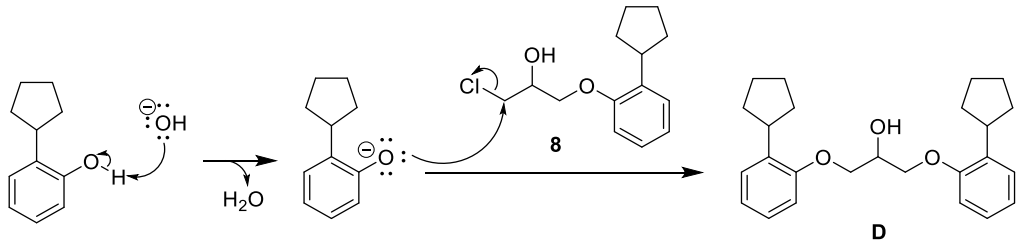

Scheme 2.2.2: Mechanism of formation of byproduct D

Dimer **D** was not isolated. This type of dimer, formed from the addition of the deprotonated starting material (here 2-cyclopentylphenolate) on the chlorohydrin product (here compound **8**) has been shown by Gundersen *et al.* [52] to be the most abundant byproduct for similar reactions.

Epoxide **7** was then opened with lithium chloride. Workup and flash chromatography purification led to compound **8** as a transparent oil with a purity of 99% (^{1}H-NMR). Those two steps gave a combined yield of 70%.

2.2.1.1 Unsuccessful attempts made to improve the yield of synthesis of chlorohydrin 8

As shown previously, after 48 hours of reaction between one equivalent of 2-cyclopentylphenol and two equivalents of epichlorohydrin in an aqueous sodium hydroxide solution (1.5 equivalents of NaOH), full conversion of 2-cyclopentylphenol into products **7** and **8** was not achieved. Increasing the time of the reaction has been tried before [53], but did not result in a significative change in the conversion.

Increasing the amounts of base from 0.5 equivalents to 1.5 equivalents has been tried before [53] and leads to an increased conversion of the starting material. For this type of compound, using more than 1.5 equivalents of sodium hydroxide could lead to the formation of more dimer **D**, as it happens for similar reactions [77]. However, the presence of the bulky cyclopentyl group in 2-cyclopentylphenol could limit its formation.

In order to improve the conversion of the starting material, different equivalents of the base and of epichlorohydrin were tested, as described in Table 2.2.1. Increasing the amount of base to

more than 1.5 equivalents while keeping 2 equivalents of chlorohydrin was attempted, but no significant differences were noticed in the conversion after 48h. Using more base leads to the formation of more epoxide and more byproducts. With three equivalents of base and six equivalents of epichlorohydrin, a better conversion and fewer byproducts were obtained than with three equivalents of base and two equivalents of epichlorohydrin. Increasing the amount of epichlorohydrin under those conditions has therefore a positive effect on the conversion of 2-cyclopentylphenol into epoxide **7** and chlorohydrin **8**. However, with 1.5 equivalents of base, increasing the amount of epichlorohydrin did not improve conversion. It did not reduce the formation of byproducts significantly either.

Table 2.2.1: Summary of the results obtained by ^{1}H-NMR analysis for epichlorohydrin addition on 2-cyclopentylphenol using sodium hydroxide (see Scheme 2.2.1) under different reaction conditions.

Time (h)	NaOH (eq)	Epichlorohydrin (eq)	2-cyclopentylphenol (%)	epoxide 7 (%)	chlorohydrin 8 (%)	byproducts (%)
48	1.5	2	13	36	39	12
48	3	2	10	52	<10	>28
48	4.5	2	12	50	<10	>28
72	3	6	6	27	44	23
48	1.5	6	21	11	57	11

In another reaction batch, potassium carbonate was used as a base and acetonitrile as a solvent for the epichlorohydrin addition on 2-cyclopentylphenol, adapting the procedure for a similar reaction described by previous master student Anna Tennfjord [77]. The reaction was performed on 80 mg of 2-cyclopentylphenol, and gave 90 mg of a mixture that, after ^{1}H-NMR analysis, revealed to be composed of 2% of the starting material, 78 % of the epoxide **7**, 7% of the chlorohydrin **8**, and around 13% of unknown impurities containing aromatic protons. Calculation based on the mass of the mixture and its approximate composition showed that the final yield would not be significantly superior to 70%. Opening epoxide **7** into product **8** was therefore not performed.

2.2.1.2 Epoxide opening alternative procedure using hydrochloric acid

In order to obtain a greener procedure for the synthesis of chlorohydrin **8** from epoxide **7** than the one using lithium chloride and tetrahydrofuran, opening of epoxide **7** with an aqueous hydrochloric acid solution (1M) was attempted. As explained in the introduction, this could lead to the formation of byproduct **A** shown in Figure 2.2.2 [69].

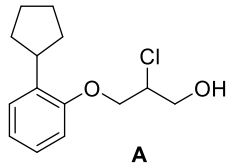

A

Figure 2.2.2: Structure of potential byproduct A.

However, since the epoxide's substituents do not particularly stabilize the formation of a carbocation, this byproduct will most likely not be the dominant product.

Only small-scale test reactions were performed for the opening of epoxide **7** with hydrochloric acid, hence yields were not calculated. The potential byproduct **A** was not present in sufficient quantities in the mixtures to be identified in the ^{1}H-NMR spectra. The reaction using a hydrochloric acid aqueous solution (1M) gave only 50% conversion after around 10 hours of reaction.

Using a concentrated hydrochloric acid aqueous solution (37%) gave total conversion of epoxide **7** to chlorohydrin **8** after 10 hours of reaction (^{1}H-NMR). However, the conditions of the reaction are then a lot harsher than when lithium chloride and acetic acid are used. The lithium chloride procedure was therefore preferred for the epoxide opening step.

2.2.1.3 Reaction mechanisms for the synthesis of chlorohydrin 8 from 2-cyclopentylphenol

The mechanism for the addition of epichlorohydrin on aromatic alcohols have been studied by Gundersen *et al.* [52], and the reaction mechanism for the formation of chlorohydrin **8** and epoxide **7** from 2-cyclopentylphenol and epichlorohydrin in a sodium hydroxide solution is shown in Scheme 2.2.3. While step ***c*** is an equilibrium reaction that depends on the amount of base used, step ***d*** is irreversible. The formation of epoxide **7** from chlorohydrin **8** is therefore plausible and explains why an increasing the amount of base from 1.5 equivalents to 3 equivalents leads to an increased amount of epoxide **7** formed over chlorohydrin **8**.

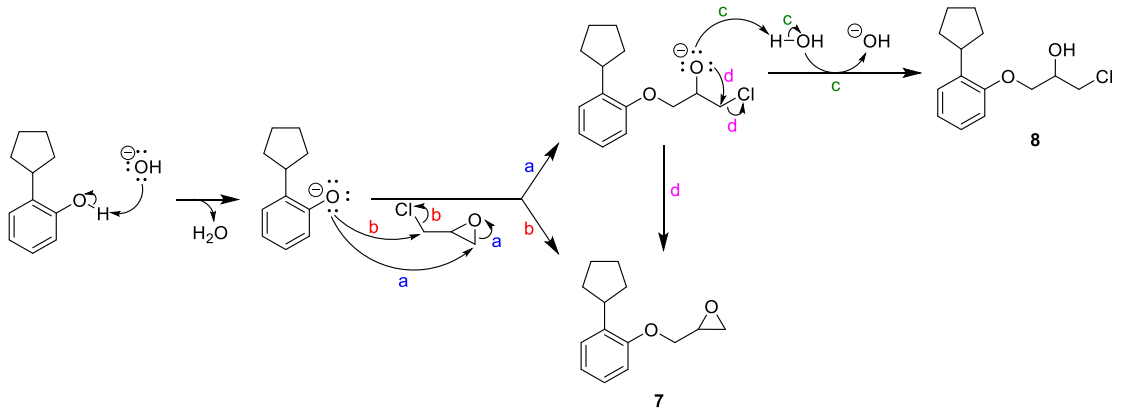

Scheme 2.2.3: Reaction mechanism for the addition of epichlorohydrin on 2-cyclopentylphenol to form epoxide **7** and chlorohydrin **8**.

The proposed mechanism for the opening of epoxide **7** with lithium chloride is shown in Scheme 2.2.4. The addition of chlorine on the least hindered carbon shows that the mechanism does not include a carbocation intermediate.

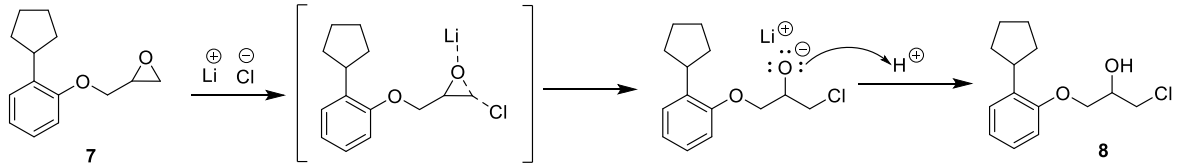

Scheme 2.2.4: Proposed mechanism for the epoxide **7** opening using lithium chloride.

The proposed mechanism for the opening of epoxide **7** using hydrochloric acid is shown in Scheme 2.2.5.

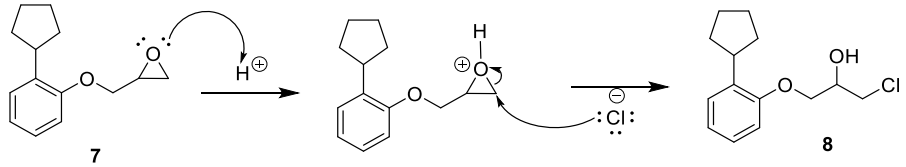

Scheme 2.2.5: Proposed mechanism for the opening of epoxide **7** using hydrochloric acid, based on the general mechanism described by Solomons [68].

2.2.1.4 Characterization of chlorohydrin 8

Characterization of the chlorohydrin **8** was carried out by NMR spectroscopy, with deuterated chloroform as solvent. Chlorohydrin **8** with numbered carbon atoms is shown in Figure 2.1.1, and assignment of chemical shifts are given in Table 2.1.2.

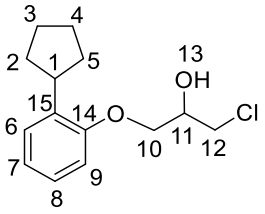

Figure 2.2.3: Chlorohydrin **8** with numbered carbon and nitrogen atoms. Assignment of chemical shifts are given in Table 2.1.2, and all spectra are given in the appendix (Part 6.2.1).

Table 2.2.2: Characterization of chlorohydrin **8** given ^{1}H-, ^{13}C-, H,H-COSY, HSQC- and HMBC-NMR (600 MHz, CDCl3), see the appendix (Part 6.2.1).

Numbered atom	^{1}H-NMR [ppm] (mult., int., ^{3}J)	^{13}C-NMR [ppm]	COSY	HMBC
1	3.37 – 3.24 (m, 1H)	39.19	2,3,4,5	2,3,4,5,6,14,15
2	2.04 – 1.56 (m, 8H)	33.12	1	1,3,4,5,15
3	2.04 – 1.56 (m, 8H)	25.62	1	1,2,4,5
4	2.04 – 1.56 (m, 8H)	25.62	1	1,2,3,5
5	2.04 – 1.56 (m, 8H)	33.12	1	1,2,3,4,15
6	7.24 (dd, *J* = 7.6, 1.7 Hz, 1H)	127.05	8	1,8,9,14
7	7.16 (td, *J* = 7.8, 1.7 Hz, 1H)	121.52	9	6,8,9,14,15
8	6.96 (td, *J* = 7.5, 1.2 Hz, 1H)	126.84	6	6,9,14,15
9	6.85 (dd, *J* = 8.1, 1.2 Hz, 1H)	111.67	7	1,6,7,8,14,15
10	4.10 (qd, *J* = 9.5, 5.2 Hz, 2H)	68.79	11	11,12,14
11	4.25 (h, *J* = 5.4 Hz, 1H)	70.20	10,12,13	10,12
12	3.78 (ddd, *J* = 13.8, 11.2, 5.0 Hz, 2H)	46.35	11	9,10,12’
13	2.48 (d, *J* = 6.1 Hz, 1H)	-	11	10,11,12
14	-	156.01	-	-
15	-	134.89	-	-

2.2.2 Derivatization of 1-chloro-3-(2-cyclopentylphenoxy)propan-2-ol (8)

A derivatization of racemic 1-chloro-3-(2-cyclopentylphenoxy)propan-2-ol (**8**) was performed in order to form racemic ester **9** and determine the retention times of its *R*- and *S*- enantiomers on chiral HPLC. Pyridine and butyric anhydride were added to a solution of compound **8** in hexane, and the mixture was heated for one hour at 60 °C, as shown in Scheme 2.2.6. The reaction mixture was washed several times with distilled water and dried over magnesium

sulfate in order to remove pyridine, butyric anhydride and its derivatives, and water, that could damage the chiral column.

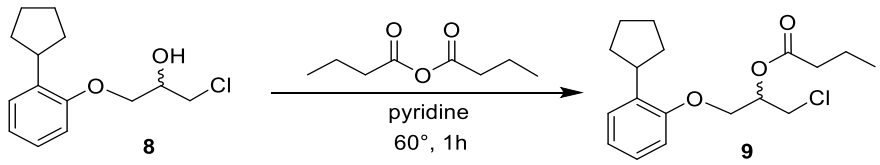

Scheme 2.2.6: Derivatization of 1-chloro-3-(2-cyclopentylphenoxy)propan-2-ol (**8**) to form racemic 1-chloro-3-(2-cyclopentylphenoxy)propan-2-yl butyrate (**9**).

Separation of the enantiomers of chlorohydrin **8** was obtained by using a Chiralcel OD-H column, a mobile phase composition of hexane (90%) and 2-propanol (10%) as eluent and a 1 mL/min flow. As shown in Figure 2.2.4, the retention times obtained are t_R((*S*)-**8**) = 6.63 min and t_R((*R*)-**8**) = 7.31 min. As expected, their peaks have the same area under the curve.

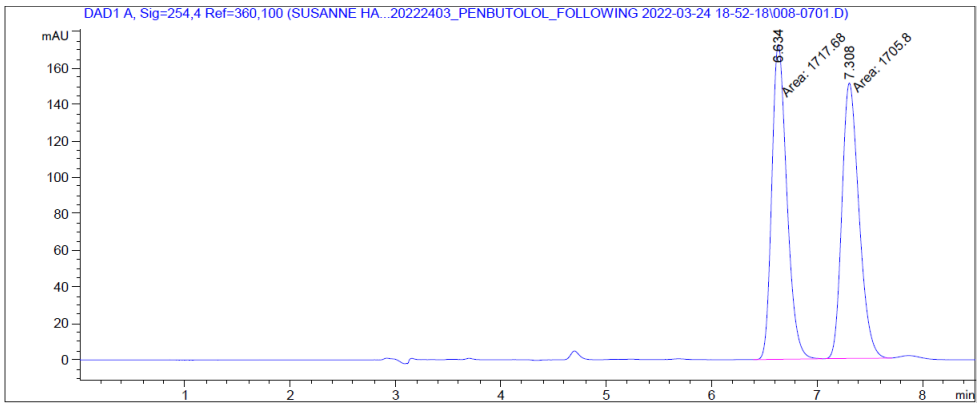

Figure 2.2.4: Chiral HPLC chromatogram of chlorohydrin **8**. The analysis was performed on a Chiralcel OD-H column with hexane and 2-propanol (90:10) as eluent and 1 mL/min flow, and with a detection wavelength of 280.8 nm. The retention times obtained are t_R((*S*)-**8**) = 6.63 min and t_R((*R*)-**8**) = 7.31 min. R_S((*S*)/(*R*)-**8**) = 2.41.

Separation of the enantiomers of ester **9** was obtained by using a Chiralcel OD-H column and a mobile phase composition of hexane (99.4%) and 2-propanol (0.6%). As shown in Figure 2.2.5, the retention times obtained are t_R((*S*)-**9**) = 8.05 min and t_R((*R*)-**9**) = 9.37 min. An unknown impurity eluted at 6.01 min. It is believed to be either butyric anhydride, introduced in excess, or butyric acid, a byproduct of the derivatization reaction. Other small impurity peaks are visible before that, but were not identified. The mobile phase was then changed to a composition of 90% of hexane and 10% of 2-propanol for 8 min, in order to elute the enantiomers of chlorohydrin **8** and traces of pyridine.

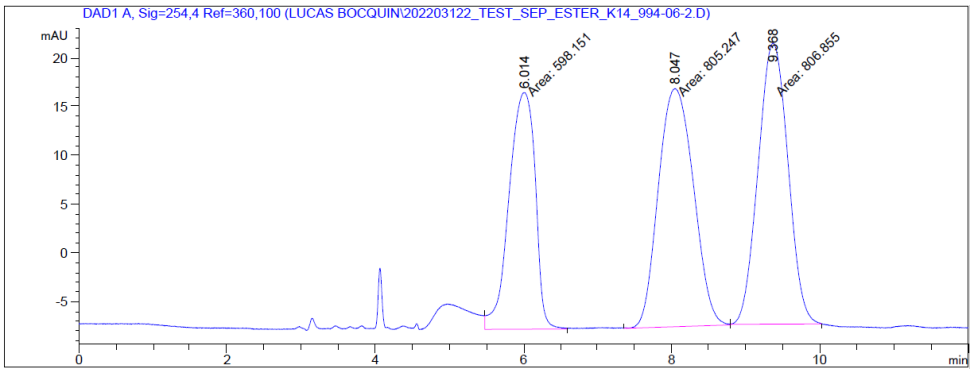

Figure 2.2.5: Chiral HPLC chromatogram of ester **9**. The analysis was performed on a Chiralcel OD-H column with hexane and 2-propanol (99.4:0.6) as eluent and 1 mL/min flow, and with a detection wavelength of 280.8 nm. The retention times obtained are t_R((*S*)-**9**) = 8.05 min and t_R((*R*)-**9**) = 9.37 min. R_S((*S*)/(*R*)-**9**) = 1.56.

2.2.3 Kinetic resolution of 1-chloro-3-(2-cyclopentylphenoxy)propan-2-ol (8) with CALB as catalyst

Kinetic resolution of 1-chloro-3-(2-cyclopentylphenoxy)propan-2-ol (**8**) was performed using CALB as the catalyst and vinyl butyrate as the acyl donor, as shown in Scheme 2.2.7. The procedure was based on the one described by Gundersen *et al.* [52] on a similar reaction.

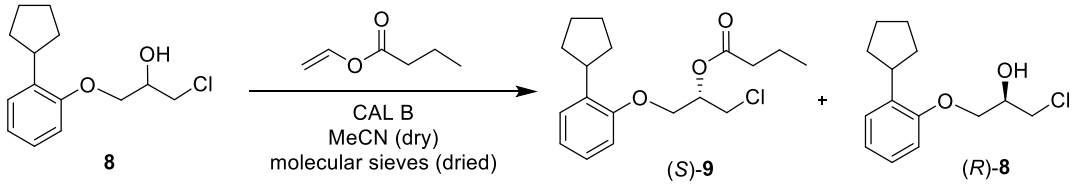

Scheme 2.2.7: Kinetic resolution of 1-chloro-3-(2-cyclopentylphenoxy)propan-2-ol with CALB as the catalyst and vinyl butanoate as the acyl donor in acetonitrile.

As explained in the introduction, plausible side reactions include hydrolysis of ester (*S*)-**9** and vinyl butyrate catalyzed by CALB. They would respectively lead to a loss in the enantiomeric excess of the chlorohydrin (*R*)-**8** obtained, and to the formation of butyric acid. To try to avoid those side reactions, activated molecular sieves were added, and the reaction was carried out in dry acetonitrile. The reaction mixture was shaken in an incubator at 38°C and 200 rpm.

2.2.3.1 Monitoring of the kinetic resolution of chlorohydrin 8

The CALB catalyzed kinetic resolution of 1-chloro-3-(2-cyclopentylphenoxy)propan-2-ol (**8**) was followed over 23 hours in order to calculate the enantiomeric ratio E of the reaction, and to know how much time is needed to get a good enantiomeric excess of the substrate **8**. Samples of the reaction mixture were collected at different time intervals and analyzed by chiral chromatography.

Chiral HPLC analyses of the samples using a mobile phase composition of hexane (90%) and 2-propanol (10%) were performed to measure the enantiomeric excess of the chlorohydrin **8** present in the reaction mixture. Chromatograms showing the enantiomeric excess of chlorohydrin **8** after 1 hour, 9 hours and 23 hours of reaction are shown in Figure 2.2.6, Figure 2.2.7 and Figure 2.2.8. The compounds eluting at 4.2 min are the enantiomers of the ester **9**. After 23 hours, chlorohydrin (*R*)-**8** is obtained with an enantiomeric excess of more than 99%.

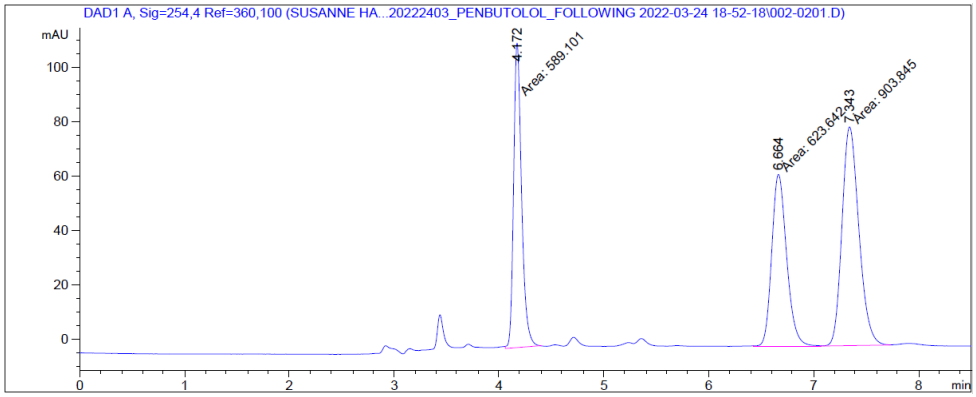

Figure 2.2.6: Chiral HPLC chromatogram of the CALB-catalyzed kinetic resolution of chlorohydrin **8** after one hour of reaction. The analysis was performed on a Chiralcel OD-H column with hexane and 2-propanol (90:10) as eluent and 1 mL/min flow, and with a detection wavelength of 254.4 nm. The retention times obtained are t_R((*S*)-**8**) = 6.66 min and t_R((*R*)-**8**) = 7.34 min.

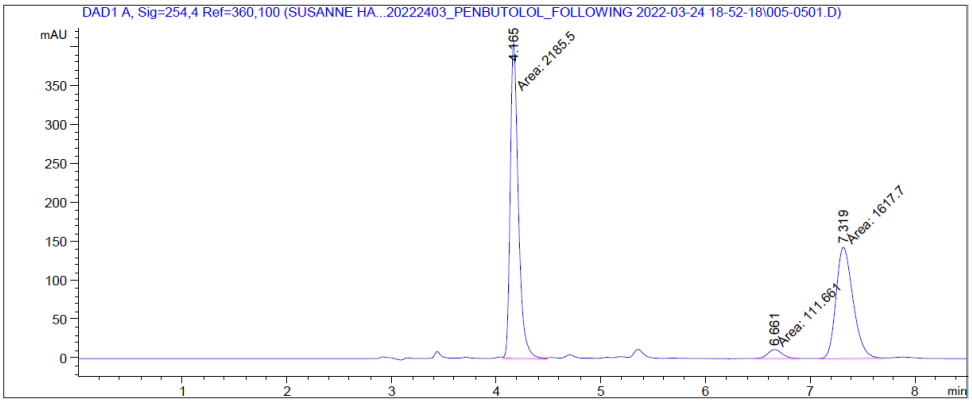

Figure 2.2.7: Chiral HPLC chromatogram of the CALB-catalyzed kinetic resolution of chlorohydrin **8** after nine hours of reaction. The retention times obtained are t_R((*S*)-**8**) = 6.66 min and t_R((*R*)-**8**) = 7.32 min.

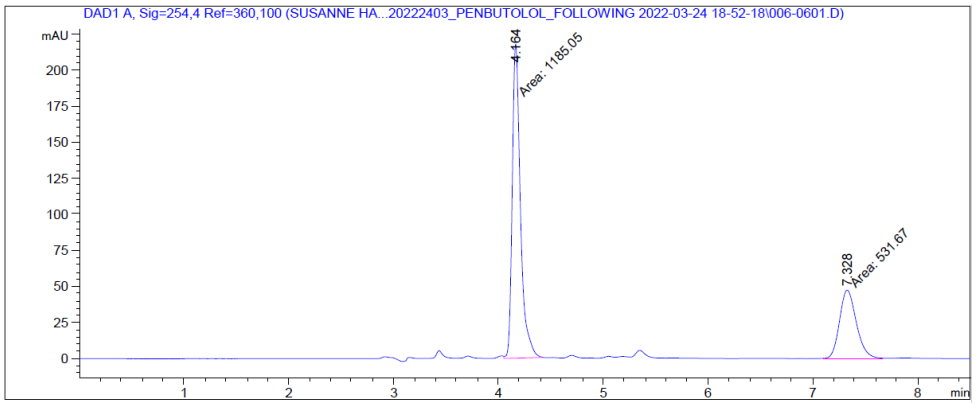

Figure 2.2.8: Chiral HPLC chromatogram of the CALB-catalyzed kinetic resolution of chlorohydrin **8** after 23 hours of reaction. The retention time obtained is t_R((*R*)-**8**) = 7.33 min.

Chiral HPLC analyses of the samples using a mobile phase composition of hexane (99.4%) and 2-propanol (0.6%) were also performed to measure the enantiomeric excess of the ester **9** produced. These values were then used to determine an enantiomeric ratio E of 183 (calculated from E&K Calculator 2.1b0 PPC [29]) from the kinetic resolution of chlorohydrin **8** with CALB, and to plot the enantiomeric excesses of ester **9** and chlorohydrin **8** as a function of conversion, as shown in Figure 2.2.9. A value of 183 is very good, and allows to obtain chlorohydrin (*R*)-**8** with a high yield and a very high enantiomeric excess.

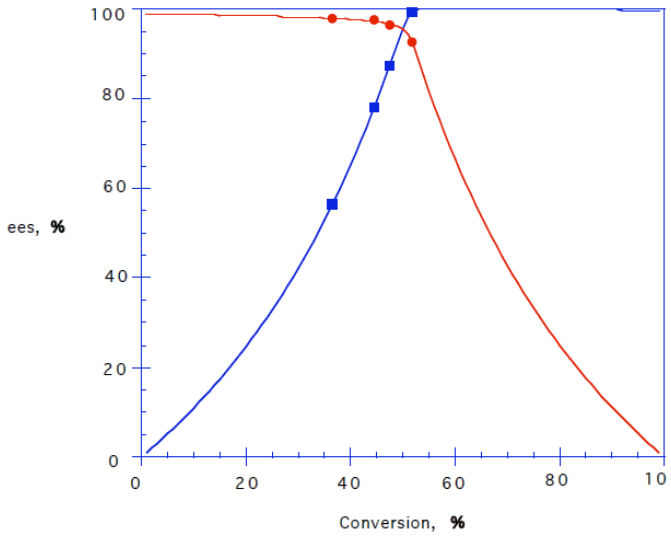

Figure 2.2.9: Enantiomeric excesses of ester **9** and chlorohydrin **8** as a function of conversion during the CALB-catalyzed kinetic resolution of chlorohydrin **8**. Enantiomeric excesses of product **9** are represented by red filled circles. Enantiomeric excesses of chlorohydrin **8** are represented by blue filled squares; E-value = 183. E-values are calculated from E&K Calculator 2.1b0 PPC [29].

2.2.3.2 Large-scale kinetic resolution of chlorohydrin 8

A large-scaled kinetic resolution of **8** was then carried out and stopped after 23 hours. The reaction mixture was washed with water several times in order to remove butyric acid.

Chlorohydrin **8** and ester **9** were then separated by flash chromatography to obtain enantiopure chlorohydrin (*R*)-**8** as a transparent oil, with a yield of 39%, an enantiomeric excess of more than 99% and a purity of 95% (^{1}H-NMR). For this type of reaction, the maximum theoretical yield is 50%, because ideally, half of the substrate is transformed into ester (*S*)-**9**. The specific rotation of (*R*)-**8** was $[\alpha]_D^{25} - 14\ (\mathrm{c}\ 1.0, \mathrm{MeOH})$, and has not been published previously. Absolute configuration was determined by the enantioselectivity of CALB which has been reported previously [30].

2.2.4 Synthesis of (*S*)-penbutolol, (*S*)-10

(*S*)-Penbutolol ((*S*)-**10**) was synthesized from (*R*)-1-chloro-3-(2-cyclopentylphenoxy)propan-2-ol ((*R*)-**8**)**,** and *tert*-butylamine, adapting the procedures described by Grundersen *et al*. [52] and Banoth and Banerjee [81] and concerning the amination of similar chlorohydrins. The general reaction for the amination of (*R*)-**8** with tert-butylamine is shown in **Scheme 2.2.8**. Two reaction procedures were tested. In the first procedure, this reaction was performed in distilled water at room temperature. In the second one, it was performed in methanol under reflux.

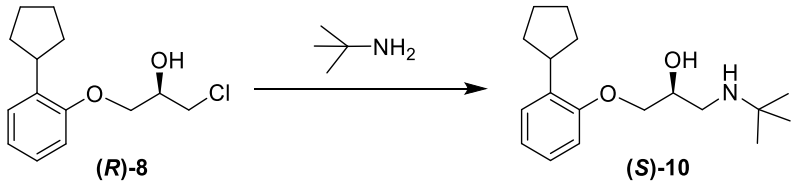

Scheme 2.2.8: Synthesis of (S)-penbutolol, (S)-**10,** from (R)-1-chloro-3-(2-cyclopentylphenoxy)propan-2-ol, (R)-**8,** and tert-butylamine.

The reactions were first carried out on racemic chlorohydrin **8**. The reaction performed in water gave after workup a mixture composed of around 64% of penbutolol (**10**), 15% of starting material **8**, and 21% of *tert*-butylamine (^{1}H-NMR). The reaction performed in methanol gave after workup penbutolol (**10**) with a purity of 93% (^{1}H-NMR), the other compound present being the starting material **8** (around 7%).

It was noticed by comparing the two ^{1}H-NMR spectra of the obtained products that some peaks, among others the *tert*-butyl peak, were slightly shifted, while others, like the aromatic peaks, were not. It was first thought that the compounds formed could have been slightly different depending on the solvent used. One potential product that could be formed instead of **10** was indeed the hydrochloric salt **10*HCl*** shown in Figure 2.2.10.

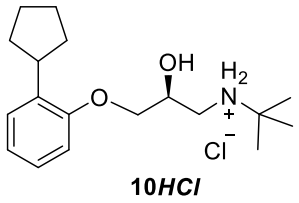

10*HCl*

Figure 2.2.10: Possible side product (S)-**10HCl** obtained during the synthesis of (S)-Penbutolol (**10**) from (R)-1-chloro-3-(2-cyclopentylphenoxy)propan-2-ol ((R)-**8**) and tert-butylamine.

The shifts were also slightly different from the previously reported data [53]. As shown in **Figure 2.2.12** and **Figure 2.2.11**, peaks number 2 are at the same shift, while peaks numbered 1, 3 and 4 have a different shift.

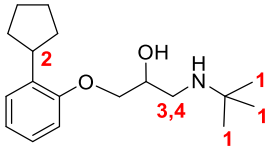

10

Figure 2.2.11: Penbutolol **10** with numbered atoms according to the spectra shown in **Figure 2.2.12**.

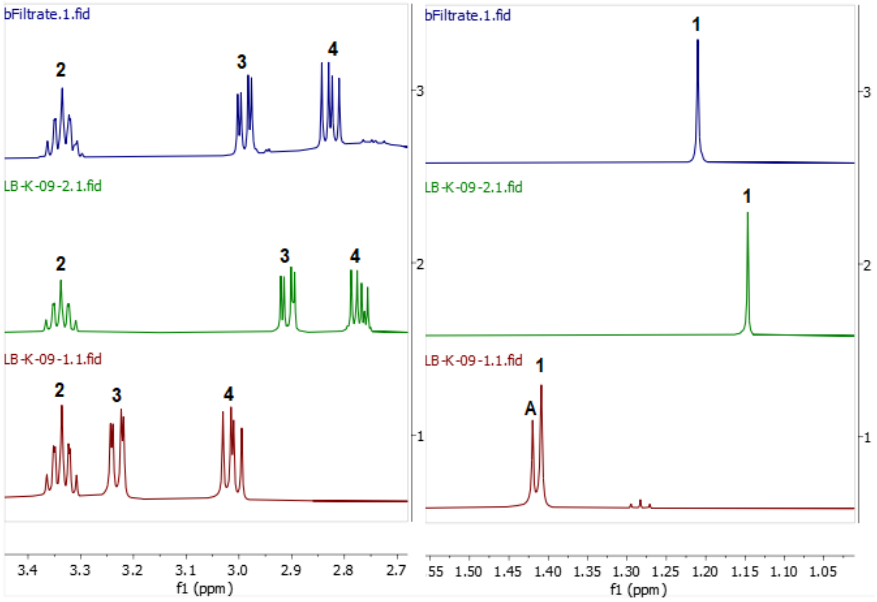

Figure 2.2.12: ^{1}H-NMR spectra of the products obtained following different methods for the amination of 1-chloro-3-(2-cyclopentylphenoxy)propan-2-ol ((R)-**8**). The upper spectrum is a previously reported (S)-**10** spectrum [53]. The middle spectrum comes from the amination reaction performed in methanol. The lower spectrum comes from the amination reaction performed in water. Peak A corresponds to remaining tert-butylamine. The other peaks are numbered according to their correspondence to protons of compound **10** shown in **Figure 2.2.11**.

After some literature search [82, 83], it was concluded that those shifts came from the fact that (*S*)-**10** was not exactly the only form of penbutolol synthesized. Our product is a mixture of (*S*)-**10**

and its hydrochloric salt (*S*)-**10*HCl***. Those two forms are in rapid exchange with each other, so the NMR instrument cannot give the peaks corresponding to each of the form separately. Instead, the peaks and their shifts are "averaged". Therefore, the shift of some peaks will be different depending on the ratio of free base (*S*)-**10** and hydrochloric salt **(*S*)-10*HCl*** present in the analyzed mixture.

It was then decided to do the amination of enantiopure chlorohydrin (*R*)-**8** in methanol. This gave (*S*)-**10** (as a mixture of (*S*)-**10** and (*S*)-**10*HCl***) as a white powder, with a purity of 99% (^{1}H-NMR) and with a yield between 73% and 82%. Specific rotation of (*S*)-**10** was $[\alpha]_D^{25} - 14\ (\mathrm{c}\ 1.0, \mathrm{MeOH})$.

Since we do not know the ratio of salt and free base present in our final products, calculating the exact yield is not possible. It was decided to add a step in the reaction process in order to form only the hydrochloric salt (*S*)-**10*HCl***. Most of the beta blockers are actually sold as a salt, sometime as a hydrochloric salt, because in this form the drug is better absorbed by the body. The salt is therefore the real final product. Moreover, the optical rotation of (*S*)-**10*HCl*** has been reported as $[\alpha]_D^{20} - 26.4\ (\mathrm{c}\ 1.0, \mathrm{MeOH})$ by Kan *et al.* [48].

Adapting the procedure from Kan *et al.*, the product was therefore dissolved in 2-propanol, and a solution of hydrochloride 2-propanol was added. The solution was stirred for one hour at 0°C, and the solvent was then removed under reduced pressure. (*S*)-Penbutolol hydrochloride ((*S*)-**10*HCl***) was obtained from chlorohydrin (*R*)-**8** with a yield of 73% and a purity of 93% (^{1}H-NMR). The product obtained had a specific rotation of $[\alpha]_D^{20} - 23\ (\mathrm{c}\ 1.0, \mathrm{MeOH})$.

Racemic **10*HCl*** was synthesized in order to determine the retention times of its (*R*)- and (*S*)-enantiomers on chiral HPLC. Separation of the enantiomers of **10*HCl*** was obtained by using a Chiralcel OD-H column, a mobile phase composition of hexane (90%) and 2-propanol containing 2% diethanolamine (10%) as the eluent and a 1 mL/min flow. The retention times obtained are t_R((*R*)-**10*HCl***) = 4.671 min and t_R((*S*)-**10*HCl***) = 7.395 min (see Figure 6.2.16 in the appendix). The resolution factor is R_S((*S*)/(*R*)-**10*HCl***) = 10.5. Diethanolamine was added to the 2-propanol in the mobile phase in order to obtain a better separation, and to deprotonate the amine in **10*HCl***, to solubilize better the analyte.

The enantiomeric excess of the (*S*)-Penbutolol hydrochloride (*S*)-**10*HCl*** synthesized was 99% (chiral HPLC).

2.2.4.1 Reaction mechanism of the amination of (*R*)-8 using tert-butylamine

A mechanism for the amination of (*R*)-1-chloro-3-(2-cyclopentylphenoxy)propan-2-ol ((*R*)-**8**) using *tert*-butylamine is shown in Scheme 2.2.9. The hydrochloric salt (*S*)-**10*HCl*** is formed even without the hydrochloric acid workup, but only in limited amounts. The equilibrium between the free base (*S*)-**10** and the hydrochloric salt (*S*)-**10*HCl*** is pushed towards (*S*)-**10*HCl*** thanks to the hydrochloric acid solution added after the amination reaction.

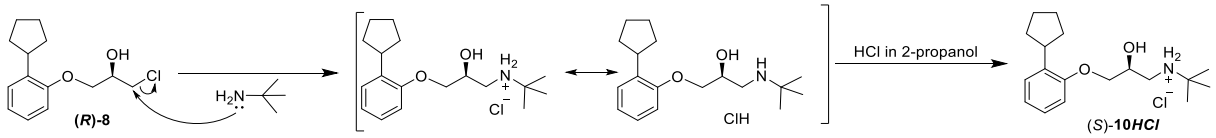

Scheme 2.2.9: Mechanism for the amination (R)-1-chloro-3-(2-cyclopentylphenoxy)propan-2-ol (**8**) using tert-butylamine.

2.2.4.2 Characterization of penbutolol hydrochloride (10*HCl*)

Characterization of the penbutolol hydrochloride (**10*HCl***) was carried out by NMR spectroscopy, with deuterated chloroform as solvent. Product **10*HCl*** with numbered carbon atoms is shown in Figure 2.2.13, and assignment of chemical shifts are given in Table 2.2.3.

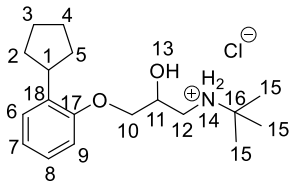

Figure 2.2.13: Penbutolol hydrochloride (**10*HCl*)** with numbered carbon and nitrogen atoms. Assignment of chemical shifts are given in Table 2.2.3, and all spectra are given in the appendix (Part 6.2.3).

Table 2.2.3: Characterization of product **10*HCl*** given ^{1}H-, ^{13}C-, H,H-COSY, HSQC- and HMBC-NMR (600 MHz, CDCl3), see the appendix (Part 6.2.3).

Numbered atom	^{1}H-NMR [ppm] (mult., int., ^{3}J)	^{13}C-NMR [ppm]	COSY	HMBC
1	3.11 (dtd, *J* = 12.3, 9.6, 2.6 Hz, 1H)	39.15	2,3,4,5	2,3,4,5,17,18
2	2.04 – 1.54 (m, 8H)	32.88	3,4,5,7	1,3,4,5,18
3	2.04 – 1.54 (m, 8H)	25.32	2,4,5,7	1,2,4,5
4	2.04 – 1.54 (m, 8H)	25.32	2,3,5,7	1,2,3,5
5	2.04 – 1.54 (m, 8H)	32.89	2,3,4,7	1,2,3,4,18
6	7.22 (dd, *J* = 7.6, 1.7 Hz, 1H)	126.74	8	1,8,9,10,17
7	7.13 (td, *J* = 7.8, 1.7 Hz, 1H)	121.19	9	6,8,9,17,18
8	6.93 (td, *J* = 7.5, 1.1 Hz, 1H)	126.70	6	6,8,9,17,18
9	6.80 (dd, *J* = 8.2, 1.2 Hz, 1H)	111.33	7	1,6,7,8,17,18
10	4.12 (dd, *J* = 9.5, 4.3 Hz, 1H), 3.98 (dd, *J* = 9.6, 6.4 Hz, 1H)	69.66	10',11	11,12,17
11	4.69 – 4.60 (m, 1H)	65.83	10,12	10,12
12	3.34 (tdd, *J* = 16.9, 9.7, 7.6 Hz, 2H)	45.92	12',11	10,11
13	-	-	-	-
14	-	-	-	-
15	1.50 (s, 9H)	25.90	-	16
16	-	57.57	-	-
17	-	155.98	-	-
18	-	134.55	-	-

2.3 Synthesis of enantiopure (*S*)-bisoprolol ((*S*)-17)

The aim of this part was to synthesize enantiopure (*S*)-bisoprolol ((*S*)-**17**) in an environmentally friendly and efficient way. Two synthesis pathways have been tried, and are shown in Scheme 2.3.1.

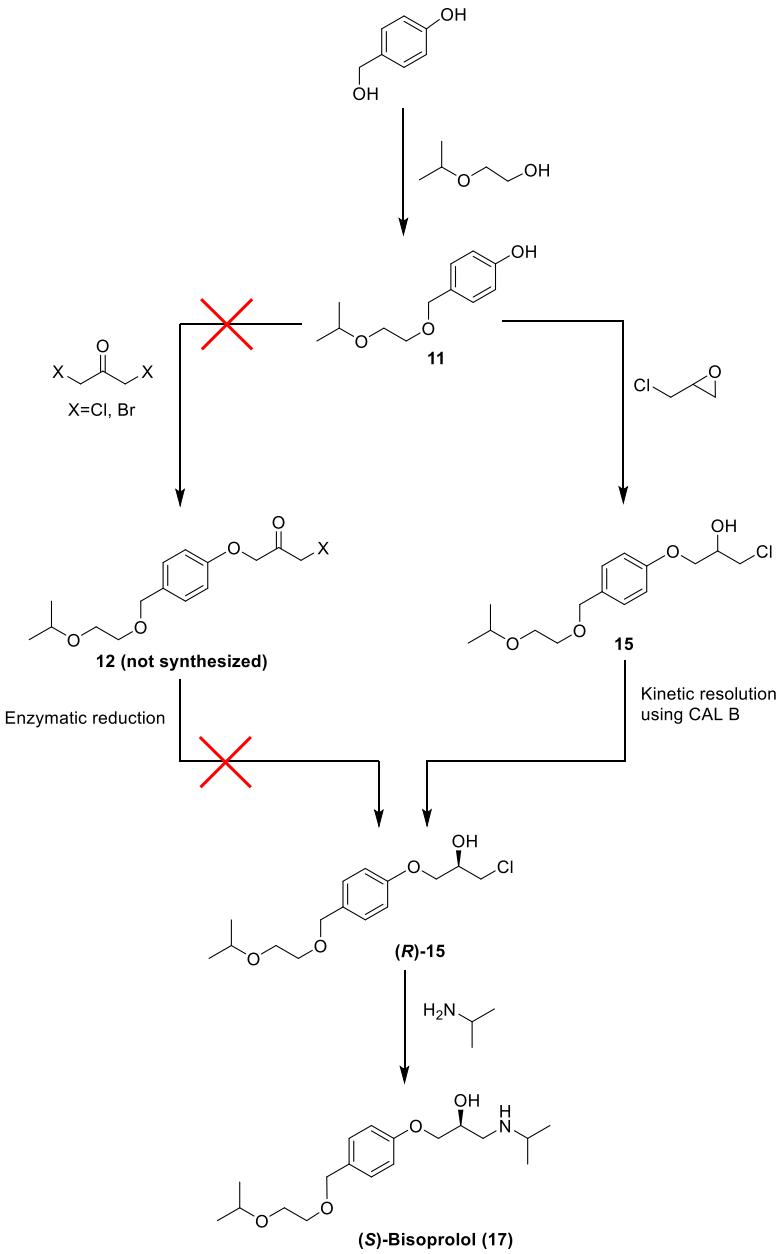

Scheme 2.3.1: Planned pathways for the synthesis of (*S*)-bisoprolol ((*S*)-**17**)

2.3.1 Synthesis of 4-((2-isopropoxyethoxy)methyl)phenol (11)

4-((2-Isopropoxyethoxy)methyl)phenol (**11**) was synthesized from 4-(hydroxymethyl)phenol and 2-isopropoxyethan-1-ol in the presence of the acid catalyst silica sulfuric acid (SSA), as

described in a patent from Morthala *et al.* [61] and shown in Scheme 2.3.2. 2-Isopropoxyethan-1-ol was introduced in large excess and plays the additional role of solvent.

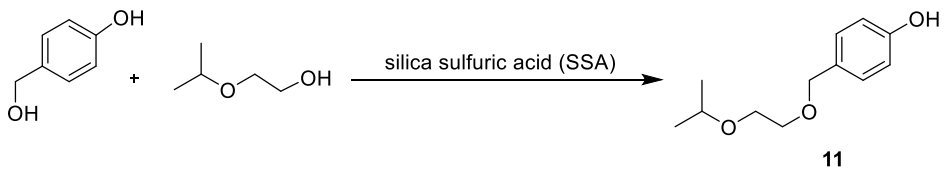

Scheme 2.3.2: Synthesis of 4-((2-isopropoxyethoxy)methyl)phenol (**11**) from 4-(hydroxymethyl)phenol and 2-isopropoxyethan-1-ol and catalyzed by silica sulfuric acid.

Silica sulfuric acid (SiO_2–H_2SO_4) was synthesized from silica and concentrated sulfuric acid (95%) in acetone following the procedure described by Chávez *et al.* [84]. 0.7 mol of sulfuric acid was used per mol of silica, as described in the patent from Morthala *et al.* [61]. The reaction is exothermic, and the sulfuric acid was added slowly. The acetone was removed under reduced pressure, and the obtained paste was let overnight in the oven, to obtain a black solid. This solid was crushed into a fine powder, and stored in a desiccator.

The catalyst was then used for the synthesis of 4-((2-isopropoxyethoxy)methyl)phenol (**11**). When it was added to the 2-isopropoxyethan-1-ol at 5 °C, the reaction mixture turned black. This could come from the silica sulfuric acid powder in suspension, but it looked more like part of the catalyst got dissolved, because even with the stirring stopped, the black color stayed uniform. 4-(Hydroxymethyl)phenol was then added to the reaction mixture, which was then stirred for one day. The patent from Morthala *et al.* indicates a simple removal of the acid catalyst by filtration. However, the filtrate was black even after the reaction mixture was filtered through a 0.25 µm filter. This color does not come from compound **11**, which is an uncolored to light yellow oil in its pure form. It was tried to filter the mixture through filter papers, syringe filters, celite, and silica, unsuccessfully.

Some colored impurities were visible by TLC (n-pentane:ethyl acetate 7:3), so the product was purified by column chromatography to give compound **11** in the form of a slightly red oil with a yield of 75% and a purity of 99% (^{1}H-NMR).

Some product was probably lost during the repeated filtering attempts done previously. The reaction was therefore performed once again, by purifying the product by flash chromatography directly after the workup, and by skipping the filtration steps. This was done as part of a project course by master student Maja Christensen under my supervision. The yield was not improved, but skipping the filtering steps simplifies the procedure and does not impact the purity of the product obtained.

2.3.1.1 Reaction mechanism for the acid-catalyzed synthesis of 4-((2-isopropoxyethoxy)methyl)phenol (11) from 4-(hydroxymethyl)phenol and 2-isopropoxyethan-1-ol

The suggested mechanisms for the acid-catalyzed synthesis of compound **11** from 4-(hydroxymethyl)phenol and 2-isopropoxyethan-1-ol are shown in Scheme 2.3.3. This reaction is an acid-catalyzed ether formation.

The Silica Sulfuric Acid catalyst could intervene more than just as a proton donor. The top mechanism is probably the main reaction happening. 2-Isopropoxyethan-1-ol is indeed mixed with the acid catalyst before the addition of 4-(hydroxymethyl)phenol. When 4-(hydroxymethyl)phenol is added, a lot of the 2-isopropoxyethan-1-ol should therefore already have been protonated.

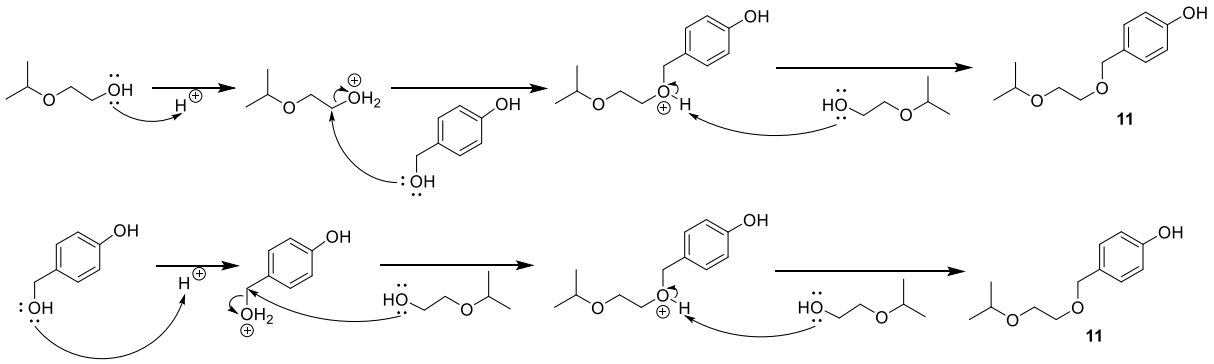

Scheme 2.3.3: Suggested mechanisms for the acid-catalyzed synthesis of 4-((2-isopropoxyethoxy)methyl)phenol (**11**) from 4-(hydroxymethyl)phenol and 2-isopropoxyethan-1-ol

Mechanisms of possible side reactions are given in Scheme 2.3.4 , as well as structures of possible impurities **B1** and **B2**. The formation of **B1** is limited by the fact that 2-isopropoxyethan-1-ol is introduced in large excess in the reaction mixture. A molecule of 4-((2-isopropoxyethoxy)methyl)phenol is therefore more likely to encounter and attack a protonated 2-isopropoxyethan-1-ol than a protonated 4-((2-isopropoxyethoxy)methyl)phenol. **B1** was not identified in the final product. The formation of **B2** is more likely to happen. However, after workup, no significant amount of **B2** was found on the ^{1}H-NMR analysis of the crude product, and **B2** was not isolated by flash chromatography. This could mean that this side reaction is negligible, or that **B2** gets removed during the workup.

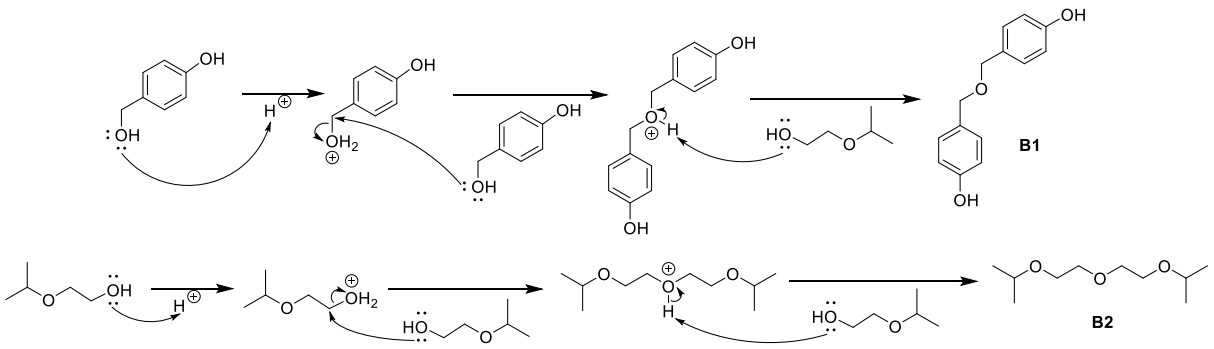

Scheme 2.3.4: Suggested mechanisms for the formation of possible side-products **B1** and **B2**.

The aromatic alcohol of 4-((2-isopropoxyethoxy)methyl)phenol does not interfere in the reaction because its oxygen atom has a lower electron density than the ones of the other alcohols in the reactions. Electrons are delocalized around the aromatic ring, lowering the capacity of this aromatic alcohol group to get protonated or to attack another molecule. The resonance forms of 4-((2-isopropoxyethoxy)methyl)phenol describing the delocalization of the electrons of aromatic alcohol into the ring is shown in Scheme 2.3.5.

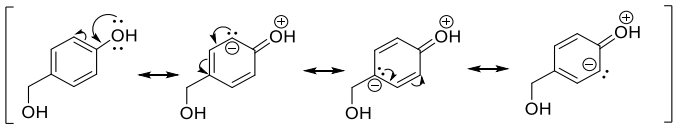

Scheme 2.3.5: Resonance forms of 4-((2-isopropoxyethoxy)methyl)phenol showing the delocalization of the electrons of aromatic alcohol into the aromatic ring

2.3.1.2 Alternative synthesis pathway using concentrated sulfuric acid as the catalyst

To see if the Silica Sulfuric Acid catalyst played an important role to limit the formation of byproducts, the same reaction was tried by using concentrated sulfuric acid instead of silica sulfuric acid as the catalyst. This was done as part of a project course by Maja Christensen under my supervision. The same amount of acid that was used to form the Silica Sulfuric Acid catalyst was added directly in the reaction mixture. The crude product was purified by column chromatography. The first fraction gave compound **11** was obtained with a yield of 52% and a purity of 97%. The second fraction gave a mixture mainly composed of compound **B2**. The loss in yield and the formation of significant amounts of **B2** when using concentrated sulfuric acid shows that the silica sulfuric acid catalyst used previously acts as more than just an acid catalyst, and prevents the formation of **B2**.

2.3.1.3 Characterization of 4-((2-isopropoxyethoxy)methyl)phenol (11)

Characterization of compound **11** was carried out by NMR spectroscopy, with deuterated chloroform as solvent. Compound **11** with numbered carbon atoms is shown in Figure 2.1.1, and assignment of chemical shifts are given in Table 2.1.2.

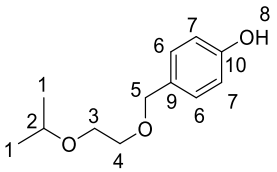

Figure 2.3.1: Compound **11** with numbered carbon and nitrogen atoms. Assignment of chemical shifts are given in Table 2.1.2, and all spectra are given in the appendix (Part 6.3.1).

Table 2.3.1: Characterization of compound **11** given ^{1}H-, ^{13}C-, H,H-COSY, HSQC- and HMBC-NMR (600 MHz, CDCl3), see the appendix (Part 6.3.1).

Atom number	**^{1}H-NMR [ppm] (mult., int., ^{3}J)**	**^{13}C-NMR [ppm]**	**COSY**	**HMBC**
1	1.20 (d, *J* = 5.9 Hz, 6H)	22.01	2	1',2
2	3.72 – 3.58 (m, 5H)	72.21	1	1,3
3	3.72 – 3.58 (m, 5H)	67.48	4	4,2
4	3.72 – 3.58 (m, 5H)	69.34	3	3,5
5	4.48 (s, 2H)	73.11	-	4,6,9
6	7.22 – 7.13 (m, 2H)	129.74	7	5,6',7,9,10
7	6.82 – 6.72 (m, 2H)	115.26	6	6,7',9,10
8	6.02 (s, 1H)	-	-	10,7

2.3.2 Attempts to synthesize 1-chloro-3-(4-((2-isopropoxyethoxy)methyl)phenoxy)propan-2-one (12)

The synthesis of 1-chloro-3-(4-((2-isopropoxyethoxy)methyl)phenoxy)propan-2-one (**12**) from 4-((2-isopropoxyethoxy)methyl)phenol (**11**) was attempted using different procedures. As described in the introduction, synthesizing compound **12** would allow the synthesis of chlorohydrin (*R*)-**15** via the preferable left pathway shown in Scheme 2.3.6. However, none of the attempts gave compound **12** in significant amounts.

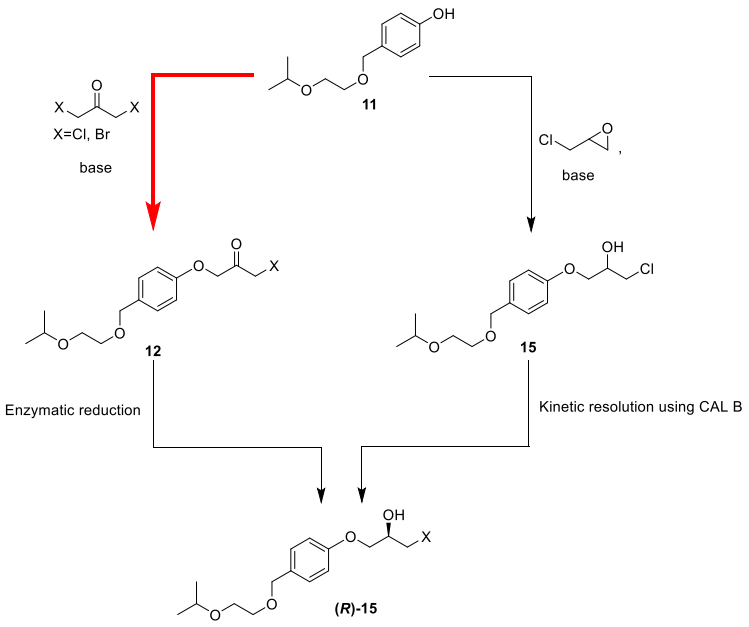

Scheme 2.3.6: Planned pathways for the synthesis of chlorohydrin (*R*)-**15**. This part will focus on the red arrow reaction.

The reaction of synthesis of compound **12** from phenol **11** and 1,3-dichloropropan-2-one (or 1,3-dibromopropan-2-one) under basic conditions should be an S_N2 reaction. Phenol **11** gets first deprotonated by the base, and attacks then one of the alpha carbons of the ketone on 1,3-dichloropropan-2-one, making one chlorine atom leave.

It was first tried to adapt a procedure used for the addition of epichlorohydrin on compounds similar to phenol **11** [58] and to use it for the addition of 1,3-dichloropropan-2-one on phenol **11**. 1,3-Dichloropropan-2-one was therefore added to a mixture of phenol **11** and potassium carbonate in dry acetonitrile. The mixture was then refluxed and stirred for 24 hours. However, the reaction mixture turned black, and no expected product was noticed at the end of the reaction time. The same thing happened when the reaction was done at room temperature. To understand if this color came from the starting material **11** reacting with the 1,3-dichloropropan-2-one, or if the starting material was not intervening in this, the same reaction was tried, but without including phenol **11**. The reaction mixture still turned black some seconds after the addition.

This indicates that 1,3-dichloropropan-2-one is not stable in this basic environment. It is believed that the molecule polymerases as shown in Scheme 2.3.7. The base helps to push the keto-enol equilibrium in 1,3-dichloropropan-2-one towards the enol, and the oxygen atom then attacks another molecule of 1,3-dichloropropan-2-one either on one carbon linked to a chlorine atom (mechanism a), or the carbon bearing the ketone (mechanism b). The reaction can then proceed, the oxygen anion attacking another molecule as previously.

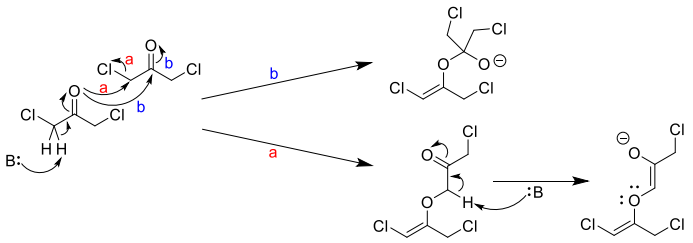

Scheme 2.3.7: Suggested mechanism for the polymerization reaction of 1,3-dichloropropan-2-one

A black color usually indicates the presence of a very long conjugated system of connected p orbitals. Repeating mechanism **a** could lead to the formation of this kind of compound. An example of a possibly formed compound with a long chain of conjugated system of connected p orbitals is shown in Figure 2.3.2. The obtained impurities were, however, not isolated.

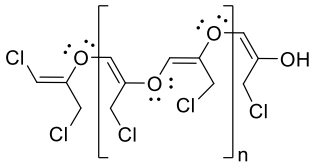

Figure 2.3.2: A possible type of degradation product of 1,3-dichloropropan-2-one in a basic environment.

The base used here leads to the degradation of 1,3-dichloropropan-2-one. However, basic conditions are necessary for the desired S_N2 reaction to happen. A base strong enough for that, but weak enough to avoid the polymerization of 1,3-dichloropropan-2-one is therefore needed.

A typical hydrogen bonded to the alpha carbon of a ketone has a pKa of around 19-20 [68]. Since the carbon bearing the acidic proton is also linked to a chlorine atom in 1,3-dichloropropan-2-one, the pKa could be slightly lower. In comparison, the aromatic alcohol on compound **11** has a predicted pKa of 9.7 [85]. Finding an adequate base should therefore be possible. However, other things need to be taken into account. For instance, the polymerization reaction pushes the equilibrium towards the enolization of 1,3-dichloropropan-2-one.

To try to prevent the polymerization reaction, 1,3-dichloropropan-2-one was added dropwise in some attempts. Several bases and solvents were tested, and are presented in Table 2.3.2. They were chosen based on published procedures on similar reactions, as described in the introduction. However, either the mixtures turned black, indicating the polymerization of 1,3-dichloropropan-2-one, or it did not, but no conversion of compound **11** was observed. Either way, no expected product was identified on the ^{1}H-NMR spectra of the crude products.

Table 2.3.2: Attempted procedures for the addition of 1,3-dichloropropan-2-one on 4-((2-isopropoxyethoxy)methyl)phenol (**11**).

Base	Solvent	Procedure	Observations
K_2CO_3	MeCN (dry)	Stirred under reflux for 40 hours	Turns black, no expected product
K_2CO_3	MeCN (dry)	Stirred at rt for 16 hours	Turns black, no expected product
$NaHCO_3$	MeCN (dry)	Addition of dichloroacetone at 0°C; Stirred at rt for 3 days	No conversion
$NaHCO_3$	DMSO	Stirred at rt for 3 days	Turns black, no expected product
$NaHCO_3$	DMF	Addition of dichloroacetone at 0°C; Stirred at rt for 3 days	Turns brown, no expected product
K_2CO_3	DMF	Addition of dichloroacetone at 0°C; Stirred at rt for 1 day	Turns black, no expected product
K_2CO_3	MeCN (dry)	Dropwise addition of dichloroacetone; Stirred at rt for 1 day	Turns brown, no expected product
NaOH	H_2O	Dropwise addition of dichloroacetone; Stirred at 35°C for 6h	Turns brown, no expected product
EtONa	EtOH	Addition at rt; reflux for 1 day	Turns black at room temperature, no expected product
NaOH	Water	Dropwise addition; Stirred for 1 day at rt	Turns light brown, no expected product formed

It was then attempted to perform the reaction with 1,3-dibromopropan-2-one. The bromine atom is bigger than chlorine, and could increase the steric hindrance around the alpha carbon of the ketone, limiting the enolization reaction. Bromine is also usually a slightly better leaving group than chlorine, which could promote the synthesis of the desired compound **12**. 1,3-dibromopropan-2-one was therefore added dropwise to a mixture of phenol **11** and sodium hydroxide in water, and the brown solution was stirred for one day at room temperature. Compound 2 was unfortunately not present in significant amounts in the crude product (^{1}H-NMR). It was therefore decided to focus on the other synthesis pathway.

2.3.3 Synthesis of racemic 1-chloro-3-(4-((2-isopropoxyethoxy)methyl)phenoxy)propan-2-ol (15)

1-Chloro-3-(4-((2-isopropoxyethoxy)methyl)phenoxy)propan-2-ol (**15**) was synthesized from 4-((2-isopropoxyethoxy)methyl)phenol (**11**) and epichlorohydrin by adapting the procedure used for a similar reaction by Gundersen *et al.* [52]. The reaction is shown in Scheme 2.3.8.

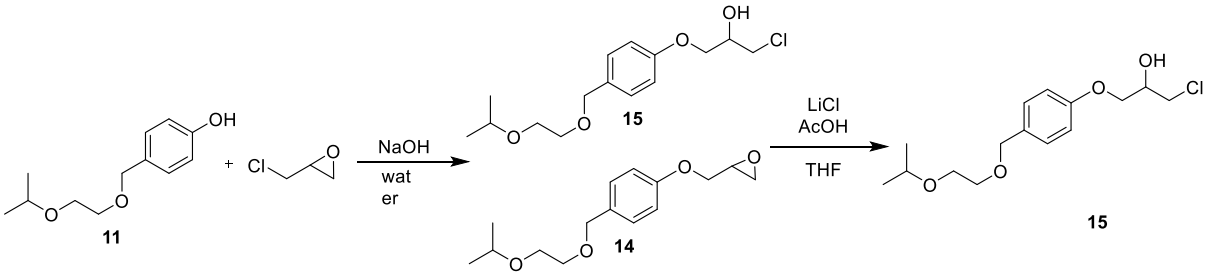

Scheme 2.3.8: Synthesis of 1-chloro-3-(4-((2-isopropoxyethoxy)methyl)phenoxy)propan-2-ol (**15**) from 4-((2-isopropoxyethoxy)methyl)phenol (**11**) and epichlorohydrin

It was attempted to follow the first step of the reaction by TLC (n-pentane:ethyl acetate 7:3) in order to see when the addition of epichlorohydrin was finished, but unfortunately the product **15** and its epoxide **14** had the same retention factor as the starting material **11**. It was, however, noticed that an oil was slowly formed at the surface of the water. After one day of stirring, a thin oil layer had been formed, and did not seem to become thicker. It is believed that the products **15** and **14** are not soluble in the sodium hydroxide aqueous solution, while starting material **11** is. The forming oil layer at the top is therefore a direct indication of the extent of the reaction. The reaction was stopped at that point, the reaction mixture was extracted with ethyl acetate and washed with water, and the solvent of the organic phase was removed under reduced pressure. An ^{1}H-NMR analysis of the obtained product revealed that it was constituted at 70% of the epoxide **14**. The other compounds present were not identifiable on the spectrum, but are probably compound **15** and dimer **D15**, shown in Figure 2.3.3. Compounds similar to **D15** have been identified as the main impurity formed during the addition of epichlorohydrin on aromatic alcohols [52]. However, the impurities were not isolated in this thesis, and the crude product was used without further purification in the next step. This has been decided because the impurities and byproducts present in the crude product are not likely to prevent the opening of epoxide **14**.

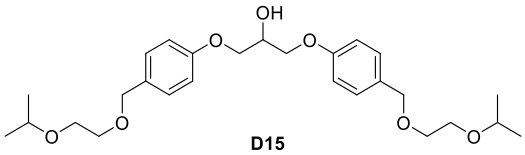

Figure 2.3.3: Dimer **D15**, a possible byproduct of the reaction.

The crude product was dissolved in THF, and acetic acid and lithium chloride were added. After 20 hours of stirring, the reaction was stopped and worked up, and the product was purified by column chromatography, to obtain pure chlorohydrin **15** with a yield of 63% and a purity of 99% (^{1}H-NMR).

2.3.3.1 Characterization of chlorohydrin 15

Characterization of chlorohydrin **15** was carried out by NMR spectroscopy, with deuterated chloroform as solvent. Chlorohydrin **15** with numbered carbon atoms is shown in Figure 2.3.4, and assignment of chemical shifts are given in Table 2.3.3.

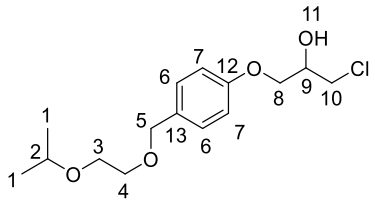

Figure 2.3.4: Chlorohydrin **15** with numbered carbon and nitrogen atoms. Assignment of chemical shifts are given in Table 2.3.3, and all spectra are given in the appendix (Part 6.3.2).

Table 2.3.3: Characterization of chlorohydrin **15** given ^{1}H-, ^{13}C-, H,H-COSY, HSQC- and HMBC-NMR (600 MHz, CDCl3), see the appendix (Part 6.3.2).

Atom number	**^{1}H-NMR [ppm] (mult., int., ^{3}J)**	**^{13}C-NMR [ppm]**	**COSY**	**HMBC**
1	1.20 (d, *J* = 6.1 Hz, 6H)	22.09	2	1',2
2	3.66 – 3.60 (m, 5H)	71.94	1	1,3
3	3.66 – 3.60 (m, 5H)	67.47	4	2,4
4	3.66 – 3.60 (m, 5H)	69.54	3	3,5
5	4.54 (s, 2H)	72.78	-	4,6,7,12,13
6	7.33 – 7.29 (m, 2H)	129.41	7	5,6',7,12
7	6.93 – 6.89 (m, 2H)	114.45	6	6,7',12,13
8	3.82 – 3.73 (m, 2H)	68.59	9	10,9,12
9	4.24 (h, *J* = 5.5 Hz, 1H)	69.87	8,10	8,10
10	4.13 – 4.08 (m, 2H)	45.98	9	8,9
11	2.57 (d, *J* = 5.9 Hz, 1H)	-	9	-
12	-	157.79	-	-
13	-	131.40	-	-

2.3.4 Derivatization of 1-chloro-3-(4-((2-isopropoxyethoxy)methyl)phenoxy)propan-2-ol (15)

A derivatization reaction of racemic chlorohydrin **15** was performed in order to form racemic ester **16** and determine the retention times of its *R*- and *S*-enantiomers. Pyridine and butyric

anhydride were added to a solution of compound **15** in hexane, and the mixture was heated for one hour at 60 °C, as shown in Scheme 2.3.9.

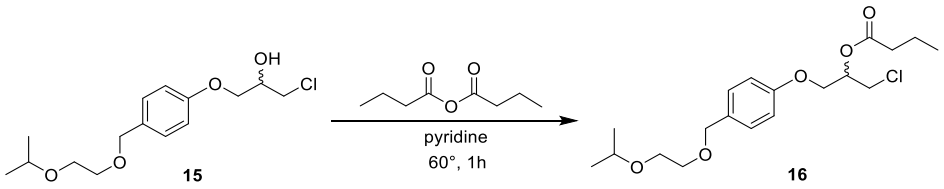

Scheme 2.3.9: Synthesis of racemic 1-chloro-3-(4-((2-isopropoxyethoxy)methyl)phenoxy)propan-2-yl propionate (**16**) from 1-chloro-3-(4-((2-isopropoxyethoxy)methyl)phenoxy)propan-2-ol (**15**)

Separation of the enantiomers of chlorohydrin **15** was obtained by using a Chiralcel OD-H column and a mobile phase composition of hexane (90%) and 2-propanol (10%) as eluent and a 1 mL/min flow. As shown in Figure 2.3.5, the retention times obtained are t_R((*R*)-**15**) = 14.81 min and t_R((*S*)-**15**) = 15.93 min. As expected, their peaks have the same area under the curve.

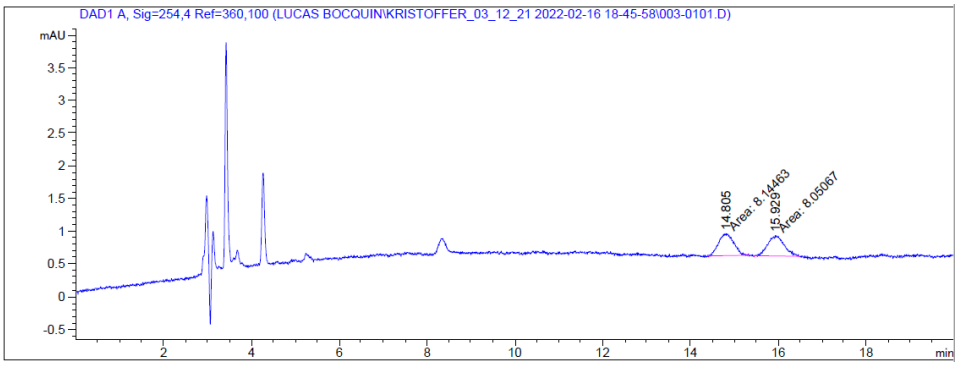

Figure 2.3.5: Chiral HPLC chromatogram of chlorohydrin **15**. The analysis was performed on a Chiralcel OD-H column with hexane and 2-propanol (90:10) as eluent and 1 mL/min flow, and with a detection wavelength of 280.8 nm. The retention times obtained are t_R((*R*)-**15**) = 14.81 min and t_R((*S*)-**15**) = 15.93 min. R_S((*S*)/(*R*)-**15**) = 1.63.

Separation of the enantiomers of ester **16** was obtained by using a Chiralcel OD-H column and a mobile phase composition of hexane (96%) and 2-propanol (4%). As shown in Figure 2.3.6, the retention times obtained are t_R((*R*)-**16**) = 11.23 min and t_R((*S*)-**16**) = 12.33 min. Some impurities elute before the enantiomers of ester **16**, but were not identified. Some of them could be butyric anhydride, introduced in excess, or butyric acid, a byproduct of the derivatization reaction. The mobile phase was then changed to a composition of 90% of hexane and 10% of 2-propanol for 8 min, in order to elute the enantiomers of chlorohydrin **15** and traces of pyridine.

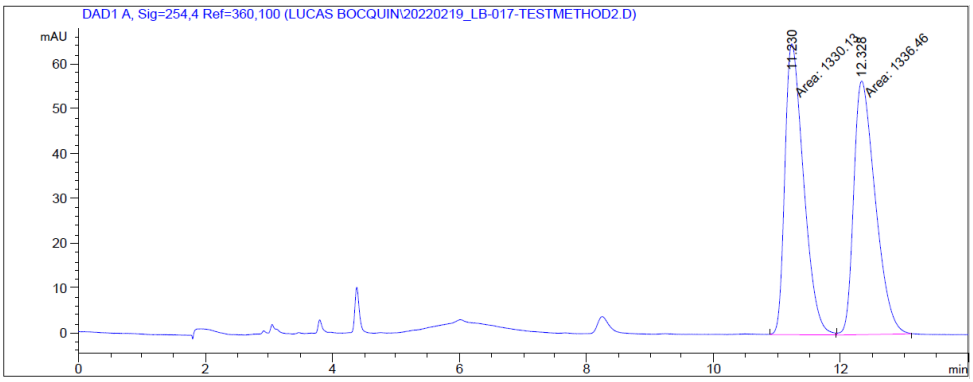

Figure 2.3.6: Chiral HPLC chromatogram of ester **16**. The analysis was performed on a Chiralcel OD-H column with hexane and 2-propanol (96:4) as eluent and 1 mL/min flow, and with a detection wavelength of 280.8 nm. The retention times obtained are t_R((*R*)-**16**) = 11.23 min and t_R((*S*)-**16**) = 12.33 min. R_S((*S*)/(*R*)-**16**) = 1.89.

2.3.5 Kinetic resolution of chlorohydrin 15 using CALB

Kinetic resolution of 1-chloro-3-(4-((2-isopropoxyethoxy)methyl)phenoxy)propan-2-ol (**15**) was performed using CALB as the catalyst and vinyl butyrate as the acyl donor, as shown in Scheme 2.3.10. The procedure was based on the one described by Gundersen *et al.* [52] on a similar reaction.

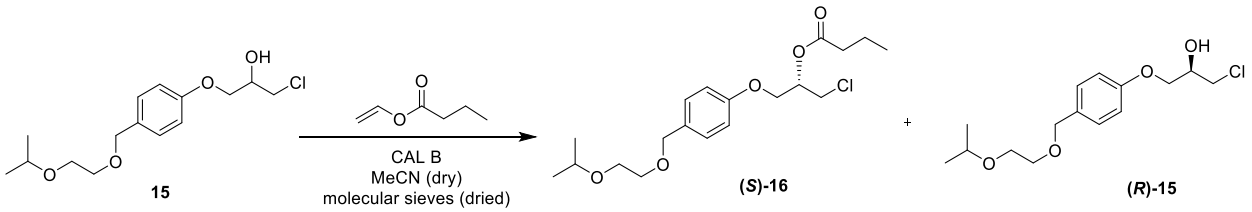

Scheme 2.3.10: Kinetic resolution of 1-chloro-3-(4-((2-isopropoxyethoxy)methyl)phenoxy)propan-2-ol (**15**) using CALB

As explained in the introduction, plausible side reactions include hydrolysis of ester (*S*)-**16** and vinyl butyrate catalyzed by CALB. They would respectively lead to a loss in the enantiomeric excess of the chlorohydrin (*R*)-**15** obtained, and to the formation of butyric acid. In order to avoid those side reactions, dry acetonitrile was used to dissolve racemic chlorohydrin **15**, and activated molecular sieves were introduced. Vinyl butyrate and CALB were then added, and the reaction mixture was shaken in an incubator at 38°C and 200 rpm.

2.3.5.1 Monitoring of the kinetic resolution of chlorohydrin 15

The CALB catalyzed kinetic resolution of chlorohydrin **15** was followed over 25 hours in order to calculate the enantiomeric ratio E of the reaction, and to know how much time is needed to get a good enantiomeric excess of the substrate **15**. Samples of the reaction mixture were collected at different time intervals and analyzed by chiral chromatography.

Chiral HPLC analyses of the samples using a mobile phase composition of hexane (90%) and 2-propanol (10%) were performed to measure the enantiomeric excess of the chlorohydrin **15** present in the reaction mixture. Chromatograms showing the enantiomeric excess of chlorohydrin **15** after 1 hour, 8 hours and 25 hours are shown in Figure 2.2.6, Figure 2.2.7 and Figure 2.2.8. The compounds eluting at 7.5 min are the enantiomers of the ester **16**. After 25 hours, chlorohydrin (*R*)-**15** is obtained with an enantiomeric excess of more than 99%.

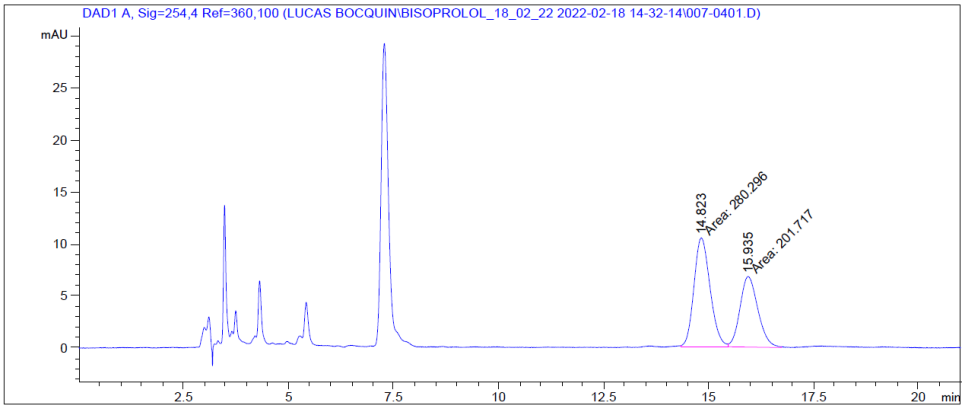

Figure 2.3.7: Chiral HPLC chromatogram of the CALB-catalyzed kinetic resolution of chlorohydrin **15** after one hour of reaction. The analysis was performed on a Chiralcel OD-H column with hexane and 2-propanol (90:10) as eluent and 1 mL/min flow, and with a detection wavelength of 254.4 nm. The retention times obtained are t_R((*R*)-**15**) = 14.82 min and t_R((*S*)-**15**) = 15.94 min.

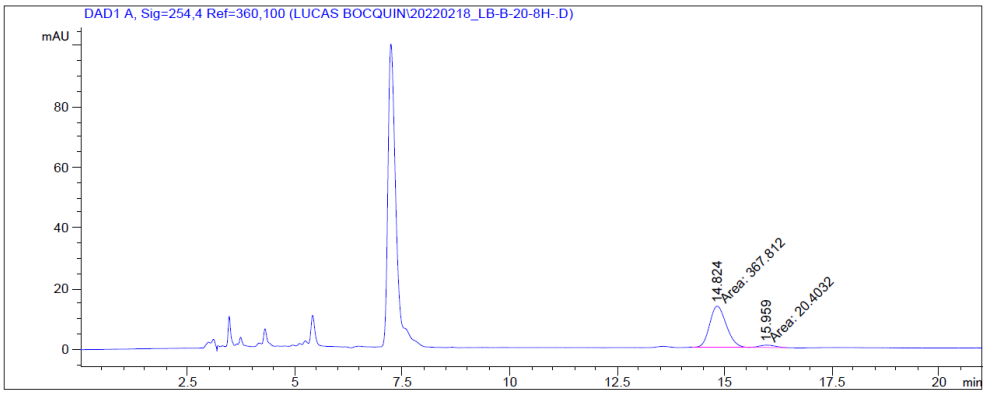

Figure 2.3.8: Chiral HPLC chromatogram of the CALB-catalyzed kinetic resolution of chlorohydrin **15** after 8 hours of reaction. The retention times obtained are t_R((*R*)-**15**) = 14.82 min and t_R((*S*)-**15**) = 15.96 min.

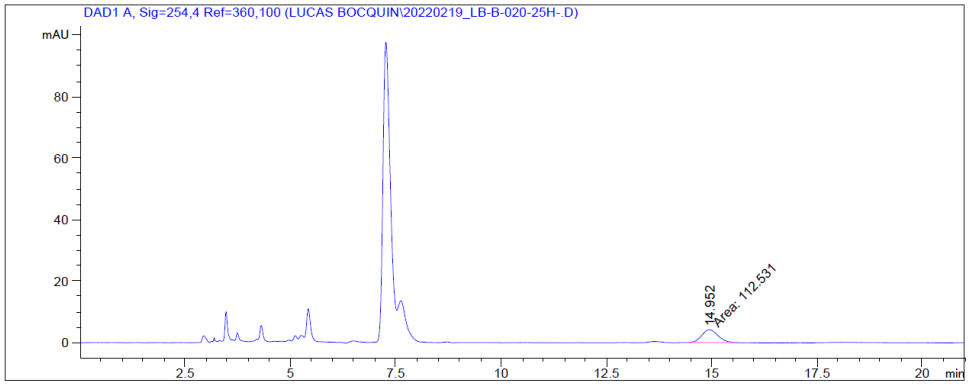

Figure 2.3.9: Chiral HPLC chromatogram of the CALB-catalyzed kinetic resolution of chlorohydrin **15** after 25 hours of reaction. The retention times obtained are t_R((R)-**15**) = 14.95 min.

Chiral HPLC analyses of the samples using a mobile phase composition of hexane (96%) and 2-propanol (4%) were also performed to measure the enantiomeric excess of the ester **16** produced. These values were then used to determine an enantiomeric ratio E of 52 (calculated from E&K Calculator 2.1b0 PPC [29]) from the kinetic resolution of chlorohydrin **15** with CALB, and to plot the enantiomeric excesses of product **16** and the chlorohydrin **15** as a function of conversion, as shown in Figure 2.2.9. A value of 52 is not as good as what was obtained with penbutolol's precursor **8**. Because of this relatively low value, it is not possible to obtain an enantiomeric excess of more than 96% for ester **16**, even at a very low conversion. However, it is still possible to obtain a very good enantiomeric excess of chlorohydrin **15**, which is the main goal of this step.

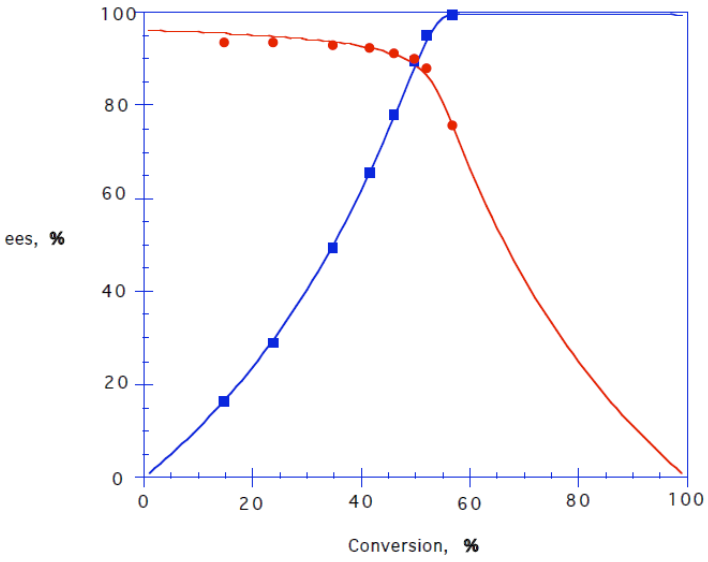

Figure 2.3.10: Enantiomeric excesses of ester **16** and chlorohydrin **15** as a function of conversion during the CALB-catalyzed kinetic resolution of chlorohydrin **15**. Enantiomeric excesses of product **16** are represented by red filled circle. Enantiomeric excesses of chlorohydrin **15** are represented by blue filled squares; E-value = 52. E-values calculated from E&K Calculator 2.1b0 PPC [29].

2.3.5.2 Large-scale kinetic resolution of chlorohydrin 15

A large-scaled kinetic resolution of **15** was then carried out and stopped after 25 hours. The reaction mixture was washed with distilled water several times in order to remove butyric acid. Chlorohydrin **15** and ester **16** were then separated by flash chromatography. The first fraction gave a mixture of ester (*S*)-**16** (68%) and butyric acid (32%) (^{1}H-NMR). The second fraction gave enantiopure chlorohydrin (*R*)-**15** as a transparent oil, with an enantiomeric excess of more than 99%, a yield of 44% and a purity of 82% (^{1}H-NMR), the other compounds present being butyric acid (around 5%) and unknown impurities (14%). For this type of reaction, the maximum theoretical yield is 50%, because ideally, half of the substrate is transformed into ester **16**. The specific rotation of the obtained chlorohydrin (*R*)-**15** was $[\alpha]_D^{20} - 17\ (\mathrm{c}\ 1.0, \mathrm{MeOH})$. Absolute configuration was determined by the enantioselectivity of CALB which has been reported previously [30].

2.3.5.3 Characterization of ester 16

Characterization of ester **16** was carried out by NMR spectroscopy, with deuterated chloroform as solvent. Ester **16** with numbered carbon atoms is shown in Figure 2.3.11, and assignment of chemical shifts are given in Table 2.3.4.

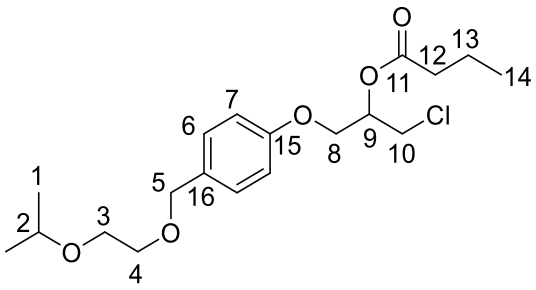

Figure 2.3.11: Ester **16** with numbered carbon and nitrogen atoms. Assignment of chemical shifts are given in Table 2.3.4, and all spectra are given in the appendix (Part 6.3.3).

Table 2.3.4: Characterization of ester **16** given ^{1}H-, ^{13}C-, H,H-COSY, HSQC- and HMBC-NMR (600 MHz, CDCl3), see the appendix (Part 6.3.3).

Atom number	^{1}H-NMR [ppm] (mult., int., ^{3}J)	^{13}C-NMR [ppm]	COSY	HMBC
1	1.17 (d, *J* = 6.1 Hz, 6H)	22.09	2	1',2
2	3.65 – 3.54 (m, 5H)	71.93	1	1,3
3	3.65 – 3.54 (m, 5H)	67.48	4	2,4
4	3.65 – 3.54 (m, 5H)	69.52	3	3,5
5	4.51 (s, 2H)	72.78	-	4,6,16
6	7.30 – 7.26 (m, 2H)	129.38	7	5,6',7,15
7	6.90 – 6.87 (m, 2H)	114.51	6	6,7',15,16
8	4.19 – 4.13 (m, 2H)	66.15	9	9,10,15
9	5.34 (p, *J* = 5.2 Hz, 1H)	70.81	8,10	8,10,11
10	3.85 (dd, *J* = 11.7, 5.0 Hz, 1H), 3.78 (dd, *J* = 11.7, 5.3 Hz, 1H)	42.62	9	8,9
11	-	172.85	-	-
12	2.41 – 2.30 (m, 2H)	36.09	13	11,13,14
13	1.68 (h, *J* = 7.4 Hz, 2H)	18.43	12,14	11,12,14
14	0.96 (t, *J* = 7.4 Hz, 3H)	13.58	13	12,13
15	-	157.81	-	-
16	-	131.39	-	-

2.3.6 Synthesis of (*S*)-bisoprolol (17)

(*S*)-Bisoprolol ((*S*)-**17**) was synthesized from chlorohydrin (*R*)-**15** and isopropylamine by adapting the procedure described by Banoth and Banerjee [81] and concerning the amination of similar chlorohydrins.

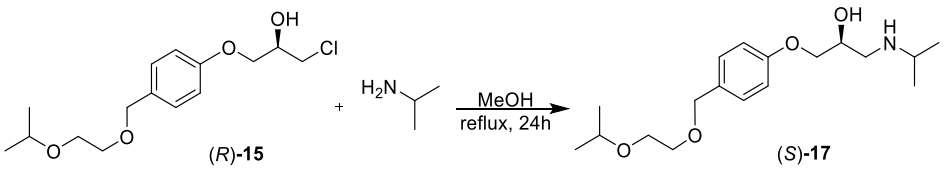

Scheme 2.3.11: Synthesis of (*S*)-Penbutolol from (*R*)-1-chloro-3-(2-cyclopentylphenoxy)propan-2-ol and tert-butylamine.

The product obtained showed a purity of 92% on the ^{1}H-NMR spectrum, but it is probably a mixture of (*S*)-**17** and its hydrochloride salt (*S*)-**17*HCl*** shown in Figure 2.3.12. More explanation on the formation of this type of mixture and their NMR analyses is given in part

2.2.4. The yield cannot be calculated exactly at this step, and depending on the amount of free base and of hydrochloric salt, it is somewhere between 83% and 92%.

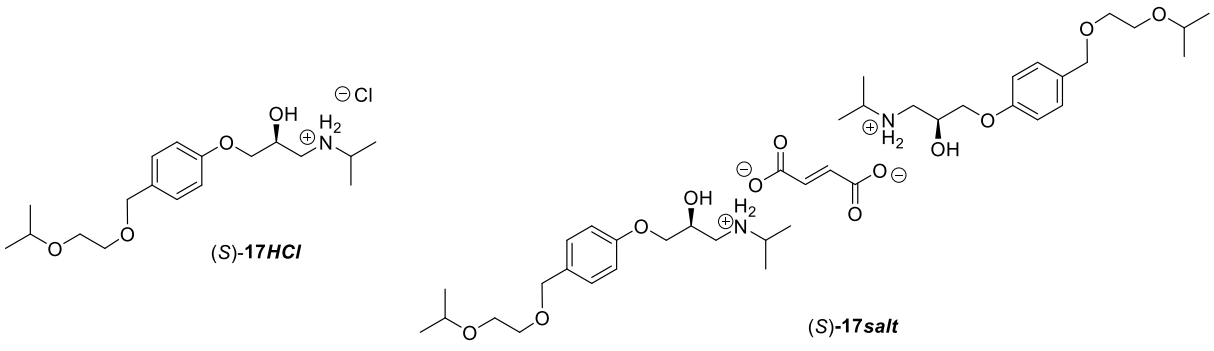

Figure 2.3.12: Structures of (*S*)-Bisoprolol hydrochloride ((*S*)-**17*HCl***) and (*S*)-bisoprolol hemifumarate ((*S*)-**17*salt***)

The specific rotations of (*S*)-bisoprolol ((*S*)-**17**) and (*S*)-bisoprolol hydrochloride ((*S*)-**17*HCl***) have not been reported, but the one of (*S*)-bisoprolol hemifumarate ((*S*)-**17*salt***) was reported to be $[\alpha]_D^{21} - 20.6$ (c 1.0, MeOH) by Kitaori *et al.* [57]. The enantiomeric excess of their product was not written. In order to compare this optical rotation with the one of the product obtained for this thesis, the procedure described in this article was followed to form (*S*)-bisoprolol hemifumarate ((*S*)-**17*salt***) from (*S*)-**17**. The structure of (*S*)-**17*salt*** is shown in Figure 2.3.12.

Racemic **17*salt*** was synthesized in order to determine the retention times of its (*R*)- and (*S*)-enantiomers on chiral HPLC. Separation of the enantiomers of **17*salt*** was obtained by using a Chiralcel OD-H column, a mobile phase composition of hexane (90%) and 2-propanol containing 2% diethanolamine (10%) as eluent and a 1 mL/min flow. The retention times obtained are t_R((R)-**17*salt***) = 7.92 min and t_R((S)-**17*salt***) = 11.8 min (see Figure 6.3.26 in the appendix). The resolution factor is R_S((S)/(R)-**17*salt***) = 7.02. Diethanolamine was added to the 2-propanol in the mobile phase in order to obtain a better separation, and to deprotonate the amine in **17*salt***, to solubilize better the analyte.

Enantiopure (*S*)-**17*salt*** was synthesized from chlorohydrin (*R*)-**15** with a yield of 92%, a purity of 90%, and an enantiomeric excess of more than 96% (chiral HPLC).

The specific rotation of the obtained product was $[\alpha]_D^{20} - 17$ (c 1.0, MeOH). This is the same sign as the specific rotation obtained by Kitaori *et al.* [57], which confirms that the enantiomer formed is (*S*)-**17*salt***.

2.3.6.1 Reaction mechanism for the amination (*R*)-15 using isopropylamine

A mechanism for the amination (*R*)-**15** using isopropylamine is suggested in Scheme 2.2.9. The hydrochloric salt **17*HCl*** is formed only in limited amounts. The next step involving the synthesis of (*S*)-bisoprolol hemifumarate ((*S*)-**17*salt***) is an acid-base reaction. Because fumaric acid has two carboxyl groups and only 0.5 equivalents of it are added, each molecule of fumarate forms a salt with two molecules of (*S*)-**17*salt***.

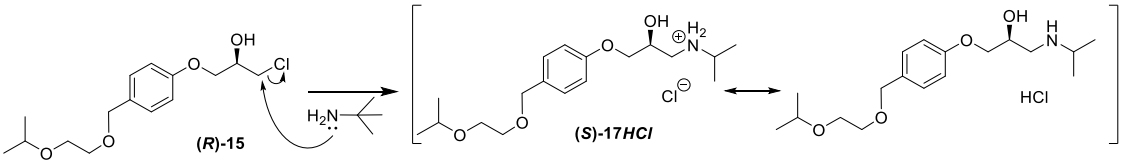

Scheme 2.3.12: Mechanism for the amination of chlorohydrin (*R*)-**15** using tert-butylamine.

2.3.6.2 Characterization of bisoprolol (17) and bisoprolol hemifumarate (17*salt*)

Characterization of compounds **17** and **17*salt*** were carried out by NMR spectroscopy, with deuterated chloroform as solvent. The compound **17** analyzed is actually probably containing compound **17*HCl*** as discussed before, but this will only affect the shift of some peaks.

Compound **17** with numbered carbon atoms is shown in Figure 2.3.13, and assignment of chemical shifts are given in Table 2.3.5.

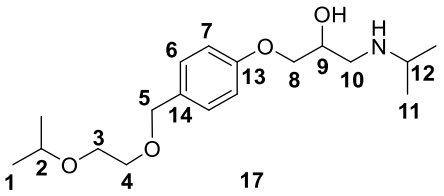

Figure 2.3.13: Compound **17** with numbered carbon and nitrogen atoms. Assignment of chemical shifts are given in Table 2.3.5, and all spectra are given in the appendix (Part 6.3.4).

Table 2.3.5: Characterization of compound **17** given ^{1}H-, ^{13}C-, H,H-COSY, HSQC- and HMBC-NMR (600 MHz, CDCl3), see the appendix (Part 6.3.4).

Atom number	**^{1}H-NMR [ppm] (mult., int., ^{3}J)**	**^{13}C-NMR [ppm]**	**COSY**	**HMBC**
1	1.10 (d, *J* = 6.1 Hz, 6H)	22.09	2	1',2
2	3.58 – 3.49 (m, 5H)	71.91	1	1,3
3	3.58 – 3.49 (m, 5H)	67.48	4	2,4
4	3.58 – 3.49 (m, 5H)	69.47	3	3,5
5	4.44 (s, 2H)	72.85	-	4,6,14
6	7.21 – 7.18 (m, 2H)	129.35	7	5,6',7,13
7	6.83 – 6.80 (m, 2H)	114.43	6	7',13,14
8	3.96 – 3.87 (m, 3H)	70.56	9	9,10,13
9	3.96 – 3.87 (m, 3H)	68.50	8,10	8,10
10	2.66 (dd, *J* = 12.1, 7.4 Hz, 1H) 2.82 (dd, *J* = 12.2, 3.7 Hz, 1H)	49.19	8,9,10',11,12	8,9,10',12
11	1.02 (d, *J* = 6.3 Hz, 6H)	23.05/23.19	12	11',12
12	2.76 (p, *J* = 6.3 Hz, 1H)	48.94	11	10,11
13	-	158.28	-	-
14	-	130.93	-	-

Compound **17*salt*** with numbered carbon atoms is shown in Figure 2.3.14, and assignment of chemical shifts are given in Table 2.3.6.

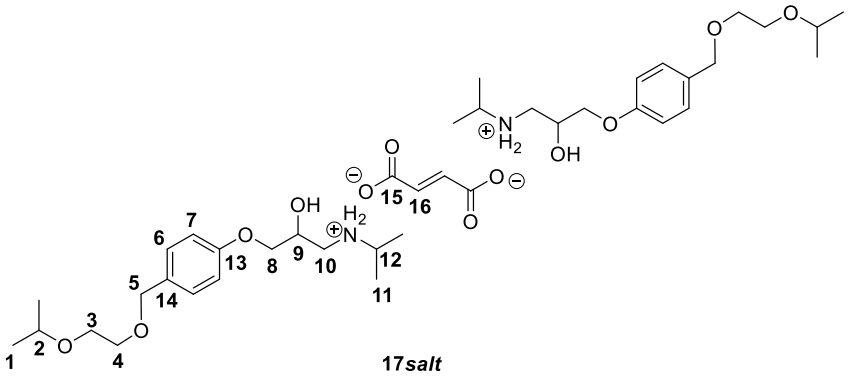

Figure 2.3.14: Compound **17*salt*** with numbered carbon and nitrogen atoms. Assignment of chemical shifts are given in Table 2.3.6, and all spectra are given in the appendix (Part 6.3.5).

Table 2.3.6: Characterization of compound **17*salt*** given ^{1}H-, ^{13}C-, H,H-COSY, HSQC- and HMBC-NMR (600 MHz, CDCl3), see the appendix (Part 6.3.5).

Atom number	**^{1}H-NMR [ppm] (mult., int., ^{3}J)**	**^{13}C-NMR [ppm]**	**COSY**	**HMBC**
1	1.16 (d, *J* = 6.1 Hz, 12H)	22.09	2	1',2
2	3.63 – 3.54 (m, 10H)	71.92	1	1,3
3	3.63 – 3.54 (m, 10H)	67.46	4	1,4
4	3.63 – 3.54 (m, 10H)	69.51	3	3,5
5	4.48 (s, 4H)	72.80	-	4,6,13,14
6	7.24 (d, *J* = 8.3 Hz, 4H)	129.37	7	5,6',7,13
7	6.87 – 6.83 (m, 4H)	114.38	6	7',13,14
8	4.04 (dd, *J* = 9.6, 4.3 Hz, 2H), 3.97 (dd, *J* = 9.7, 6.1 Hz, 2H)	70.11	9	9,10,13
9	4.52 (dt, *J* = 11.6, 6.1 Hz, 2H)	65.25	8,10	-
10	3.04 (dd, *J* = 12.1, 2.8 Hz, 2H), 3.14 (t, *J* = 11.2 Hz, 2H)	48.29	9	8,9,12
11	1.36 (d, *J* = 6.5 Hz, 6H), 1.32 (d, *J* = 6.5 Hz, 6H)	19.60, 19.06	12	11',12
12	3.28 (p, *J* = 6.5 Hz, 2H)	50.63	11	10,11
13	-	157.99	-	-
14	-	131.10	-	-
15	-	173.28	-	-
16	6.65 (s, 2H)	136.16	-	15,16'

3 Conclusion

Sotalol precursor (*R*)-**5** was synthesized from aniline in three steps with a combined yield of 53%. The obtained product had an enantiomeric excess of 81%. The reaction carried out to synthesize (*R*)-sotalol precursor (*R*)-**5** and other derivatives, as well as the yields obtained, are shown in Scheme 3.1.

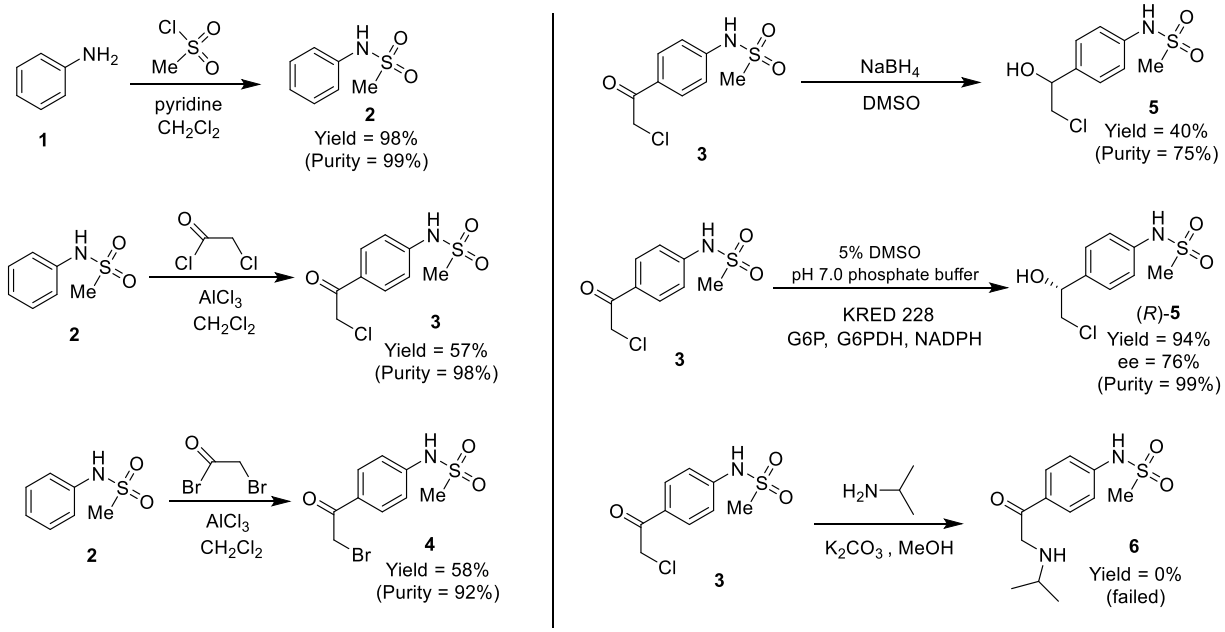

Scheme 3.1: Summary of the reactions carried out to synthesize (*R*)-N-(4-(2-chloro-1-hydroxyethyl)phenyl)methanesulfonamide ((*R*)-**5**)

(*S*)-Penbutolol hydrochloride ((*S*)-**10*HCl***) was obtained from 2-cyclopentylphenol in five steps with a combined yield of 20% and an enantiomeric excess of 99%. The reaction performed to synthesize (*S*)-penbutolol hydrochloride ((*S*)-**10*HCl***), as well as the yields obtained, are shown in Scheme 3.2.

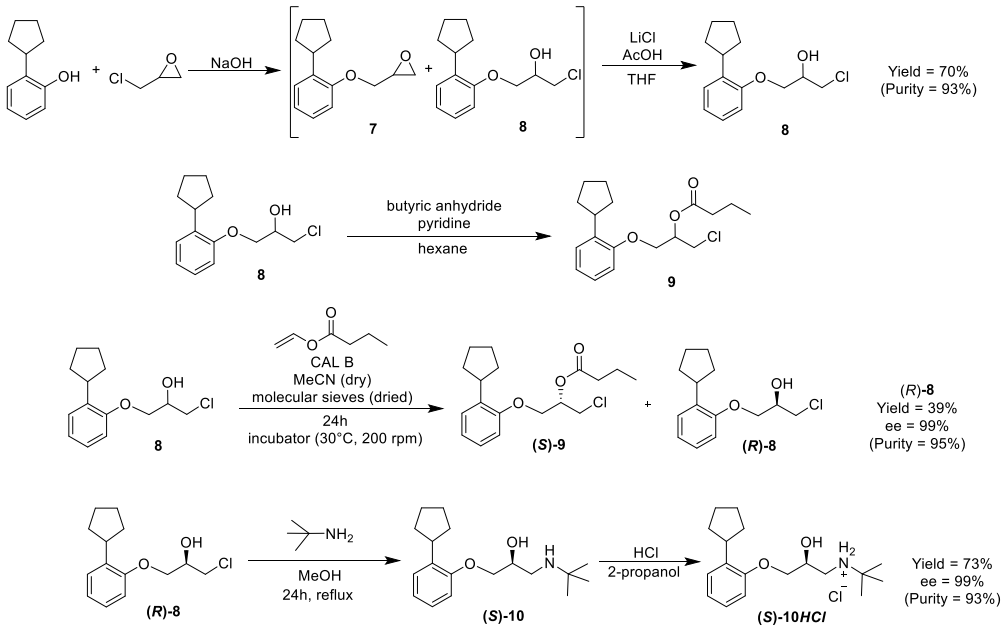

Scheme 3.2: Summary of the reactions carried out to synthesize (*S*)-penbutolol.

(*S*)-Bisoprolol hemifumarate ((*S*)-**17*salt***) was synthesized from 4-(hydroxymethyl)phenol in six steps with a combined yield of 19% and an enantiomeric excess of more than 96%. The reaction carried out to synthesize (*S*)-bisoprolol ((*S*)-**17**), as well as the yields obtained, are shown in Scheme 3.3.

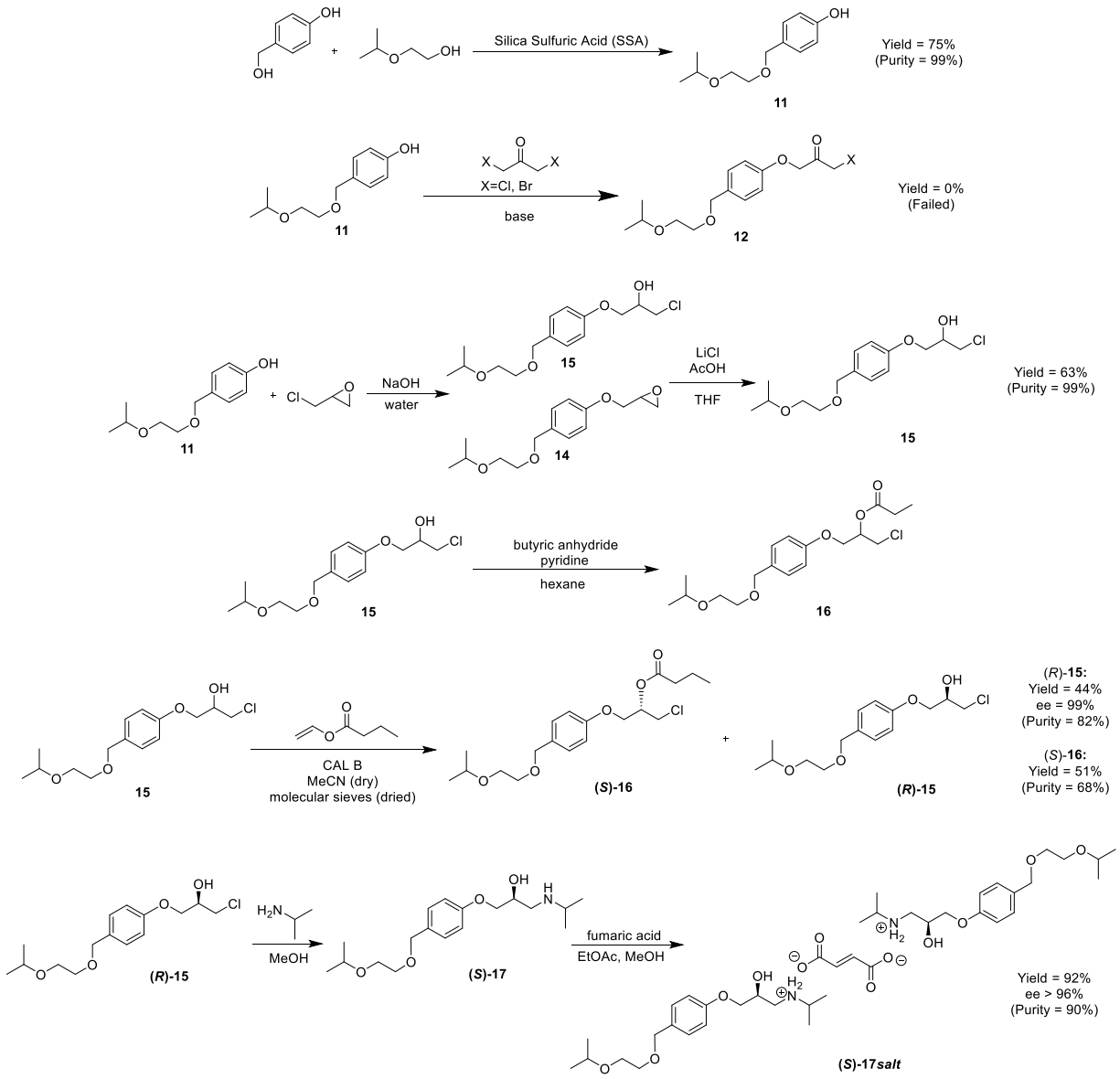

Scheme 3.3: Summary of the reactions carried out to synthesize (*S*)-bisoprolol.

4 Experimental

4.1 General methods

All experiments and analyses were carried out at the Department of Chemistry, in the Faculty of Natural Sciences of the University of Science and Technology (NTNU), Trondheim, Norway.

4.1.1 Chemicals, solvents and enzymes

Chemicals used in this thesis are all commercially available and of analytical quality. The non-enzymatic chemicals were bought from Sigma Aldrich (Oslo, Norway), VWR (Oslo, Norway). The water used was of distilled grade, and heating was performed using an oil bath. The laboratory work has been carried out following the university's HSE guidelines.

All solvents used for HPLC analyses were of HPLC grade.

Activation of molecular sieves

Molecular sieves (1/8 pellets, pore diameter 4Å) were dried at 1000 °C for 24 hours and stored in a desiccator.

Dry solvents

Dry solvents were obtained from a solvent purifier from MBraun (Munich, Germany) and use right afterwards or stored under nitrogen and in the presence of molecular sieves.

Enzymes

Candida antarctica Lipase B (activity > 10 000 PLU/g, lot no. 20170315) immobilized on styrene/methacrylate polymer was gifted from SyncoZymes Co, Ltd. (Shanghai,China). Crystalline KRED 228, KRED 130 and KRED 113 were gifted from SyncoZymes Co, Ltd. (Shanghai,China).

Glucose-6-phosphate dehydrogenase from *Leuconostoc mesenteroides* (G6P-DH, lyophilized powder, 550-1100 U/mg, lot no. G5885-2KU) and from *S. cerevisae* (G6P-DH, ammonium sulfate suspension, 5787 U/mL, lot no. SLCB1507) were purchased from Sigma-Aldrich. Glucose-6-phosphate (G6P, lot no. 10127647001) was purchased from Sigma-Aldrich.

Dihydronicotinamide-adenine dinucleotide phosphate (NADPH, lot no. 20160712-2) was gifted from SyncoZymes Co, Ltd. (Shanghai,China).

4.1.2 Chromatographic analyses

Thin layer chromatography (TLC)

TLC analyses were carried out using precoated Merck silica gel 60 F_{245} (0.2 mm) plates bought from Sigma Aldrich (Oslo, Norway). Identification of the compounds was performed under ultraviolet light (254 nm).

Flash chromatography

Silica gel used in flash chromatography was bought from Sigma Aldrich (pore size 60 Å, 230-240 mesh particle size, 40-63 μm particle size).

Chiral HPLC

Chiral HPLC analyses were performed Agilent HPLC 1200 (Series system Santa Clara, CA, USA) equipped with an autosampler and a variable wavelength detector (VWD), set to 254 nm unless otherwise stated. Separations were performed using a Chiralcel OD-H column (250 mm L × 4.6 mm ID; 5 μm) (Chiral Technologies Europe, Gonthier d´Andernach, Illkirch, France).

4.1.3 Spectroscopic analyses

Nuclear magnetic resonance (NMR)

NMR characterizations were performed on a 600 MHz Bruker Avance III UltraShield from Bruker Corporation (Fällanden, Switzerland), equipped with a CryoProbe 5 mm TCI probehead. Some other analyses were performed on a 400 MHz Bruker Avance III HD NMR Spectrometer from Bruker Corporation (Fällanden, Switzerland), equipped with a SmartProbe 5 mm probehead. The spectroscopic data were analyzed with Mestrelab Research software MestReNova 14.2.0-26256.

Mass spectrometry (MS)

Accurate mass determination in positive and negative mode was performed on a "Synapt G2-S" Q-TOF instrument from Water TM. Samples were ionized by the use of ASAP probe (APCI) or ESI probe. No chromatographic separation was used previous to the mass analysis. Calculated exact mass and spectra processing was done by Waters TM Software Masslynx V4.1 SCN871.

4.1.4 Other methods

Shaker

Enzymatic reactions were performed in a New Brunswick G24 Environmental Shaker from New Brunswick Co. (Edison, New Jersey, USA).

Optical rotation

Optical rotation measurements were performed using an Anton Paar MCP 5100 polarimeter with a 10 mm long cell from Dipl. Ing. Houm AS (Oslo, Norway). Analyses were carried out at 20°C unless otherwise stated, and at a wavelength of 589 nm.

4.2 Synthesis of chemical compounds

N-phenylmethanesulfonamide (**1**)

A mixture of aniline (49 μL, 50 mg, 0.54 mmol) and pyridine (44 μL, 43 mg, 0.54 mmol) in CH_2Cl_2 (15 mL) under inert atmosphere was cooled down to 0 °C. Methanesulfonyl chloride (46 μL, 68 mg, 0.60 mmol) was added dropwise, and the reaction mixture was stirred for 1 h at 0 °C. The solution was then warmed to rt, and stirred for 24 h. Pyridine and the solvent were then removed under reduced pressure, and the obtained product was dissolved in CH_2Cl_2 (10 mL). The organic phase was washed with dist. H_2O (10 mL), and the aqueous phase was extracted with CH_2Cl_2 (10 mL). The combined organic layers were then washed with a saturated $MgSO_4$ solution (5 × 15 mL) until the color of the solution had almost completely disappeared. The organic phase was then dried over anhydrous $MgSO_4$, filtered, and the solvent was evaporated under reduced pressure. N-phenylmethanesulfonamide (**1**) was obtained as a white solid (90 mg, 0.53 mmol, 98% yield, 99% purity (^{1}H-NMR)). ^{1}H NMR (600 MHz, DMSO) δ 9.72 (s, 1H), 7.37 - 7.30 (m, 2H), 7.25 - 7.18 (m, 2H), 7.13 - 7.06 (m, 1H), 2.98 (s, 3H). ^{13}C NMR (151 MHz, DMSO) δ 138.86, 129.76, 124.31, 120.26, 39.64. The analysis is consistent with previously reported data [86].

N-(4-(2-chloroacetyl)phenyl)methanesulfonamide (**2**)

$AlCl_3$ (8.04 g, 60 mmol) in suspension in CH_2Cl_2 (15 mL) and under inert atmosphere was cooled down to –10 °C. 2-Chloroacetyl chloride (3.25 mL, 4.62 g, 40.9 mmol) diluted in CH_2Cl_2 (15 mL) was added dropwise to the reaction mixture, followed by N-phenylmethanesulfonamide (**1**) (3.42 g, 20 mmol) in CH_2Cl_2 (20 mL). The solution was stirred for 1 h at –10 °C, and for 24 h at rt. The solution was then poured into a mixture of concentrated

HCl (25 mL) and ice-cold water (80 mL). The solution was filtrated, and the obtained solid was dissolved in EtOAc (500 mL). The organic phase was washed with dist. H_2O (100 mL) and with a saturated NaCl solution (3 × 80 mL), and dried over anhydrous $MgSO_4$. The solvent was removed under reduced pressure, and the obtained solid was recrystallized from MeOH to give compound **2** as light brown crystals (2.81 g, 11.3 mmol, 57% yield, 98% purity (^{1}H-NMR)). ^{1}H NMR (600 MHz, DMSO) δ 10.43 (s, 1H), 8.01 - 7.92 (m, 2H), 7.34 - 7.25 (m, 2H), 5.12 (s, 2H), 3.14 (s, 3H). ^{13}C NMR (151 MHz, DMSO) δ 190.64, 144.10, 130.70, 129.34, 117.92, 47.76, 40.49. The ^{1}H-NMR analysis is consistent with previously reported data [72].

N-(4-(2-bromoacetyl)phenyl)methanesulfonamide (**3**)

$AlCl_3$ (8.04 g, 60 mmol) in suspension in CH_2Cl_2 (15 mL) and under inert atmosphere was cooled down to –10 °C. 2-Bromoacetyl chloride (3.25 mL, 4.62 g, 40.9 mmol) diluted in CH_2Cl_2 (15 mL) was added dropwise to the reaction mixture, followed by N-phenylmethanesulfonamide (**1**) (3.42 g, 20 mmol) in CH_2Cl_2 (20 mL). The solution was stirred for 1 h at –10 °C, and for 24 h at rt. The solution was then poured into a mixture of concentrated HCl (25 mL) and ice-cold water (80 mL). The solution was filtrated, and the obtained solid was dissolved in EtOAc (500 mL). The organic phase was washed with dist. H_2O (100 mL) and with a saturated NaCl solution (3 × 80 mL), and dried over anhydrous $MgSO_4$. The solvent was removed under reduced pressure, and the obtained solid was recrystallized from MeOH to give compound **3** as light brown crystals (2.81 g, 11.3 mmol, 58% yield, 92% purity (^{1}H-NMR)). ^{1}H NMR (600 MHz, DMSO) δ 10.44 (s, 1H), 8.01 - 7.97 (m, 2H), 7.32 - 7.28 (m, 2H), 4.85 (s, 2H), 3.14 (s, 3H). ^{13}C NMR (151 MHz, DMSO) δ 190.82, 144.12, 131.13, 128.98, 117.89, 40.53, 34.14.

N-(4-(2-chloro-1-hydroxyethyl)phenyl)methanesulfonamide (**4**)

To a solution of N-(4-(2-chloroacetyl)phenyl)methanesulfonamide (**2**) (0.30 g, 1.21 mmol) in DMSO (10mL) was added slowly $NaBH_4$ (0.09 g, 2.42 mmol). The reaction mixture was stirred for 4 d, and then poured into 15mL of ice-water. An aqueous HCl solution (2.5 mL, 1 M) was added, and the mixture was stirred for 10 min. The product was extracted with EtOAc (2 × 20mL), and the organic layer was washed with a saturated NaCl solution (7 × 20mL) and dried over anhydrous $MgSO_4$. The solvent was removed under reduced pressure, and the product was placed under vacuum overnight to remove any remaining DMSO. The obtained product was purified by flash chromatography (n-pentane: ethyl acetate, 6:4, v/v) to give compound **4** as a white solid (120 mg, 0.48 mmol, 40% yield, 75% purity (^{1}H-NMR)). Chiral

HPLC eluent: hexane:*i*-PrOH (90:10), flow 1 mL/min. t_R((*S*)-**4**) = 50.51 min and t_R((*R*)-**4**) = 63.51 min. R_S ((R)/(S)-**4**) = 3.45. ^{1}H NMR (600 MHz, DMSO) δ 9.72 (s, 1H), 7.38 – 7.33 (m, 2H), 7.20 - 7.16 (m, 2H), 5.75 (d, *J* = 4.7 Hz, 1H), 4.73 (dt, *J* = 7.1, 4.7 Hz, 1H), 3.73 (dd, *J* = 11.0, 4.6 Hz, 1H), 3.65 (dd, *J* = 11.0, 7.1 Hz, 1H), 2.98 (s, 3H). ^{13}C NMR (151 MHz, DMSO) δ 137.77, 137.58, 127.32, 119.52, 71.96, 50.22, 40.43. The ^{1}H-NMR analysis is consistent with previously reported data [44].

(*R*)-N-(4-(2-chloro-1-hydroxyethyl)phenyl)methanesulfonamide ((*R*)-**4**)

To a solution of KRED 228 (5.5 mg), NADPH (1.5 mg), G6P (41 mg), G6PDH (0.6 mg) in a potassium phosphate buffer (0.1 M, pH 7.4, 5 mL) was added N-(4-(2-chloroacetyl)phenyl)methanesulfonamide (**2**) (20 mg, 81 μmol) in DMSO (0.25 mL). The reaction was run for 18 h in an incubator at 200 rpm and 38°C. The product was extracted with EtOAc (5 × 10 mL) and washed with dist. H_2O (2 × 20 mL). The organic phase was dried over anhydrous $MgSO_4$. The solvent was removed under reduced pressure to give (*R*)-N-(4-(2-chloro-1-hydroxyethyl)phenyl)methanesulfonamide ((*R*)-**4**) as a white solid (19 mg, 76 μmol, 94% yield, 99% purity (^{1}H-NMR), ee = 76% (chiral HPLC)). $[\alpha]_D^{20} - 17.5$ (c 1.03, EtOH). ^{1}H NMR (600 MHz, DMSO) δ 9.72 (s, 1H), 7.38 - 7.33 (m, 2H), 7.20 - 7.16 (m, 2H), 5.75 (d, *J* = 4.7 Hz, 1H), 4.73 (dt, *J* = 7.1, 4.7 Hz, 1H), 3.73 (dd, *J* = 11.0, 4.6 Hz, 1H), 3.65 (dd, *J* = 11.0, 7.1 Hz, 1H), 2.98 (s, 3H). The analysis is consistent with previously reported data [44].

Attempt to synthesize N-(4-(isopropylglycyl)phenyl)methanesulfonamide (**5**)

To a solution of N-(4-(2-chloroacetyl)phenyl)methanesulfonamide (**2**) (142 mg, 0.57 mmol) in MeOH (10 mL) was added K_2CO_3 (158 mg, 1.14 mmol) and *i*-$PrNH_2$ (977 μL, 674 mg). The reaction mixture was stirred at rt for 18 h. Methanol and remaining *i*-$PrNH_2$ were removed under reduced pressure. The obtained product was dissolved into CH_2Cl_2 (30 mL), and washed with a saturated NaCl solution (10 mL). The organic phase was dried over anhydrous $MgSO_4$, and the solvent was removed under reduced pressure. The desired product was not isolated.

Synthesis of 1-chloro-3-(2-cyclopentylphenoxy)propan-2-ol (**8**) using NaOH as a base

To a solution of NaOH (160 mg, 4.00 mmol) in dist. H_2O (4 mL) was added 2-cyclopentylphenol (432 mg, 2.66 mmol). The reaction mixture was stirred for 1 min, and 2-(chloromethyl)oxirane (epichlorohydrin) (431 μL, 509 mg, 5.50 mmol) was added. The mixture was stirred at rt for 48 h. Dist. H_2O (10 mL) was then added and the product was extracted with

EtOAc (3 × 10 mL). The combined organic phases were washed with a saturated NaCl solution (10 mL), dried over anhydrous MgSO4, and the solvent was removed under reduced pressure, yielding 619 mg of a mixture of 2-cyclopentylphenol, 2-((2-cyclopentylphenoxy)methyl)oxirane (**7**) and 1-chloro-3-(2-cyclopentylphenoxy)propan-2-ol (**8**) as a slightly yellow oil.

A mixture of **7**/**8** (570 mg) was dissolved in THF (3 mL). AcOH (409 μL, 429 mg, 7.14 mmol) and LiCl (303 mg, 7.15 mmol) were added. The reaction mixture was stirred at rt for 24 h. The solution was then concentrated under reduced pressure. The obtained product was dissolved in EtOAc (10 mL), and washed with dist. H_2O (10 mL). The aqueous phase was extracted with EtOAc (10 mL). The combined organic phases were washed with a saturated NaCl solution (10 mL), dried over anhydrous $MgSO_4$, and the solvent was removed under reduced pressure. The product was purified by flash chromatography (n-pentane:ethyl acetate, 9:1, v/v) yielding chlorohydrin **8** as a colorless oil (435 mg, 1.71 mmol, 70% yield, 93% (^{1}H-NMR)). TLC (n-pentane:ethyl acetate, 9:1, v/v) Rf = 0.34 for product **8**. Chiral HPLC eluent: hexane:*i*-PrOH (90:10), flow 1 mL/min. t_R((S)-**8**) = 6.63 min and t_R((R)-**8**) = 7.31 min. R_S((S)/(R)-**8**) = 2.41. ^{1}H NMR (600 MHz, $CDCl_3$) δ 7.24 (dd, *J* = 7.5, 1.7 Hz, 1H), 7.16 (ddd, *J* = 8.1, 7.4, 1.7 Hz, 1H), 6.96 (td, *J* = 7.5, 1.2 Hz, 1H), 6.86 (dd, *J* = 8.2, 1.2 Hz, 1H), 4.25 (h, *J* = 5.3 Hz, 1H), 4.13 (dd, *J* = 9.4, 5.1 Hz, 1H), 4.09 (dd, *J* = 9.4, 5.4 Hz, 1H), 3.82 (dd, *J* = 11.2, 5.2 Hz, 1H), 3.76 (dd, *J* = 11.2, 5.6 Hz, 1H), 3.35 - 3.26 (m, 1H), 2.48 (d, *J* = 6.2 Hz, 1H), 2.04 - 1.56 (m, 8H). ^{13}C NMR (151 MHz, $CDCl_3$) δ 156.01, 134.89, 127.05, 126.84, 121.52, 111.67, 70.20, 68.79, 46.35, 39.19, 33.12, 25.62. The ^{1}H-NMR analysis is consistent with previously reported data [53].

Synthesis of 1-chloro-3-(2-cyclopentylphenoxy)propan-2-ol (**8**) using K_2CO_3 as a base

To a solution of 2-cyclopentylphenol (80 mg, 0.49 mmol) dissolved in MeCN (4 mL) was added K_2CO_3 (137 mg, 0.99 mmol). The reaction mixture was stirred for 1 min, and 2-(chloromethyl)oxirane (epichlorohydrin) (116 μL, 137 mg, 1.48 mmol) was added. The mixture was stirred under reflux for 48 h. It was then filtered, and the filtrate was concentrated under reduced pressure. The obtained product was dissolved in EtOAc (10 mL), and washed with dist. H_2O (10 mL). The aqueous phase was extracted with EtOAc (3 × 5 mL). The combined organic phases were washed with a saturated NaCl solution (10 mL), dried over anhydrous $MgSO_4$, and the solvent was removed under reduced pressure. A mixture of epoxide **7** (78%), chlorohydrin **8** (7%), 2-cyclopentylphenol (2%) and byproducts (13%) was obtained

as a colorless oil (90 mg) (^{1}H-NMR). The opening reaction of epoxide **7** into chlorohydrin **8** was not performed.

Derivatization reaction of 1-chloro-3-(2-cyclopentylphenoxy)propan-2-ol (**8**)

To a solution of 1-chloro-3-(2-cyclopentylphenoxy)propan-2-ol (**8**) (6 mg, 0.02 mmol) in hexane (0.5 mL) was added pyridine (one drop) and butyric anhydride (one drop). The reaction mixture was heated at 60°C for 1 h. Hexane (5 mL) was then added, and the solution was washed with dist. H_2O (5 × 0.5 mL). The organic phase was then dried over anhydrous $MgSO_4$ and filtered. The filtrate was analyzed by chiral HPLC. Chiral HPLC eluent: hexane:*i*-PrOH (99.4:0.6), flow 1 mL/min. t_R((*S*)-**9**) = 8.05 min and t_R((*R*)-**9**) = 9.37 min. R_S((S)/(R)-**9**) = 1.56.

Monitored CALB catalyzed kinetic resolution of 1-chloro-3-(2-cyclopentylphenoxy)propan-2-ol (**8**)

To a solution of 1-chloro-3-(2-cyclopentylphenoxy)propan-2-ol (**8**) (20 mg, 79 μmol) dissolved in dry MeCN (2.5 mL) were added activated molecular sieves (4Å), vinyl butyrate (50 μL, 45 mg, 0.39 mmol) and CALB (36 mg). The mixture was placed in an incubator shaker (38 °C, 200 rpm.). Samples of 125 μL were taken regularly until 23 h of reaction. For each sample, hexane (1.5 mL) was added and the solution was washed with dist. H_2O (5 × 1 mL). The organic phase was then dried over anhydrous $MgSO_4$ and analyzed by chiral HPLC. ee_s, ee_p and c were calculated from the chromatograms.

Large-scale CALB catalyzed kinetic resolution of 1-chloro-3-(2-cyclopentylphenoxy)propan-2-ol (**8**)

To a solution of 1-chloro-3-(2-cyclopentylphenoxy)propan-2-ol (**8**) (163 mg, 0.63 mmol) dissolved in dry MeCN (20 mL) were added activated molecular sieves (4Å), vinyl butyrate (408 μL, 364 mg, 3.18 mmol) and CALB (280 mg). The mixture was placed in an incubator shaker (38 °C, 200 rpm.) for 23 h. Enzymes and molecular sieves were filtered off and solvents were removed in vacuo. The obtained product was dissolved in EtOAc (10 mL), and was washed with dist. H_2O (3 × 15 mL) and a saturated NaCl solution (10 mL). The solution was dried over anhydrous $MgSO_4$, and the solvent was removed under reduced pressure. (*R*)-1-chloro-3-(2-cyclopentylphenoxy)propan-2-ol ((*R*)-**8**) and (*S*)-1-chloro-3-(2-cyclopentylphenoxy)propan-2-yl butyrate ((*S*)-**9**) were separated by flash chromatography (n-pentane: ethyl acetate, 9:1, v/v). (*R*)-**8** was obtained as a colorless oil (63 mg, 0.243 mmol, 39%

yield, 95% purity (^{1}H-NMR), ee = 99% (chiral HPLC)). $[\alpha]_D^{25} -14$ (c 1.0, MeOH). ^{1}H NMR (600 MHz, $CDCl_3$) δ 7.31 - 7.26 (m, 2H), 6.91 - 6.87 (m, 2H), 4.51 (s, 2H), 4.21 (q, *J* = 5.1 Hz, 1H), 4.12 - 4.05 (m, 2H), 3.80 - 3.70 (m, 2H), 3.66 - 3.53 (m, 5H), 2.51 (d, *J* = 5.9 Hz, 1H), 1.17 (d, *J* = 6.1 Hz, 6H).

Synthesis of racemic penbutolol (**10**) in water

To a mixture of 1-chloro-3-(2-cyclopentylphenoxy)propan-2-ol (**8**) (22 mg, 0.09 mmol) in dist. H_2O (0.36 mL) was added *tert*-butylamine (1.20 mL, 0.84 g, 11 mmol). The mixture was stirred at rt for 24 h. EtOAc (10 mL) was added, and the organic layer was washed with dist. H_2O (5 mL). The organic phase was dried over anhydrous $MgSO_4$, and the solvent was removed under reduced pressure to give penbutolol (**10**) as a white solid (16 mg, 0.05 mmol, 64% purity (^{1}H-NMR)). ^{1}H NMR (600 MHz, $CDCl_3$) δ 7.22 (dd, *J* = 7.5, 1.7 Hz, 1H), 7.18 - 7.11 (m, 1H), 6.93 (td, *J* = 7.5, 1.1 Hz, 1H), 6.83 (dd, *J* = 8.2, 1.1 Hz, 1H), 4.10 (dd, *J* = 9.5, 4.6 Hz, 1H), 3.98 (dd, *J* = 9.5, 6.1 Hz, 1H), 3.31 (tt, *J* = 9.4, 7.4 Hz, 1H), 3.21 (dd, *J* = 12.2, 2.8 Hz, 1H), 2.99 (dd, *J* = 12.2, 9.2 Hz, 1H), 2.03 - 1.56 (m, 8H), 1.39 (d, *J* = 6.6 Hz, 9H).

Synthesis of (*S*)-penbutolol hydrochloride ((*S*)-**10*HCl***) in methanol

To a mixture of (*R*)-1-chloro-3-(2-cyclopentylphenoxy)propan-2-ol ((*R*)-**8**) (31 mg, 0.12 mmol) in MeOH (2 mL) was added *tert*-butylamine (0.18 mL, 0.13 g, 1.71 mmol). The mixture was stirred under reflux for 24 h, and was then concentrated under reduced pressure. The obtained product was dissolved in EtOAc (10 mL) and washed with dist. H_2O (5 mL). The organic phase was dried over anhydrous $MgSO_4$, and the solvent was removed under reduced pressure to give a mixture of (*S*)-penbutolol ((*S*)-**10**) and (*S*)-penbutolol HCl ((*S*)-**10*HCl***) as a white solid (29 mg, 93% purity (^{1}H-NMR), ee = 99% (chiral HPLC)). $[\alpha]_D^{20} -14$ (c 1.0, MeOH). ^{1}H NMR (600 MHz, $CDCl_3$) δ 7.22 (dd, *J* = 7.5, 1.7 Hz, 1H), 7.17 - 7.11 (m, 1H), 6.92 (td, *J* = 7.4, 1.2 Hz, 1H), 6.85 (dd, *J* = 8.2, 1.2 Hz, 1H), 4.05 - 4.00 (m, 1H), 3.97 (ddt, *J* = 8.6, 7.0, 4.6 Hz, 2H), 3.35 - 3.28 (m, 1H), 2.88 (dd, *J* = 11.9, 3.7 Hz, 1H), 2.78 - 2.72 (m, 1H), 2.07 - 1.53 (m, 8H), 1.12 (s, 9H). ^{13}C NMR (151 MHz, $CDCl_3$) δ 156.48, 134.62, 126.78, 126.62, 120.84, 111.39, 70.61, 68.78, 50.32, 44.78, 39.30, 32.94, 32.87, 29.14, 25.46, 25.45.

The obtained mixture (10.0 mg) was then dissolved in *i*-PrOH (40 μL), and a solution of HCl in *i*-PrOH (5 %, 80 μL) was added. The reaction was run for 1 h, and the solvent was removed under reduced pressure to give (*S*)-penbutolol HCl ((*S*)-**10*HCl***) as a colorless solid (10.0 mg, 30.4 μmol, 73% yield, 93% purity (^{1}H-NMR), ee = 99% (chiral HPLC)). $[\alpha]_D^{20} -23$ (c 1.0, MeOH). ^{1}H NMR (600 MHz, $CDCl_3$) δ 9.81 (s, 1H), 8.32 (s, 1H), 7.22 (dd, *J* = 7.6,

1.7 Hz, 1H), 7.13 (td, *J* = 7.8, 1.7 Hz, 1H), 6.93 (td, *J* = 7.5, 1.1 Hz, 1H), 6.80 (dd, *J* = 8.2, 1.2 Hz, 1H), 4.69 - 4.60 (m, 1H), 4.12 (dd, *J* = 9.5, 4.3 Hz, 1H), 3.98 (dd, *J* = 9.6, 6.4 Hz, 1H), 3.34 (tdd, *J* = 16.9, 9.7, 7.6 Hz, 2H), 3.11 (dtd, *J* = 12.3, 9.6, 2.6 Hz, 1H), 2.04 - 1.54 (m, 8H), 1.50 (s, 9H). ^{13}C NMR (151 MHz, $CDCl_3$) δ 155.98, 134.55, 126.74, 126.70, 121.19, 111.33, 69.66, 65.83, 57.57, 45.92, 39.15, 32.89, 32.88, 25.90, 25.32.

Silica Sulfuric Acid catalyst

To a mixture of SiO_2 (10 g) in acetone (30 mL) was added slowly concentrated sulfuric acid (95 %, 6.5 mL). The solution was stirred for 1 h at rt, and the solvent was then removed under reduced pressure. The black paste obtained was placed in the oven at 180 °C overnight, and the obtained solid was crushed into a fine powder. The product was then stored in a desiccator.

4-((2-isopropoxyethoxy)methyl)phenol (**11**)

To a solution of 2-isopropoxyethan-1-ol (26.0 mL, 23.5 g, 0.23 mol) at 0 °C were added Silica Sulfuric Acid catalyst (2.01 g) and 4-(hydroxymethyl)phenol (1.99 g, 16.0 mmol). The reaction mixture was stirred for 24 h at rt, filtered, and the black filtrate was concentrated under reduced pressure. EtOAc (20 mL) was added, and the solution was washed with a saturated NaCl solution (3 × 15 mL). The aqueous phase was then extracted with EtOAc (15 mL). The combined organic layers were dried over anhydrous $MgSO_4$, and the solvent was removed under reduced pressure. The obtained product was purified by flash chromatography (n-pentane: ethyl acetate, 7:3, v/v) to give 4-((2-isopropoxyethoxy)methyl)phenol (**11**) as a slightly red oil (2.56 g, 12.2 mmol, 75% yield, 99% purity (^{1}H-NMR)). ^{1}H NMR (600 MHz, $CDCl_3$) δ 7.22 - 7.13 (m, 2H), 6.82 - 6.72 (m, 2H), 6.02 (s, 1H), 4.48 (s, 2H), 3.72 - 3.58 (m, 5H), 1.20 (d, *J* = 5.9 Hz, 6H). ^{13}C NMR (151 MHz, $CDCl_3$) δ 155.55, 129.75, 129.74, 115.26, 73.11, 72.21, 69.34, 67.48, 22.01. The analysis is consistent with previous reported data [87].

Attempts to synthesize 1-chloro-3-(4-((2-isopropoxyethoxy)methyl)phenoxy)propan-2-one (**12**)

The different procedures attempted are summarized in Table 2.3.2. None gave the desired product **12** in significant amounts. One of the procedures is detailed below.

To a solution of 4-((2-isopropoxyethoxy)methyl)phenol (25 mg, 0.12 mmol) in dry MeCN (5 mL) was added K_2CO_3 (67 mg, 0.34 mmol). 1,3-Dichloropropan-2-one (11 μL at 45 °C, 15 mg, 0.12 mmol) diluted in MeCN (5 mL) was added dropwise during 30 min. The

reaction mixture was stirred at rt for 24 h, filtered, and concentrated under reduced pressure. EtOAc (15 mL) were added, and the solution was washed with dist. H_2O (3 × 10 mL) and with a saturated NaCl solution (10 mL). The organic phase was dried over anhydrous $MgSO_4$, and the solvent was removed under reduced pressure to give a brown paste (31 mg) that did not contain compound **12** in significant amounts (^{1}H-NMR).

1-Chloro-3-(4-((2-isopropoxyethoxy)methyl)phenoxy)propan-2-ol (**15**)

To a solution of NaOH (80 mg, 2.00 mmol) in dist. H_2O (2 mL) was added 4-((2-isopropoxyethoxy)methyl)phenol (**11**) (209 mg, 0.99 mmol). The reaction mixture was stirred for 1 min, and 2-(chloromethyl)oxirane (epichlorohydrin) (157 µL, 185 mg, 2.00 mmol) was added. The mixture was stirred at rt for 48 h. Dist. H_2O (5 mL) was then added and the product was extracted with EtOAc (3 × 5 mL). The combined organic phases were washed with a saturated NaCl solution (15 mL), dried over anhydrous MgSO4, and the solvent was removed under reduced pressure, yielding 241 mg of a mixture mainly composed of 2-((4-((2-isopropoxyethoxy)methyl)phenoxy)methyl)oxirane (**14**) and 1-chloro-3-(4-((2-isopropoxyethoxy)methyl)phenoxy)propan-2-ol (**15**) (^{1}H-NMR) as a slightly yellow oil.

The obtained mixture (238 mg) was dissolved in THF (1 mL). AcOH (153 µL, 161 mg, 2.68 mmol) and LiCl (116 mg, 2.74 mmol) were added. The reaction mixture was stirred at rt for 24 h. The solution was then concentrated under reduced pressure. The obtained product was dissolved in EtOAc (10 mL), and washed with dist. H_2O (10 mL). The aqueous phase was extracted with EtOAc (2 × 10 mL). The combined organic phases were washed with a saturated NaCl solution (15 mL), dried over anhydrous $MgSO_4$, and the solvent was removed under reduced pressure. The product was purified by flash chromatography (n-pentane:ethyl acetate, 7:3, v/v) yielding 1-chloro-3-(4-((2-isopropoxyethoxy)methyl)phenoxy)propan-2-ol (**15**) as an uncolored oil (188 mg, 0.62 mmol, 63% yield, 99% purity (^{1}H-NMR)). TLC (n-pentane:ethyl acetate, 7:3, v/v): Rf = 0.45 for product **15**. Chiral HPLC eluent: hexane:*i*-PrOH (90:10), flow 1 mL/min. t_R((*R*)-**15**) = 14.81 min and t_R((*S*)-**15**) = 15.93 min. R_S((S)/(R)-**15**) = 1.63. ^{1}H NMR (600 MHz, $CDCl_3$) δ 7.33 - 7.29 (m, 2H), 6.93 - 6.89 (m, 2H), 4.54 (s, 2H), 4.24 (h, *J* = 5.5 Hz, 1H), 4.13 - 4.08 (m, 2H), 3.82 - 3.73 (m, 2H), 3.66 - 3.60 (m, 5H), 2.57 (d, *J* = 5.9 Hz, 1H), 1.20 (d, *J* = 6.1 Hz, 6H). ^{13}C NMR (151 MHz, $CDCl_3$) δ 157.79, 131.40, 129.41, 114.45, 72.78, 71.94, 69.87, 69.54, 68.59, 67.47, 45.98, 22.09.

Derivatization of 1-chloro-3-(4-((2-isopropoxyethoxy)methyl)phenoxy)propan-2-ol (**15**)

To a solution of 1-chloro-3-(4-((2-isopropoxyethoxy)methyl)phenoxy)propan-2-ol (**15**) (5 mg, 0.02 mmol) in hexane (0.5 mL) was added pyridine (one drop) and butyric anhydride (one drop). The reaction mixture was heated at 60°C for 1 h. Hexane (3 mL) was then added, and the solution was washed with dist. H_2O (5 × 0.5 mL). The organic phase was then dried over anhydrous $MgSO_4$ and filtered. The filtrate was analyzed by chiral HPLC (Chiralcel OD-H column, hexane:*i*-PrOH (96:4), 1 mL/min flow). t_R((R)-**16**) = 11.23 min and t_R((S)-**16**) = 12.33 min. R_S((S)/(R)-**16**) = 1.89.

Monitored CALB catalyzed kinetic resolution of 1-chloro-3-(4-((2-isopropoxyethoxy)methyl)phenoxy)propan-2-ol (**15**)

To a solution of 1-chloro-3-(4-((2-isopropoxyethoxy)methyl)phenoxy)propan-2-ol (**15**) (39 mg, 129 μmol) dissolved in dry MeCN (3.3 mL) were added activated molecular sieves (4Å), vinyl butyrate (83 μL, 75 mg, 0.65 mmol) and CALB (104 mg). The mixture was placed in an incubator shaker (38 °C, 200 rpm.). Samples of 100 μL were taken regularly until 23 h of reaction. For each sample, hexane (1.5 mL) was added and the solution was washed with dist. H_2O (5 × 1 mL). The organic phase was then dried over anhydrous $MgSO_4$ and analyzed by chiral HPLC. ee_s, ee_p and c were calculated from the chromatograms.

Large-scale CALB catalyzed kinetic resolution of 1-chloro-3-(4-((2-isopropoxyethoxy)methyl)phenoxy)propan-2-ol (**15**)

To a solution of 1-chloro-3-(4-((2-isopropoxyethoxy)methyl)phenoxy)propan-2-ol (**15**) (303 mg, 1.00 mmol) dissolved in dry MeCN (24 mL) were added activated molecular sieves (4Å), vinyl butyrate (623 μL, 556 mg, 4.86 mmol) and CALB (746 mg). The mixture was placed in an incubator shaker (38 °C, 200 rpm.) for 25 h. Enzymes and molecular sieves were filtered off and solvents were removed in vacuo. The obtained product was dissolved in EtOAc (15 mL), and was washed with a saturated NaCl solution (2 × 10 mL). The solution was dried over anhydrous $MgSO_4$, and the solvent was removed under reduced pressure. (*R*)-1-chloro-3-(4-((2-isopropoxyethoxy)methyl)phenoxy)propan-2-ol ((*R*)-**15**) and (*S*)-1-chloro-3-(4-((2-isopropoxyethoxy)methyl)phenoxy)propan-2-yl butyrate ((*S*)-**16**) were separated by flash chromatography (n-pentane: ethyl acetate, 7:3, v/v). (*R*)-1-Chloro-3-(4-((2-isopropoxyethoxy)methyl)phenoxy)propan-2-ol ((*R*)-**15**) was obtained as a colorless oil (134 mg, 0.44 mmol, 44% yield, 82% purity (^{1}H-NMR), ee=99% (chiral HPLC)). $[\alpha]_D^{20} -7$ (c 1.0, MeOH). ^{1}H NMR (600 MHz, $CDCl_3$) δ 7.31 - 7.26 (m, 2H), 6.91 - 6.87 (m, 2H), 4.51

(s, 2H), 4.21 (q, *J* = 5.1 Hz, 1H), 4.12 - 4.05 (m, 2H), 3.80 - 3.70 (m, 2H), 3.66 - 3.53 (m, 5H), 2.51 (d, *J* = 5.9 Hz, 1H), 1.17 (d, *J* = 6.1 Hz, 6H).

(*S*)-1-Chloro-3-(4-((2-isopropoxyethoxy)methyl)phenoxy)propan-2-yl butyrate ((*S*)-**16**) was obtained as a colorless oil (191 mg, 0.51 mmol, 51% yield, 68% purity (^{1}H-NMR)). ^{1}H NMR (600 MHz, $CDCl_3$) δ 7.30 - 7.25 (m, 2H), 6.92 - 6.85 (m, 2H), 5.34 (p, *J* = 5.1 Hz, 1H), 4.51 (s, 2H), 4.20 - 4.12 (m, 2H), 3.85 (dd, *J* = 11.7, 5.0 Hz, 1H), 3.78 (dd, *J* = 11.7, 5.3 Hz, 1H), 3.65 - 3.55 (m, 5H), 2.41 - 2.30 (m, 2H), 1.73 - 1.63 (m, 2H), 1.17 (d, *J* = 6.1 Hz, 6H), 1.00 - 0.94 (m, 3H).

(*S*)-Bisoprolol hemifumarate ((*S*)-**17*salt***):

To a mixture of (*R*)-1-chloro-3-(4-((2-isopropoxyethoxy)methyl)phenoxy)propan-2-ol ((*R*)-**15**) (40 mg, 0.13 mmol) in MeOH (2.5 mL) was added *i*-$PrNH_2$ (0.16 mL, 1.82 mmol). The mixture was stirred under reflux for 25 h, and was then concentrated under reduced pressure. The obtained product was dissolved in EtOAc (20 mL) and washed with dist. H_2O (10 mL). The aqueous phase was extracted with EtOAc (10 mL), and the combined organic phases were washed with brine (5 mL) and dried over anhydrous $MgSO_4$. The solvent was removed under reduced pressure to give a mixture of (*S*)-bisoprolol ((*S*)-**16**) and (*S*)-bisoprolol HCl ((*S*)-**16*HCl***) as a white solid (39 mg, 91% purity (^{1}H-NMR)). ^{1}H NMR (600 MHz, $CDCl_3$) δ 7.21 - 7.18 (m, 2H), 6.83 - 6.80 (m, 2H), 4.44 (s, 2H), 3.96 - 3.87 (m, 3H), 3.58 - 3.49 (m, 5H), 2.82 (dd, *J* = 12.2, 3.7 Hz, 1H), 2.76 (p, *J* = 6.3 Hz, 1H), 2.66 (dd, *J* = 12.1, 7.4 Hz, 1H), 1.10 (d, *J* = 6.1 Hz, 6H), 1.02 (d, *J* = 6.3 Hz, 6H). ^{13}C NMR (151 MHz, $CDCl_3$) δ 158.28, 130.93, 129.35, 114.43, 72.85, 71.91, 70.56, 69.47, 68.50, 67.48, 49.19, 48.94, 23.19, 23.05, 22.09.

The obtained mixture (10.0 mg) was then dissolved in EtOAc (15 μL) and MeOH (145 μL) and heated to 50°C. Fumaric acid (1.8 mg, 15 μmol) was added. The reaction was run for 1 h, and the solvent was removed under reduced pressure to give (*S*)-bisoprolol hemifumarate ((*S*)-**17*salt***) as a white solid (11.8 mg, 15 μmol, 92% yield, 90% purity (^{1}H-NMR), ee > 96% (chiral HPLC)). $[\alpha]_D^{20} - 17$ (c 1.0, MeOH). ^{1}H NMR (600 MHz, $CDCl_3$) δ 7.24 (d, *J* = 8.3 Hz, 4H), 6.87 - 6.83 (m, 4H), 6.65 (s, 2H), 4.52 (dt, *J* = 11.6, 6.1 Hz, 2H), 4.48 (s, 4H), 4.04 (dd, *J* = 9.6, 4.3 Hz, 2H), 3.97 (dd, *J* = 9.7, 6.1 Hz, 2H), 3.63 - 3.54 (m, 11H), 3.28 (p, *J* = 6.5 Hz, 2H), 3.14 (t, *J* = 11.2 Hz, 2H), 3.04 (dd, *J* = 12.1, 2.8 Hz, 2H), 1.36 (d, *J* = 6.5 Hz, 6H), 1.32 (d, *J* = 6.5 Hz, 6H), 1.16 (d, *J* = 6.1 Hz, 12H). ^{13}C NMR (151 MHz, $CDCl_3$) δ 173.28, 157.99, 136.16, 131.10, 129.37, 114.38, 72.80, 71.92, 70.11, 69.51, 67.46, 65.25, 50.63, 48.29, 22.09, 19.60, 19.06.

5 References

1. Mane, S., Racemic drug resolution: A comprehensive guide. *Analytical Methods* **2016,** *8*, 7567-7586.
2. Nguyen, L. A.; He, H.; Pham-Huy, C., Chiral drugs: an overview. *Int J Biomed Sci* **2006,** *2* (2), 85-100.
3. Vargesson, N., Thalidomide-induced teratogenesis: history and mechanisms. *Birth Defects Res C Embryo Today* **2015,** *105* (2), 140-156.
4. Calcaterra, A.; D'Acquarica, I., The market of chiral drugs: Chiral switches versus de novo enantiomerically pure compounds. *J. Pharm. Biomed. Anal.* **2018,** *147*, 323-340.
5. Agranat, I.; Caner, H., Intellectual property and chirality of drugs. *Drug Discovery Today* **1999,** *4* (7), 313-321.
6. Agranat, I.; Caner, H.; Caldwell, J., Putting chirality to work: the strategy of chiral switches. *Nature Reviews Drug Discovery* **2002,** *1* (10), 753-768.
7. Pifferi, G.; Perucca, E., The cost benefit ratio of enantiomeric drugs. *Eur J Drug Metab Pharmacokinet* **1995,** *20* (1), 15-25.
8. Long, A. S.; Zhang, A. D.; Meyer, C. E.; Egilman, A. C.; Ross, J. S.; Wallach, J. D., Evaluation of Trials Comparing Single-Enantiomer Drugs to Their Racemic Precursors: A Systematic Review. *JAMA Network Open* **2021,** *4* (5), e215731-e215731.
9. Diaconu, C.; Marcu, D.; Bratu, O.; Stănescu, A.; Gina, G.; Velnic, A.-A.; Mischianu, D.; Manea, M., Beta-blockers in Cardiovascular Therapy: A Review. *Journal of Mind & Behavior* **2019,** *6*, 216-223.
10. Yang, Y.; Wang, Y.; Bao, Z.; Yang, Q.; Zhang, Z.; Ren, Q., Progress in the Enantioseparation of β-Blockers by Chromatographic Methods. *Molecules* **2021,** *26* (2), 468.
11. Taylor, M. R., Pharmacogenetics of the human beta-adrenergic receptors. *Pharmacogenomics J* **2007,** *7* (1), 29-37.
12. Baker, J. G., The selectivity of beta-adrenoceptor antagonists at the human beta1, beta2 and beta3 adrenoceptors. *Br J Pharmacol* **2005,** *144* (3), 317-322.
13. Čižmáriková, R.; Habala, L.; Valentová, J.; Markuliak, M., Survey of Pharmacological Activity and Pharmacokinetics of Selected β-Adrenergic Blockers in Regard to Their Stereochemistry. *Applied Sciences* **2019,** *9* (4).
14. Sotalol hydrochloride injection for intravenous use. U.S. Food and Drug Administration: July 2009.
15. Waldo, A. L.; Camm, A. J.; deRuyter, H.; Friedman, P. L.; MacNeil, D. J.; Pauls, J. F.; Pitt, B.; Pratt, C. M.; Schwartz, P. J.; Veltri, E. P., Effect of d-sotalol on mortality in patients with left ventricular dysfunction after recent and remote myocardial infarction. The SWORD Investigators. Survival With Oral d-Sotalol. *Lancet* **1996,** *348* (9019), 7-12.
16. Hussain, S. S.; Aboul-Enein, H. Y.; al-Dakan, A.; Hannan, M. A., Mutagenicity of enantiomers of penbutolol. *Drug Chem Toxicol* **1989,** *12* (1), 77-83.
17. Johns, T. E.; Lopez, L. M., Bisoprolol: Is This Just Another Beta-Blocker for Hypertension or Angina? *Annals of Pharmacotherapy* **1995,** *29* (4), 403-414.
18. Most Prescribed Beta Blockers in the U.S. definitivehc.com/blog/beta-blocker-prescription-patterns (accessed April 2022).
19. Dutta, A.; Lanc, R.; Begg, E.; Robson, R.; Sia, L.; Dukart, G.; Desjardins, R.; Yacobi, A., Dose Proportionality of Bisoprolol Enantiomers in Humans After Oral Administration of the Racemate. *The Journal of Clinical Pharmacology* **1994,** *34* (8), 829-836.
20. Zelaszczyk, D.; Kieć-Kononowicz, K., Biocatalytic approaches to optically active beta-blockers. *Curr Med Chem* **2007,** *14* (1), 53-65.
21. Stoschitzky, K.; Lindner, W.; Zernig, G., Racemic beta-blockers - fixed combinations of different drugs. *Journal of clinical and basic cardiology* **1998,** *1*, 15-19.
22. Anastas, P.; Eghbali, N., Green Chemistry: Principles and Practice. *Chemical Society Reviews* **2010,** *39* (1), 301-312.
23. Anastas, P. T. W. J. C., *Green chemistry : theory and practice*. Oxford University Press: Oxford [England]; New York, 1998.

24. Anastas, P. T., Green Chemistry: Thirty Years of Holding Up Our End of the Bargain. *ACS Sustainable Chemistry & Engineering* **2021,** *9* (48), 16005-16006.
25. Masson-Delmotte, V., P. Zhai, A. Pirani, S.L. Connors, C. Péan, S. Berger, N. Caud, Y. Chen, L. Goldfarb, M.I. Gomis, M. Huang, K. Leitzell, E. Lonnoy, J.B.R. Matthews, T.K. Maycock, T. Waterfield, O. Yelekçi, R. Yu, B. Zhou *Climate Change 2021: The Physical Science Basis. Contribution of Working Group I to the Sixth Assessment Report of the Intergovernmental Panel on Climate Change*; IPCC: 2021.
26. Sheldon, R. A., Biocatalysis and Green Chemistry. In *Green Biocatalysis*, 2016; pp 1-15.
27. Faber, K., *Biotransformations in organic chemistry: a textbook*. Springer: 2011.
28. Dakin, H. D., The hydrolysis of optically inactive esters by means of enzymes. *The Journal of Physiology* **1903,** *30* (3-4), 253-263.
29. Anthonsen, H. W.; Hoff, B. H.; Anthonsen, T., Calculation of enantiomer ratio and equilibrium constants in biocatalytic ping-pong bi-bi resolutions. *Tetrahedron: Asymmetry* **1996,** *7* (9), 2633-2638.
30. Jacobsen, E. E.; Hoff, B. H.; Anthonsen, T., Enantiopure derivatives of 1,2-alkanediols: substrate requirements of lipase B from Candida antarctica. *Chirality* **2000,** *12* (9), 654-9.
31. Li, C.; Tan, T.; Zhang, H.; Feng, W., Analysis of the Conformational Stability and Activity of Candida antarctica Lipase B in Organic Solvents: INSIGHT FROM MOLECULAR DYNAMICS AND QUANTUM MECHANICS/SIMULATIONS*. *Journal of Biological Chemistry* **2010,** *285* (37), 28434-28441.
32. Wong, C.-H.; Whitesides, G. M., Enzyme-catalyzed organic synthesis: NAD(P)H cofactor regeneration by using glucose-6-phosphate and the glucose-5-phosphate dehydrogenase from Leuconostoc mesenteroides. *Journal of the American Chemical Society* **1981,** *103* (16), 4890-4899.
33. Weckbecker, A.; Gröger, H.; Hummel, W., Regeneration of Nicotinamide Coenzymes: Principles and Applications for the Synthesis of Chiral Compounds. In *Biosystems Engineering I: Creating Superior Biocatalysts*, Wittmann, C.; Krull, R., Eds. Springer Berlin Heidelberg: Berlin, Heidelberg, 2010; pp 195-242.
34. Dalgliesh, C. E., 756. The optical resolution of aromatic amino-acids on paper chromatograms. *Journal of the Chemical Society (Resumed)* **1952,** (0), 3940-3942.
35. Feitsma, K. G.; Drenth, B. F., Chromatographic separation of enantiomers. *Pharm Weekbl Sci* **1988,** *10* (1), 1-11.
36. Mayer, S.; Schurig, V., Enantiomer separation by electrochromatography on capillaries coated with chirasil-dex. Dedicated to Professor Ernst Bayer on the occasion of his 65th birthday. *Journal of High Resolution Chromatography* **1992,** *15* (2), 129-131.
37. Berthod, A., Chapter 1 - Fundamentals of countercurrent chromatography. In *Comprehensive Analytical Chemistry*, Berthod, A., Ed. Elsevier: 2002; Vol. 38, pp 1-20.
38. Clayden, J.; Greeves, N.; Warren, S., *Organic Chemistry*. OUP Oxford: 2012.
39. Covington, C. L.; Polavarapu, P. L., Specific Optical Rotations and the Horeau Effect. *Chirality* **2016,** *28* (3), 181-5.
40. Smith, P.; Brodfuehrer, P. R.; Dillon, J. L.; Vemishetti, P., A Short Synthesis of d-Sotalol. *Synthetic Communications* **1995,** *25* (7), 1093-1098.
41. Brodfuehrer, P. R.; Smith, P.; Dillon, J. L.; Vemishetti, P., Asymmetric Synthesis of the Antiarrhythmia Agent d-Sotalol. *Organic Process Research & Development* **1997,** *1* (2), 176-178.
42. Phukan, P.; Jagtap, H.; Sudalai, A., A Convenient Synthesis of d-Sotalol. *Indian Journal of Chemistry* **2000,** *39B*, 950-953.
43. Patel, R. N.; Banerjee, A.; McNamee, C. G.; Szarka, L. J., Stereoselective microbial reduction of N-(4-(1-oxo-2-chloroacetyl ethyl) phenyl methane sulfonamide. *Applied Microbiology and Biotechnology* **1993,** *40* (2), 241-245.
44. Kamal, A.; Sandbhor, M.; Ali Shaik, A., Chemoenzymatic synthesis of (S) and (R)-propranolol and sotalol employing one-pot lipase resolution protocol. *Bioorg Med Chem Lett* **2004,** *14* (17), 4581-3.
45. Kapoor, M.; Anand, N.; Ahmad, K.; Koul, S.; Chimni, S. S.; Taneja, S. C.; Qazi, G. N., Synthesis of β-adrenergic blockers (R)-(−)-nifenalol and (S)-(+)-sotalol via a highly efficient resolution of a bromohydrin precursor. *Tetrahedron: Asymmetry* **2005,** *16* (3), 717-725.

46. Zhu, D.; Mukherjee, C.; Hua, L., 'Green' synthesis of important pharmaceutical building blocks: enzymatic access to enantiomerically pure α-chloroalcohols. *Tetrahedron: Asymmetry* **2005,** *16* (19), 3275-3278.
47. Hamaguchi, S.; Asada, M.; Hasegawa, J.; Watanabe, K., Asymmetric hydrolysis of racemic 2-oxazolidinone esters with lipases. *Agricultural and biological chemistry* **1984,** *48*, 2331-2337.
48. Kan, K.; Miyama, A.; Hamaguchi, S.; Ohashi, T.; Watanabe, K., Synthesis of (S)-β-Blockers from(S)5-Hydroxymethyl-3-tert butyl-2-oxazolidinone or(S)-5-Hydroxymethyl-3-isopropyl-2-oxazolidinone. *Agricultural and Biological Chemistry* **1985,** *49* (1), 207-210.
49. Ader, U.; Schneider, M. P., Enzyme assisted preparation of enantiomerically pure β-adrenergic blockers III. Optically active chlorohydrin derivatives and their conversion. *Tetrahedron: Asymmetry* **1992,** *3* (4), 521-524.
50. Klunder, J. M.; Onami, T.; Sharpless, K. B., Arenesulfonate derivatives of homochiral glycidol: versatile chiral building blocks for organic synthesis. *The Journal of Organic Chemistry* **1989,** *54* (6), 1295-1304.
51. Phukan, P.; Sudalai, A., Regioselective alkylation of phenol with cyclopentanol over montmorillonite K10: An efficient synthesis of 1-(2-cyclopentylphenoxy)-3-[(1,1-dimethylethyl)amino]propan-2-ol {(S)-penbutolol}. *Journal of the Chemical Society, Perkin Transactions 1* **1999,** (20), 3015-3018.
52. Gundersen, M. A.; Austli, G. B.; Løvland, S. S.; Hansen, M. B.; Rødseth, M.; Jacobsen, E. E., Lipase Catalyzed Synthesis of Enantiopure Precursors and Derivatives for β-Blockers Practolol, Pindolol and Carteolol. *Catalysts* **2021,** *11* (4), 503.
53. Klungseth, K. Chemo-enzymatic synthesis of enantiopure penbutolol and penbutolol derivative 1-tertbutylamino)-3-(4-cyclopentylphenoxy)propan-2-ol. Master's thesis, Norwegian University of Science and Technology, 2021.
54. Jun, Y.; Xian, Z.; Ying-ming, W.; Hong-wei, A. N., Research in synthesis of chiral drug bisoprolol fumarate. *河北科技大学英文界面* **2010,** *31* (4), 317-320.
55. Fumin, Z. Preparation method of chiral bisoprolol fumarate. Chinese Patent CN112194587A, January 08, 2021.
56. Soloviev, D. V.; Matarrese, M.; Moresco, R. M.; Todde, S.; Bonasera, T. A.; Sudati, F.; Simonelli, P.; Magni, F.; Colombo, D.; Carpinelli, A.; Kienle, M. G.; Fazio, F., Asymmetric synthesis and preliminary evaluation of (R)- and (S)-[11C]bisoprolol, a putative beta1-selective adrenoceptor radioligand. *Neurochem Int* **2001,** *38* (2), 169-80.
57. Kitaori, K.; Furukawa, Y.; Yoshimoto, H.; Otera, J., CsF in organic synthesis. The first and convenient synthesis of enantiopure bisoprolol by use of glycidyl nosylate. *Tetrahedron Letters* **1998,** *39* (20), 3173-3176.
58. Lund, I.; Bøckmann, P.; Jacobsen, E., Highly enantioselective CALB-catalyzed kinetic resolution of building blocks for β-blocker atenolol. *Tetrahedron* **2016,** *72*.
59. Shioya, T.; Akiyama, T.; Yokoyama, T.; Matsumoto, Y., Formation rate of benzyl cation intermediate from p-Hydroxyphenyl, guaiacyl, or syringyl nucleus in acidolysis of lignin. *Journal of Wood Chemistry and Technology* **2017,** *37* (2), 75-86.
60. Stein;, I. D.; Gantzert;, L.; Strohmenger;, A.; Bokel;, H. D.; Eberle, H. G. D. Continuous production of hydroxy-benzyl alkyl ether. German Patent DE4434823A1, 1994.
61. Morthala, R. R.; Gharpure, M.; Jagtap, A.; Mhaskar, M.; Krishnmurthy, D. An Improved Process for the Preparation of Bisoprolol and its Intermediate. International Patent WO2016135616A1, Sep 1, 2016.
62. Bøckmann, P. L. Synthesis of enantiopure β-blocker (S)-metoprolol and derivatives by lipase catalysis. Master's thesis, Norwegian University of Science and Technology, 2016.
63. Sibley, G. E. M.; Malmstroem, L. J.; Larsson, J. M. Preparation of Diazine Compounds for Treatment of Fungal Infections. International Patent WO2017009651, Jan 01, 2017.
64. Kubo, Y.; Ando, M.; Tanaka, H.; Osaka, S.; Matsumoto, T.; Nakata, H.; Terada, D.; Nitabaru, T. Preparation of Morpholine Derivatives or their Salts as ATM Inhibitors for Therapeutic Agents and Anticancer Drug Sensitivity Enhancers. European Patent EP3042900, Sep 13, 2016.
65. Hassan, A. Y.; Sarg, M. T.; El Deeb, M. A.; Bayoumi, A. H.; El Rabeb, S. I., Facile Synthesis and Anticancer Activity Study of Novel Series of Substituted and Fused Coumarin Derivatives. *Journal of Heterocyclic Chemistry* **2018,** *55* (6), 1426-1443.

66. Zhou, Y. Preparation Method of Propranolole Hydrochloride. Chinese Patent CN108586273, Sep 28, 2018.
67. Stroech, K.; Böckmann, K.; Plempel, M. Antimykotische Mittel. European Patent

EP0308783A2, Sep 29, 1989.
68. Solomons, T. W. G.; Fryhle, C. B.; Snyder, S. A., Organic chemistry. **2014**, p841; p969.
69. Carey, F. A.; Sundberg, R. J., Advanced Organic Chemistry : Part B: Reactions and Synthesis. **2013**, pages 909-916.
70. Lis, R.; Marisca, A. J., Methanesulfonanilides and the Mannich reaction. *The Journal of Organic Chemistry* **1987,** *52* (19), 4377-4379.
71. King, J. F., Return of sulfenes. *Accounts of Chemical Research* **1975,** *8* (1), 10-17.
72. Lis, R.; Morgan, T. K., Jr.; DeVita, R. J.; Davey, D. D.; Lumma, W. C., Jr.; Wohl, R. A.; Diamond, J.; Wong, S. S.; Sullivan, M. E., Synthesis and antiarrhythmic activity of novel 3-alkyl-1-[omega-[4-[(alkylsulfonyl)amino]phenyl]-omega- hydroxyalkyl]-1H-imidazolium salts and related compounds. *J Med Chem* **1987,** *30* (4), 696-704.
73. Kayser, M. M.; Eliev, S.; Eisenstein, O., Reduction of ketones by sodium borohydride in the absence of protic solvents. Inter versus intramolecular mechanism. *Tetrahedron Letters* **1983,** *24* (10), 1015-1018.
74. Zeynizadeh, B.; Behyar, T., Wet THF as a Suitable Solvent for a Mild and Convenient Reduction of Carbonyl Compounds with NaBH4. *Bulletin of the Chemical Society of Japan* **2005,** *78* (2), 307-315.
75. Yakabe, S.; Hirano, M.; Takashi, M., Alumina-assisted reduction of carbonyl compounds with sodium borohydride in hexane. *Canadian Journal of Chemistry* **1998,** *76* (12), 1916-1921.
76. Blindheim, F. H.; Hansen, M. B.; Evjen, S.; Zhu, W.; Jacobsen, E. E., Chemoenzymatic Synthesis of Synthons as Precursors for Enantiopure Clenbuterol and Other β2-Agonists. *Catalysts* **2018,** *8* (11).
77. Tennfjord, A. L. Synthesis of enantiopure ß-blocker (S)-esmolol. Master's thesis, Norwegian University of Science and Technology, 2021.
78. Montero, G.; Gloria Quintanilla, M.; Barba, F., A new carbene route for the electrochemical reduction of phenacyl bromide. *Journal of Electroanalytical Chemistry* **1993,** *345* (1), 457-461.
79. Kapur, S.; Mathur, N. C.; McManus, K.; Pincock, A. L.; Pincock, J. A., Substituent effects on the rate of carbene formation in the pyrolysis of indenyl diazo compounds. *Canadian Journal of Chemistry* **1988,** *66* (11), 2888-2893.
80. Guha, A.; Boruah, A.; Hazarika, M.; Kaman, S., Switching of carbene spin states: effect of hydrogen bond donors. *Reports in Theoretical Chemistry* **2015**, 1.
81. Banoth, L.; Banerjee, U. C., New chemical and chemo-enzymatic synthesis of (RS)-, (R)-, and (S)-esmolol. *Arabian Journal of Chemistry* **2017,** *10*, S3603-S3613.
82. Metaxas, A. E.; Cort, J. R., Counterion influence on chemical shifts in strychnine salts. *Magnetic Resonance in Chemistry* **2013,** *51* (5), 292-298.
83. Richards, S. A.; Hollerton, J. C., *Essential Practical NMR for Organic Chemistry*. Wiley: 2010.
84. Chávez, F.; Godinez, R., Sulfuric Acid Adsorbed on Silica Gel. An Efficient Catalyst for the Tetrahydropyranylation of Alcohols. *Synthetic Communications* **1992,** *22* (1), 159-164.
85. *ChemBioDraw Ultra*, CambridgeSoft Corporation: 2014.
86. Sánchez-Cantalejo, F.; Priest, J. D.; Davies, P. W., A Gold Carbene Manifold to Prepare Fused γ-Lactams by Oxidative Cyclisation of Ynamides. *Chemistry – A European Journal* **2018,** *24* (65), 17215-17219.
87. Bhaskar, G.; Solomon, M.; Babu, G.; Muralidharan, D.; Perumal, P. T., A simple and an efficient indium trichloride catalyzed benzyl etherification. *Indian Journal of Chemistry* **2010,** *IJC-B Vol.49B [2010]*, 795-801.

6 Appendix

6.1 Sotalol synthesis

6.1.1 N-phenylmethanesulfonamide (1)

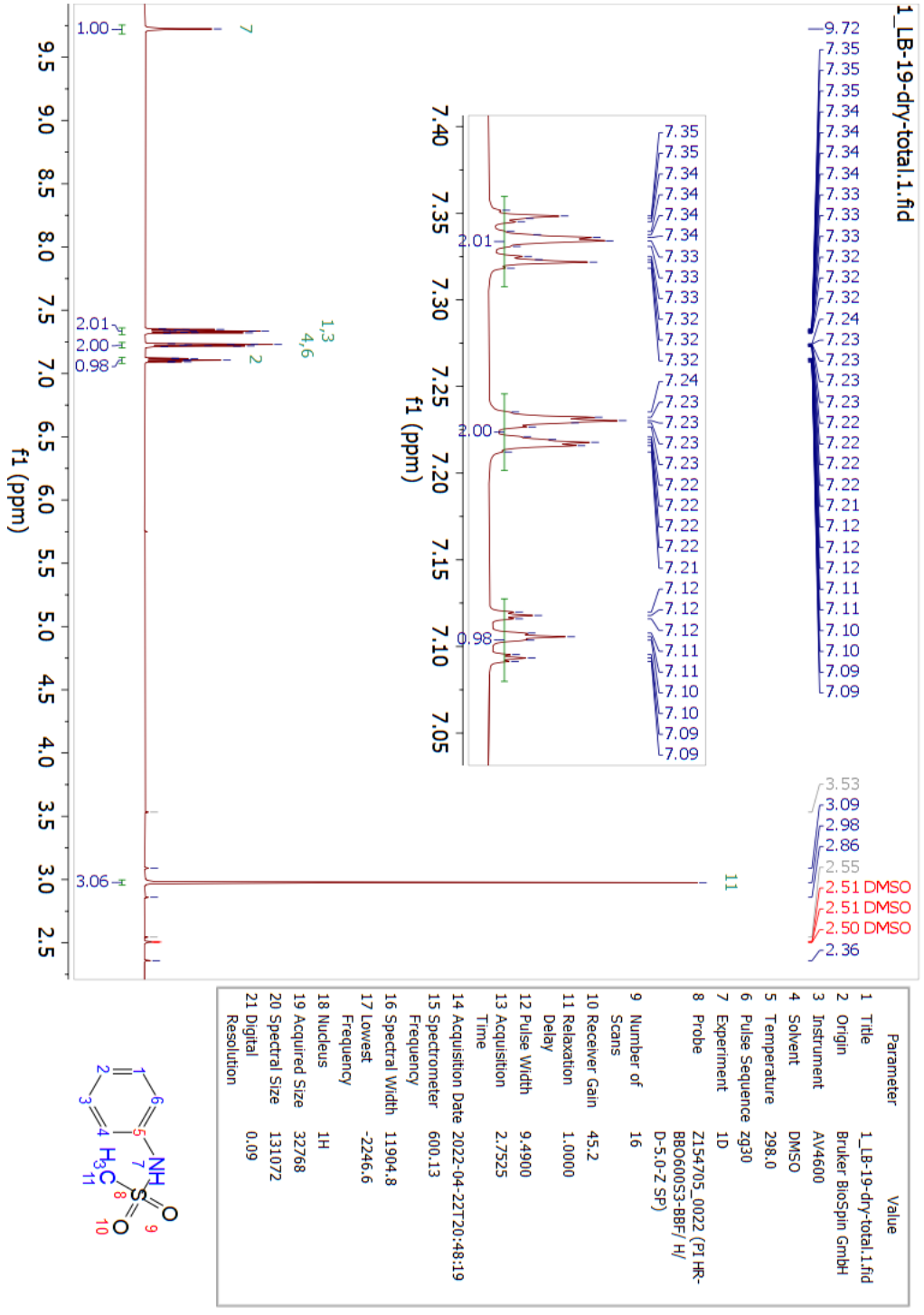

Figure 6.1.1: ^{1}H-NMR spectrum (600 MHz, d6-DMSO) of N-phenylmethanesulfonamide (**1**).

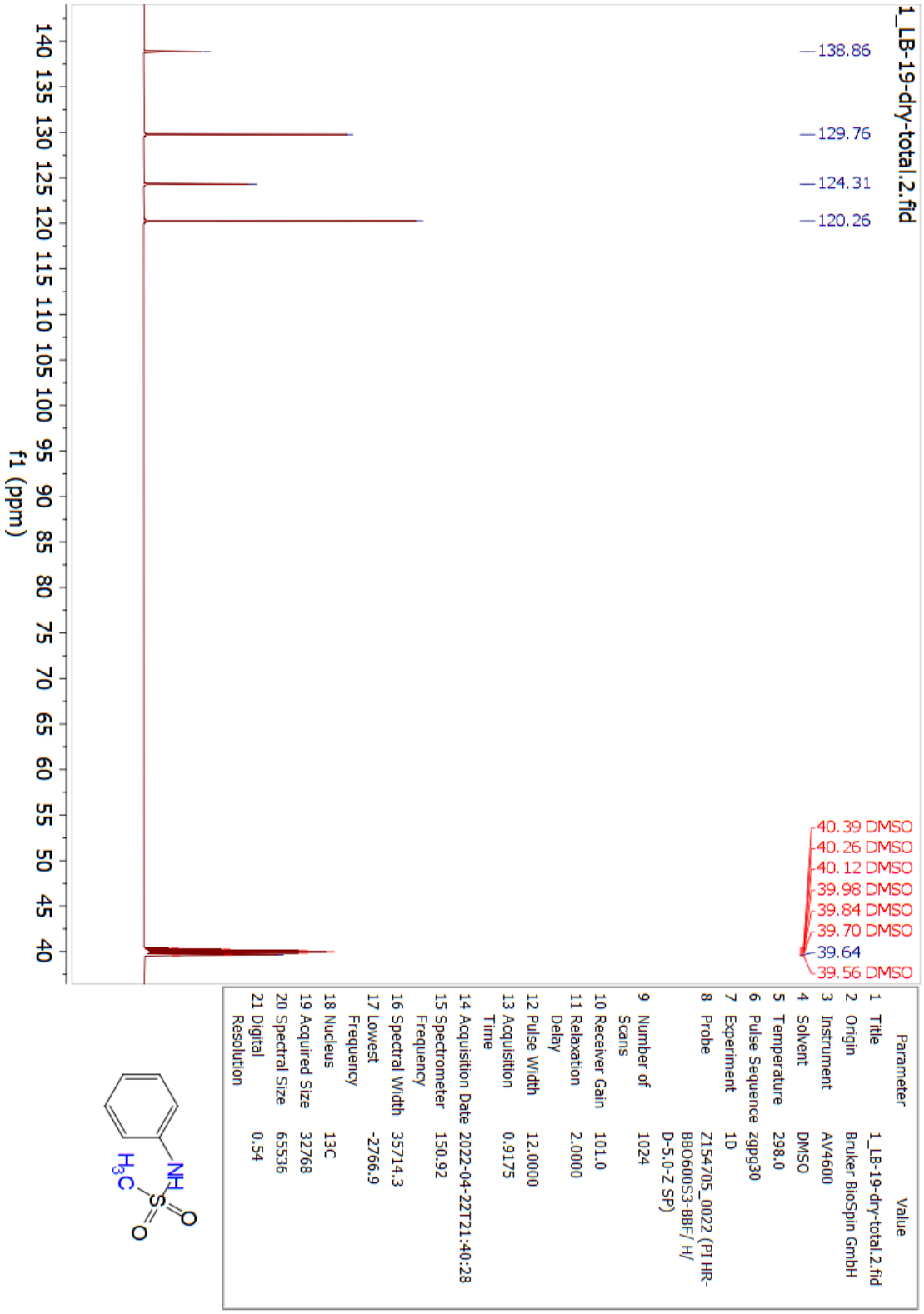

Figure 6.1.2: ^{13}C-NMR spectrum (600 MHz, d6-DMSO) of N-phenylmethanesulfonamide (**1**).

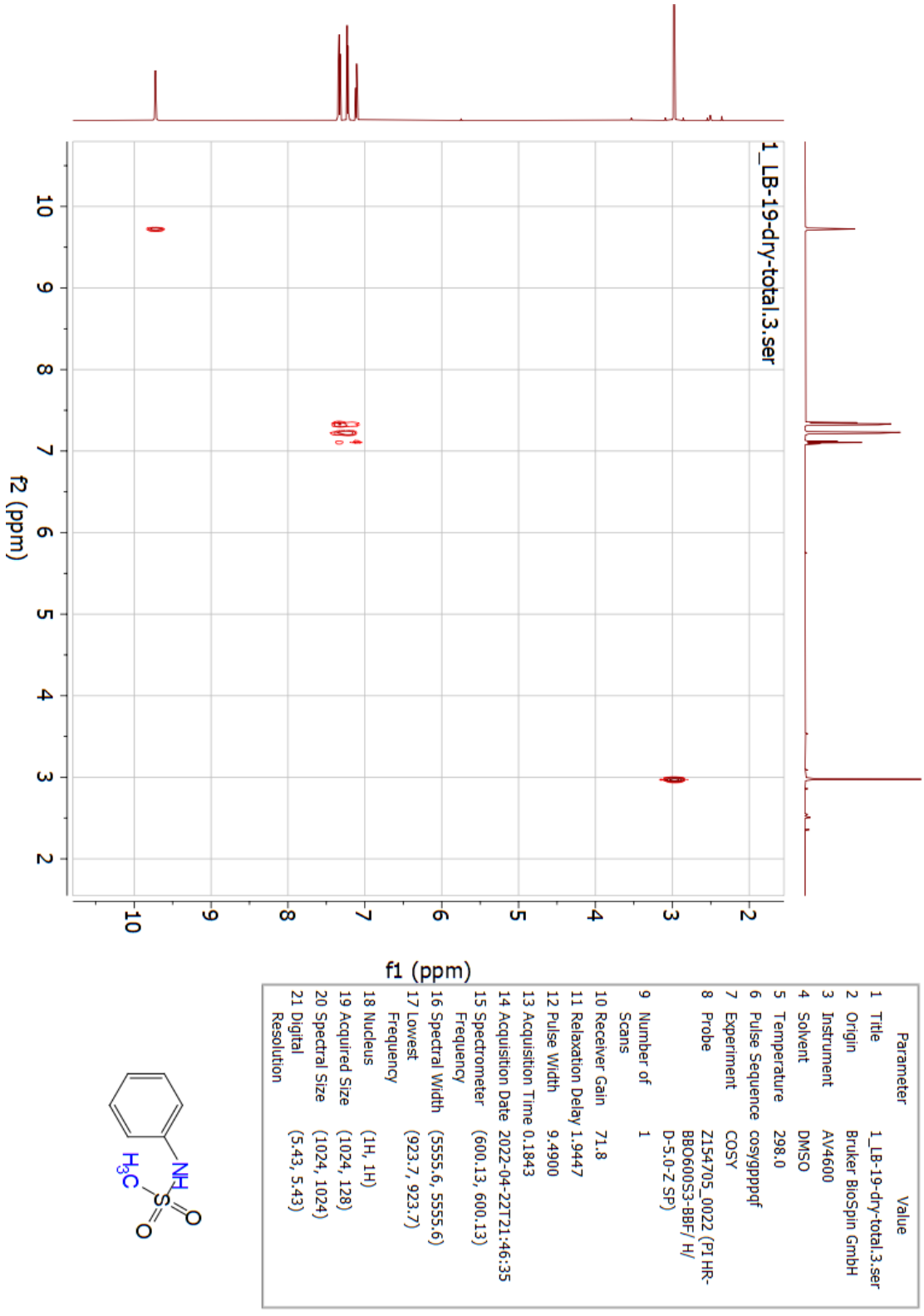

Figure 6.1.3: H,H-COSY-NMR spectrum (600 MHz, d6-DMSO) of N-phenylmethanesulfonamide (**1**).

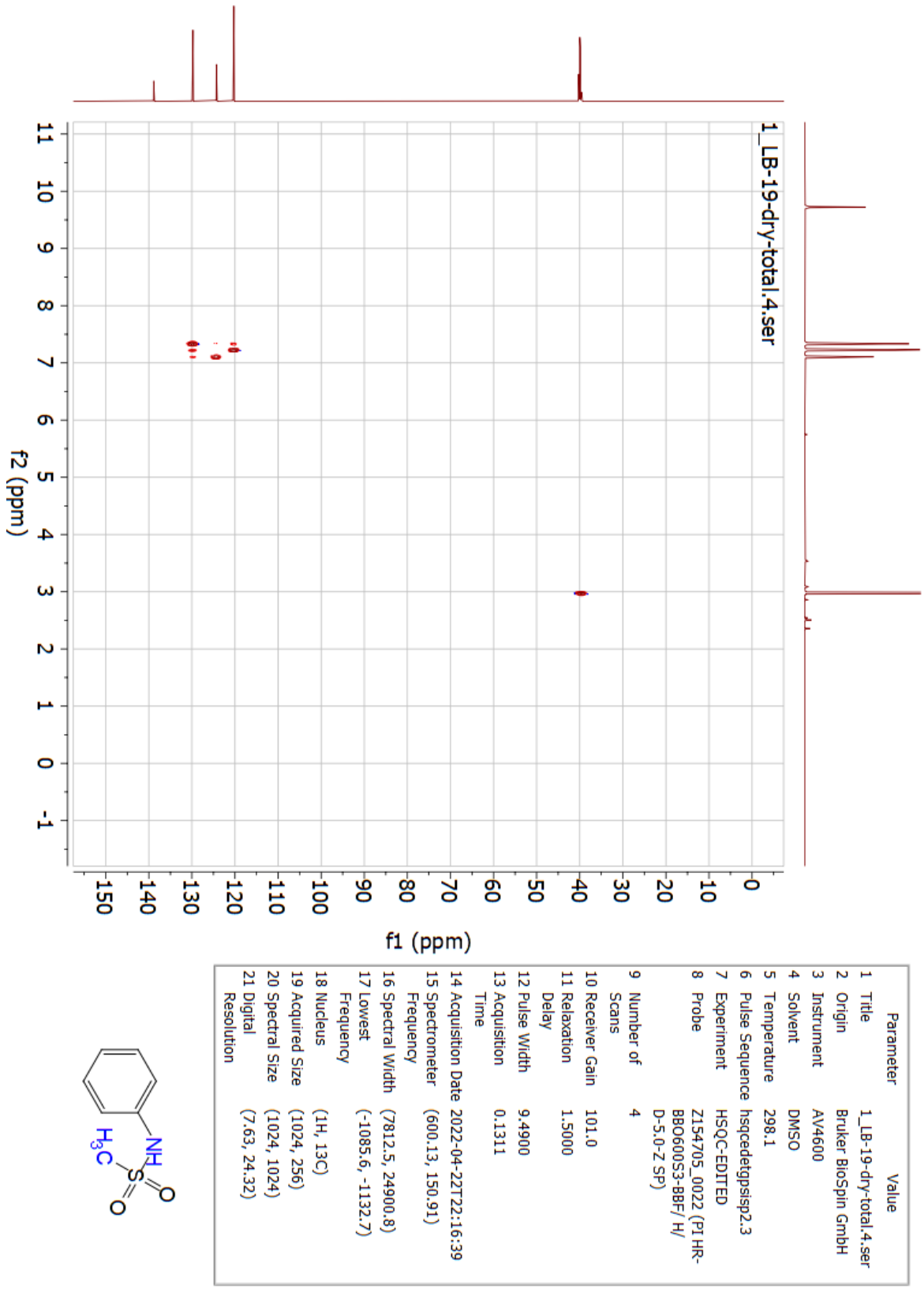

	Parameter	Value
1	Title	1_LB-19-dry-total.4.ser
2	Origin	Bruker BioSpin GmbH
3	Instrument	AV4600
4	Solvent	DMSO
5	Temperature	298.1
6	Pulse Sequence	hsqcedetgpsisp2.3
7	Experiment	HSQC-EDITED
8	Probe	Z154705_0022 (PI HR-BBO600S3-BBF/ H/ D-5.0-Z SP)
9	Number of Scans	4
10	Receiver Gain	101.0
11	Relaxation Delay	1.5000
12	Pulse Width	9.4900
13	Acquisition Time	0.1311
14	Acquisition Date	2022-04-22T22:16:39
15	Spectrometer Frequency	(600.13, 150.91)
16	Spectral Width	(7812.5, 24900.8)
17	Lowest Frequency	(-1085.6, -1132.7)
18	Nucleus	(1H, 13C)
19	Acquired Size	(1024, 256)
20	Spectral Size	(1024, 1024)
21	Digital Resolution	(7.63, 24.32)

Figure 6.1.4: HSQC-NMR spectrum (600 MHz, d6-DMSO) of N-phenylmethanesulfonamide (**1**).

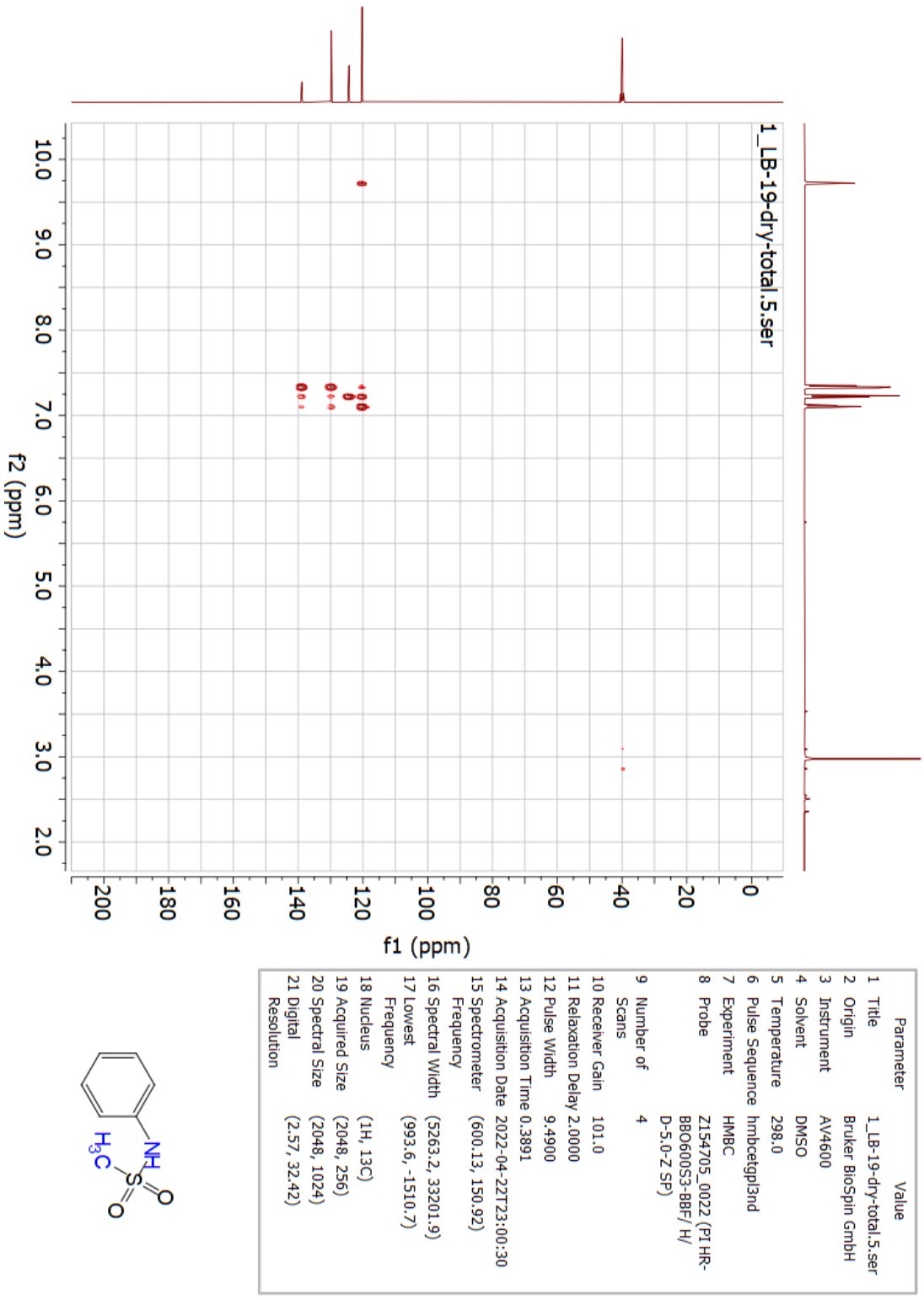

Figure 6.1.5: HMBC-NMR spectrum (600 MHz, d6-DMSO) of N-phenylmethanesulfonamide (**1**).

6.1.2 N-(4-(2-chloroacetyl)phenyl)methanesulfonamide (2)

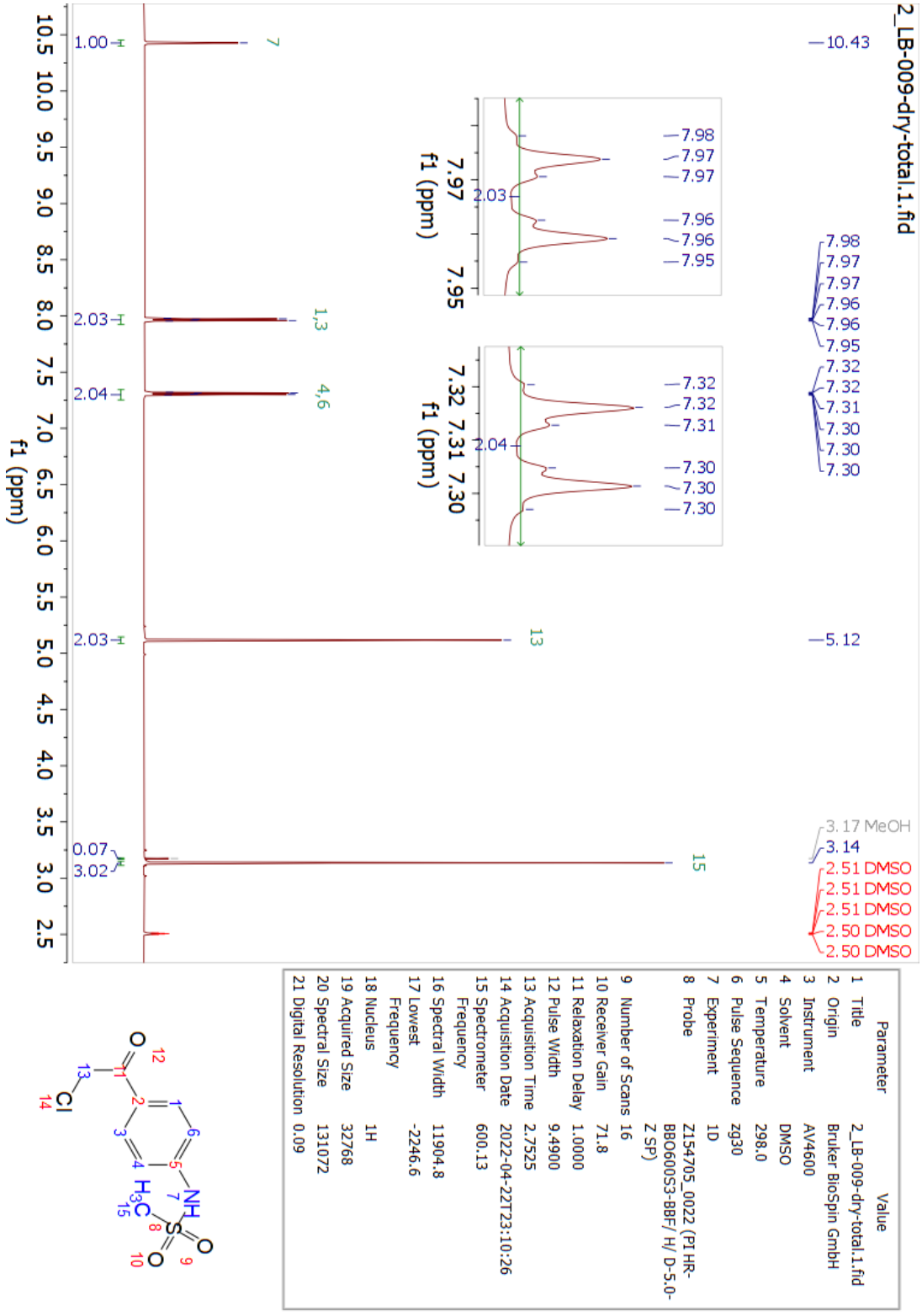

Figure 6.1.6: ^{1}H-NMR spectrum (600 MHz, d6-DMSO) of N-(4-(2-chloroacetyl)phenyl)methanesulfonamide (**2**).

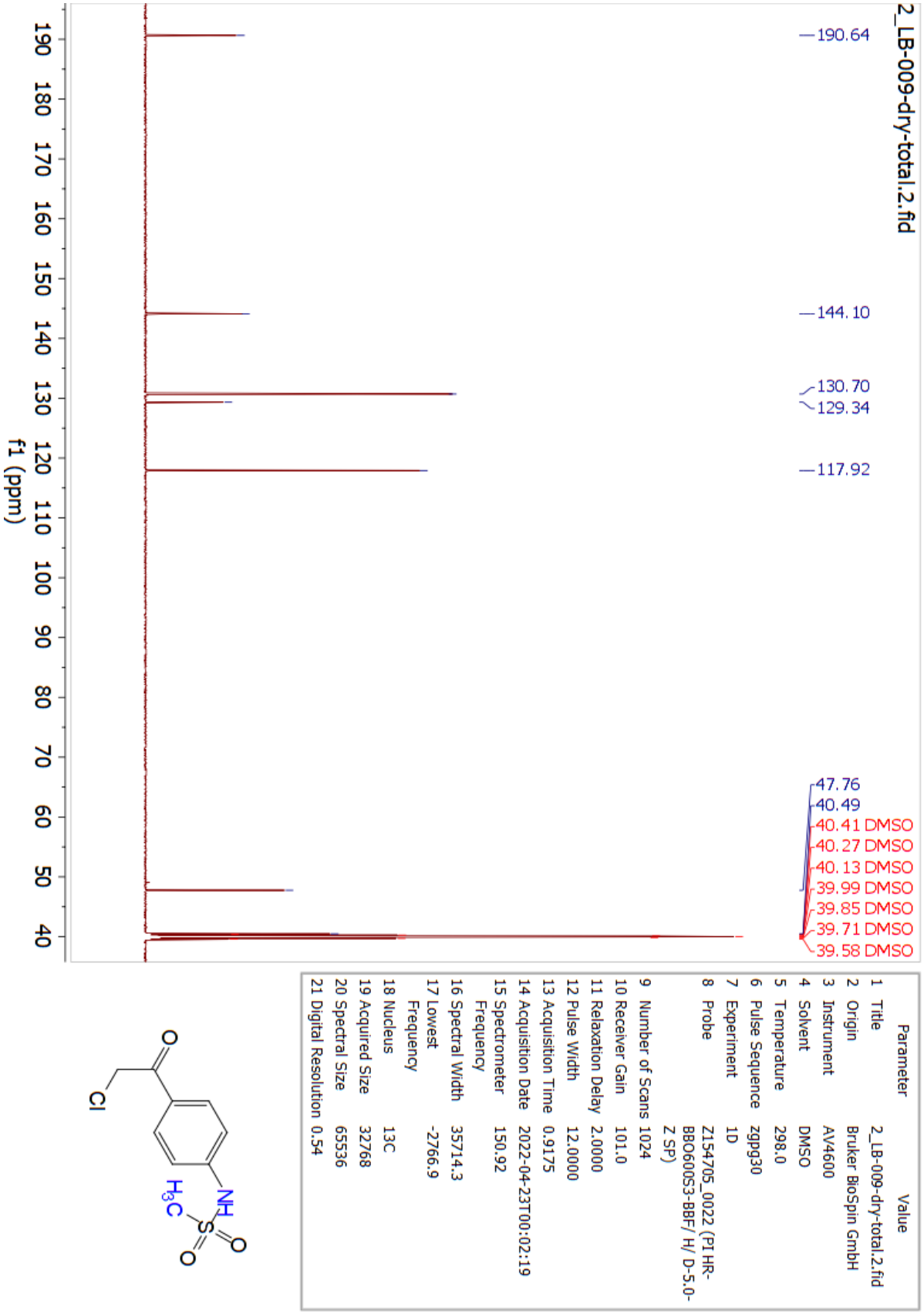

Figure 6.1.7: ^{13}C-NMR spectrum (600 MHz, d6-DMSO) of N-(4-(2-chloroacetyl)phenyl)methanesulfonamide (**2**).

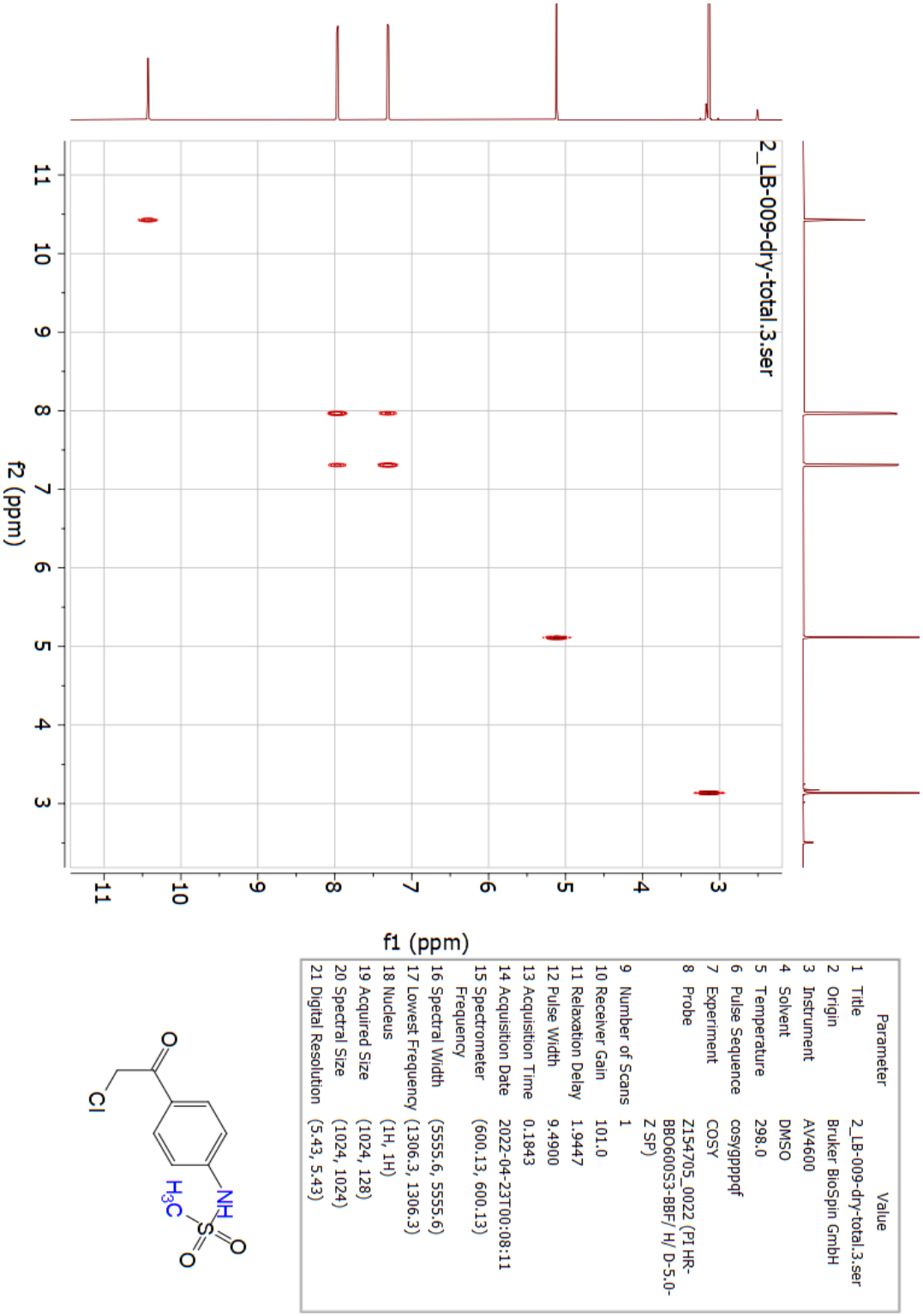

	Parameter	Value
1	Title	2_LB-009-dry-total.3.ser
2	Origin	Bruker BioSpin GmbH
3	Instrument	AV4600
4	Solvent	DMSO
5	Temperature	298.0
6	Pulse Sequence	cosygpppqf
7	Experiment	COSY
8	Probe	Z154705_0022 (PI HR-BBO600S3-BBF/ H/ D-5.0-Z SP)
9	Number of Scans	1
10	Receiver Gain	101.0
11	Relaxation Delay	1.9447
12	Pulse Width	9.4900
13	Acquisition Time	0.1843
14	Acquisition Date	2022-04-23T00:08:11
15	Spectrometer Frequency	(600.13, 600.13)
16	Spectral Width	(5555.6, 5555.6)
17	Lowest Frequency	(1306.3, 1306.3)
18	Nucleus	(1H, 1H)
19	Acquired Size	(1024, 128)
20	Spectral Size	(1024, 1024)
21	Digital Resolution	(5.43, 5.43)

Figure 6.1.8: H,H-COSY-NMR spectrum (600 MHz, d6-DMSO) of N-(4-(2-chloroacetyl)phenyl)methanesulfonamide (**2**).

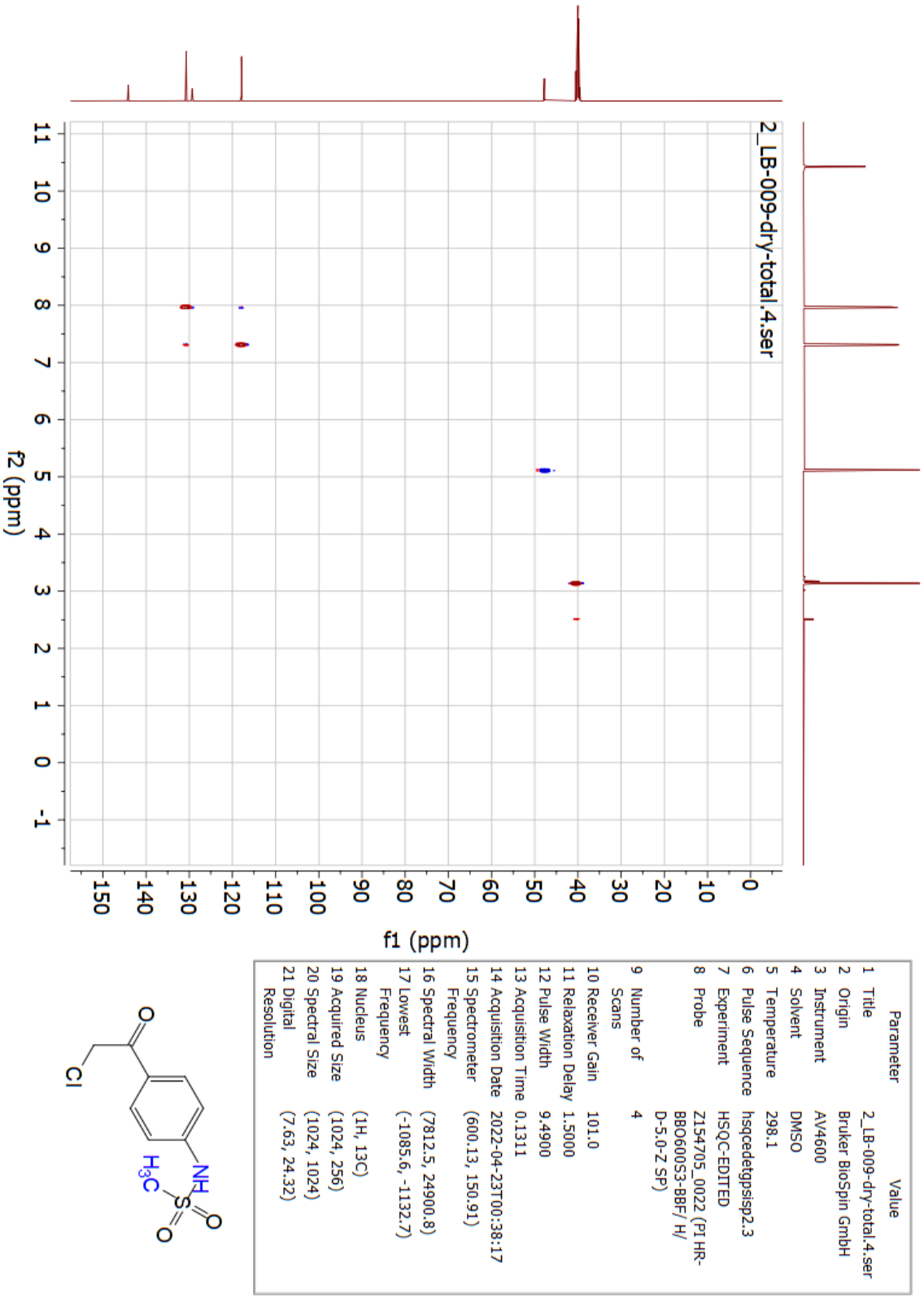

	Parameter	Value
1	Title	2_LB-009-dry-total.4.ser
2	Origin	Bruker BioSpin GmbH
3	Instrument	AV4600
4	Solvent	DMSO
5	Temperature	298.1
6	Pulse Sequence	hsqcedetgpsisp2.3
7	Experiment	HSQC-EDITED
8	Probe	Z154705_0022 (PI HR-BBO600S3-BBF/ H/D-5.0-Z SP)
9	Number of Scans	4
10	Receiver Gain	101.0
11	Relaxation Delay	1.5000
12	Pulse Width	9.4900
13	Acquisition Time	0.1311
14	Acquisition Date	2022-04-23T00:38:17
15	Spectrometer Frequency	(600.13, 150.91)
16	Spectral Width	(7812.5, 24900.8)
17	Lowest Frequency	(-1085.6, -1132.7)
18	Nucleus	(1H, 13C)
19	Acquired Size	(1024, 256)
20	Spectral Size	(1024, 1024)
21	Digital Resolution	(7.63, 24.32)

Figure 6.1.9: HSQC-NMR spectrum (600 MHz, d6-DMSO) of N-(4-(2-chloroacetyl)phenyl)methanesulfonamide (**2**).

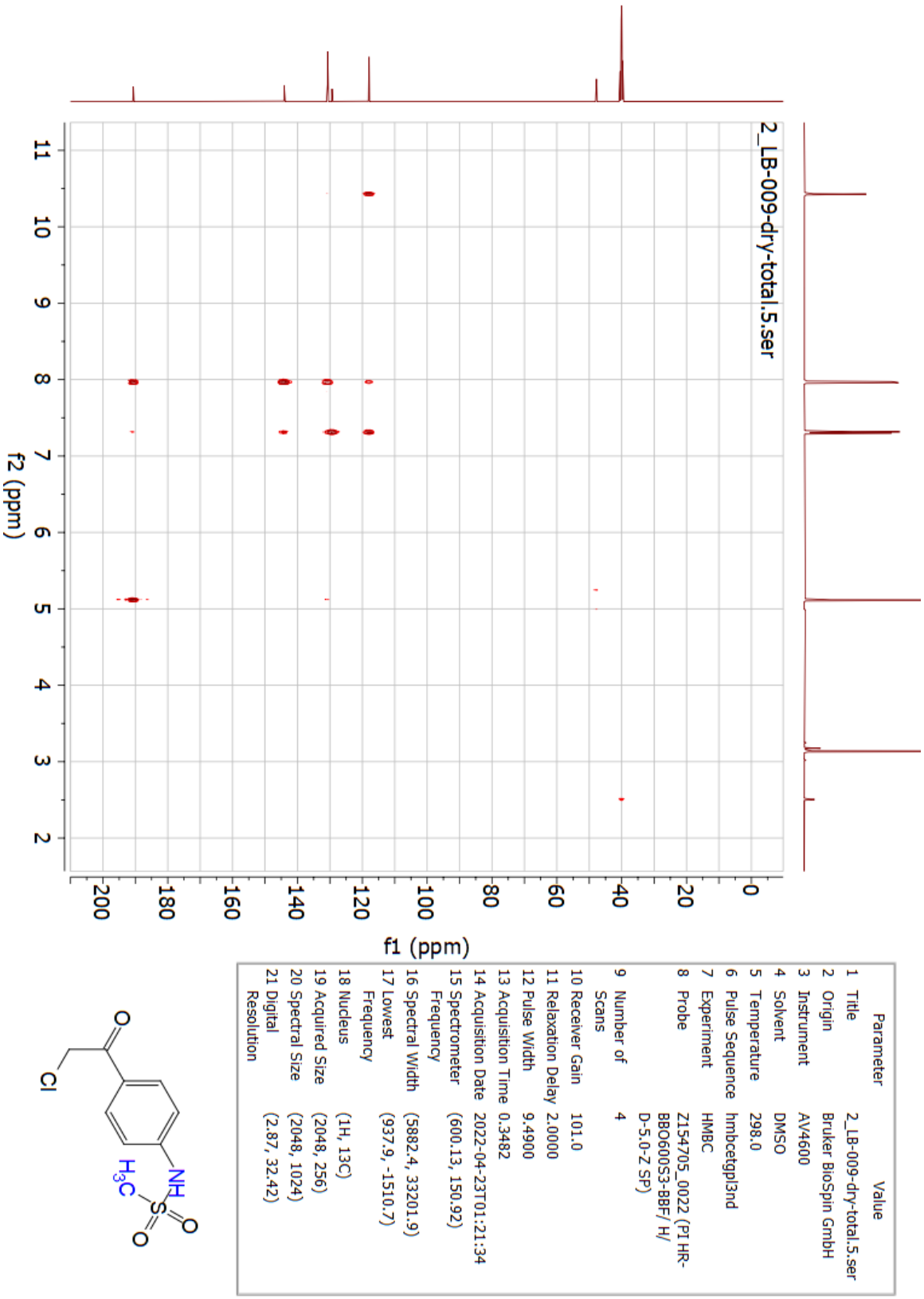

Figure 6.1.10: HMBC-NMR spectrum (600 MHz, d6-DMSO) of N-(4-(2-chloroacetyl)phenyl)methanesulfonamide (**2**).

6.1.3 N-(4-(2-bromoacetyl)phenyl)methanesulfonamide (3)

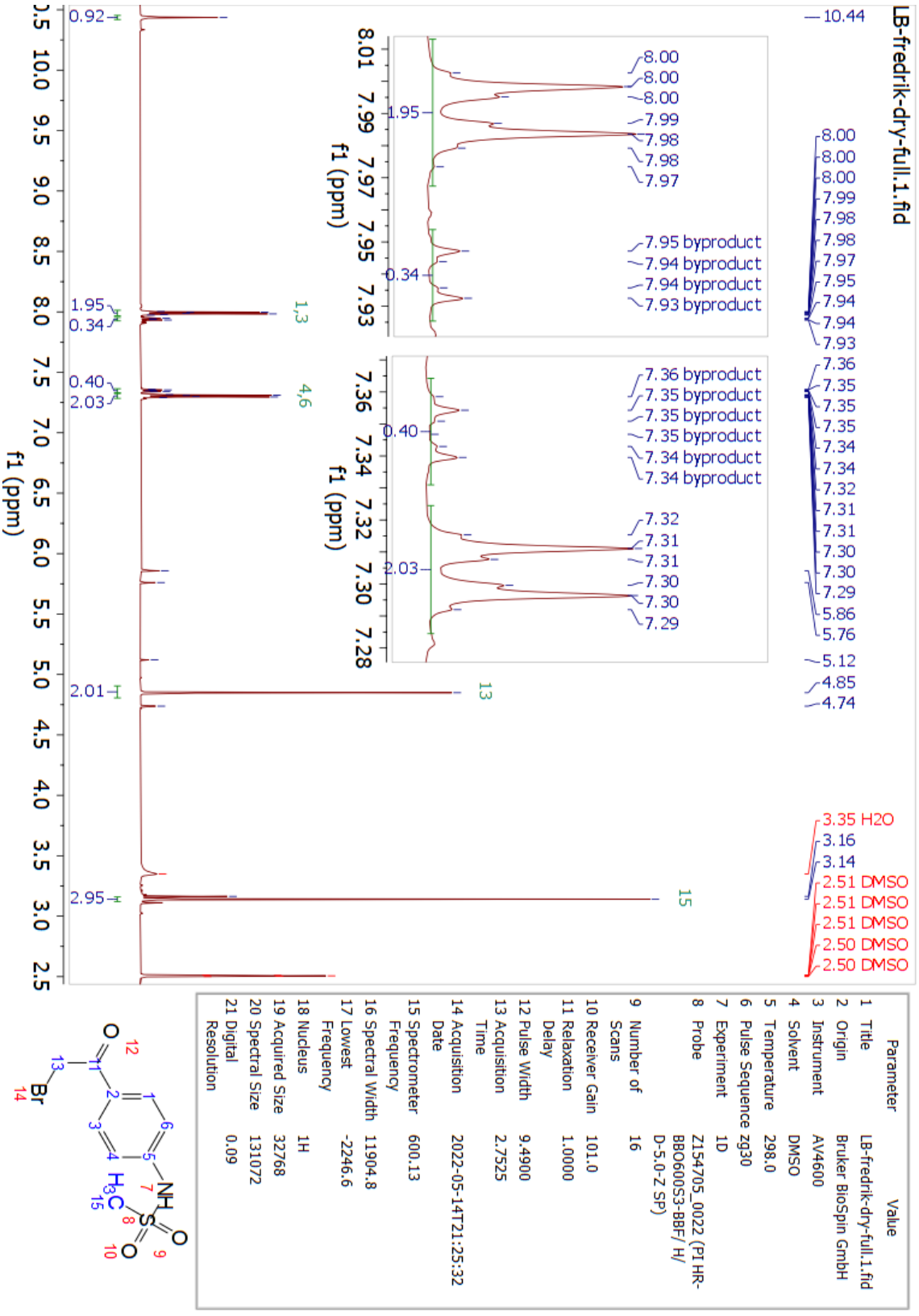

Parameter	Value
1 Title	LB-fredrik-dry-full.1.fid
2 Origin	Bruker BioSpin GmbH
3 Instrument	AV4600
4 Solvent	DMSO
5 Temperature	298.0
6 Pulse Sequence	zg30
7 Experiment	1D
8 Probe	Z154705_0022 (PI HR-BBO600S3-BBF/ H/ D-5.0-Z SP)
9 Number of Scans	16
10 Receiver Gain	101.0
11 Relaxation Delay	1.0000
12 Pulse Width	9.4900
13 Acquisition Time	2.7525
14 Acquisition Date	2022-05-14T21:25:32
15 Spectrometer Frequency	600.13
16 Spectral Width	11904.8
17 Lowest Frequency	-2246.6
18 Nucleus	1H
19 Acquired Size	32768
20 Spectral Size	131072
21 Digital Resolution	0.09

Figure 6.1.11: [1]H-NMR spectrum (600 MHz, d6-DMSO) of N-(4-(2-bromoacetyl)phenyl)methanesulfonamide (**3**).

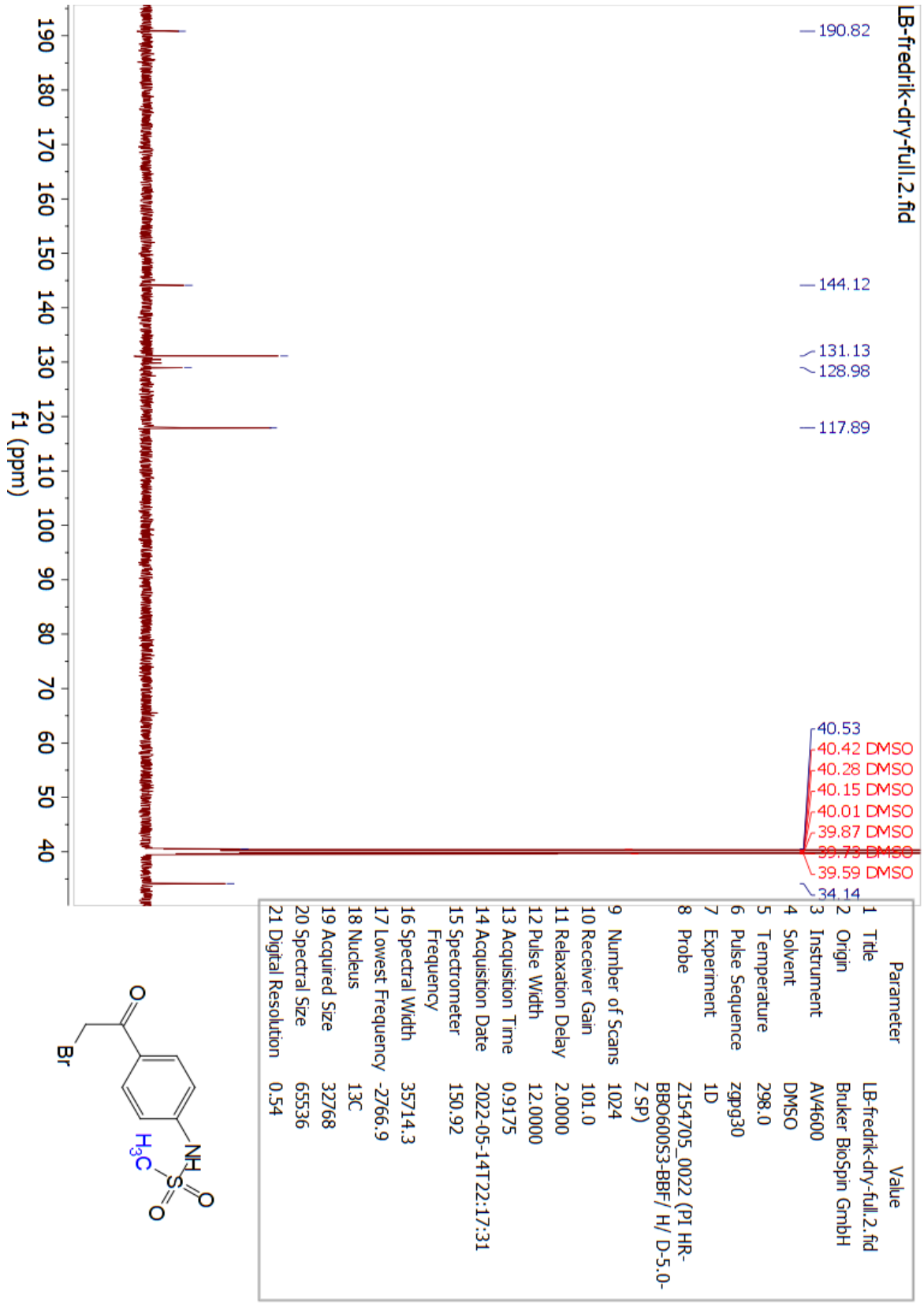

Figure 6.1.12: ^{13}C-NMR spectrum (600 MHz, d6-DMSO) of N-(4-(2-bromoacetyl)phenyl)methanesulfonamide (**3**).

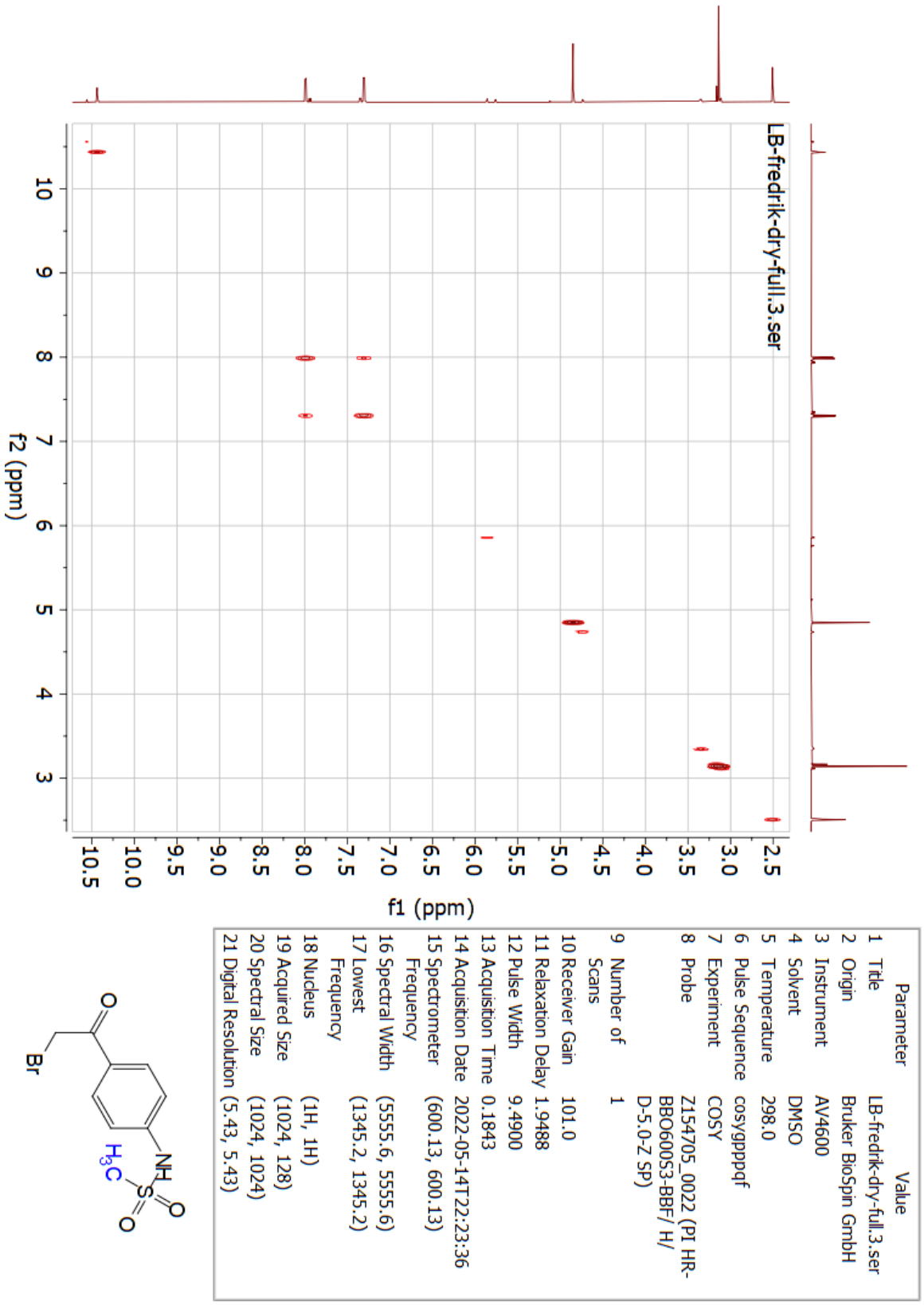

	Parameter	Value
1	Title	LB-fredrik-dry-full.3.ser
2	Origin	Bruker BioSpin GmbH
3	Instrument	AV4600
4	Solvent	DMSO
5	Temperature	298.0
6	Pulse Sequence	cosygpppqf
7	Experiment	COSY
8	Probe	Z154705_0022 (PI HR-BBO600S3-BBF/ H/ D-5.0-Z SP)
9	Number of Scans	1
10	Receiver Gain	101.0
11	Relaxation Delay	1.9488
12	Pulse Width	9.4900
13	Acquisition Time	0.1843
14	Acquisition Date	2022-05-14T22:23:36
15	Spectrometer Frequency	(600.13, 600.13)
16	Spectral Width	(5555.6, 5555.6)
17	Lowest Frequency	(1345.2, 1345.2)
18	Nucleus	(1H, 1H)
19	Acquired Size	(1024, 128)
20	Spectral Size	(1024, 1024)
21	Digital Resolution	(5.43, 5.43)

Figure 6.1.13: H,H-COSY-NMR spectrum (600 MHz, d6-DMSO) of N-(4-(2-bromoacetyl)phenyl)methanesulfonamide (**3**).

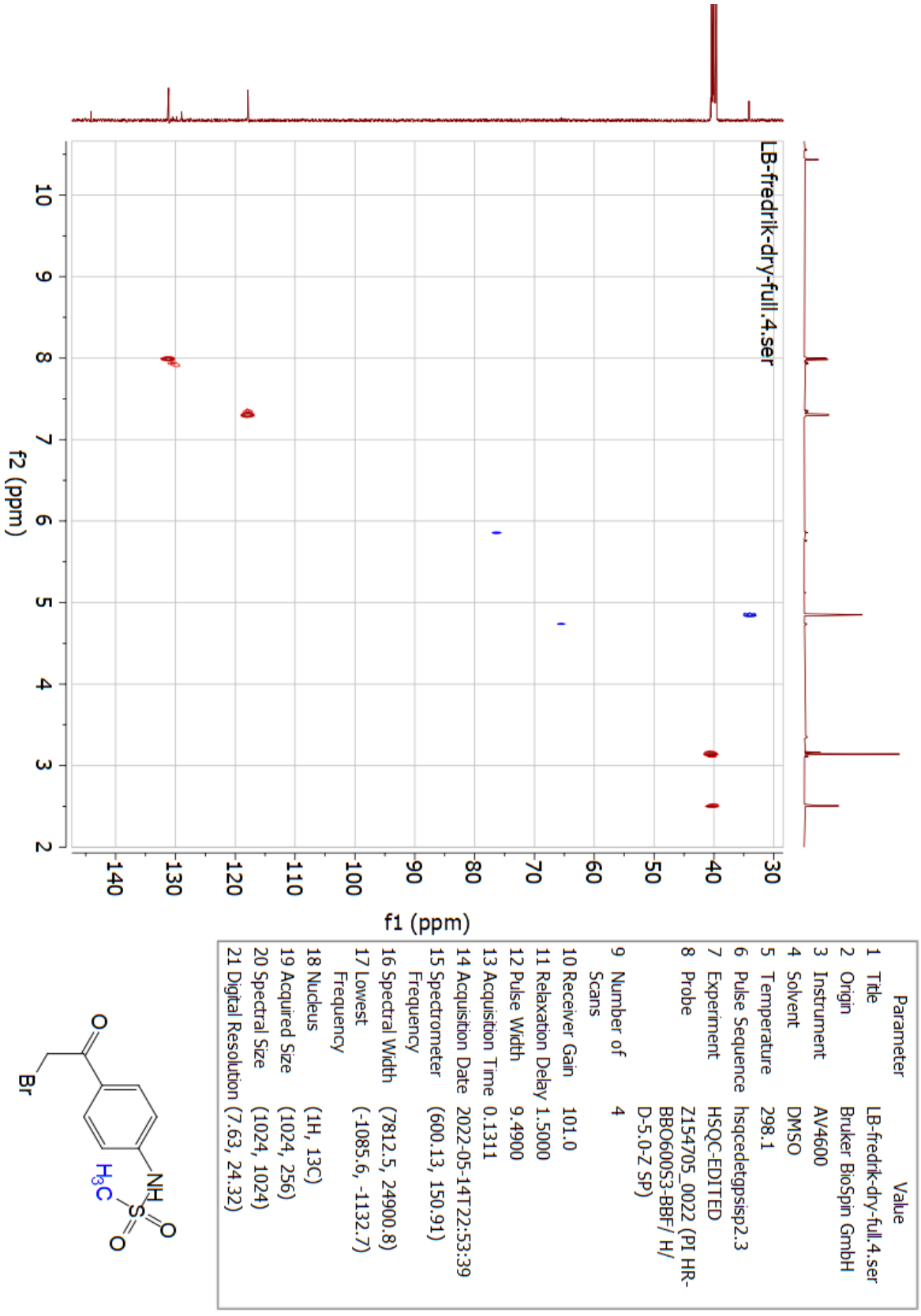

Parameter	Value
1 Title	LB-fredrik-dry-full.4.ser
2 Origin	Bruker BioSpin GmbH
3 Instrument	AV4600
4 Solvent	DMSO
5 Temperature	298.1
6 Pulse Sequence	hsqcedetgpsisp2.3
7 Experiment	HSQC-EDITED
8 Probe	Z154705_0022 (PI HR-BBO600S3-BBF/ H/ D-5.0-Z SP)
9 Number of Scans	4
10 Receiver Gain	101.0
11 Relaxation Delay	1.5000
12 Pulse Width	9.4900
13 Acquisition Time	0.1311
14 Acquisition Date	2022-05-14T22:53:39
15 Spectrometer Frequency	(600.13, 150.91)
16 Spectral Width	(7812.5, 24900.8)
17 Lowest Frequency	(-1085.6, -1132.7)
18 Nucleus	(1H, 13C)
19 Acquired Size	(1024, 256)
20 Spectral Size	(1024, 1024)
21 Digital Resolution	(7.63, 24.32)

Figure 6.1.14: HSQC-NMR spectrum (600 MHz, d6-DMSO) of N-(4-(2-bromoacetyl)phenyl)methanesulfonamide (**3**).

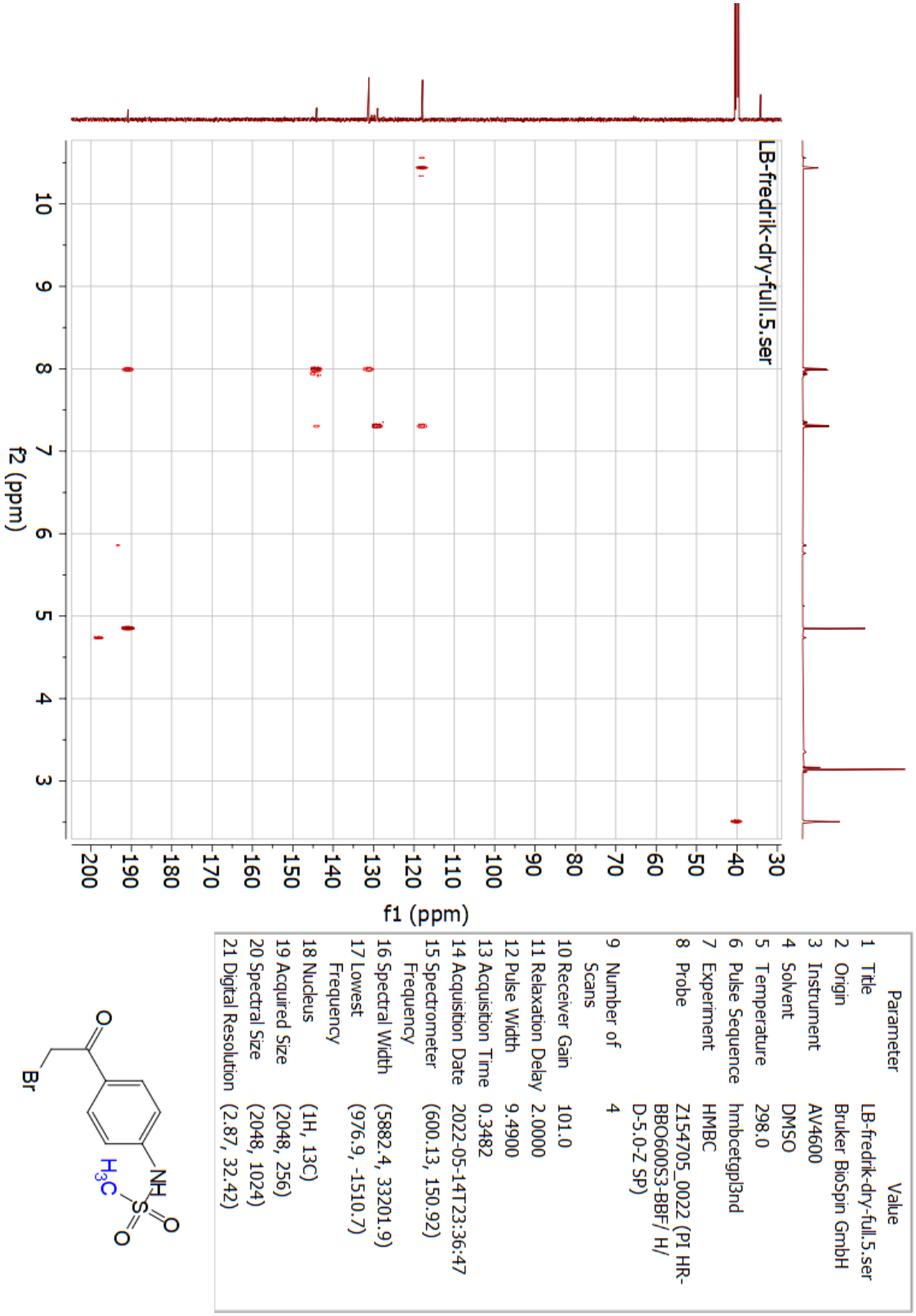

Parameter	Value
1 Title	LB-fredrik-dry-full.5.ser
2 Origin	Bruker BioSpin GmbH
3 Instrument	AV4600
4 Solvent	DMSO
5 Temperature	298.0
6 Pulse Sequence	hmbcetgpl3nd
7 Experiment	HMBC
8 Probe	Z154705_0022 (PI HR-BBO600S3-BBF/ H/ D-5.0-Z SP)
9 Number of Scans	4
10 Receiver Gain	101.0
11 Relaxation Delay	2.0000
12 Pulse Width	9.4900
13 Acquisition Time	0.3482
14 Acquisition Date	2022-05-14T23:36:47
15 Spectrometer Frequency	(600.13, 150.92)
16 Spectral Width	(5882.4, 33201.9)
17 Lowest Frequency	(976.9, -1510.7)
18 Nucleus	(1H, 13C)
19 Acquired Size	(2048, 256)
20 Spectral Size	(2048, 1024)
21 Digital Resolution	(2.87, 32.42)

Figure 6.1.15: HMBC-NMR spectrum (600 MHz, d6-DMSO) of N-(4-(2-bromoacetyl)phenyl)methanesulfonamide (**3**).

6.1.4 N-(4-(2-chloro-1-hydroxyethyl)phenyl)methanesulfonamide (4)

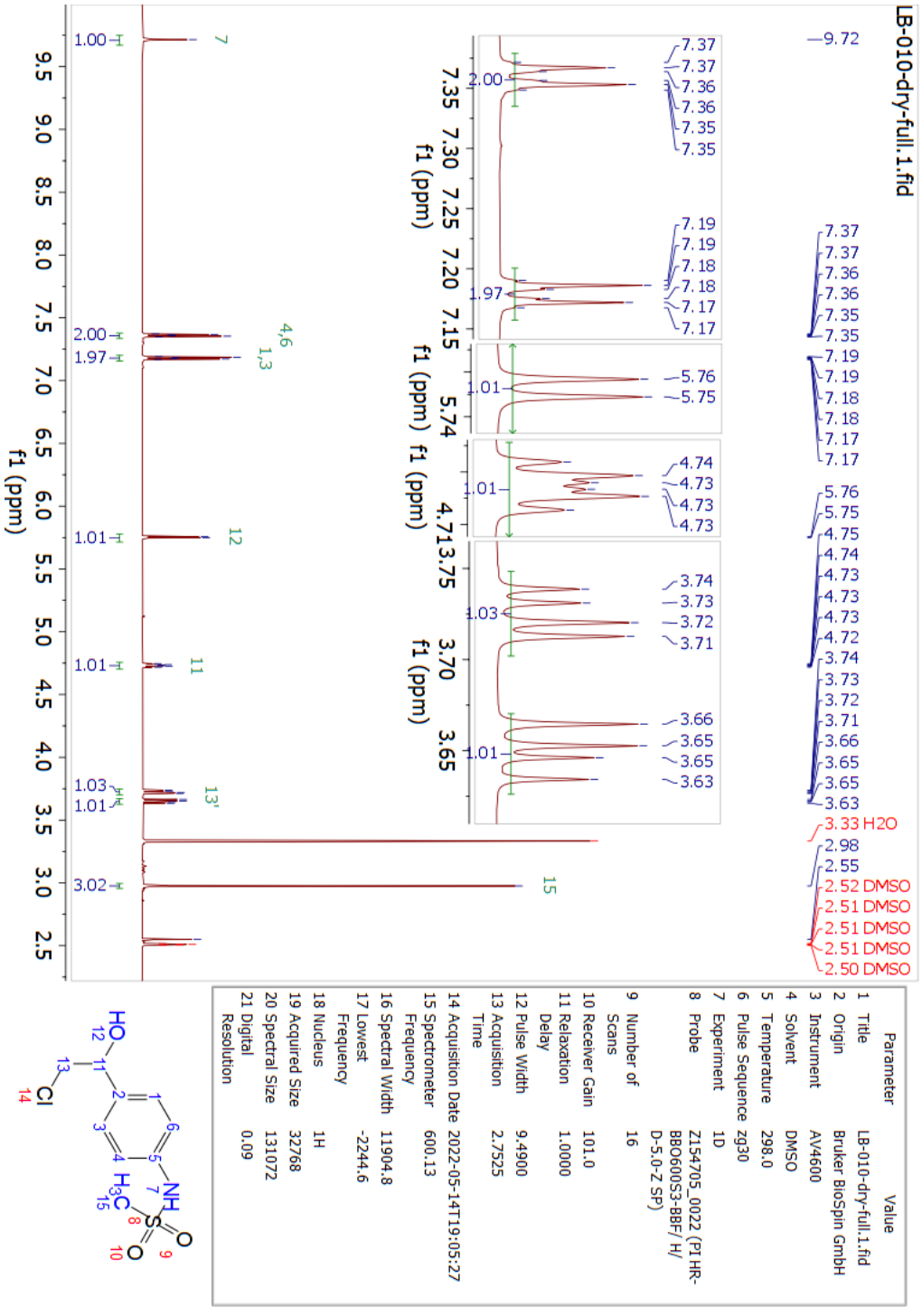

Figure 6.1.16: ^{1}H-NMR spectrum (600 MHz, d6-DMSO) of N-(4-(2-chloro-1-hydroxyethyl)phenyl)methanesulfonamide (**4**).

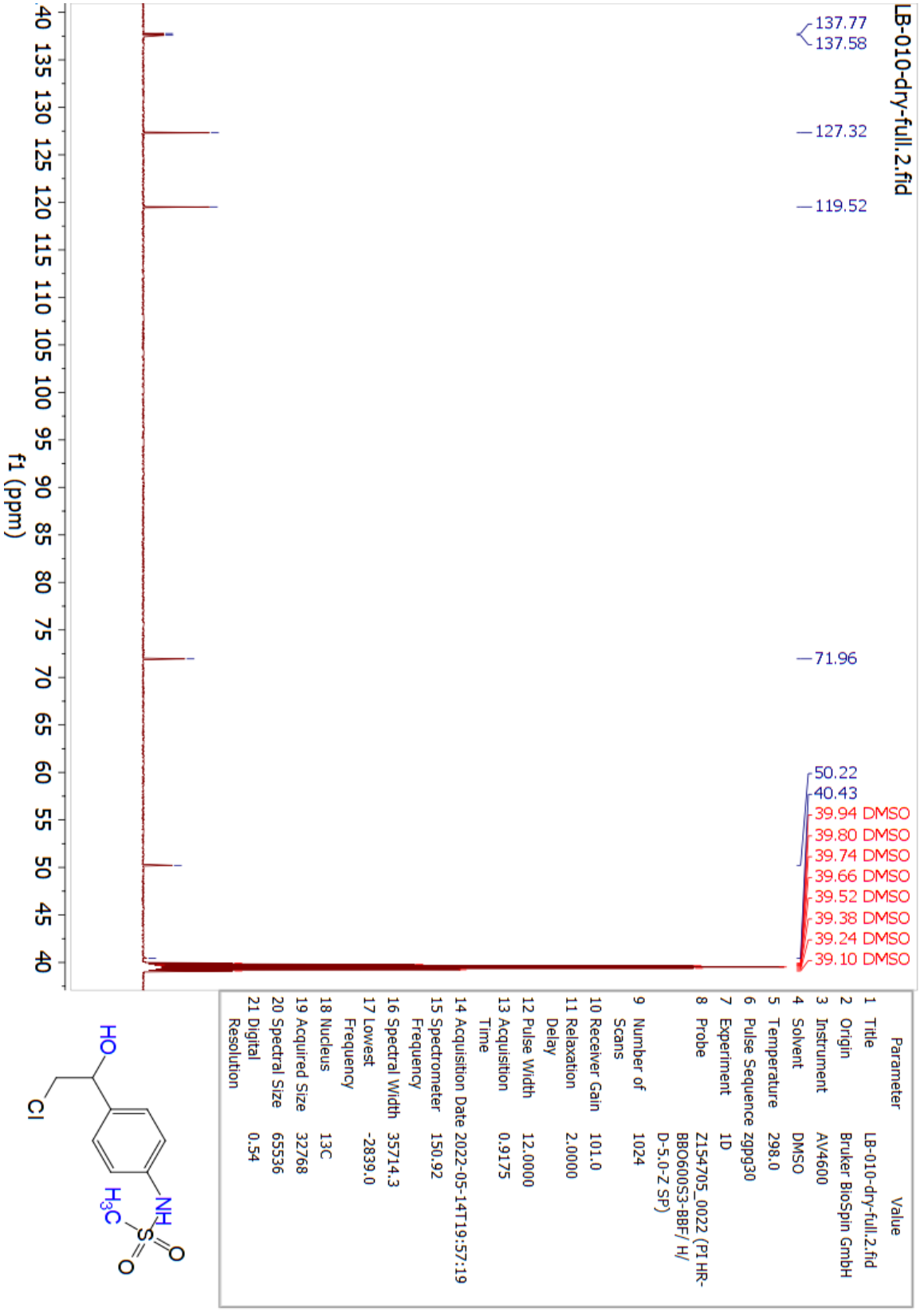

Figure 6.1.17: ^{13}C-NMR spectrum (600 MHz, d6-DMSO) of N-(4-(2-chloro-1-hydroxyethyl)phenyl)methanesulfonamide (**4**).

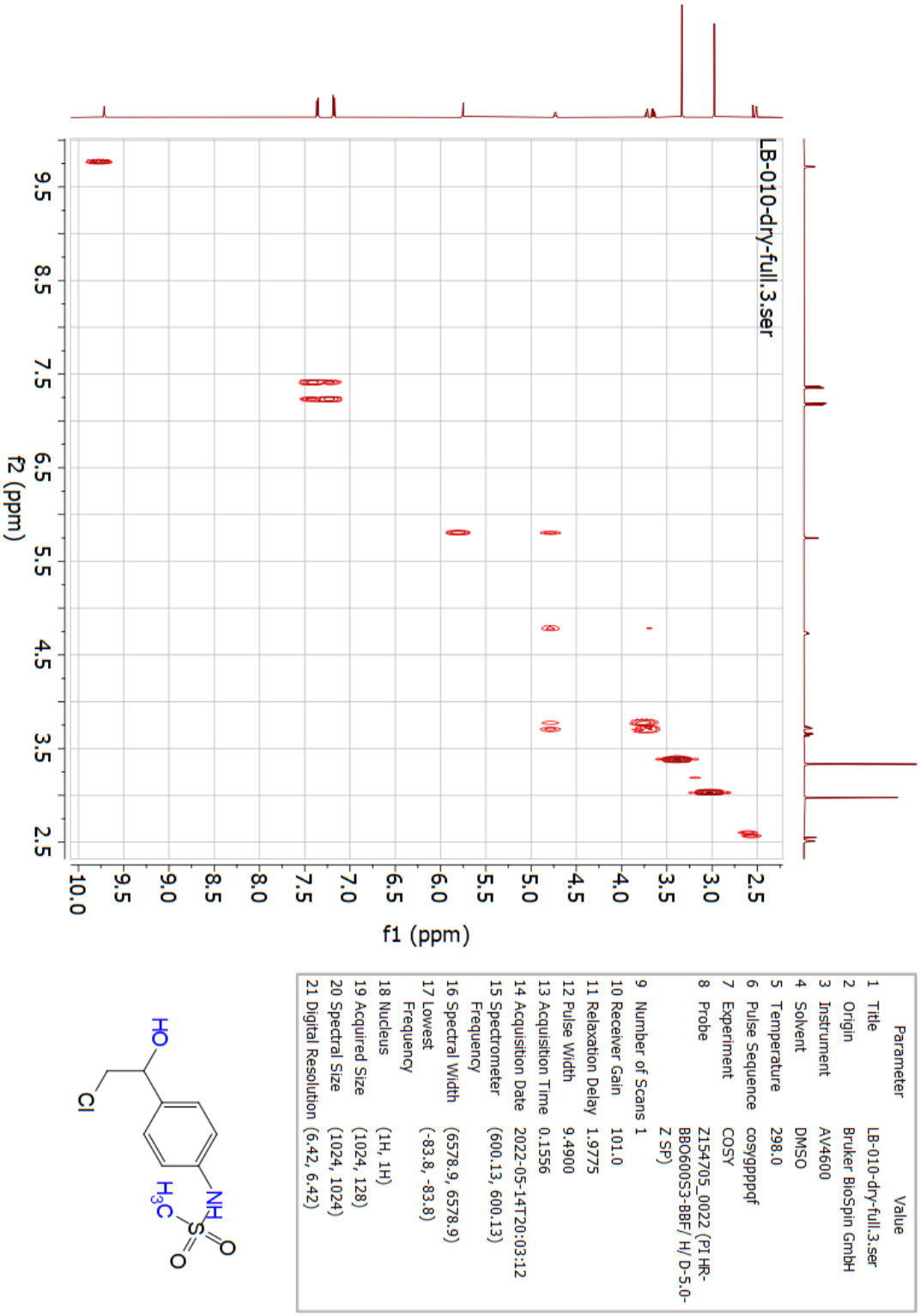

	Parameter	Value
1	Title	LB-010-dry-full.3.ser
2	Origin	Bruker BioSpin GmbH
3	Instrument	AV4600
4	Solvent	DMSO
5	Temperature	298.0
6	Pulse Sequence	cosygpppqf
7	Experiment	COSY
8	Probe	Z154705_0022 (PI HR-BBO600S3-BBF/ H/ D-5.0-Z SP)
9	Number of Scans	1
10	Receiver Gain	101.0
11	Relaxation Delay	1.9775
12	Pulse Width	9.4900
13	Acquisition Time	0.1556
14	Acquisition Date	2022-05-14T20:03:12
15	Spectrometer Frequency	(600.13, 600.13)
16	Spectral Width	(6578.9, 6578.9)
17	Lowest Frequency	(-83.8, -83.8)
18	Nucleus	(1H, 1H)
19	Acquired Size	(1024, 128)
20	Spectral Size	(1024, 1024)
21	Digital Resolution	(6.42, 6.42)

Figure 6.1.18: H,H-COSY-NMR spectrum (600 MHz, d6-DMSO) of N-(4-(2-chloro-1-hydroxyethyl)phenyl)methanesulfonamide (**4**).

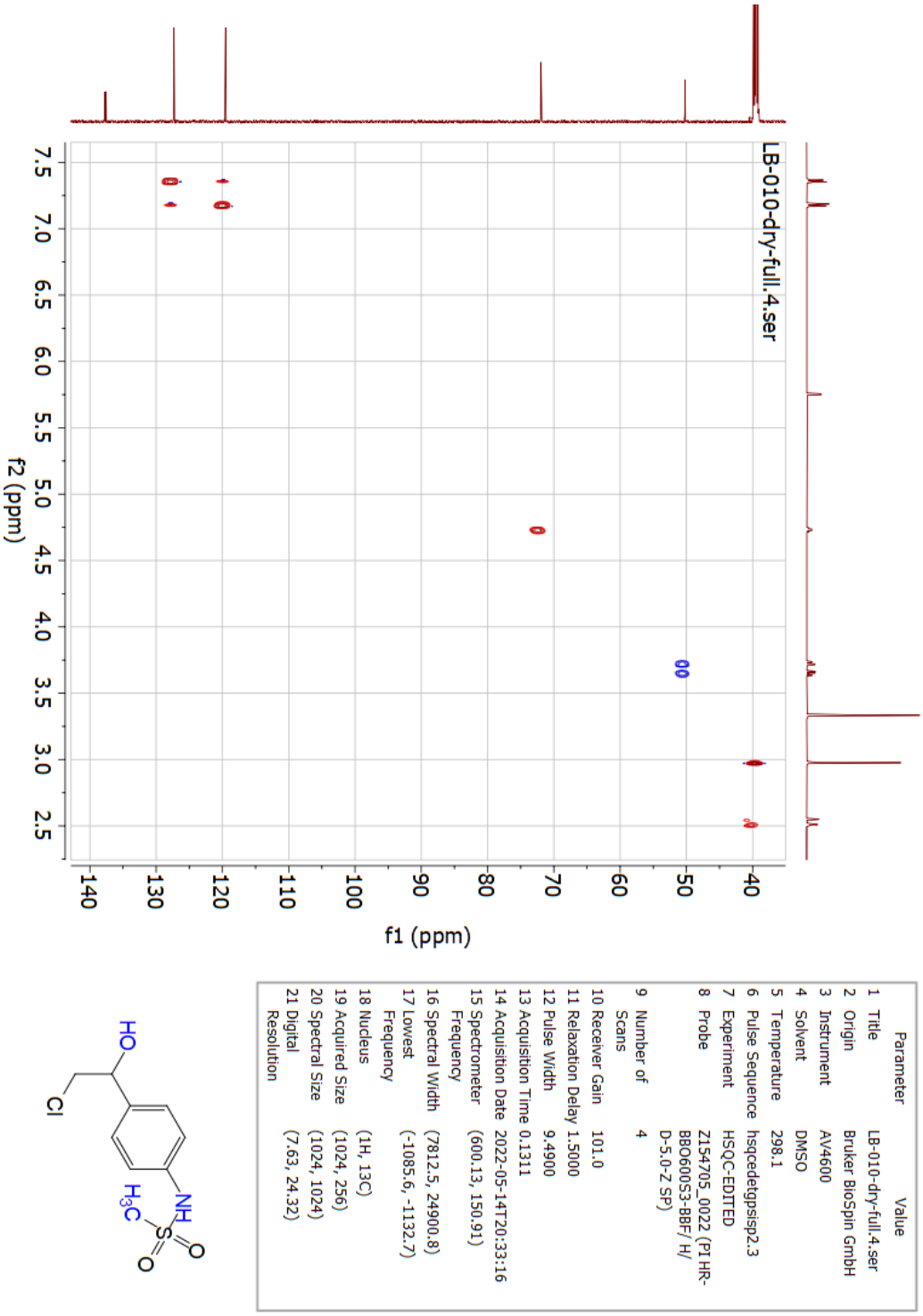

	Parameter	Value
1	Title	LB-010-dry-full.4.ser
2	Origin	Bruker BioSpin GmbH
3	Instrument	AV4600
4	Solvent	DMSO
5	Temperature	298.1
6	Pulse Sequence	hsqcedetgpsisp2.3
7	Experiment	HSQC-EDITED
8	Probe	Z154705_0022 (PI HR-BBO600S3-BBF/ H/ D-5.0-Z SP)
9	Number of Scans	4
10	Receiver Gain	101.0
11	Relaxation Delay	1.5000
12	Pulse Width	9.4900
13	Acquisition Time	0.1311
14	Acquisition Date	2022-05-14T20:33:16
15	Spectrometer Frequency	(600.13, 150.91)
16	Spectral Width	(7812.5, 24900.8)
17	Lowest Frequency	(-1085.6, -1132.7)
18	Nucleus	(1H, 13C)
19	Acquired Size	(1024, 256)
20	Spectral Size	(1024, 1024)
21	Digital Resolution	(7.63, 24.32)

Figure 6.1.19: HSQC-NMR spectrum (600 MHz, d6-DMSO) of N-(4-(2-chloro-1-hydroxyethyl)phenyl)methanesulfonamide (**4**).

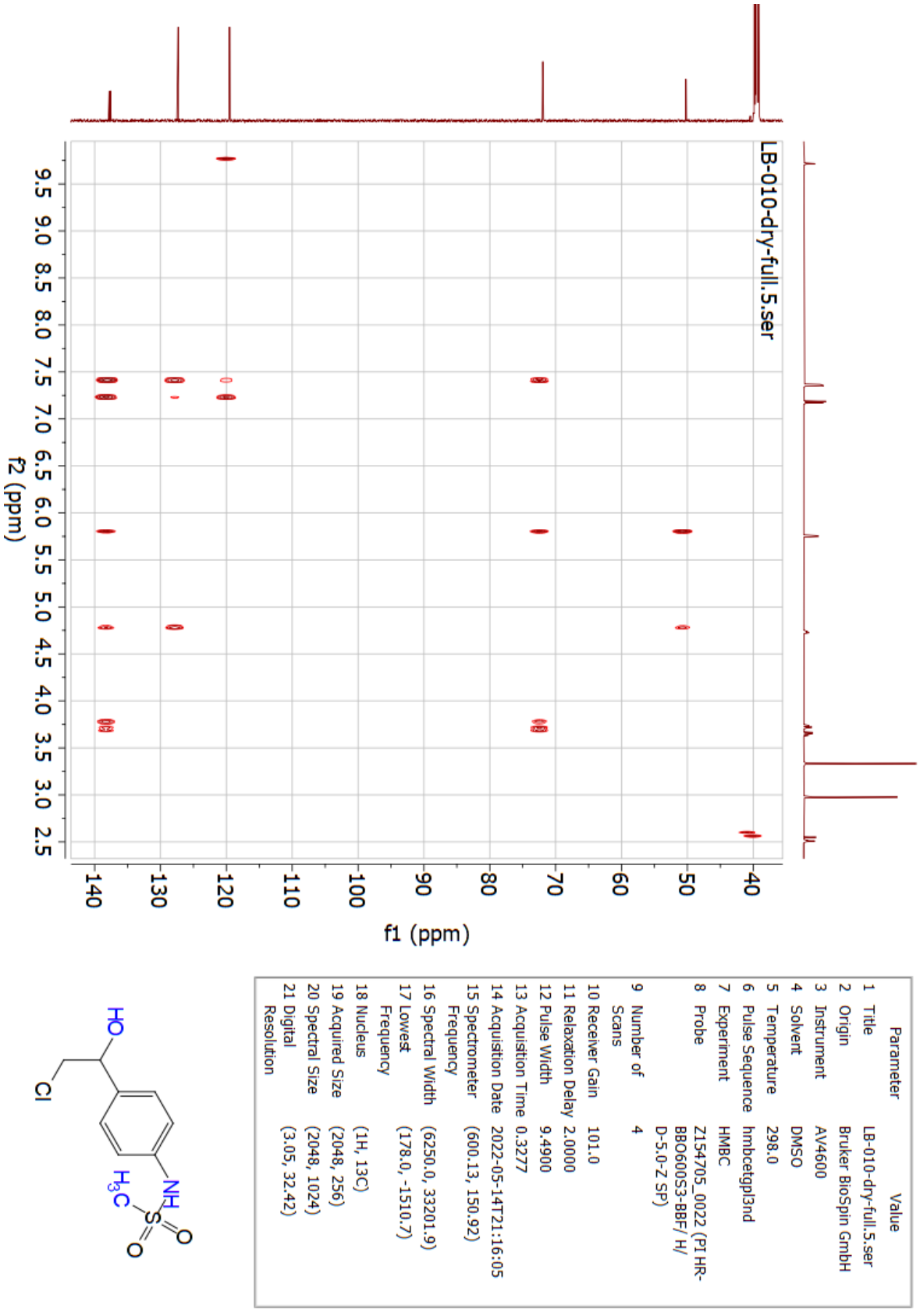

Parameter	Value
1 Title	LB-010-dry-full.5.ser
2 Origin	Bruker BioSpin GmbH
3 Instrument	AV4600
4 Solvent	DMSO
5 Temperature	298.0
6 Pulse Sequence	hmbcetgpl3nd
7 Experiment	HMBC
8 Probe	Z154705_0022 (PI HR-BBO600S3-BBF/ H/D-5.0-Z SP)
9 Number of Scans	4
10 Receiver Gain	101.0
11 Relaxation Delay	2.0000
12 Pulse Width	9.4900
13 Acquisition Time	0.3277
14 Acquisition Date	2022-05-14T21:16:05
15 Spectrometer Frequency	(600.13, 150.92)
16 Spectral Width	(6250.0, 33201.9)
17 Lowest Frequency	(178.0, -1510.7)
18 Nucleus	(1H, 13C)
19 Acquired Size	(2048, 256)
20 Spectral Size	(2048, 1024)
21 Digital Resolution	(3.05, 32.42)

Figure 6.1.20: HMBC-NMR spectrum (600 MHz, d6-DMSO) of N-(4-(2-chloro-1-hydroxyethyl)phenyl)methanesulfonamide (**4**).

6.1.5 N-(4-(2-Methoxyacetyl)phenyl)methanesulfonamide (M)

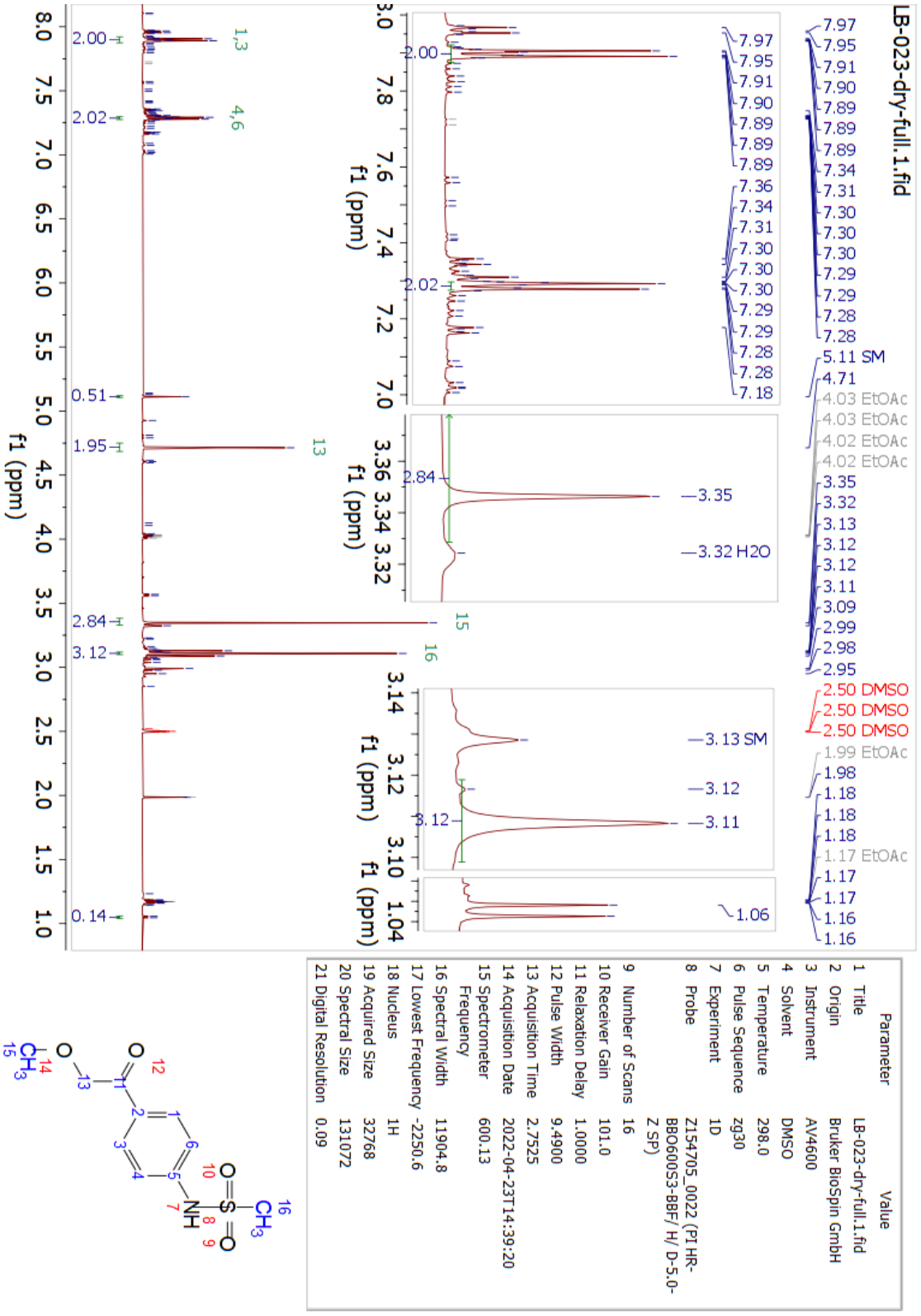

Figure 6.1.21: ^{1}H-NMR spectrum (600 MHz, d6-DMSO) of byproduct **M**.

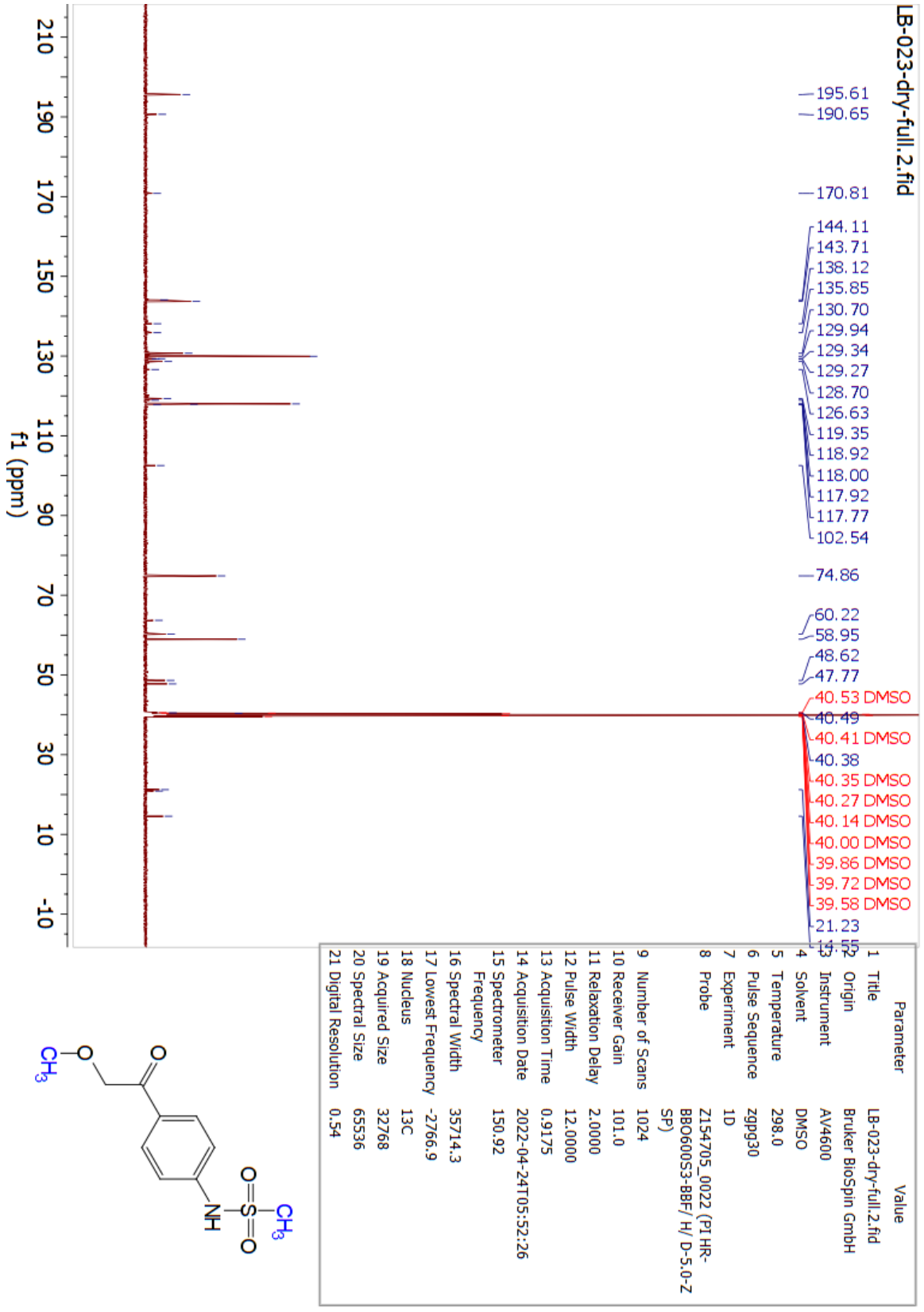

Figure 6.1.22: ^{13}C-NMR spectrum (600 MHz, d6-DMSO) of byproduct **M**.

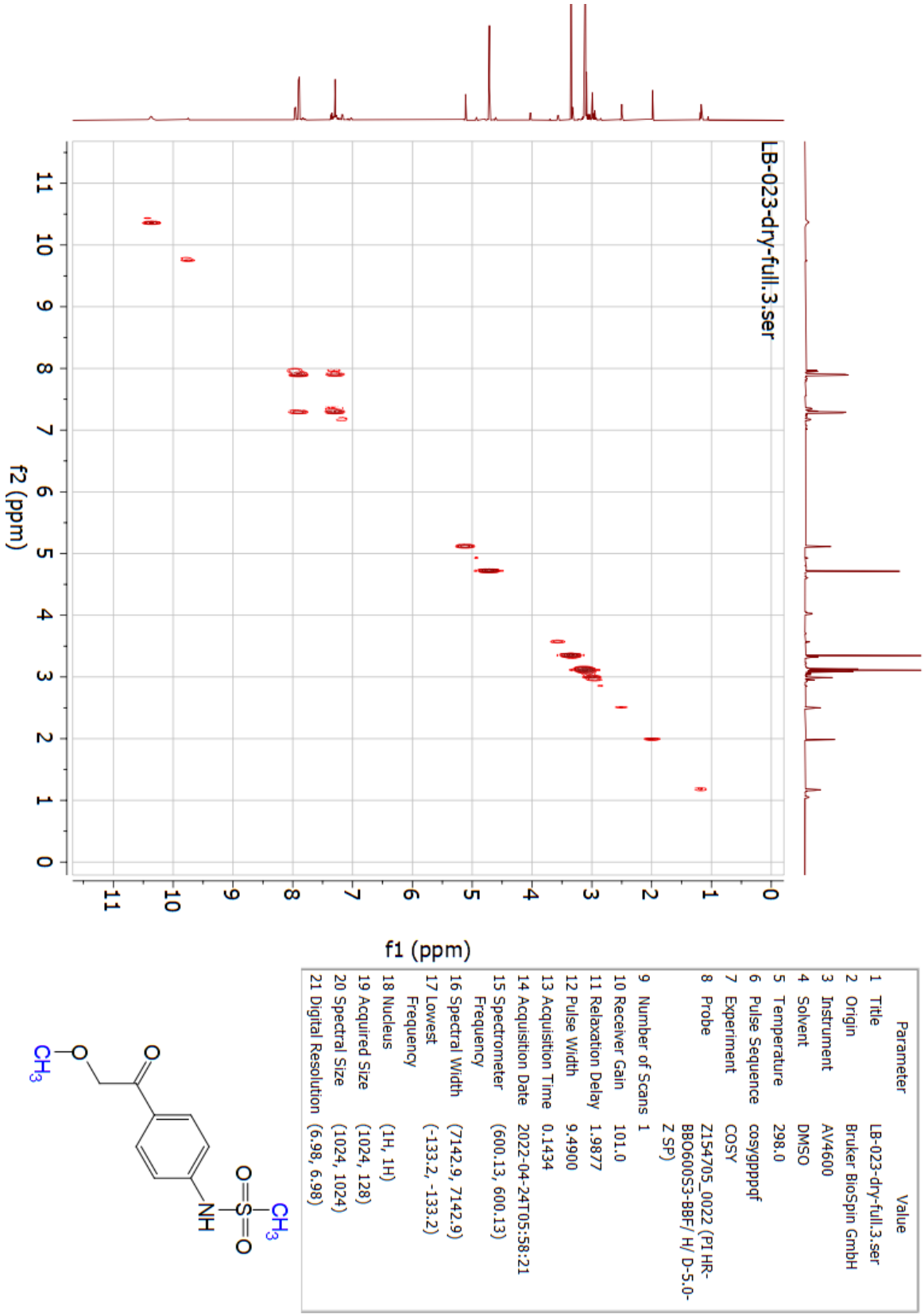

Figure 6.1.23: H,H-COSY-NMR spectrum (600 MHz, d6-DMSO) of byproduct **M**.

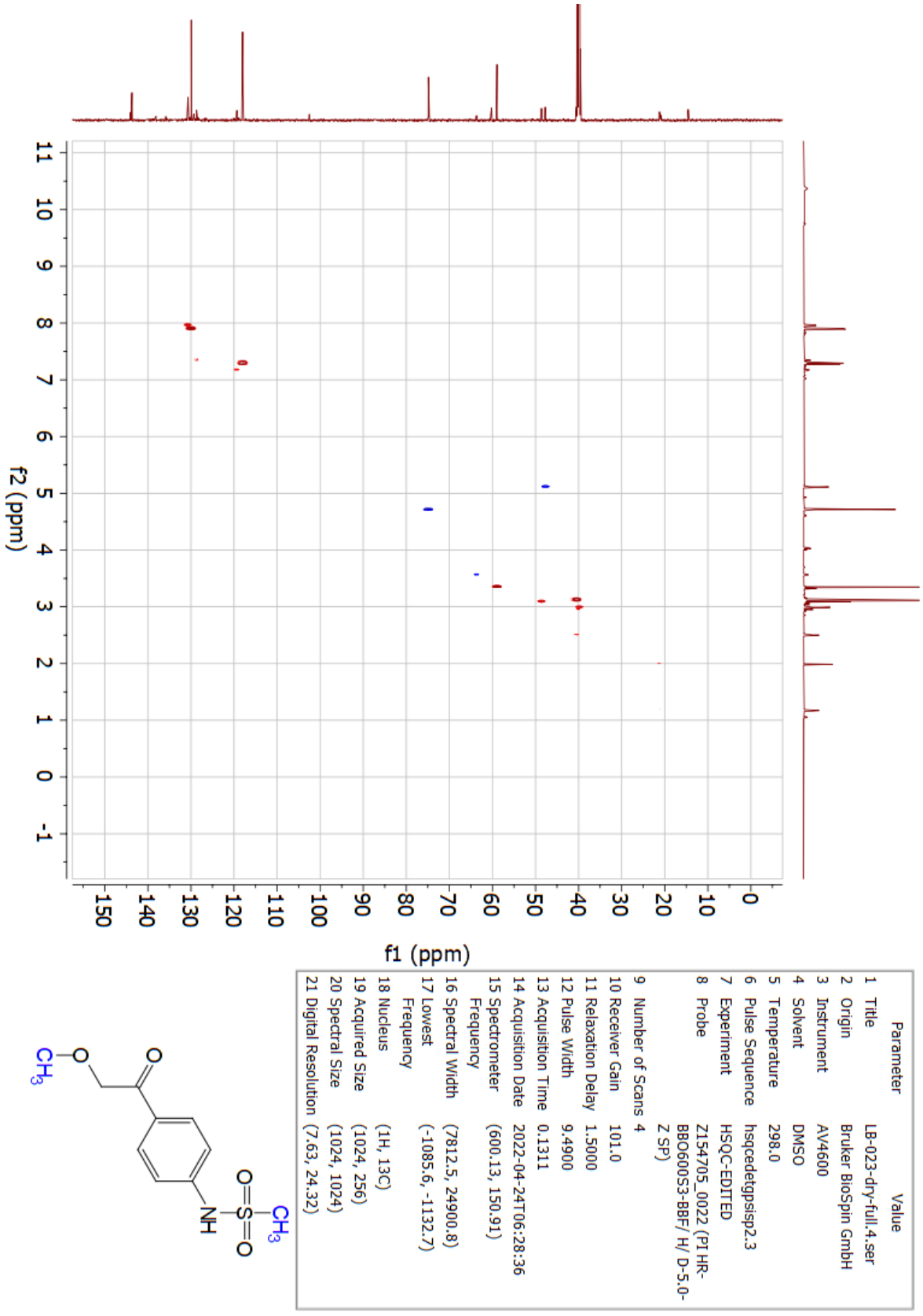

Figure 6.1.24: HSQC-NMR spectrum (600 MHz, d6-DMSO) of byproduct **M**.

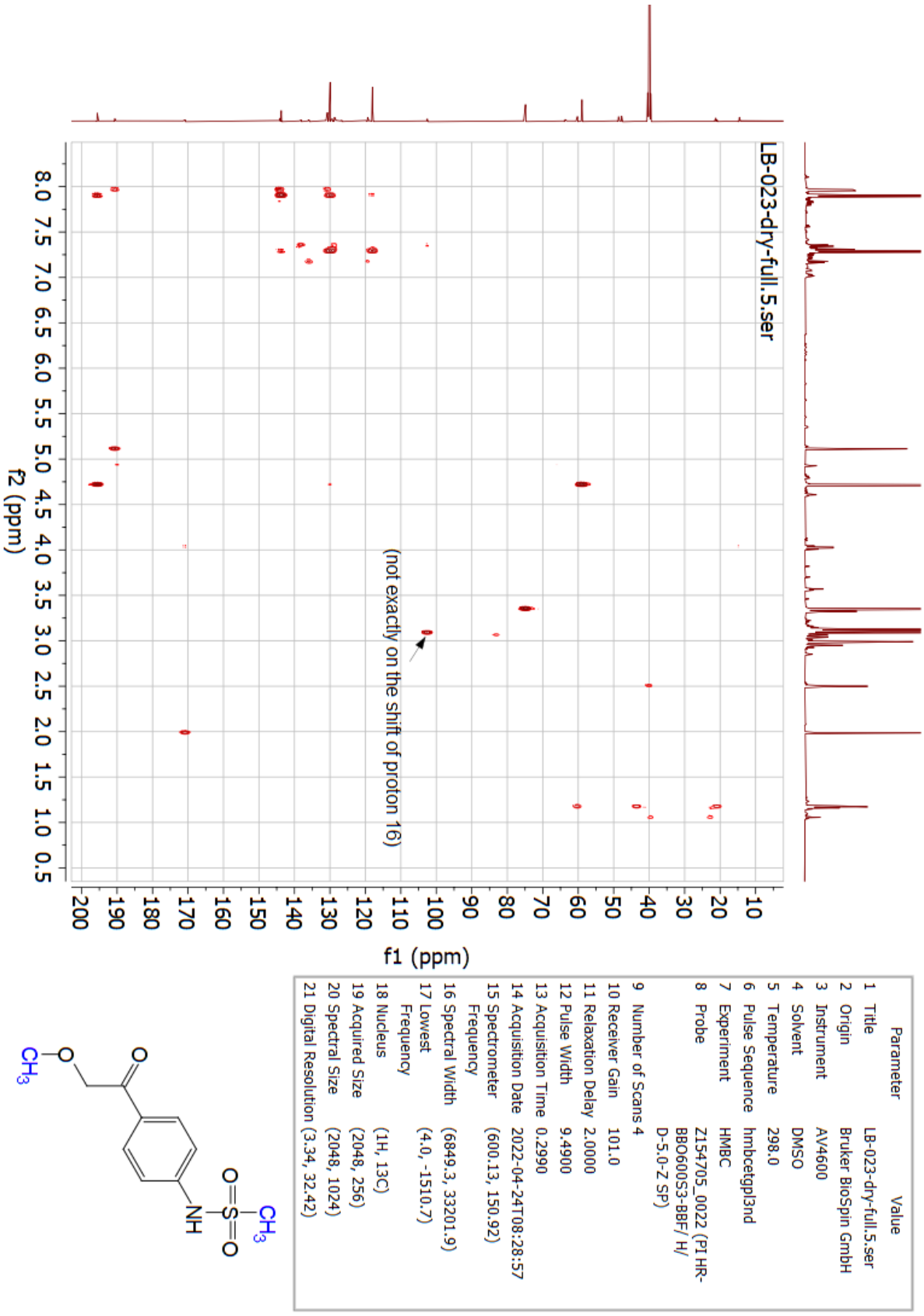

Figure 6.1.25: HMBC-NMR spectrum (600 MHz, d6-DMSO) of byproduct **M**.

Single Mass Analysis
Tolerance = 5.0 PPM / DBE: min = -10.0, max = 50.0
Element prediction: Off
Number of isotope peaks used for i-FIT = 6

Monoisotopic Mass, Even Electron Ions
158 formula(e) evaluated with 1 results within limits (all results (up to 1000) for each mass)
Elements Used:
C: 0-100 H: 0-200 N: 0-2 O: 0-5 S: 0-1
ReqID1503 74 (0.707) AM2 (Ar,35000.0,0.00,0.00); Cm (61:88)
1: TOF MS ES+

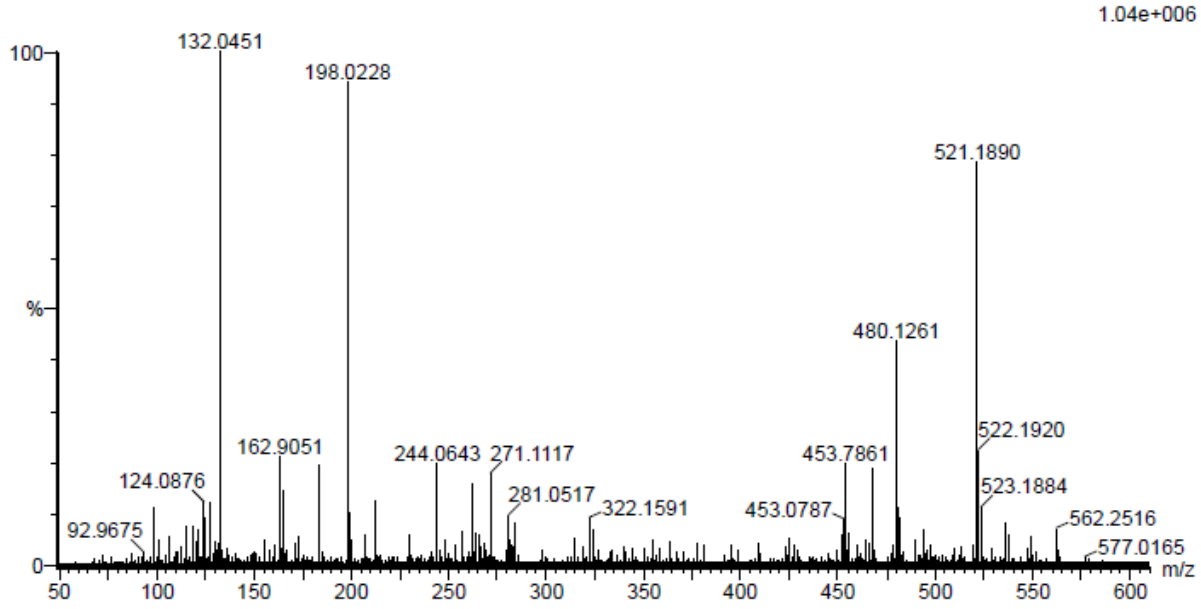

Minimum:				-10.0				
Maximum:		1000.0	5.0	50.0				
Mass	Calc. Mass	mDa	PPM	DBE	i-FIT	Norm	Conf(%)	Formula
244.0643	244.0644	-0.1	-0.4	4.5	3421.1	n/a	n/a	C10 H14 N O4 S

Figure 6.1.26: MS analysis of the mixture containing byproduct **M**. Accurate mass determination in positive and negative mode was performed on a "Synapt G2-S" Q-TOF instrument from Water TM. Samples were ionized by the use of ASAP probe (APCI) or ESI probe. No chromatographic separation was used previous to the mass analysis. Calculated exact mass and spectra processing was done by Waters TM Software Masslynx V4.1 SCN871.

6.2 Penbutolol synthesis

6.2.1 1-chloro-3-(2-cyclopentylphenoxy)propan-2-ol (8)

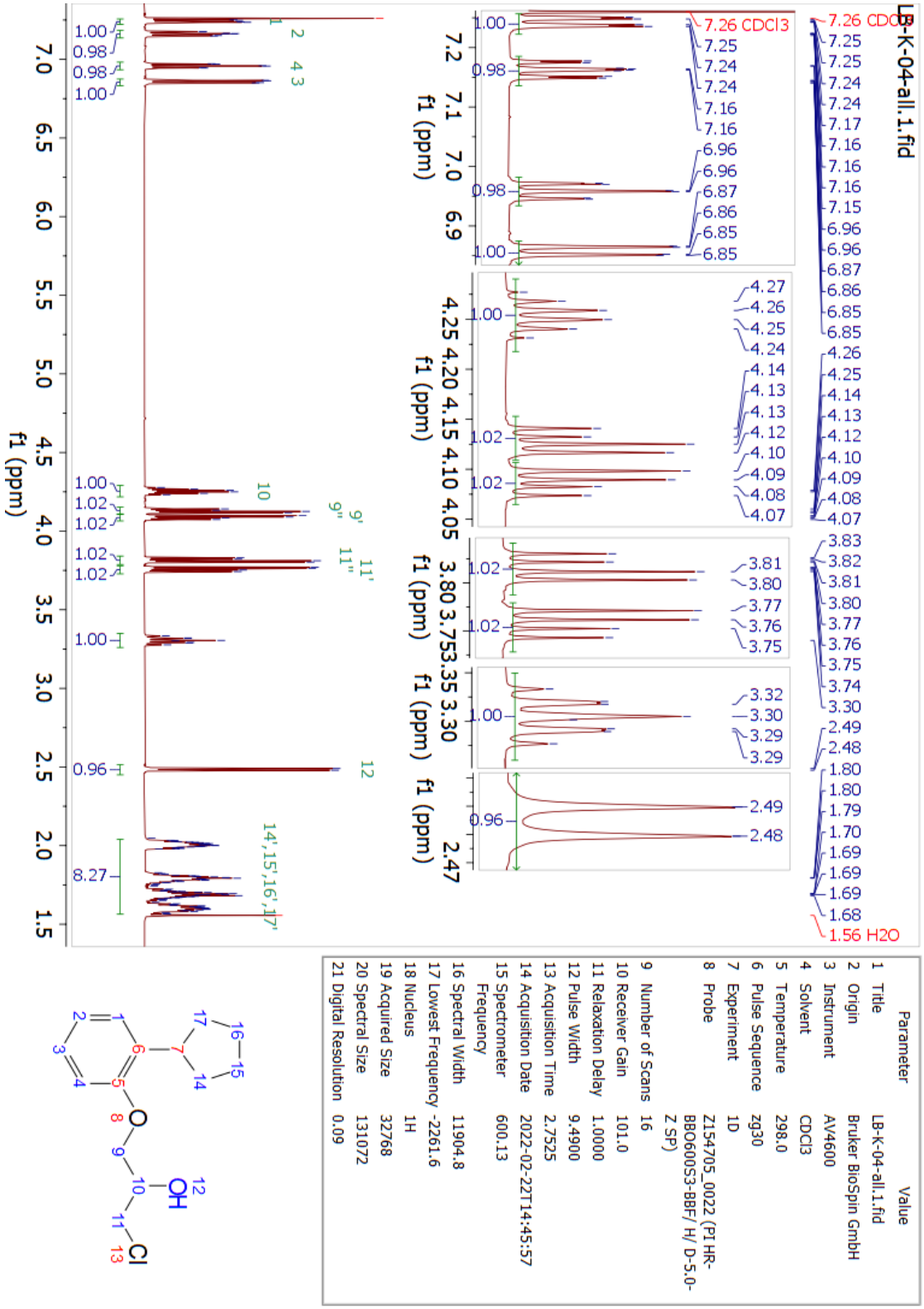

Figure 6.2.1: ^{1}H-NMR spectrum (600 MHz, $CDCl_3$) of 1-chloro-3-(2-cyclopentylphenoxy)propan-2-ol (**8**).

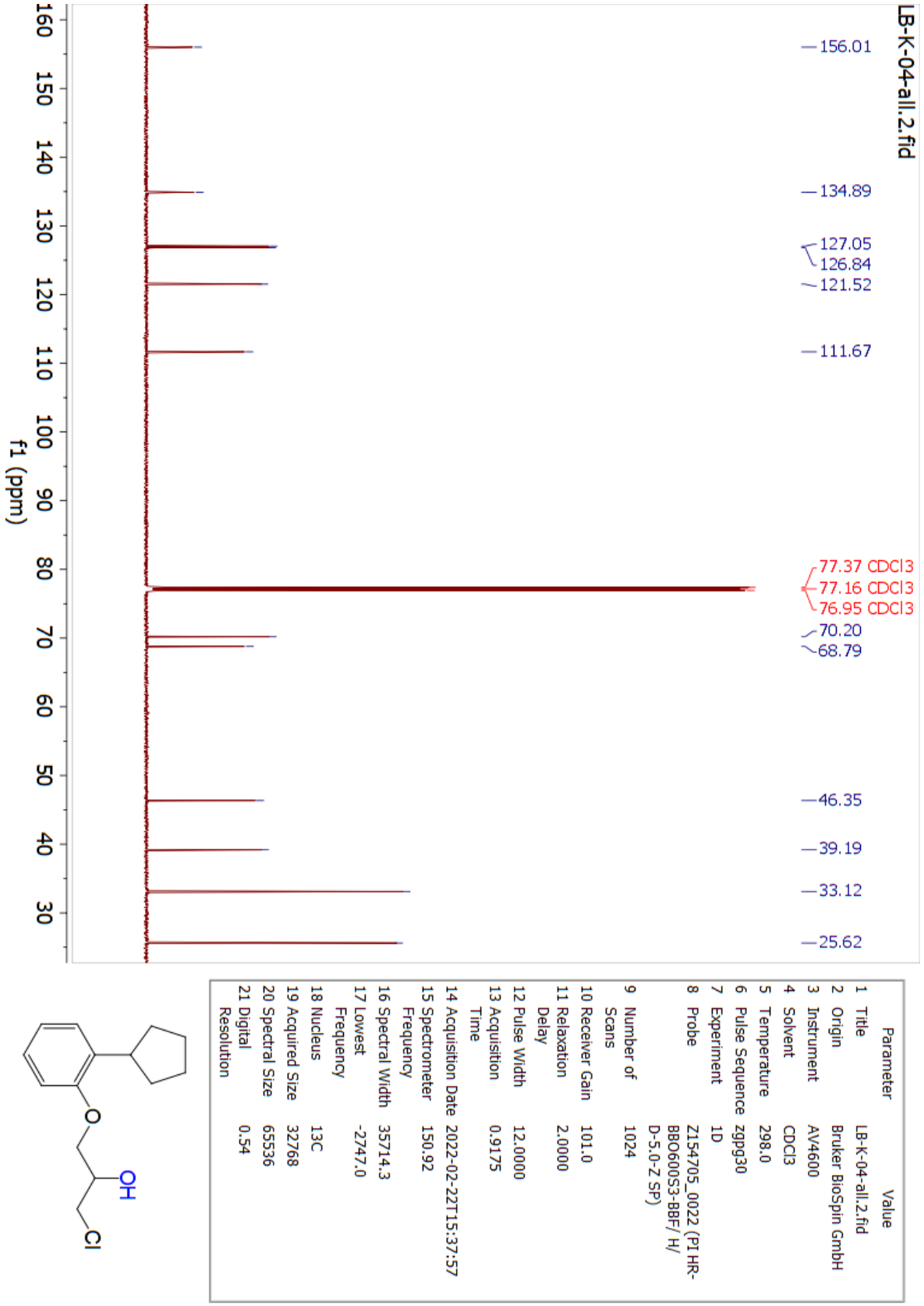

Parameter	Value
1 Title	LB-K-04-all.2.fid
2 Origin	Bruker BioSpin GmbH
3 Instrument	AV4600
4 Solvent	CDCl3
5 Temperature	298.0
6 Pulse Sequence	zgpg30
7 Experiment	1D
8 Probe	Z154705_0022 (PI HR-BBO600S3-BBF/ H/ D-5.0-Z SP)
9 Number of Scans	1024
10 Receiver Gain	101.0
11 Relaxation Delay	2.0000
12 Pulse Width	12.0000
13 Acquisition Time	0.9175
14 Acquisition Date	2022-02-22T15:37:57
15 Spectrometer Frequency	150.92
16 Spectral Width	35714.3
17 Lowest Frequency	-2747.0
18 Nucleus	13C
19 Acquired Size	32768
20 Spectral Size	65536
21 Digital Resolution	0.54

Figure 6.2.2: ^{13}C-NMR spectrum (600 MHz, $CDCl_3$) of 1-chloro-3-(2-cyclopentylphenoxy)propan-2-ol (**8**).

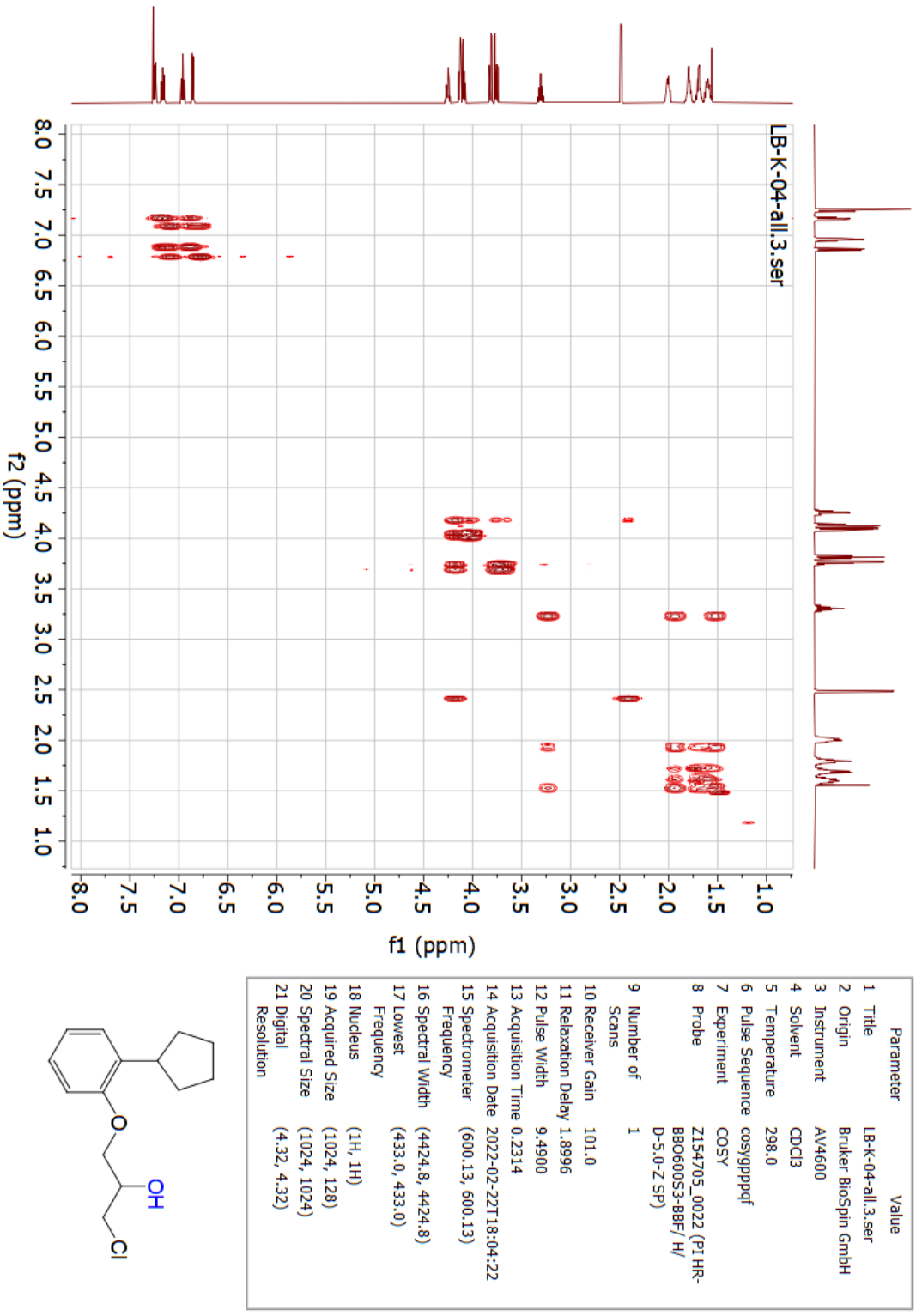

Parameter	Value
1 Title	LB-K-04-all.3.ser
2 Origin	Bruker BioSpin GmbH
3 Instrument	AV4600
4 Solvent	CDCl3
5 Temperature	298.0
6 Pulse Sequence	cosygpppqf
7 Experiment	COSY
8 Probe	Z154705_0022 (PI HR-BBO600S3-BBF/ H/ D-5.0-Z SP)
9 Number of Scans	1
10 Receiver Gain	101.0
11 Relaxation Delay	1.8996
12 Pulse Width	9.4900
13 Acquisition Time	0.2314
14 Acquisition Date	2022-02-22T18:04:22
15 Spectrometer Frequency	(600.13, 600.13)
16 Spectral Width	(4424.8, 4424.8)
17 Lowest Frequency	(433.0, 433.0)
18 Nucleus	(1H, 1H)
19 Acquired Size	(1024, 128)
20 Spectral Size	(1024, 1024)
21 Digital Resolution	(4.32, 4.32)

Figure 6.2.3: H,H-COSY-NMR spectrum (600 MHz, $CDCl_3$) of 1-chloro-3-(2-cyclopentylphenoxy)propan-2-ol (**8**).

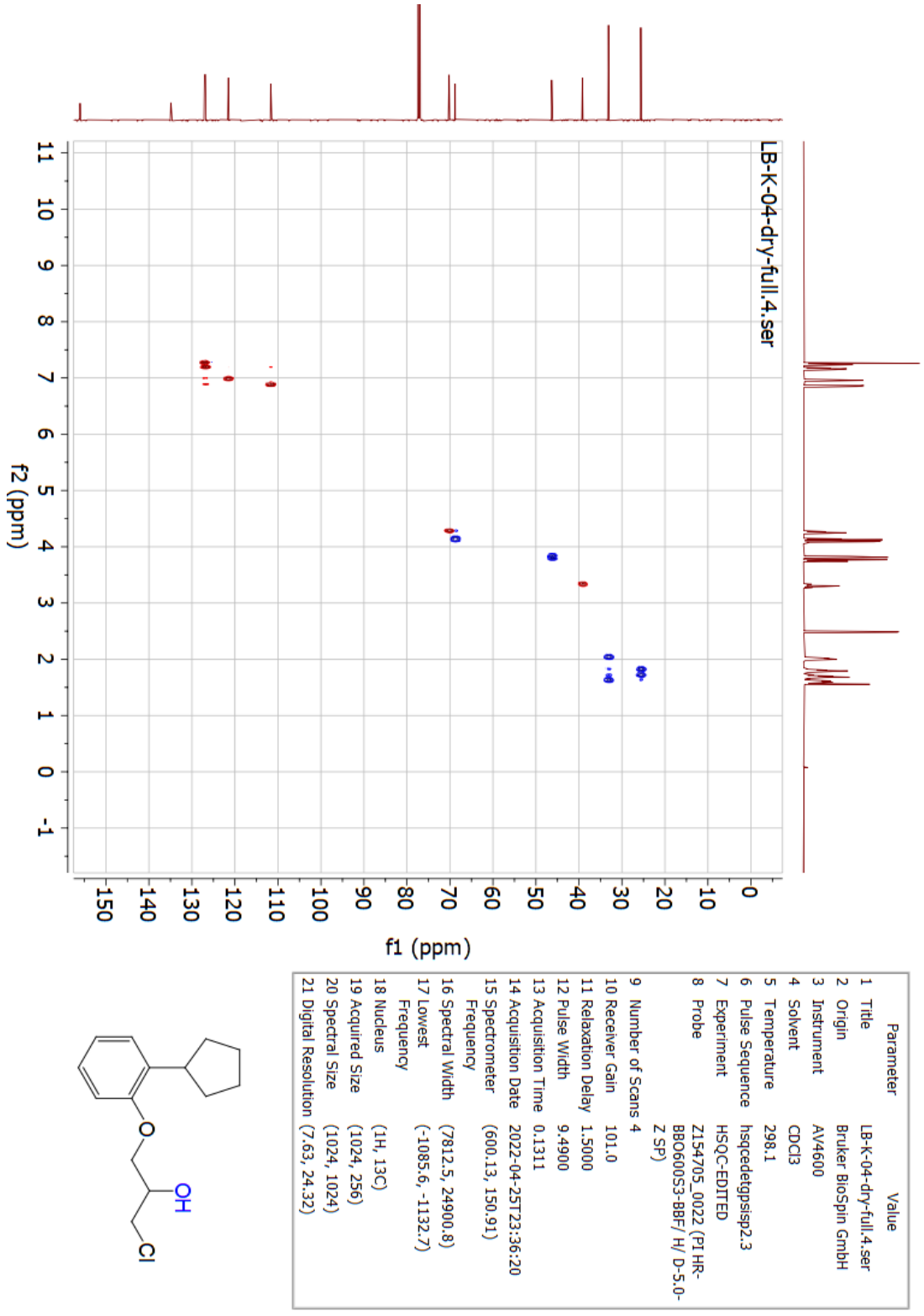

	Parameter	Value
1	Title	LB-K-04-dry-full.4.ser
2	Origin	Bruker BioSpin GmbH
3	Instrument	AV4600
4	Solvent	CDCl3
5	Temperature	298.1
6	Pulse Sequence	hsqcedetgpsisp2.3
7	Experiment	HSQC-EDITED
8	Probe	Z154705_0022 (PI HR-BBO600S3-BBF/ H/ D-5.0-Z SP)
9	Number of Scans	4
10	Receiver Gain	101.0
11	Relaxation Delay	1.5000
12	Pulse Width	9.4900
13	Acquisition Time	0.1311
14	Acquisition Date	2022-04-25T23:36:20
15	Spectrometer Frequency	(600.13, 150.91)
16	Spectral Width	(7812.5, 24900.8)
17	Lowest Frequency	(-1085.6, -1132.7)
18	Nucleus	(1H, 13C)
19	Acquired Size	(1024, 256)
20	Spectral Size	(1024, 1024)
21	Digital Resolution	(7.63, 24.32)

Figure 6.2.4: HSQC-NMR spectrum (600 MHz, $CDCl_3$) of 1-chloro-3-(2-cyclopentylphenoxy)propan-2-ol (**8**).

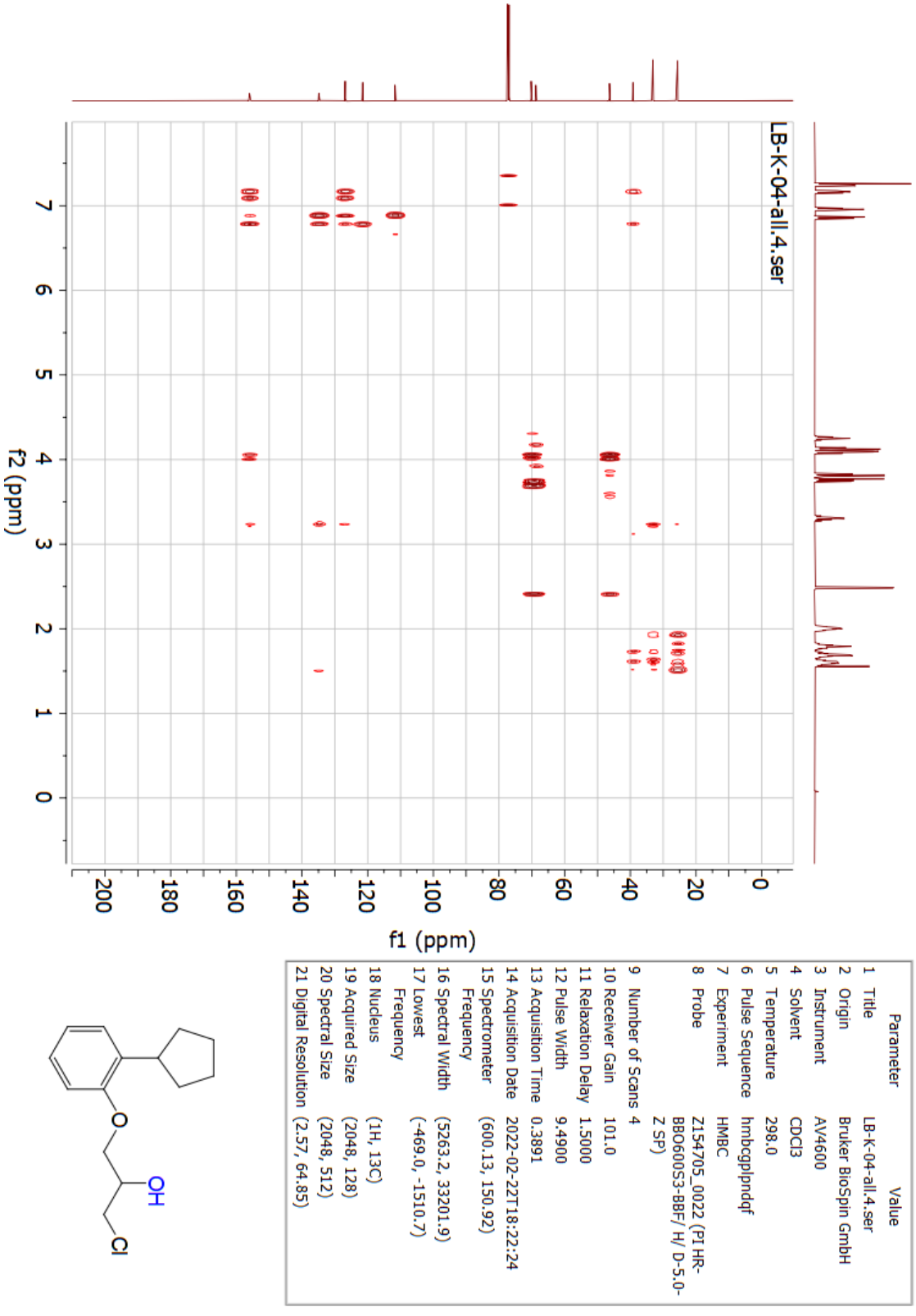

Parameter	Value
1 Title	LB-K-04-all.4.ser
2 Origin	Bruker BioSpin GmbH
3 Instrument	AV4600
4 Solvent	CDCl3
5 Temperature	298.0
6 Pulse Sequence	hmbcgplpndqf
7 Experiment	HMBC
8 Probe	Z154705_0022 (PI HR-BBO600S3-BBF/ H/ D-5.0-Z SP)
9 Number of Scans	4
10 Receiver Gain	101.0
11 Relaxation Delay	1.5000
12 Pulse Width	9.4900
13 Acquisition Time	0.3891
14 Acquisition Date	2022-02-22T18:22:24
15 Spectrometer Frequency	(600.13, 150.92)
16 Spectral Width	(5263.2, 33201.9)
17 Lowest Frequency	(-469.0, -1510.7)
18 Nucleus	(1H, 13C)
19 Acquired Size	(2048, 128)
20 Spectral Size	(2048, 512)
21 Digital Resolution	(2.57, 64.85)

Figure 6.2.5: HMBC-NMR spectrum (600 MHz, $CDCl_3$) of 1-chloro-3-(2-cyclopentylphenoxy)propan-2-ol (**8**).

6.2.2 Penbutolol (10)

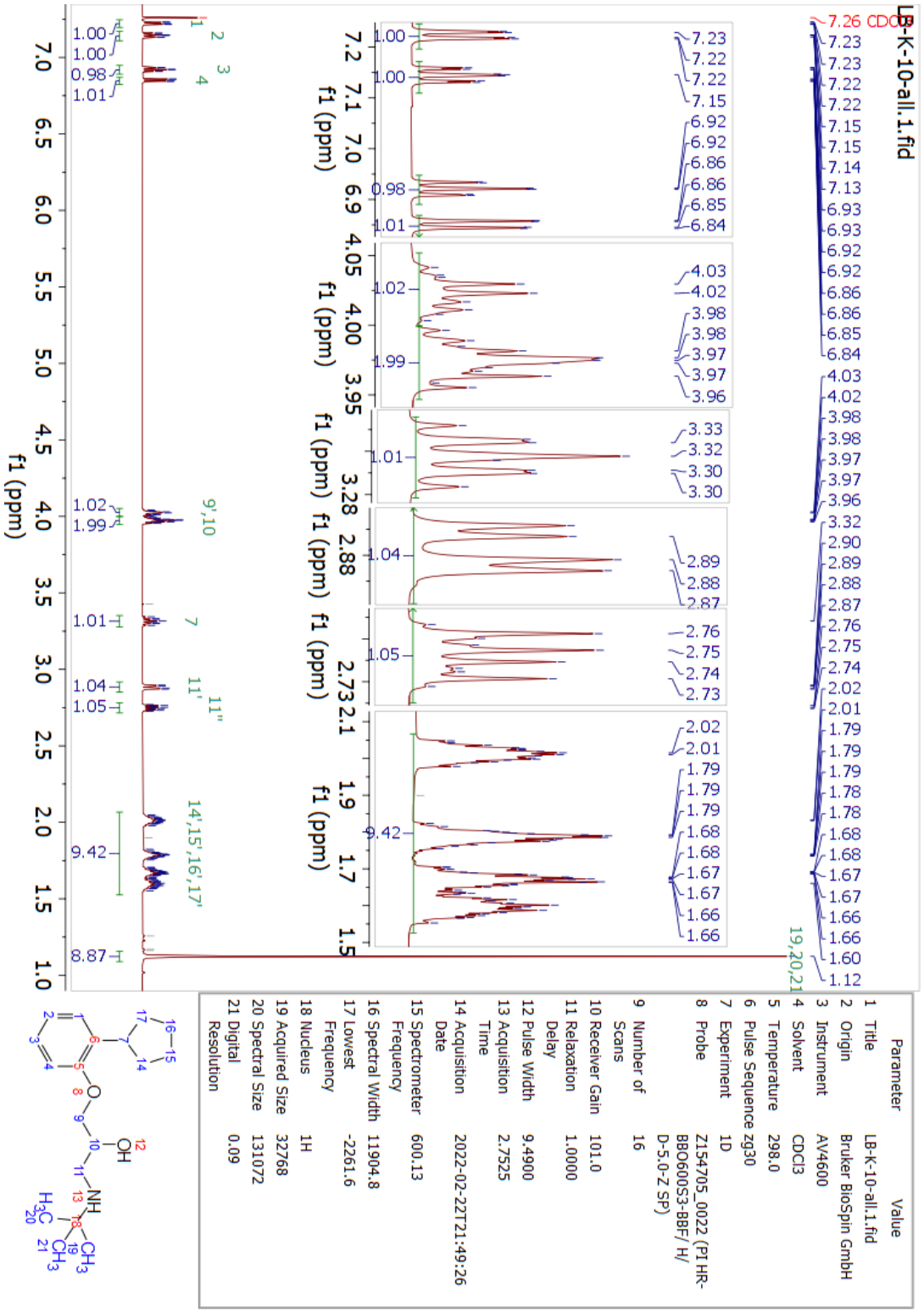

Figure 6.2.6: ^{1}H-NMR spectrum (600 MHz, $CDCl_3$) of penbutolol (**10**).

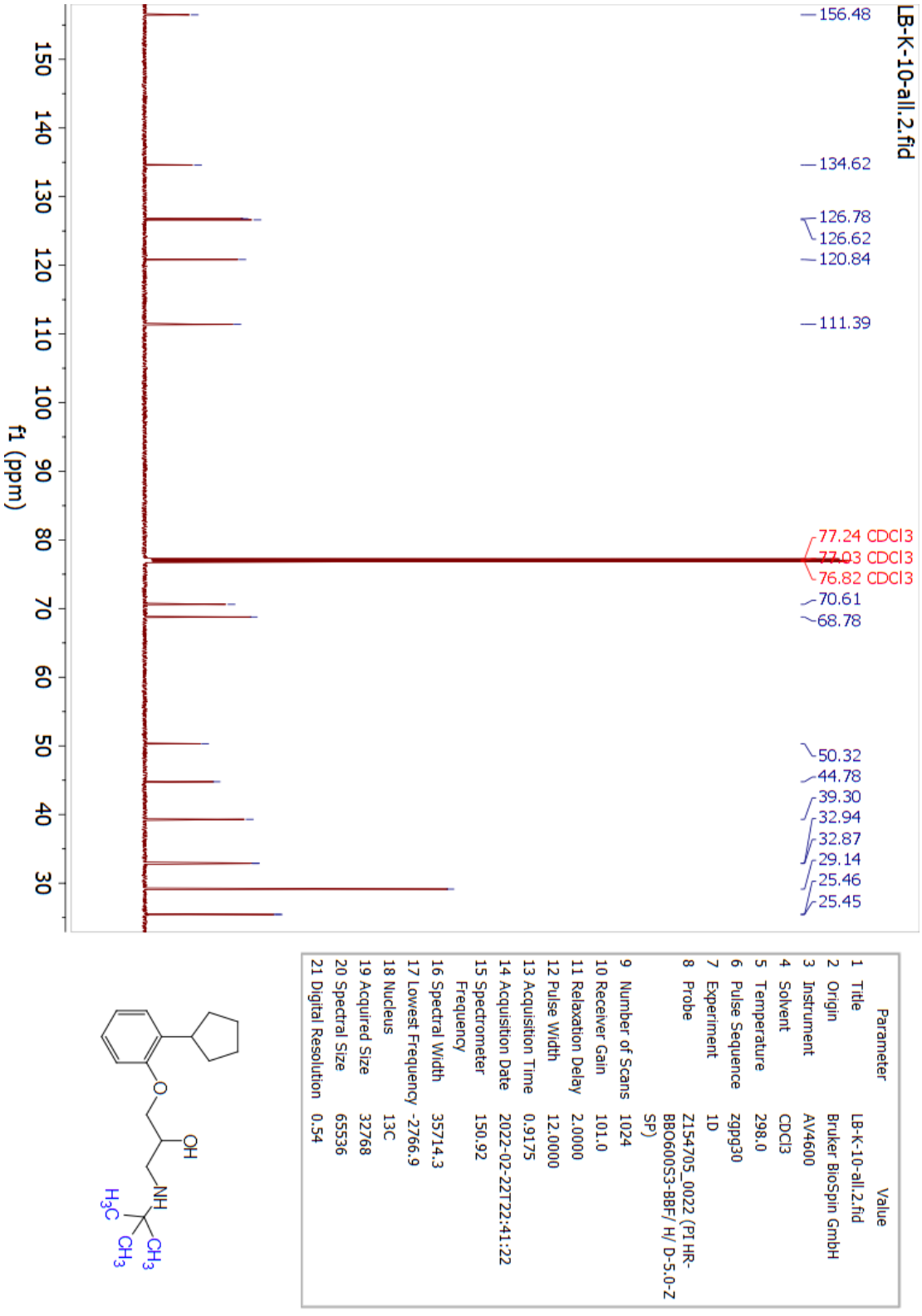

Parameter	Value
1 Title	LB-K-10-all.2.fid
2 Origin	Bruker BioSpin GmbH
3 Instrument	AV4600
4 Solvent	CDCl3
5 Temperature	298.0
6 Pulse Sequence	zgpg30
7 Experiment	1D
8 Probe	Z154705_0022 (PI HR-BBO600S3-BBF/ H/ D-5.0-Z SP)
9 Number of Scans	1024
10 Receiver Gain	101.0
11 Relaxation Delay	2.0000
12 Pulse Width	12.0000
13 Acquisition Time	0.9175
14 Acquisition Date	2022-02-22T22:41:22
15 Spectrometer Frequency	150.92
16 Spectral Width	35714.3
17 Lowest Frequency	-2766.9
18 Nucleus	13C
19 Acquired Size	32768
20 Spectral Size	65536
21 Digital Resolution	0.54

Figure 6.2.7: ^{13}C-NMR spectrum (600 MHz, $CDCl_3$) of penbutolol (**10**).

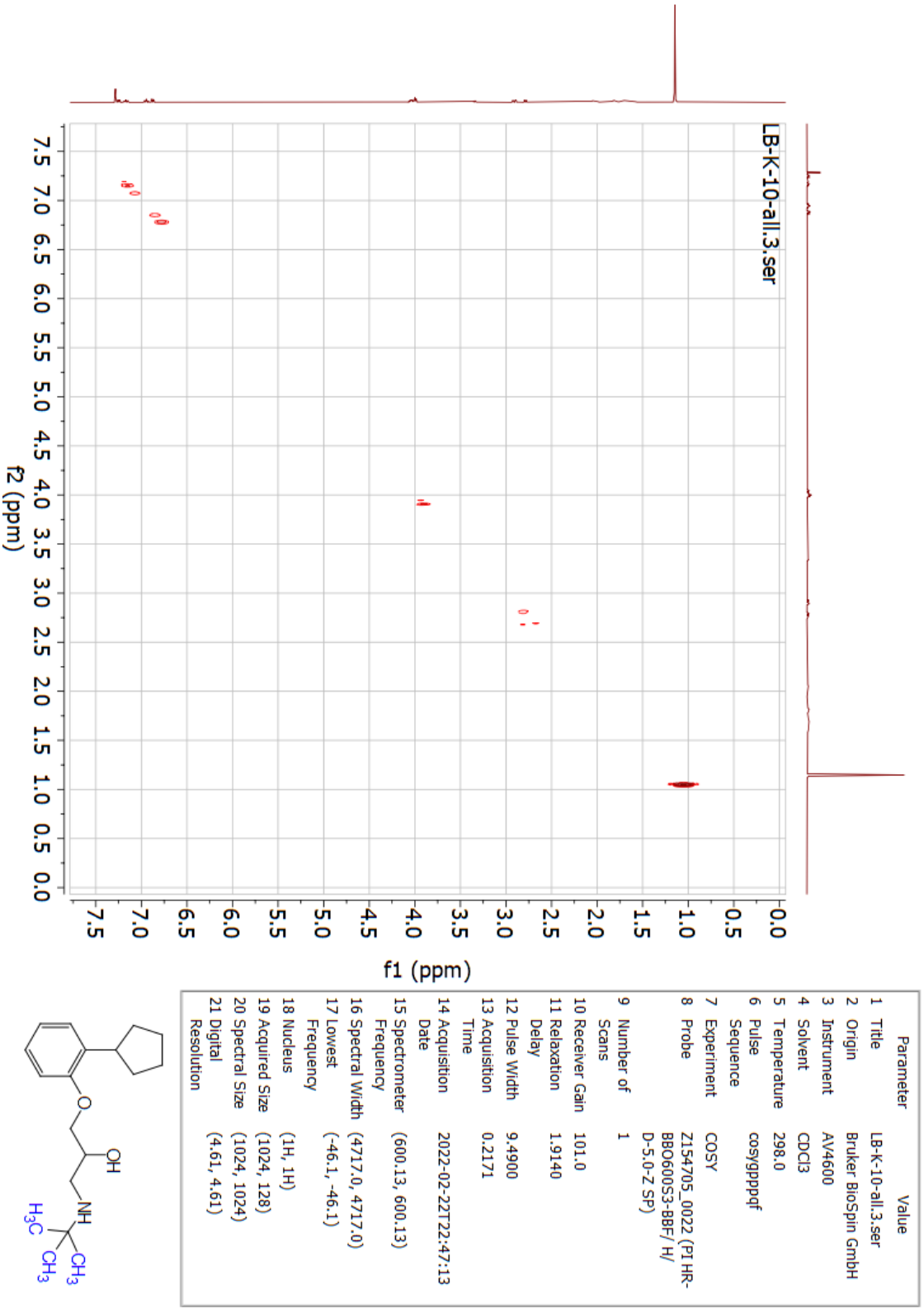

	Parameter	Value
1	Title	LB-K-10-all.3.ser
2	Origin	Bruker BioSpin GmbH
3	Instrument	AV4600
4	Solvent	CDCl3
5	Temperature	298.0
6	Pulse Sequence	cosygpppqf
7	Experiment	COSY
8	Probe	Z154705_0022 (PI HR-BBO600S3-BBF/ H/ D-5.0-Z SP)
9	Number of Scans	1
10	Receiver Gain	101.0
11	Relaxation Delay	1.9140
12	Pulse Width	9.4900
13	Acquisition Time	0.2171
14	Acquisition Date	2022-02-22T22:47:13
15	Spectrometer Frequency	(600.13, 600.13)
16	Spectral Width	(4717.0, 4717.0)
17	Lowest Frequency	(-46.1, -46.1)
18	Nucleus	(1H, 1H)
19	Acquired Size	(1024, 128)
20	Spectral Size	(1024, 1024)
21	Digital Resolution	(4.61, 4.61)

Figure 6.2.8: H,H-COSY-NMR spectrum (600 MHz, $CDCl_3$) of penbutolol (**10**).

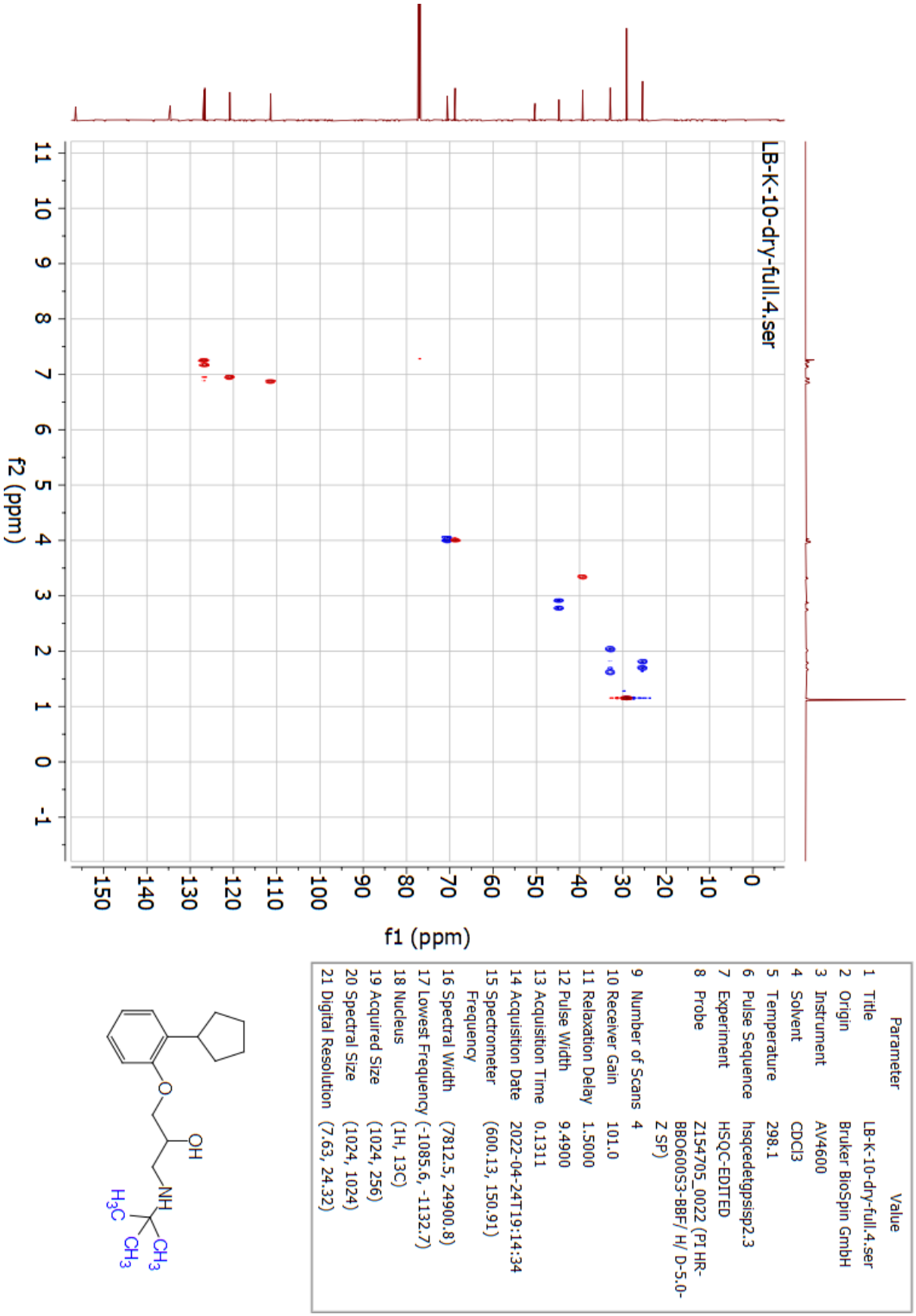

Parameter	Value
1 Title	LB-K-10-dry-full.4.ser
2 Origin	Bruker BioSpin GmbH
3 Instrument	AV4600
4 Solvent	CDCl3
5 Temperature	298.1
6 Pulse Sequence	hsqcedetgpsisp2.3
7 Experiment	HSQC-EDITED
8 Probe	Z154705_0022 (PI HR-BBO600S3-BBF/ H/ D-5.0-Z SP)
9 Number of Scans	4
10 Receiver Gain	101.0
11 Relaxation Delay	1.5000
12 Pulse Width	9.4900
13 Acquisition Time	0.1311
14 Acquisition Date	2022-04-24T19:14:34
15 Spectrometer Frequency	(600.13, 150.91)
16 Spectral Width	(7812.5, 24900.8)
17 Lowest Frequency	(-1085.6, -1132.7)
18 Nucleus	(1H, 13C)
19 Acquired Size	(1024, 256)
20 Spectral Size	(1024, 1024)
21 Digital Resolution	(7.63, 24.32)

Figure 6.2.9: HSQC-NMR spectrum (600 MHz, $CDCl_3$) of penbutolol (**10**).

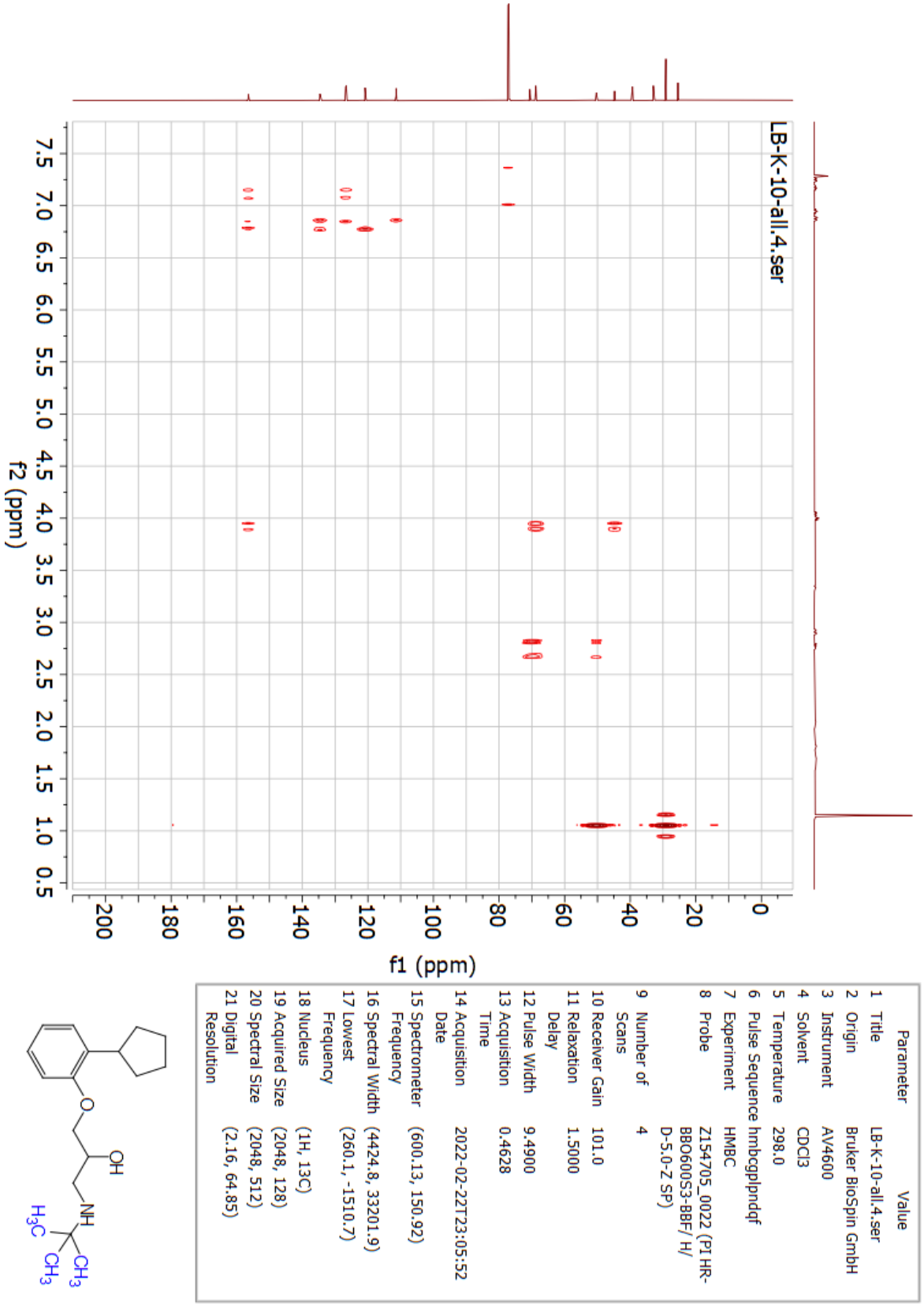

Parameter	Value
1 Title	LB-K-10-all.4.ser
2 Origin	Bruker BioSpin GmbH
3 Instrument	AV4600
4 Solvent	CDCl3
5 Temperature	298.0
6 Pulse Sequence	hmbcgplpndqf
7 Experiment	HMBC
8 Probe	Z154705_0022 (PI HR-BBO600S3-BBF/ H/ D-5.0-Z SP)
9 Number of Scans	4
10 Receiver Gain	101.0
11 Relaxation Delay	1.5000
12 Pulse Width	9.4900
13 Acquisition Time	0.4628
14 Acquisition Date	2022-02-22T23:05:52
15 Spectrometer Frequency	(600.13, 150.92)
16 Spectral Width	(4424.8, 33201.9)
17 Lowest Frequency	(260.1, -1510.7)
18 Nucleus	(1H, 13C)
19 Acquired Size	(2048, 128)
20 Spectral Size	(2048, 512)
21 Digital Resolution	(2.16, 64.85)

Figure 6.2.10: HMBC-NMR spectrum (600 MHz, $CDCl_3$) of penbutolol (**10**).

6.2.3 Penbutolol hydrochloride (10*HCl*)

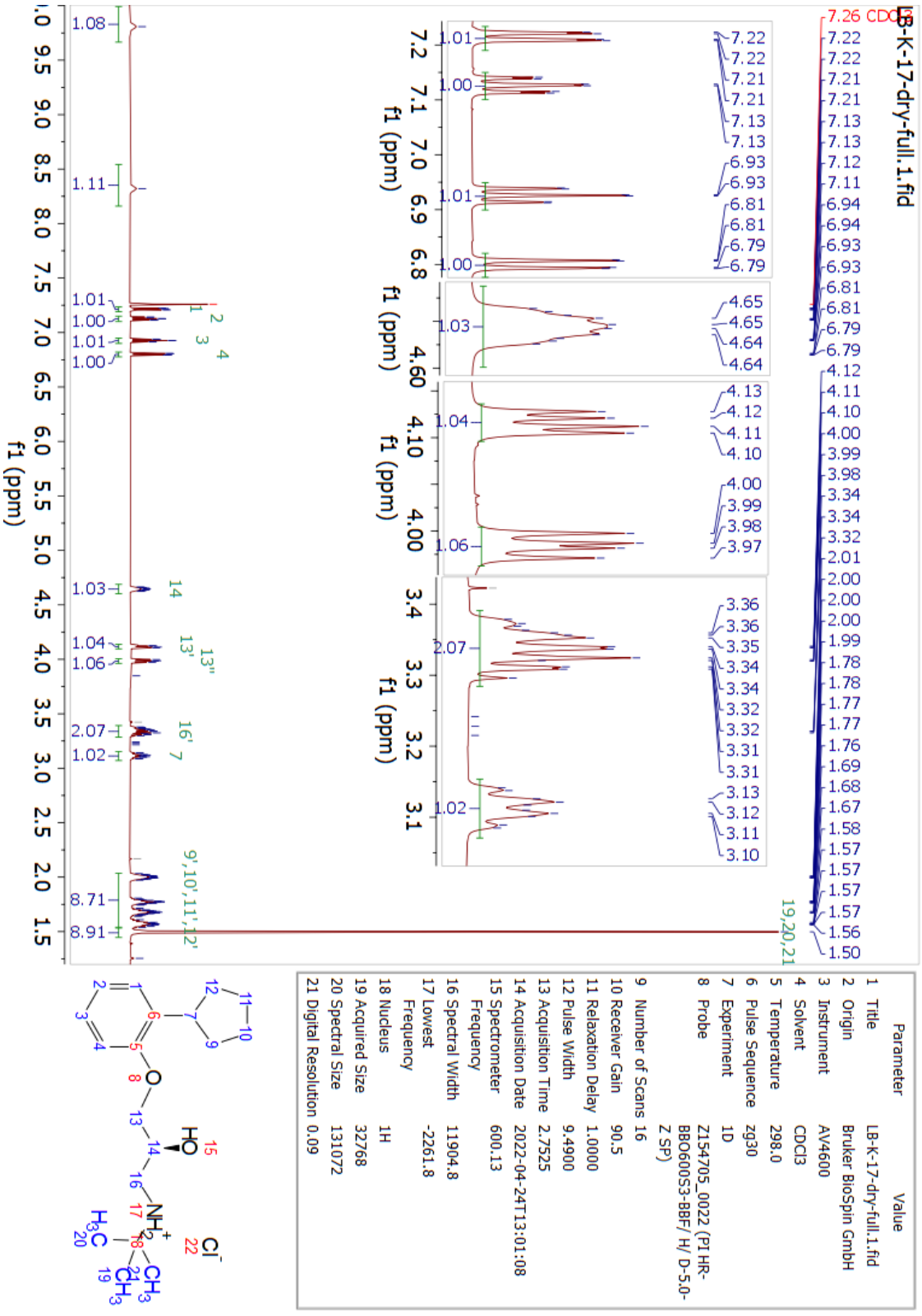

Figure 6.2.11: ^{1}H-NMR spectrum (600 MHz, $CDCl_3$) of penbutolol hydrochloride (**10*HCl***).

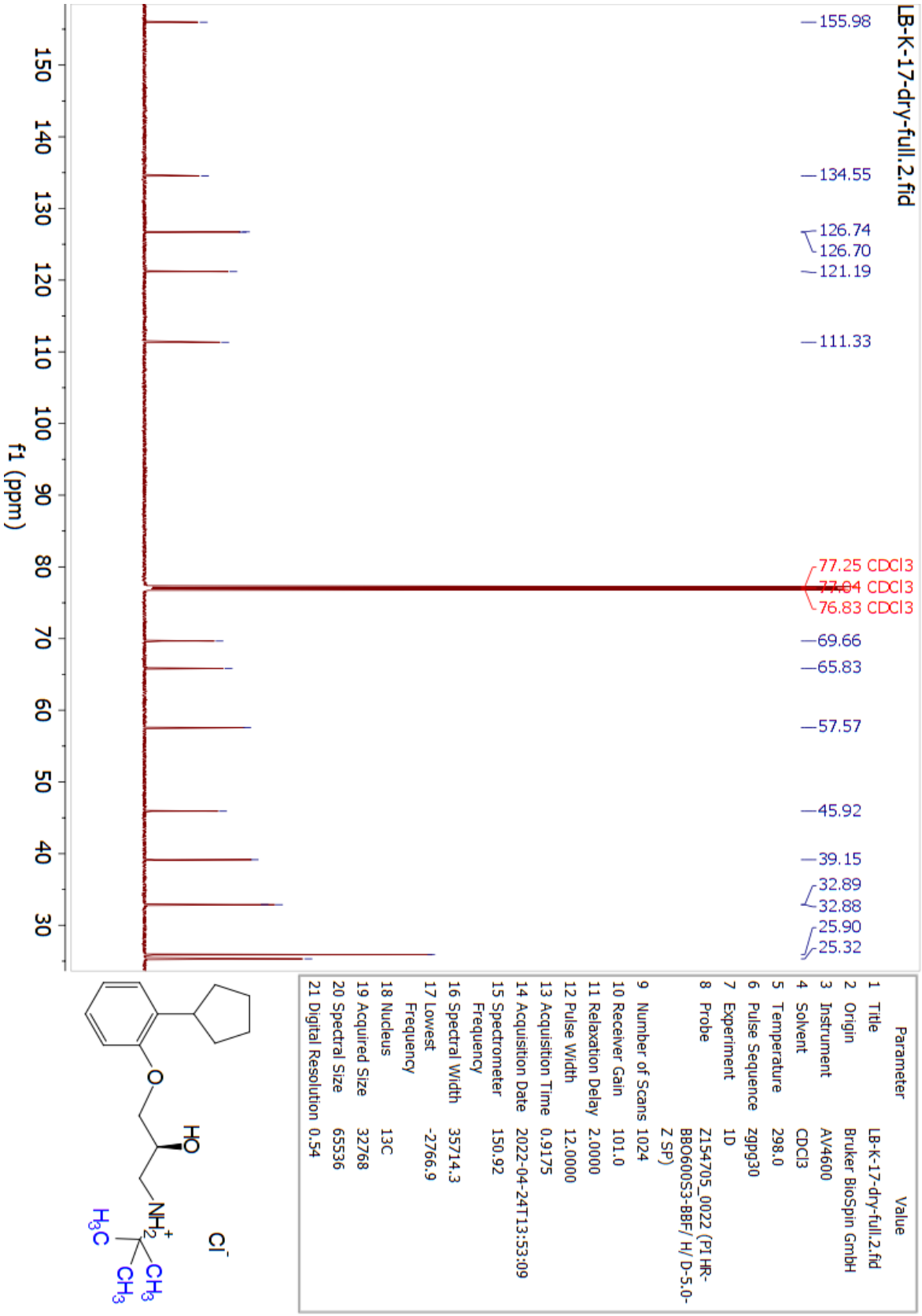

Figure 6.2.12: ^{13}C-NMR spectrum (600 MHz, $CDCl_3$) of penbutolol hydrochloride (**10*HCl***).

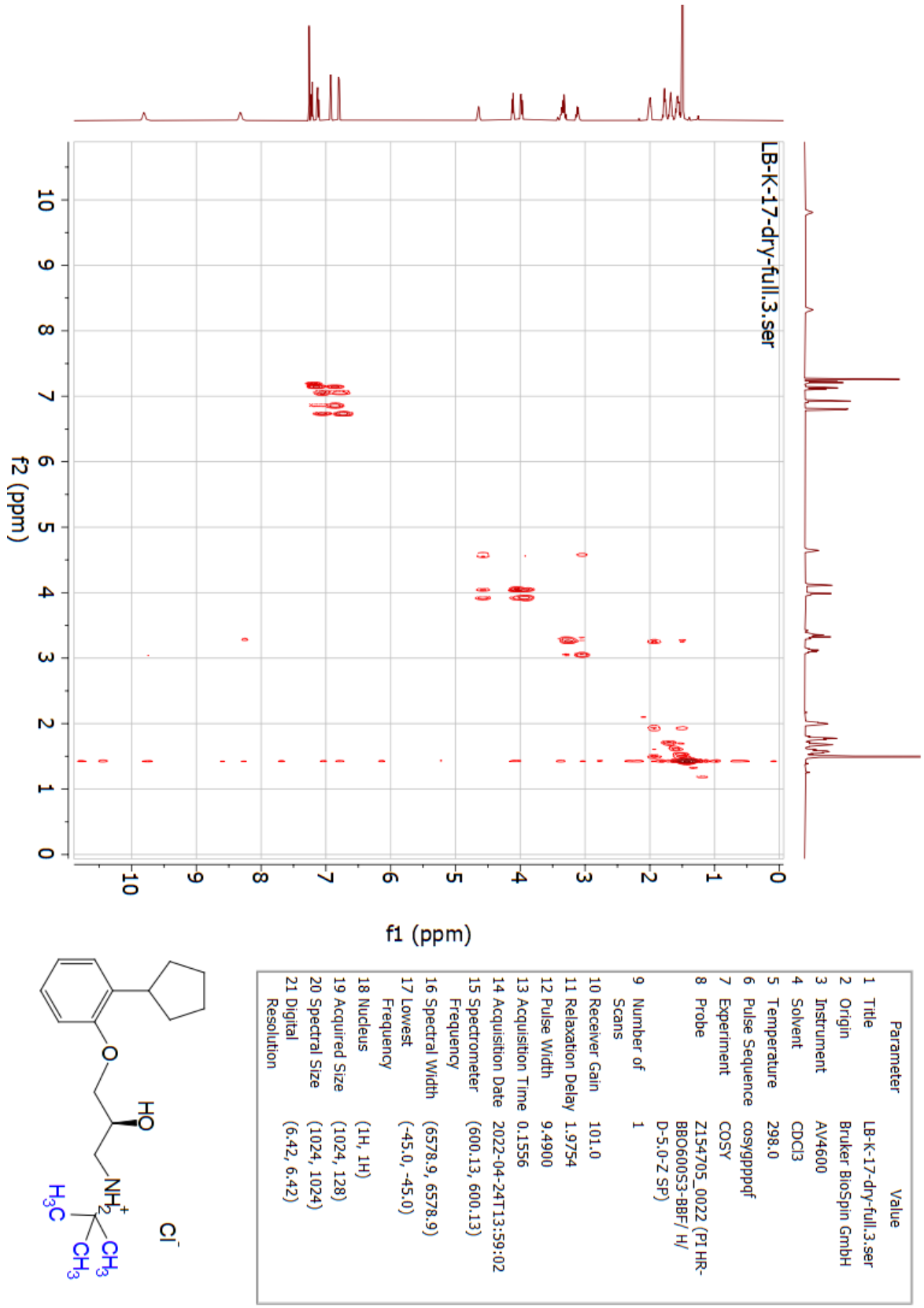

	Parameter	Value
1	Title	LB-K-17-dry-full.3.ser
2	Origin	Bruker BioSpin GmbH
3	Instrument	AV4600
4	Solvent	CDCl3
5	Temperature	298.0
6	Pulse Sequence	cosygpppqf
7	Experiment	COSY
8	Probe	Z154705_0022 (PI HR-BBO600S3-BBF/ H/ D-5.0-Z SP)
9	Number of Scans	1
10	Receiver Gain	101.0
11	Relaxation Delay	1.9754
12	Pulse Width	9.4900
13	Acquisition Time	0.1556
14	Acquisition Date	2022-04-24T13:59:02
15	Spectrometer Frequency	(600.13, 600.13)
16	Spectral Width	(6578.9, 6578.9)
17	Lowest Frequency	(-45.0, -45.0)
18	Nucleus	(1H, 1H)
19	Acquired Size	(1024, 128)
20	Spectral Size	(1024, 1024)
21	Digital Resolution	(6.42, 6.42)

Figure 6.2.13: H,H-COSY-NMR spectrum (600 MHz, $CDCl_3$) of penbutolol hydrochloride (**10*HCl***).

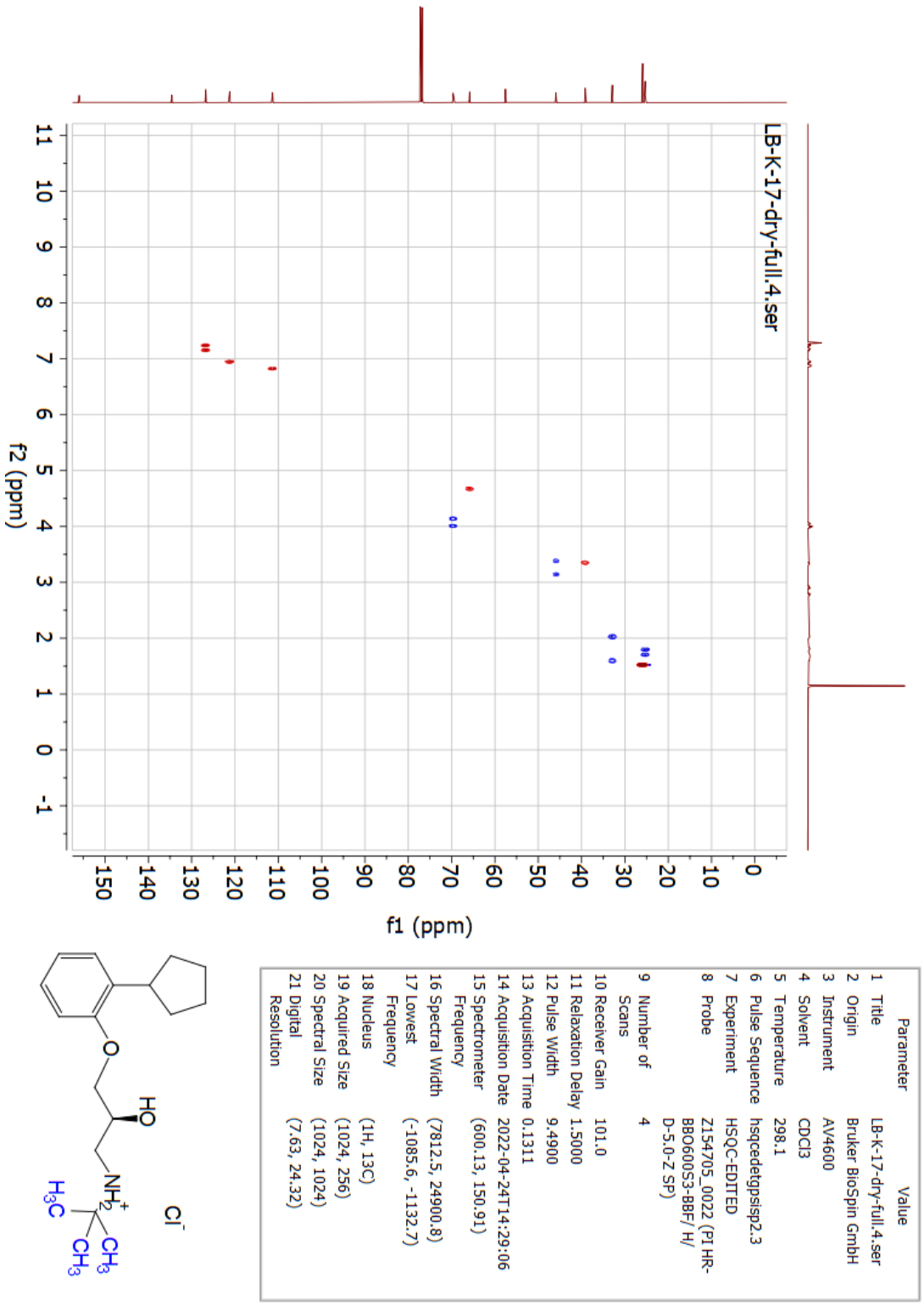

Parameter	Value
1 Title	LB-K-17-dry-full.4.ser
2 Origin	Bruker BioSpin GmbH
3 Instrument	AV4600
4 Solvent	CDCl3
5 Temperature	298.1
6 Pulse Sequence	hsqcedetgpsisp2.3
7 Experiment	HSQC-EDITED
8 Probe	Z154705_0022 (PI HR-BBO600S3-BBF/ H/ D-5.0-Z SP)
9 Number of Scans	4
10 Receiver Gain	101.0
11 Relaxation Delay	1.5000
12 Pulse Width	9.4900
13 Acquisition Time	0.1311
14 Acquisition Date	2022-04-24T14:29:06
15 Spectrometer Frequency	(600.13, 150.91)
16 Spectral Width	(7812.5, 24900.8)
17 Lowest Frequency	(-1085.6, -1132.7)
18 Nucleus	(1H, 13C)
19 Acquired Size	(1024, 256)
20 Spectral Size	(1024, 1024)
21 Digital Resolution	(7.63, 24.32)

Figure 6.2.14: HSQC-NMR spectrum (600 MHz, $CDCl_3$) of penbutolol hydrochloride (**10*HCl***).

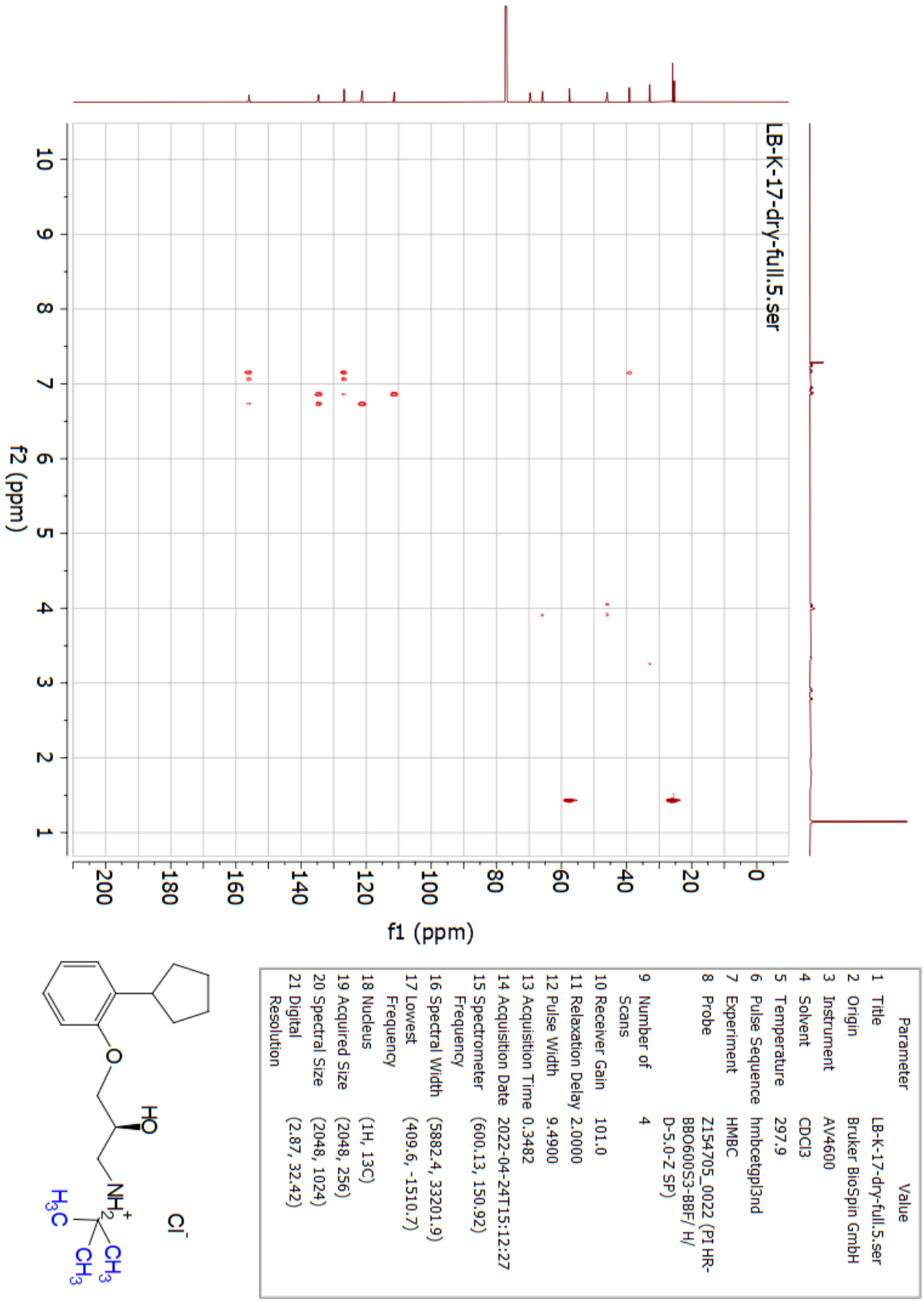

	Parameter	Value
1	Title	LB-K-17-dry-full.5.ser
2	Origin	Bruker BioSpin GmbH
3	Instrument	AV4600
4	Solvent	CDCl3
5	Temperature	297.9
6	Pulse Sequence	hmbcetgpl3nd
7	Experiment	HMBC
8	Probe	Z154705_0022 (PI HR-BBO600S3-BBF/ H/ D-5.0-Z SP)
9	Number of Scans	4
10	Receiver Gain	101.0
11	Relaxation Delay	2.0000
12	Pulse Width	9.4900
13	Acquisition Time	0.3482
14	Acquisition Date	2022-04-24T15:12:27
15	Spectrometer Frequency	(600.13, 150.92)
16	Spectral Width	(5882.4, 33201.9)
17	Lowest Frequency	(409.6, -1510.7)
18	Nucleus	(1H, 13C)
19	Acquired Size	(2048, 256)
20	Spectral Size	(2048, 1024)
21	Digital Resolution	(2.87, 32.42)

Figure 6.2.15: HMBC-NMR spectrum (600 MHz, $CDCl_3$) of penbutolol hydrochloride (**10*HCl***).

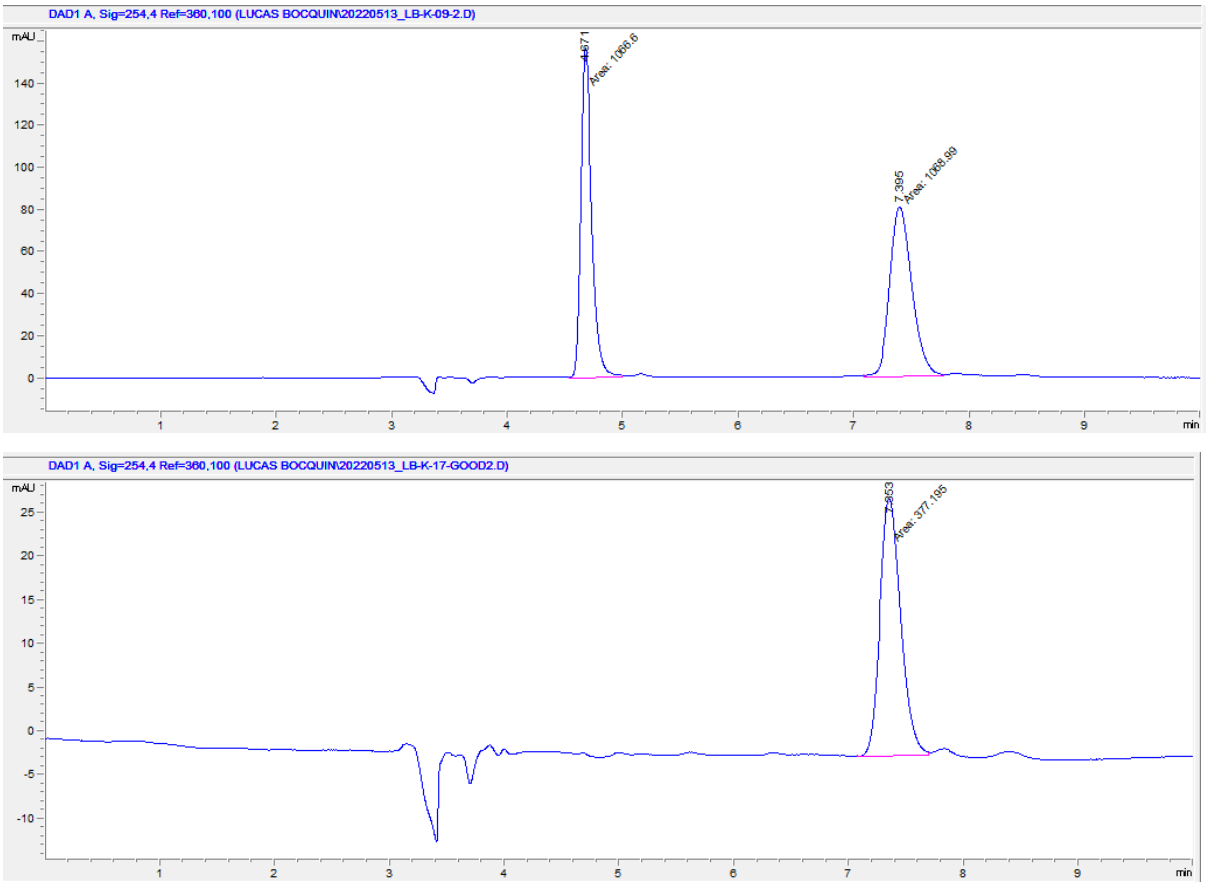

Figure 6.2.16: Chiral HPLC chromatogram of racemic of racemic penbutolol hydrochloride (**10*HCl***) (upper chromatogram) and enantiopure (R)-**10*HCl*** (bottom chromatogram). The analysis was performed on a Chiralcel OD-H column with hexane (90%) and 2-propanol containing 2% diethanolamine (10%) as eluent and 1 mL/min flow, and with a detection wavelength of 254.4 nm. The retention times obtained in the upper chromatogram are t_R((*R*)-**10*HCl***) = 4.671 min and t_R((*S*)-**10*HCl***) = 7.395 min. The resolution factor in the upper chromatogram is R_S((*S*)/(*R*)-**10*HCl***) = 10.5.

6.3 Bisoprolol synthesis

6.3.1 4-((2-Isopropoxyethoxy)methyl)phenol (11)

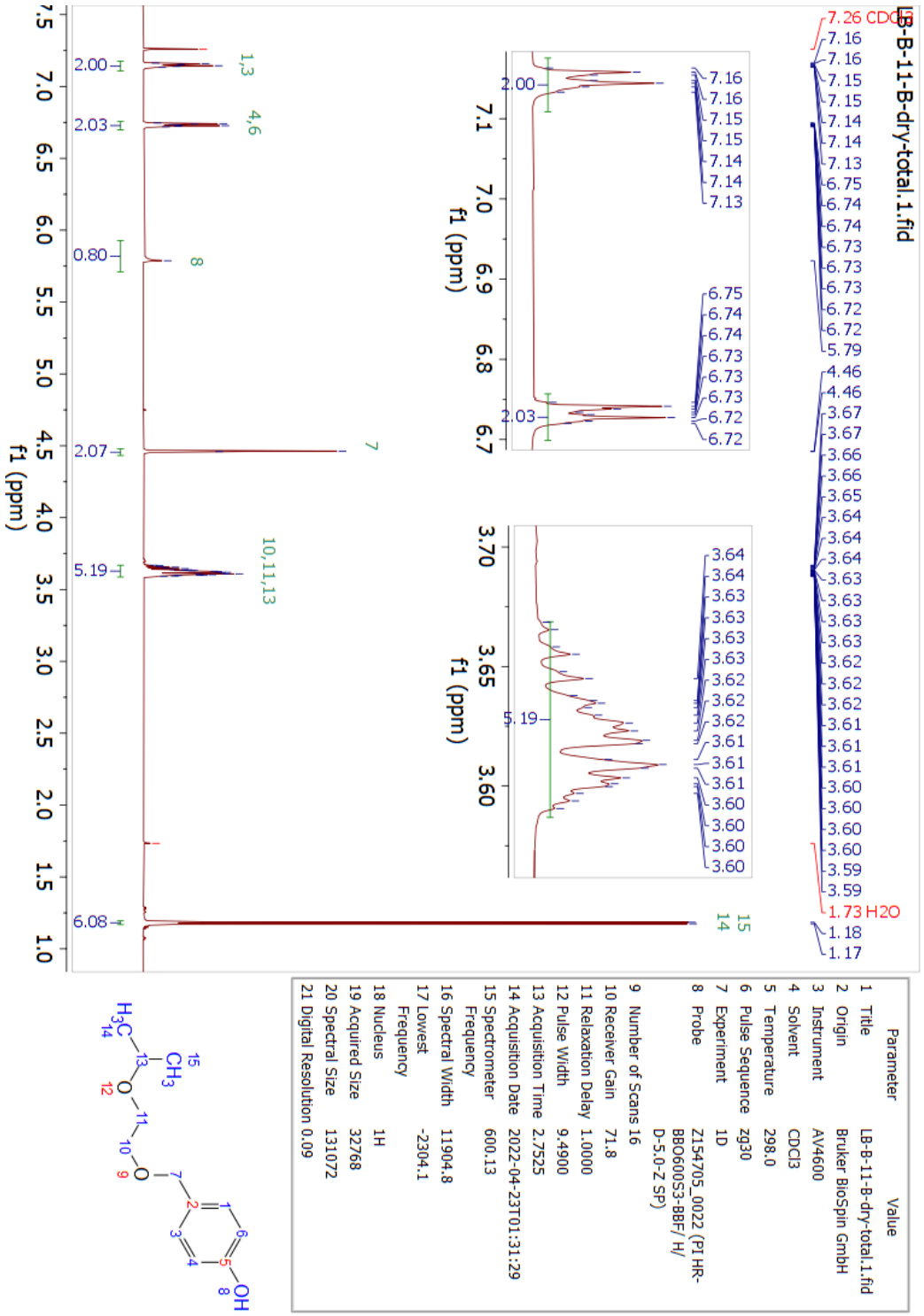

Figure 6.3.1: ^{1}H-NMR spectrum (600 MHz, $CDCl_3$) of 4-((2-isopropoxyethoxy)methyl)phenol (**11**).

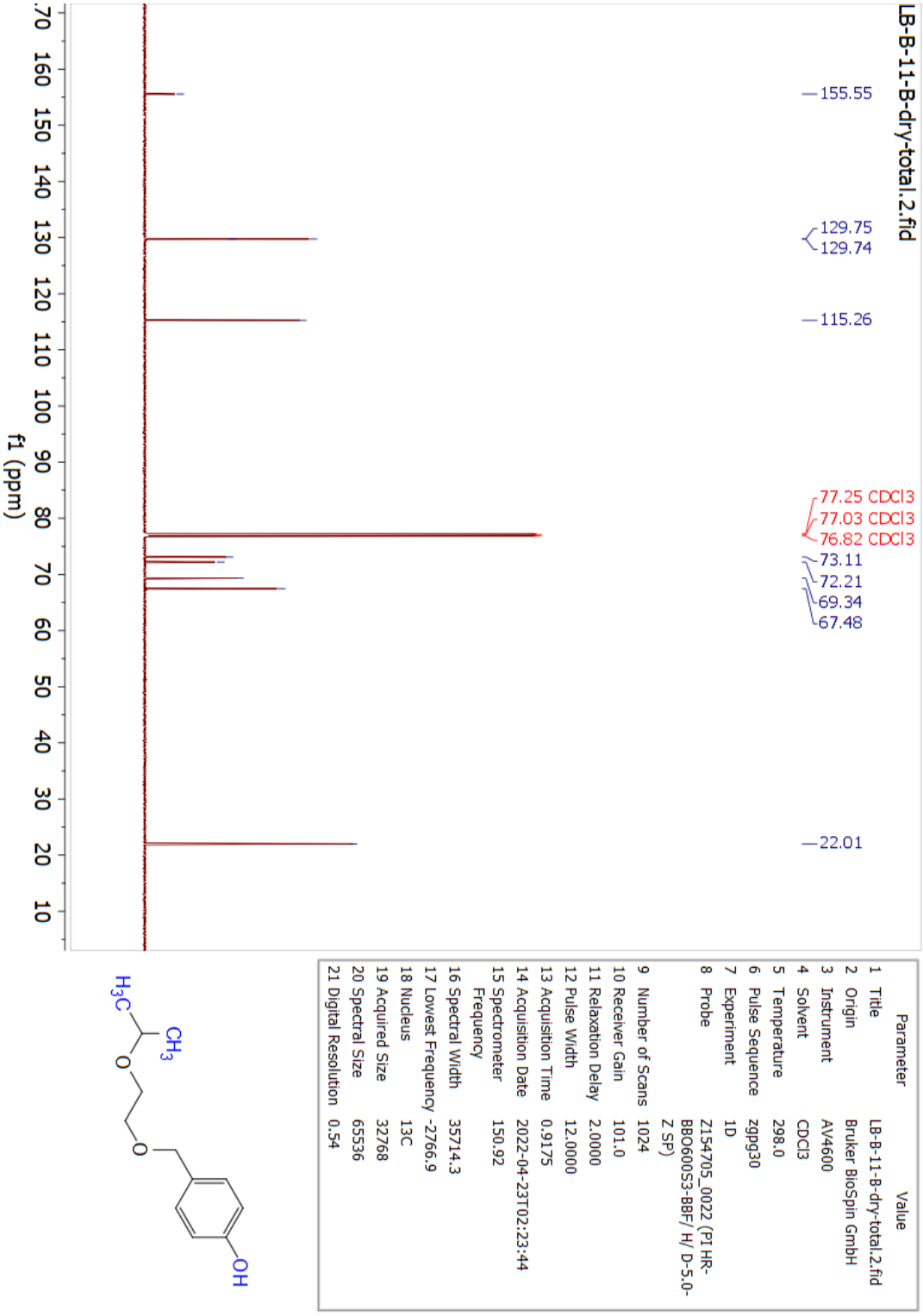

Figure 6.3.2: ^{13}C-NMR spectrum (600 MHz, $CDCl_3$) of 4-((2-isopropoxyethoxy)methyl)phenol (**11**).

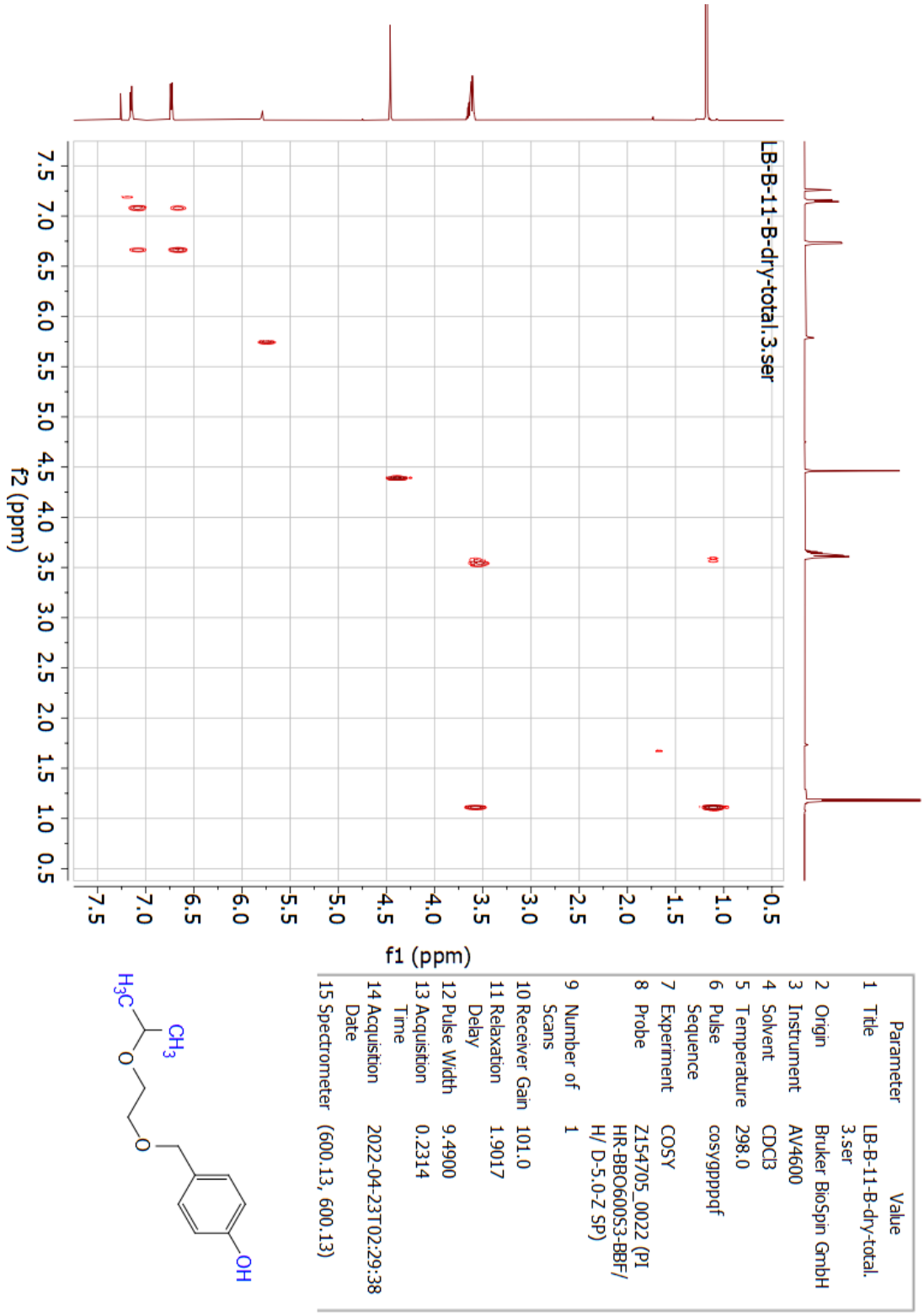

Parameter	Value
1 Title	LB-B-11-B-dry-total.3.ser
2 Origin	Bruker BioSpin GmbH
3 Instrument	AV4600
4 Solvent	CDCl3
5 Temperature	298.0
6 Pulse Sequence	cosygpppqf
7 Experiment	COSY
8 Probe	Z154705_0022 (PI HR-BBO600S3-BBF/ H/ D-5.0-Z SP)
9 Number of Scans	1
10 Receiver Gain	101.0
11 Relaxation Delay	1.9017
12 Pulse Width	9.4900
13 Acquisition Time	0.2314
14 Acquisition Date	2022-04-23T02:29:38
15 Spectrometer	(600.13, 600.13)

Figure 6.3.3: H,H-COSY-NMR spectrum (600 MHz, $CDCl_3$) of 4-((2-isopropoxyethoxy)methyl)phenol (**11**).

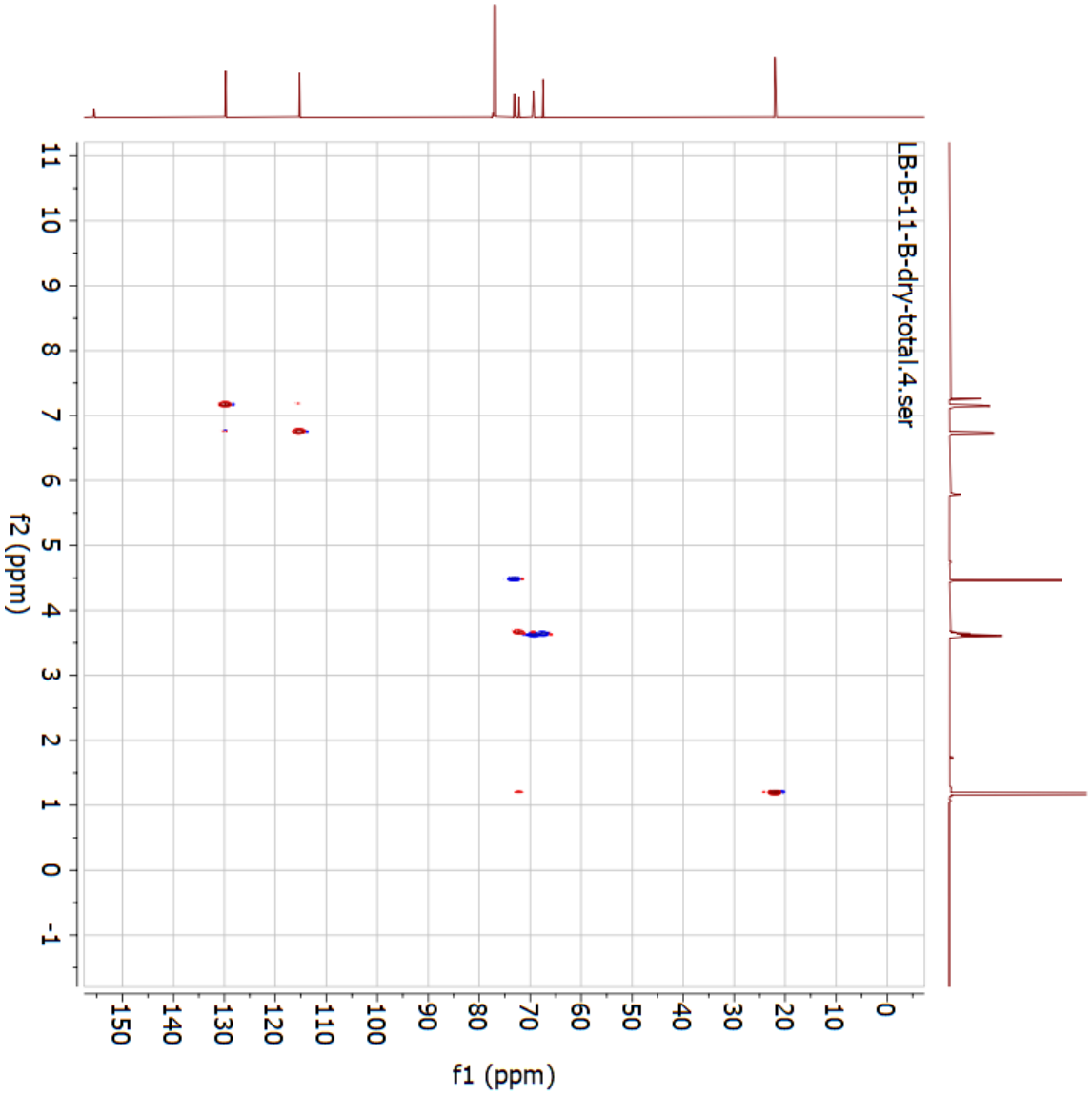

	Parameter	Value
1	Title	LB-B-11-B-dry-total.4.ser
2	Origin	Bruker BioSpin GmbH
3	Instrument	AV4600
4	Solvent	CDCl3
5	Temperature	298.1
6	Pulse Sequence	hsqcedetgpsisp2.3
7	Experiment	HSQC-EDITED
8	Probe	Z154705_0022 (PI HR-BBO600S3-BBF/ H/ D-5.0-Z SP)
9	Number of Scans	4
10	Receiver Gain	101.0
11	Relaxation Delay	1.5000
12	Pulse Width	9.4900
13	Acquisition Time	0.1311
14	Acquisition Date	2022-04-23T02:59:44
15	Spectrometer Frequency	(600.13, 150.91)
16	Spectral Width	(7812.5, 24900.8)
17	Lowest Frequency	(-1085.6, -1132.7)
18	Nucleus	(1H, 13C)
19	Acquired Size	(1024, 256)
20	Spectral Size	(1024, 1024)
21	Digital Resolution	(7.63, 24.32)

Figure 6.3.4: HSQC-NMR spectrum (600 MHz, $CDCl_3$) of 4-((2-isopropoxyethoxy)methyl)phenol (**11**).

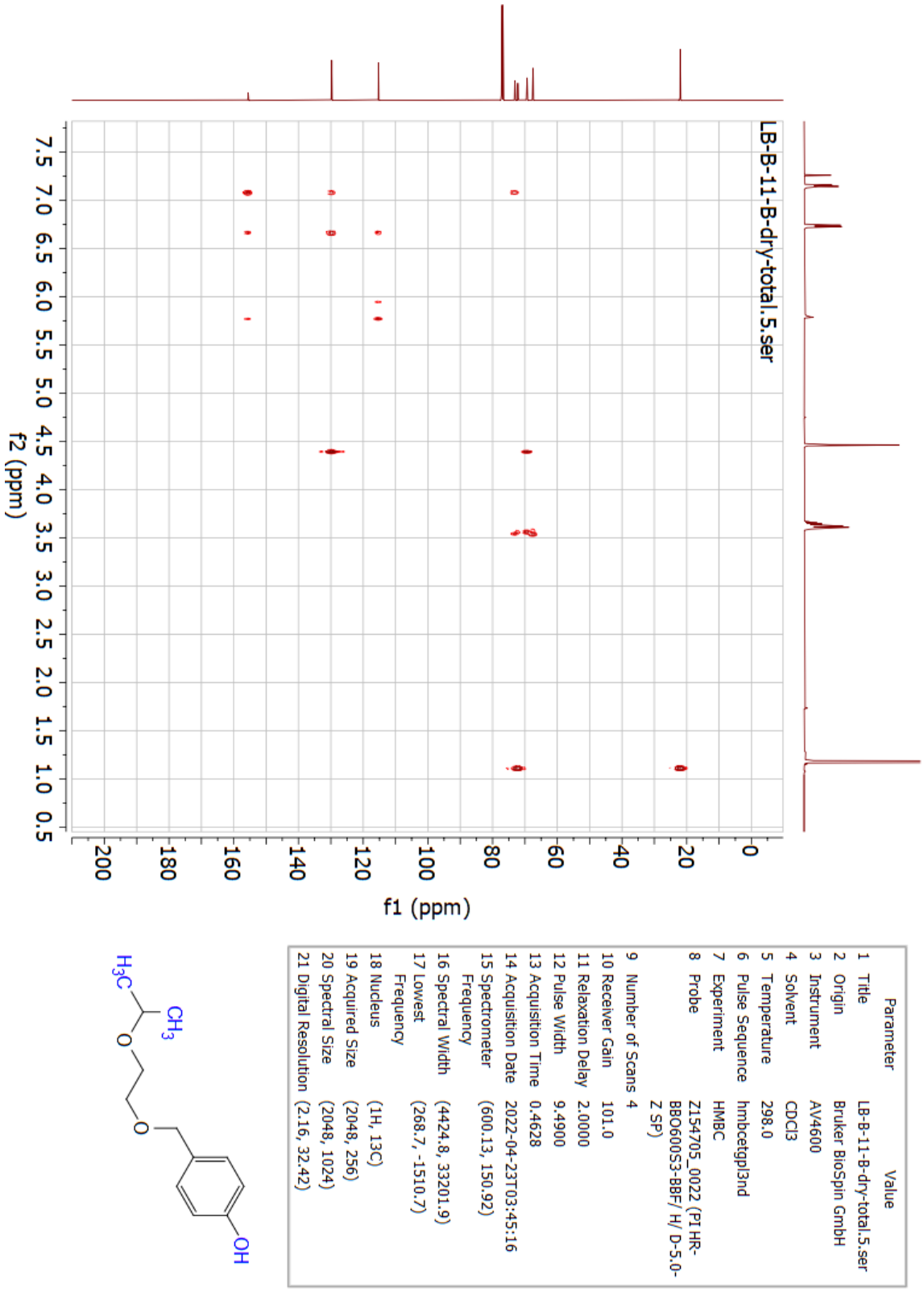

	Parameter	Value
1	Title	LB-B-11-B-dry-total.5.ser
2	Origin	Bruker BioSpin GmbH
3	Instrument	AV4600
4	Solvent	CDCl3
5	Temperature	298.0
6	Pulse Sequence	hmbcetgpl3nd
7	Experiment	HMBC
8	Probe	Z154705_0022 (PI HR-BBO600S3-BBF/ H/ D-5.0-Z SP)
9	Number of Scans	4
10	Receiver Gain	101.0
11	Relaxation Delay	2.0000
12	Pulse Width	9.4900
13	Acquisition Time	0.4628
14	Acquisition Date	2022-04-23T03:45:16
15	Spectrometer Frequency	(600.13, 150.92)
16	Spectral Width	(4424.8, 33201.9)
17	Lowest Frequency	(268.7, -1510.7)
18	Nucleus	(1H, 13C)
19	Acquired Size	(2048, 256)
20	Spectral Size	(2048, 1024)
21	Digital Resolution	(2.16, 32.42)

Figure 6.3.5: HMBC-NMR spectrum (600 MHz, $CDCl_3$) of 4-((2-isopropoxyethoxy)methyl)phenol (**11**).

6.3.2 1-Chloro-3-(4-((2-isopropoxyethoxy)methyl)phenoxy)propan-2-ol (15)

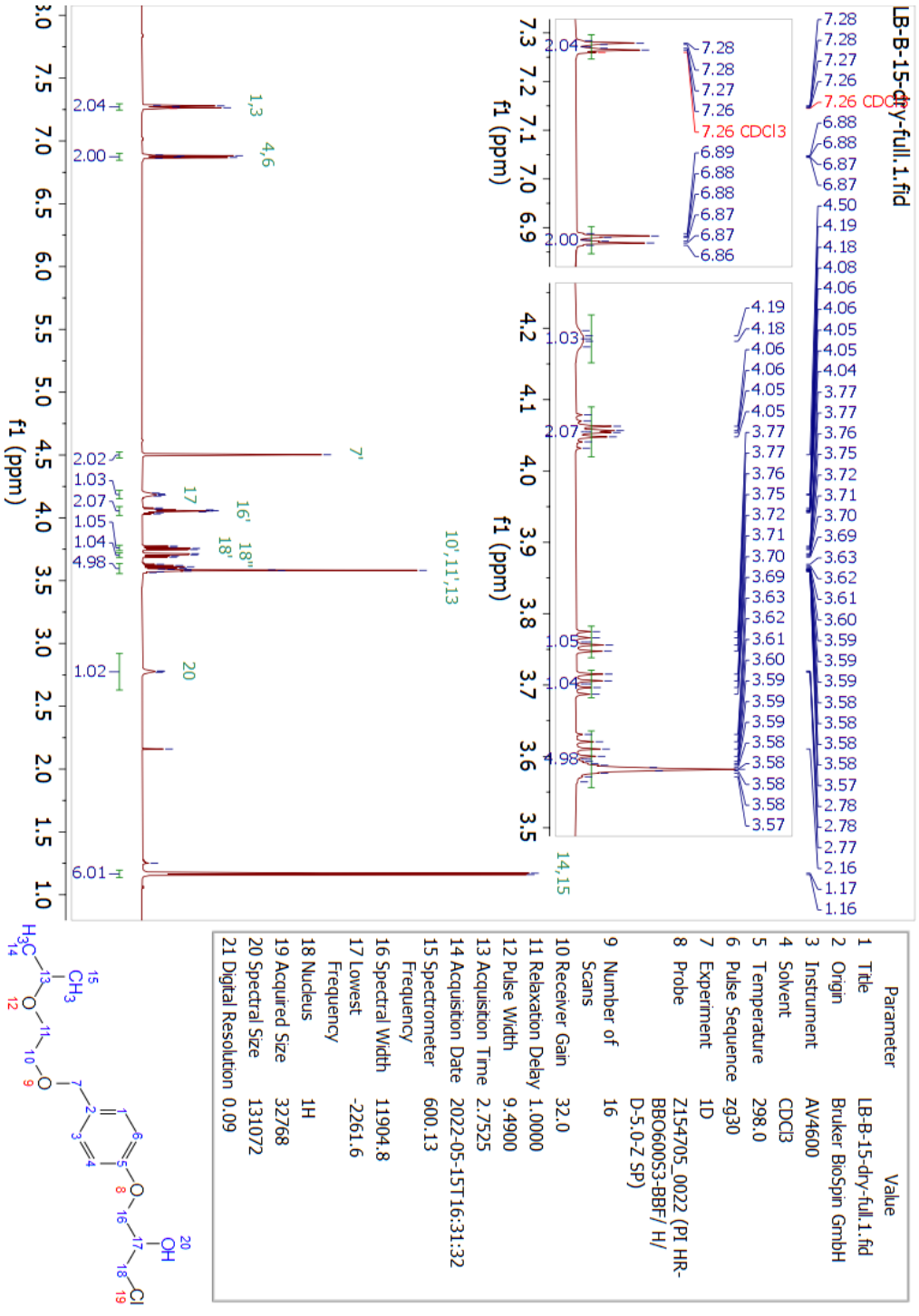

Figure 6.3.6: ^{1}H-NMR spectrum (600 MHz, $CDCl_3$) of 1-chloro-3-(4-((2-isopropoxyethoxy)methyl)phenoxy)propan-2-ol (**15**).

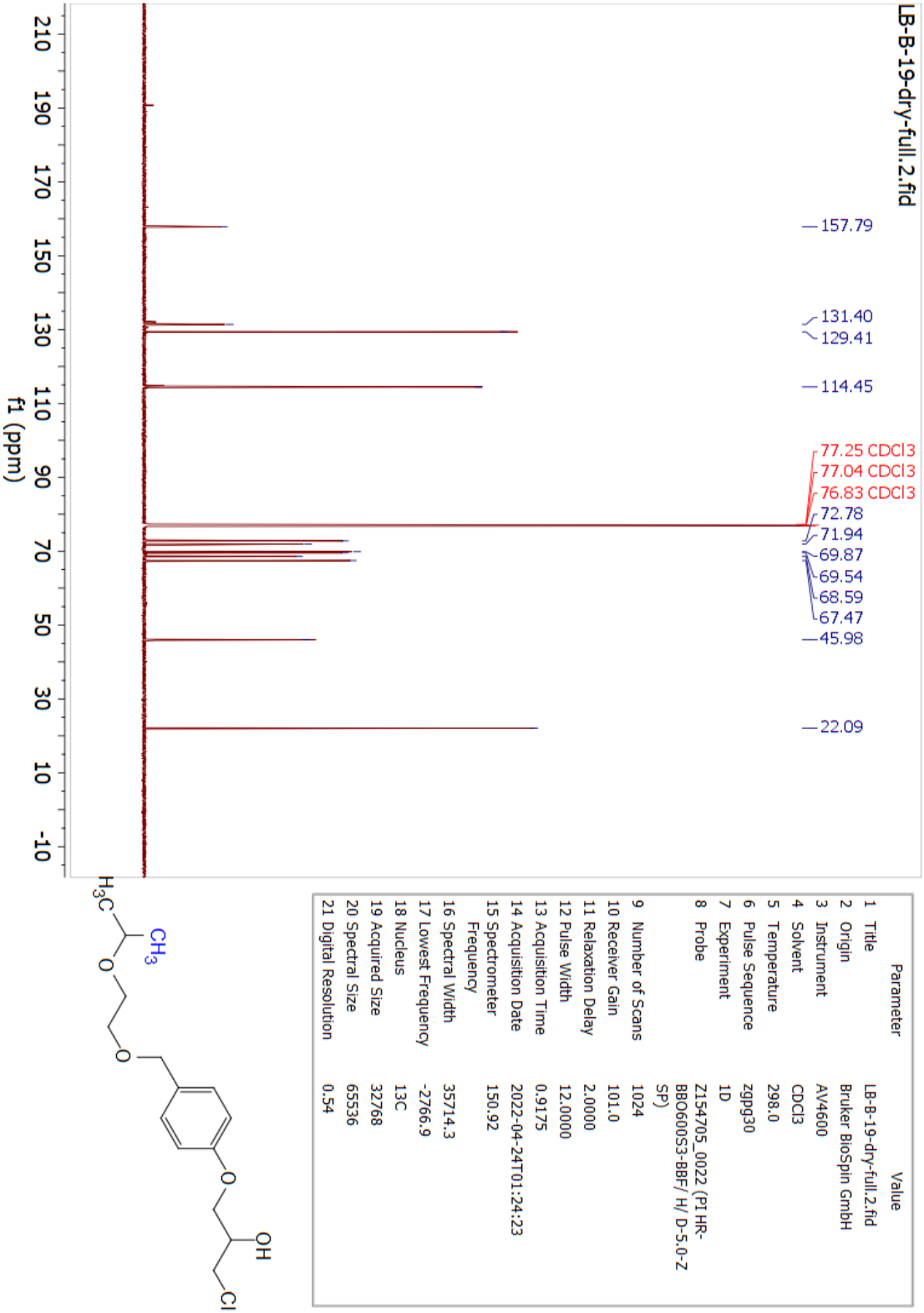

Parameter	Value
1 Title	LB-B-19-dry-full.2.fid
2 Origin	Bruker BioSpin GmbH
3 Instrument	AV4600
4 Solvent	CDCl3
5 Temperature	298.0
6 Pulse Sequence	zgpg30
7 Experiment	1D
8 Probe	Z154705_0022 (PI HR-BBO600S3-BBF/ H/ D-5.0-Z SP)
9 Number of Scans	1024
10 Receiver Gain	101.0
11 Relaxation Delay	2.0000
12 Pulse Width	12.0000
13 Acquisition Time	0.9175
14 Acquisition Date	2022-04-24T01:24:23
15 Spectrometer Frequency	150.92
16 Spectral Width	35714.3
17 Lowest Frequency	-2766.9
18 Nucleus	13C
19 Acquired Size	32768
20 Spectral Size	65536
21 Digital Resolution	0.54

Figure 6.3.7: ^{13}C-NMR spectrum (600 MHz, $CDCl_3$) of 1-chloro-3-(4-((2-isopropoxyethoxy)methyl)phenoxy)propan-2-ol (**15**).

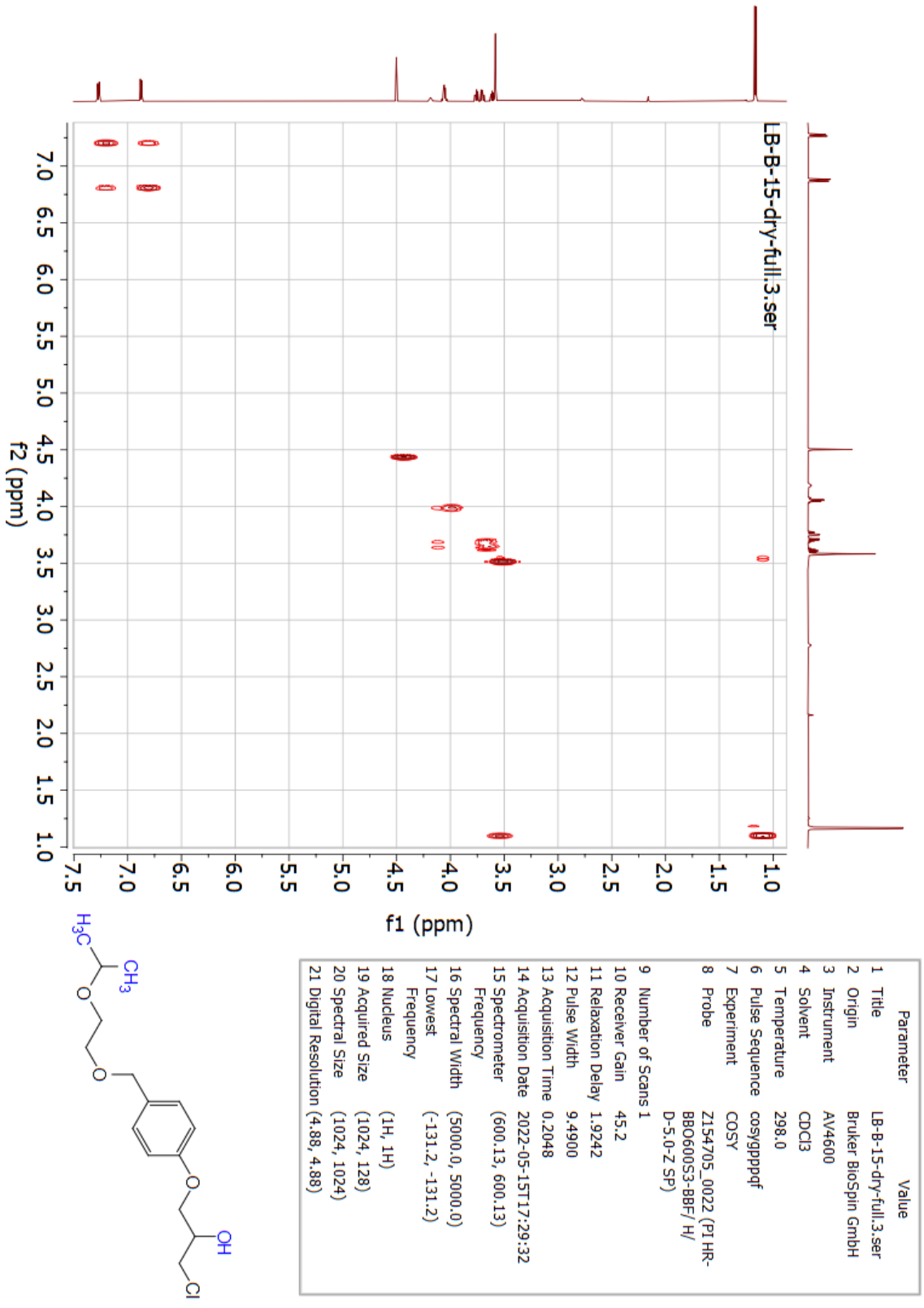

	Parameter	Value
1	Title	LB-B-15-dry-full.3.ser
2	Origin	Bruker BioSpin GmbH
3	Instrument	AV4600
4	Solvent	CDCl3
5	Temperature	298.0
6	Pulse Sequence	cosygpppqf
7	Experiment	COSY
8	Probe	Z154705_0022 (PI HR-BBO600S3-BBF/ H/ D-5.0-Z SP)
9	Number of Scans	1
10	Receiver Gain	45.2
11	Relaxation Delay	1.9242
12	Pulse Width	9.4900
13	Acquisition Time	0.2048
14	Acquisition Date	2022-05-15T17:29:32
15	Spectrometer Frequency	(600.13, 600.13)
16	Spectral Width	(5000.0, 5000.0)
17	Lowest Frequency	(-131.2, -131.2)
18	Nucleus	(1H, 1H)
19	Acquired Size	(1024, 128)
20	Spectral Size	(1024, 1024)
21	Digital Resolution	(4.88, 4.88)

Figure 6.3.8: H,H-COSY-NMR spectrum (600 MHz, $CDCl_3$) of 1-chloro-3-(4-((2-isopropoxyethoxy)methyl)phenoxy)propan-2-ol (**15**).

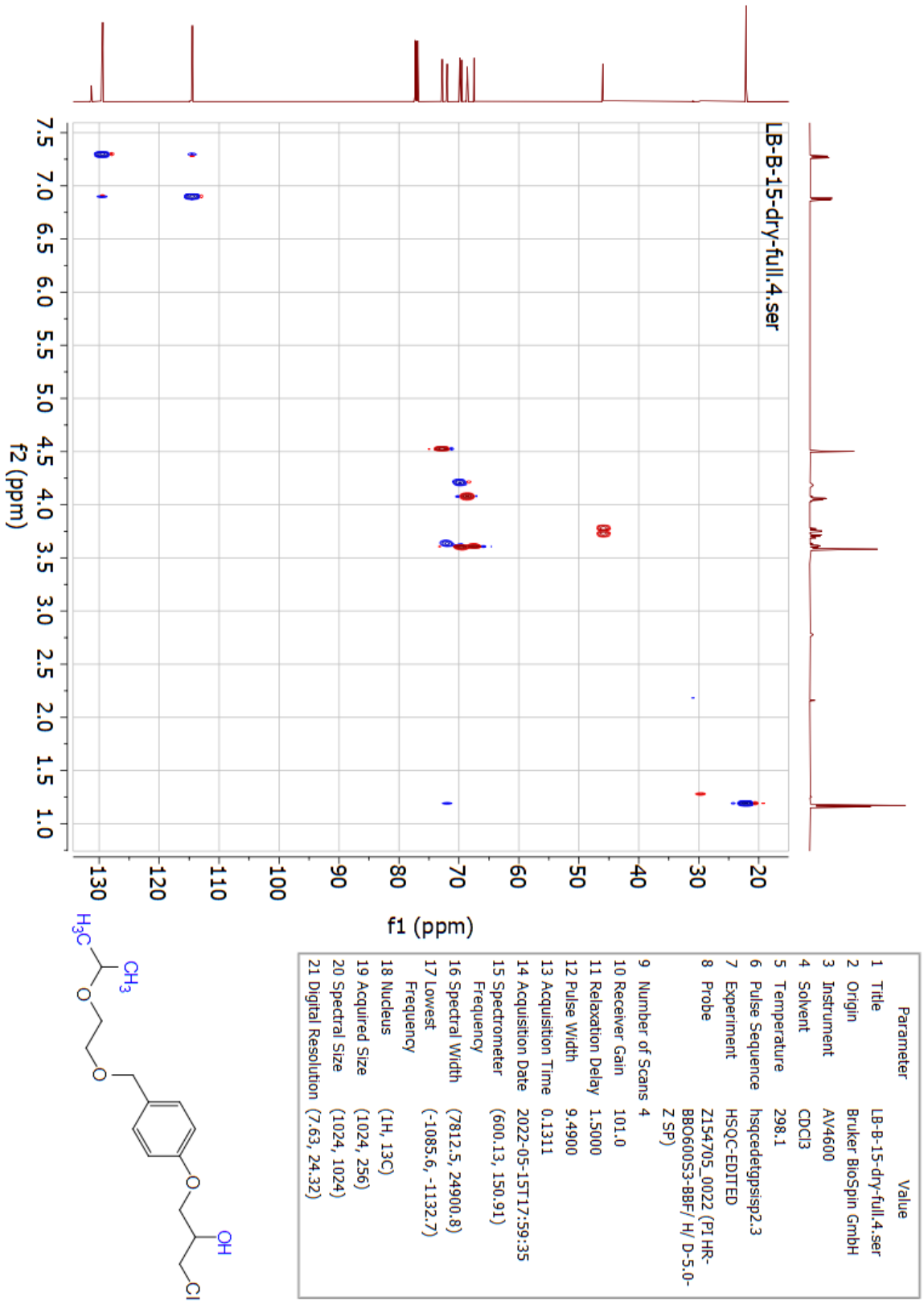

	Parameter	Value
1	Title	LB-B-15-dry-full.4.ser
2	Origin	Bruker BioSpin GmbH
3	Instrument	AV4600
4	Solvent	CDCl3
5	Temperature	298.1
6	Pulse Sequence	hsqcedetgpsisp2.3
7	Experiment	HSQC-EDITED
8	Probe	Z154705_0022 (PI HR-BBO600S3-BBF/ H/ D-5.0-Z SP)
9	Number of Scans	4
10	Receiver Gain	101.0
11	Relaxation Delay	1.5000
12	Pulse Width	9.4900
13	Acquisition Time	0.1311
14	Acquisition Date	2022-05-15T17:59:35
15	Spectrometer Frequency	(600.13, 150.91)
16	Spectral Width	(7812.5, 24900.8)
17	Lowest Frequency	(-1085.6, -1132.7)
18	Nucleus	(1H, 13C)
19	Acquired Size	(1024, 256)
20	Spectral Size	(1024, 1024)
21	Digital Resolution	(7.63, 24.32)

Figure 6.3.9: HSQC-NMR spectrum (600 MHz, $CDCl_3$) of 1-chloro-3-(4-((2-isopropoxyethoxy)methyl)phenoxy)propan-2-ol (**15**).

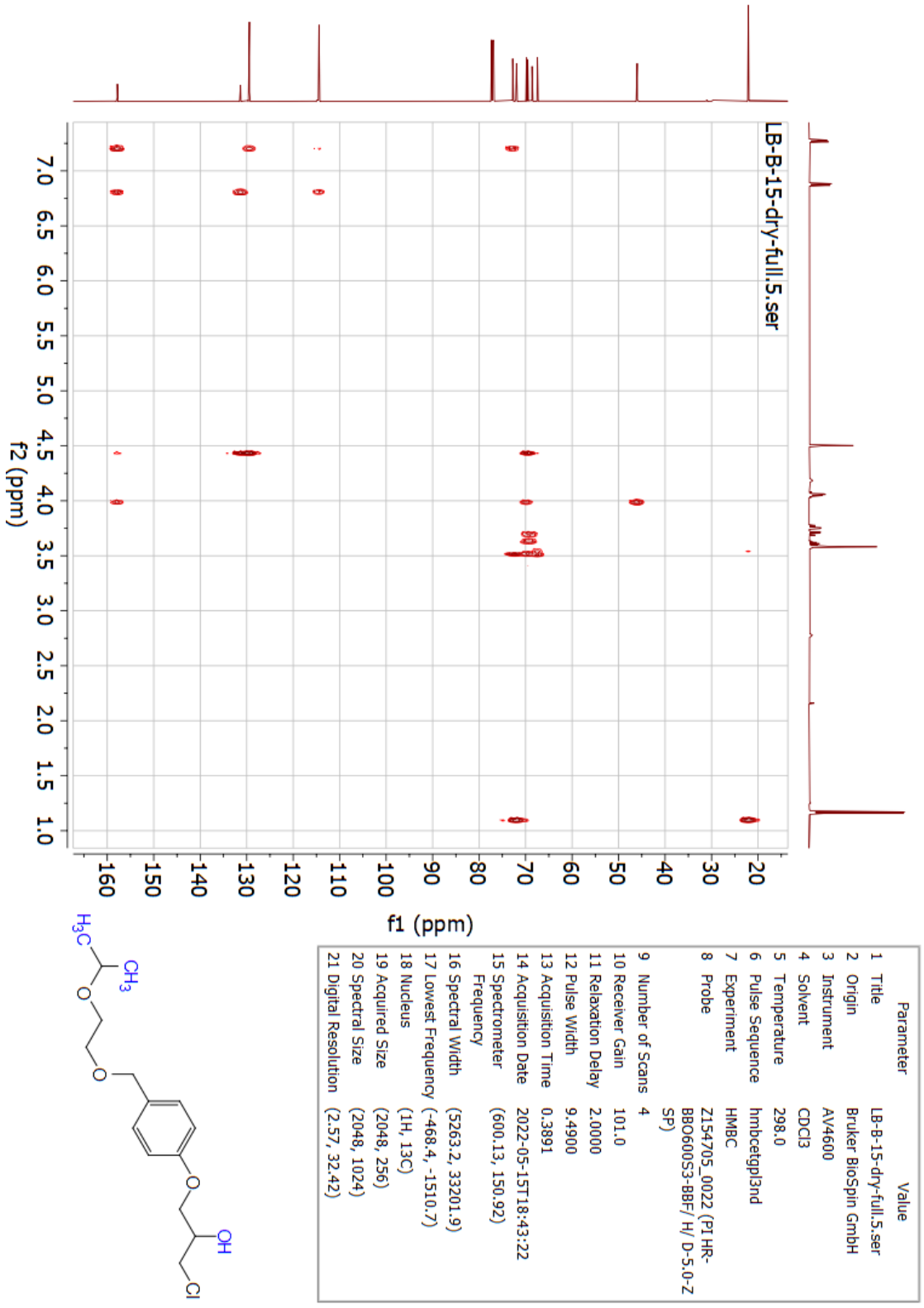

	Parameter	Value
1	Title	LB-B-15-dry-full.5.ser
2	Origin	Bruker BioSpin GmbH
3	Instrument	AV4600
4	Solvent	CDCl3
5	Temperature	298.0
6	Pulse Sequence	hmbcetgpl3nd
7	Experiment	HMBC
8	Probe	Z154705_0022 (PI HR-BBO600S3-BBF/ H/ D-5.0-Z SP)
9	Number of Scans	4
10	Receiver Gain	101.0
11	Relaxation Delay	2.0000
12	Pulse Width	9.4900
13	Acquisition Time	0.3891
14	Acquisition Date	2022-05-15T18:43:22
15	Spectrometer Frequency	(600.13, 150.92)
16	Spectral Width	(5263.2, 33201.9)
17	Lowest Frequency	(-468.4, -1510.7)
18	Nucleus	(1H, 13C)
19	Acquired Size	(2048, 256)
20	Spectral Size	(2048, 1024)
21	Digital Resolution	(2.57, 32.42)

Figure 6.3.10: HMBC-NMR spectrum (600 MHz, $CDCl_3$) of 1-chloro-3-(4-((2-isopropoxyethoxy)methyl)phenoxy)propan-2-ol (**15**).

6.3.3 1-Chloro-3-(4-((2-isopropoxyethoxy)methyl)phenoxy)propan-2-yl butyrate (16)

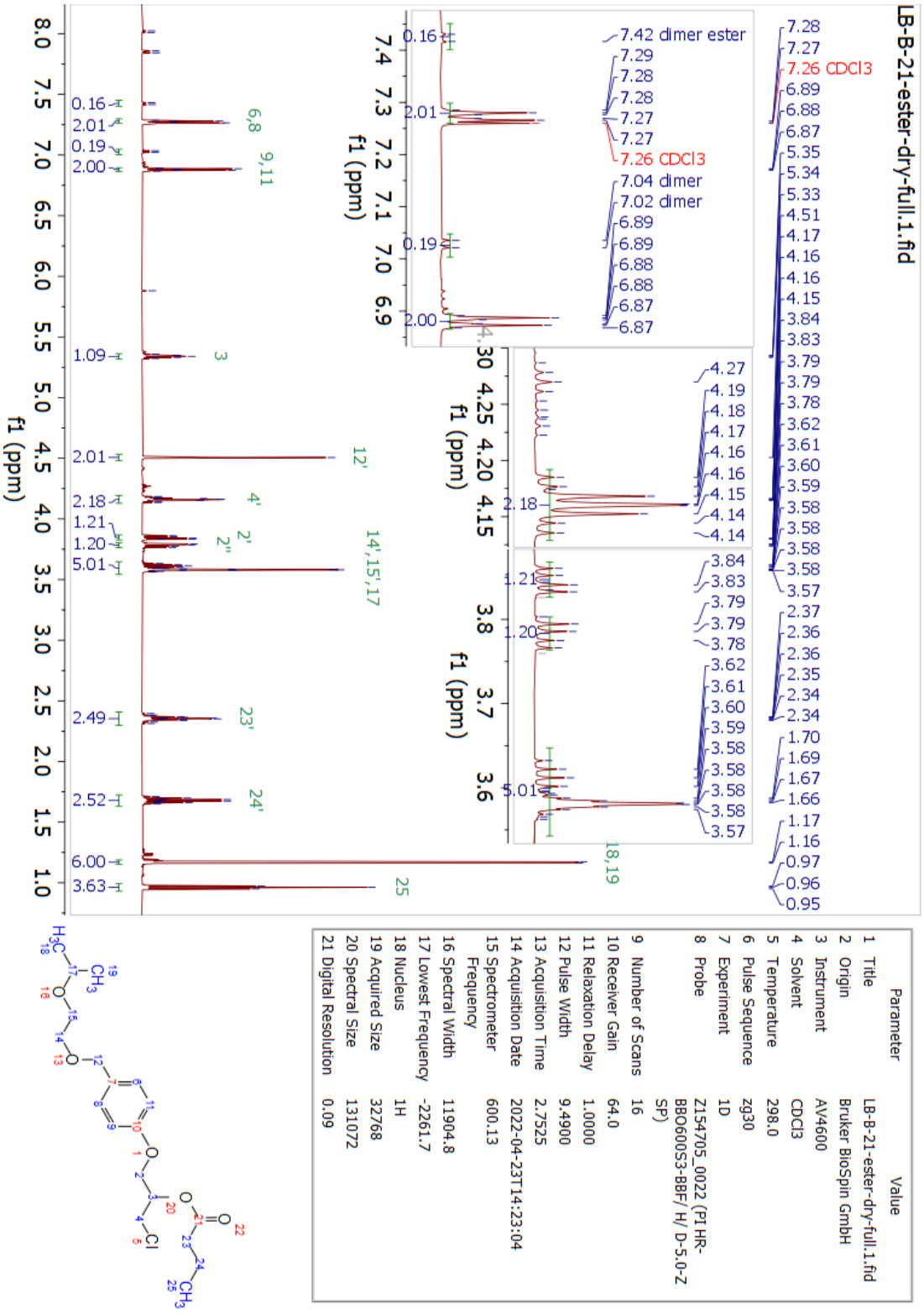

Figure 6.3.11: ^{1}H-NMR spectrum (600 MHz, $CDCl_3$) of 1-chloro-3-(4-((2-isopropoxyethoxy)methyl)phenoxy)propan-2-yl butyrate (**16**).

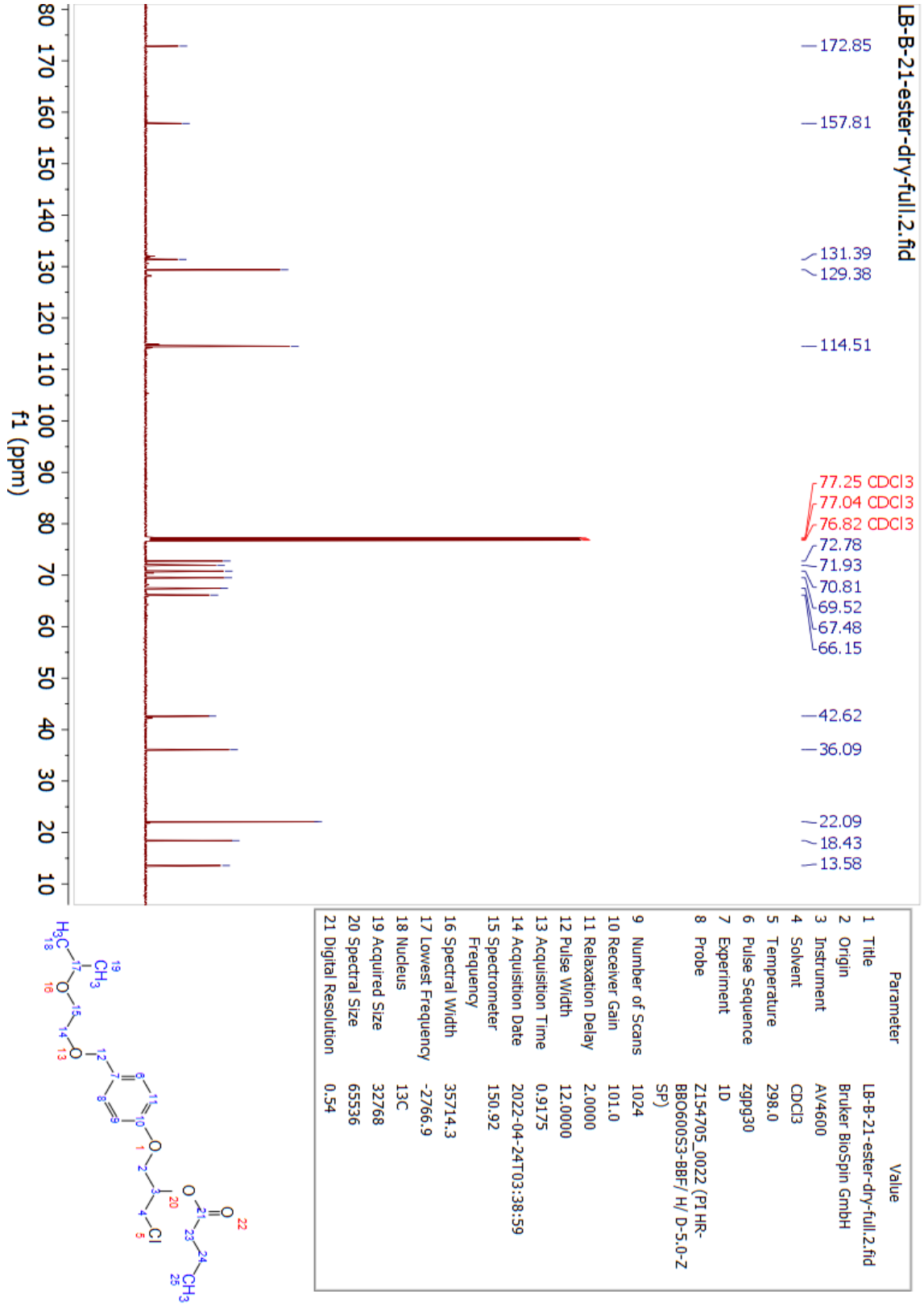

Figure 6.3.12: ^{13}C-NMR spectrum (600 MHz, $CDCl_3$) of 1-chloro-3-(4-((2-isopropoxyethoxy)methyl)phenoxy)propan-2-yl butyrate (**16**).

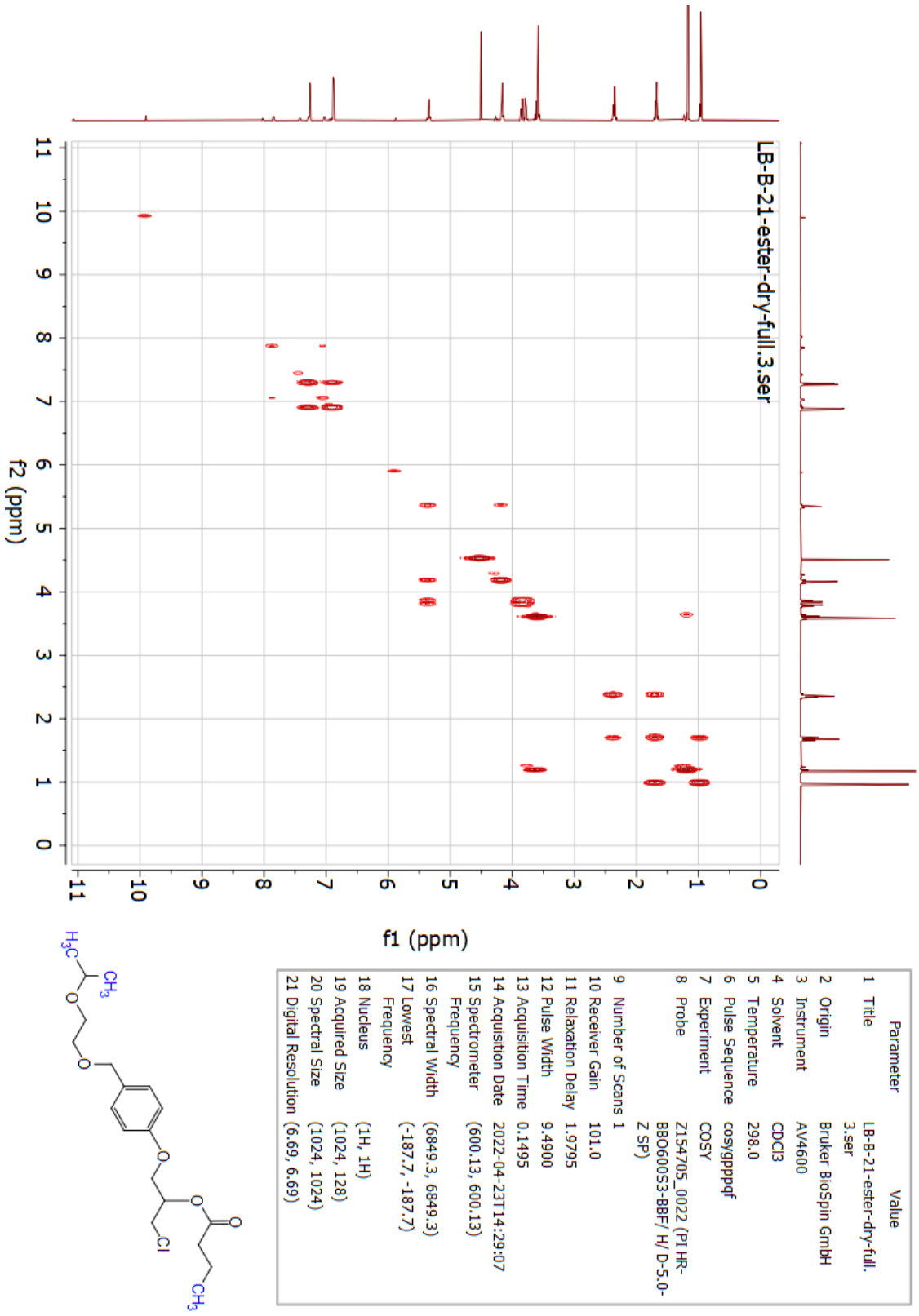

	Parameter	Value
1	Title	LB-B-21-ester-dry-full.3.ser
2	Origin	Bruker BioSpin GmbH
3	Instrument	AV4600
4	Solvent	CDCl3
5	Temperature	298.0
6	Pulse Sequence	cosygpppqf
7	Experiment	COSY
8	Probe	Z154705_0022 (PI HR-BBO600S3-BBF/ H/ D-5.0-Z SP)
9	Number of Scans	1
10	Receiver Gain	101.0
11	Relaxation Delay	1.9795
12	Pulse Width	9.4900
13	Acquisition Time	0.1495
14	Acquisition Date	2022-04-23T14:29:07
15	Spectrometer Frequency	(600.13, 600.13)
16	Spectral Width	(6849.3, 6849.3)
17	Lowest Frequency	(-187.7, -187.7)
18	Nucleus	(1H, 1H)
19	Acquired Size	(1024, 128)
20	Spectral Size	(1024, 1024)
21	Digital Resolution	(6.69, 6.69)

Figure 6.3.13: H,H-COSY-NMR spectrum (600 MHz, $CDCl_3$) of 1-chloro-3-(4-((2-isopropoxyethoxy)methyl)phenoxy)propan-2-yl butyrate (**16**).

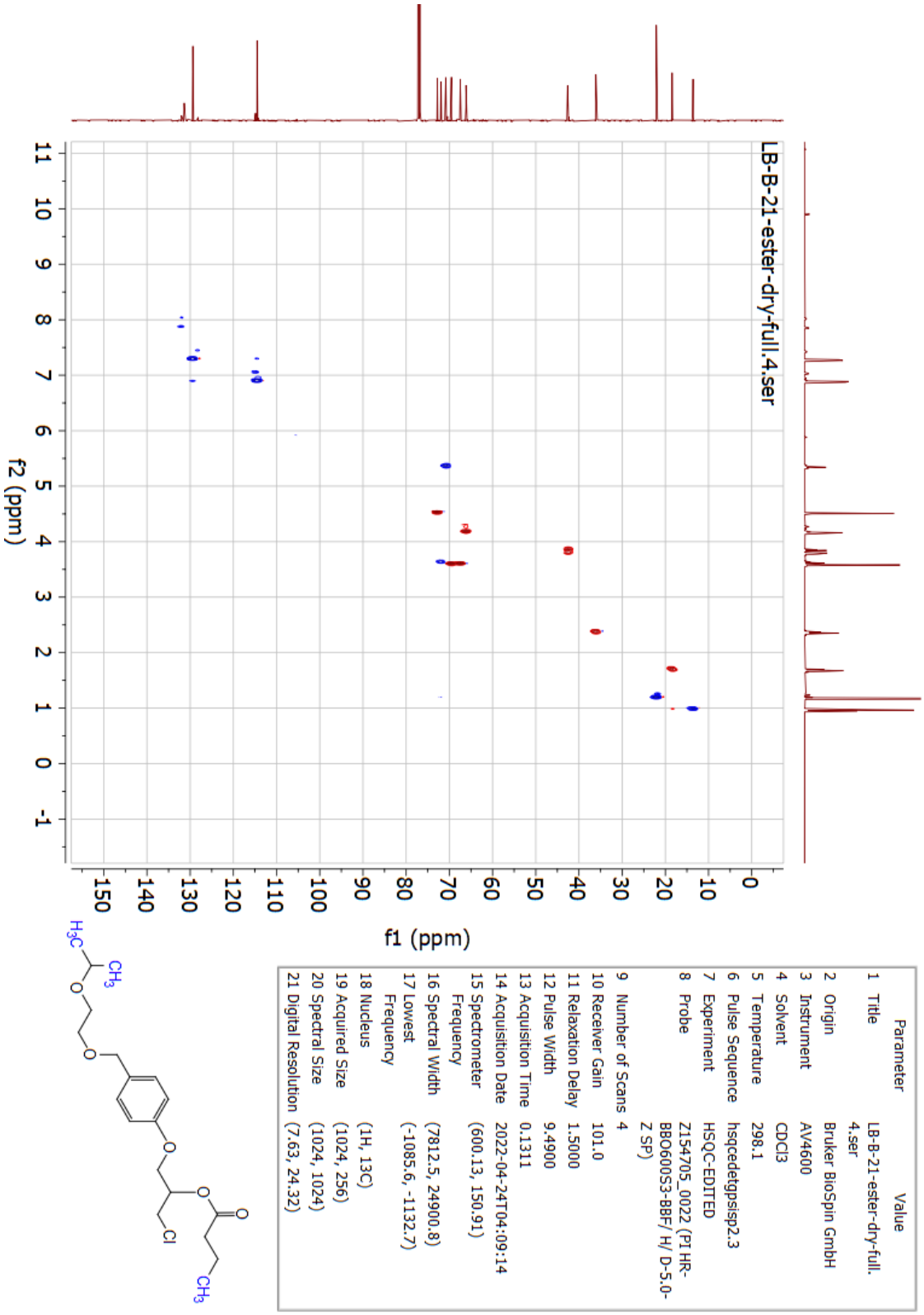

Figure 6.3.14: HSQC-NMR spectrum (600 MHz, $CDCl_3$) of 1-chloro-3-(4-((2-isopropoxyethoxy)methyl)phenoxy)propan-2-yl butyrate (**16**).

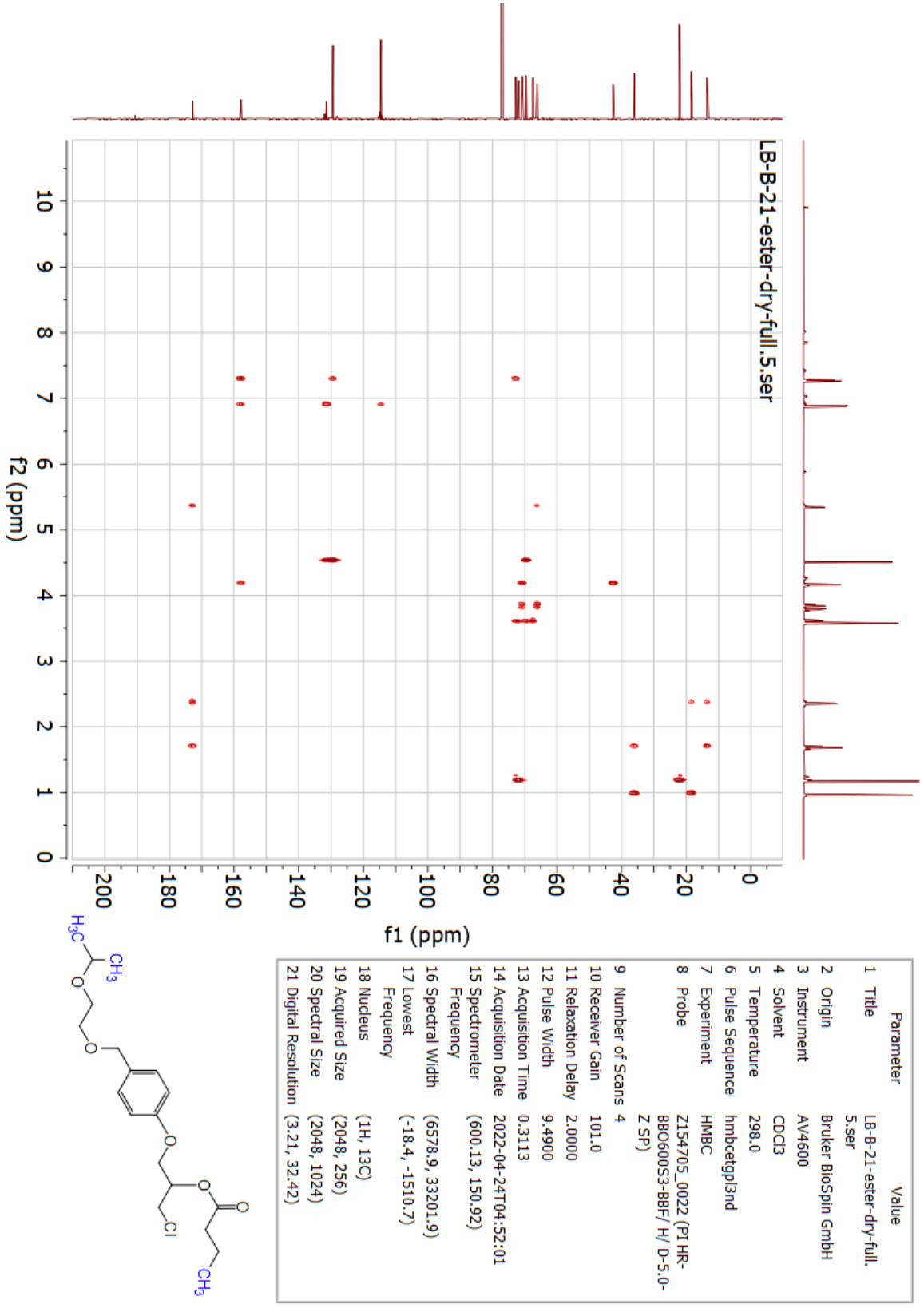

Figure 6.3.15: HMBC-NMR spectrum (600 MHz, $CDCl_3$) of 1-chloro-3-(4-((2-isopropoxyethoxy)methyl)phenoxy)propan-2-yl butyrate (**16**).

6.3.4 Bisoprolol (17)

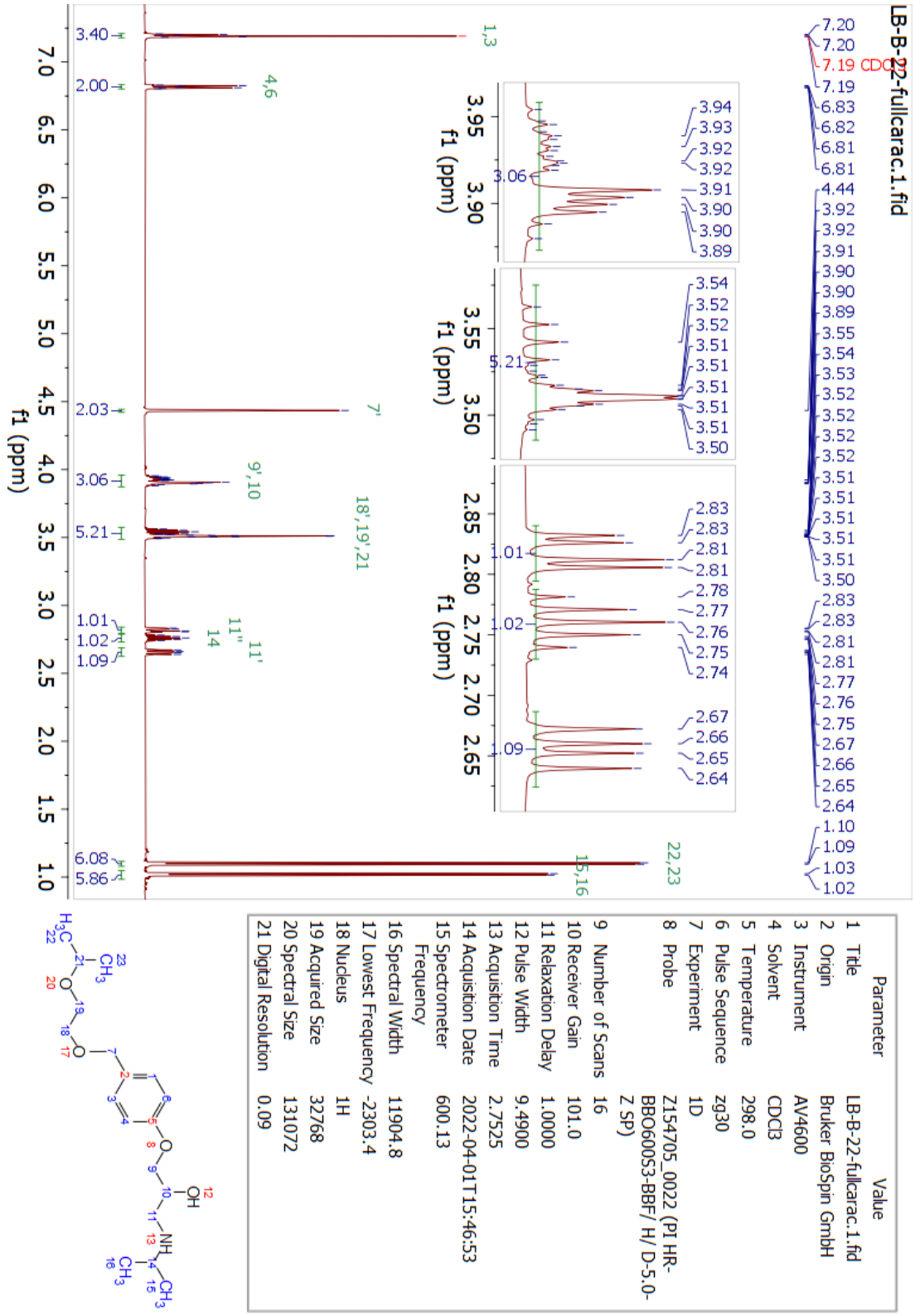

Figure 6.3.16: ^{1}H-NMR spectrum (600 MHz, $CDCl_3$) of bisoprolol (**17**).

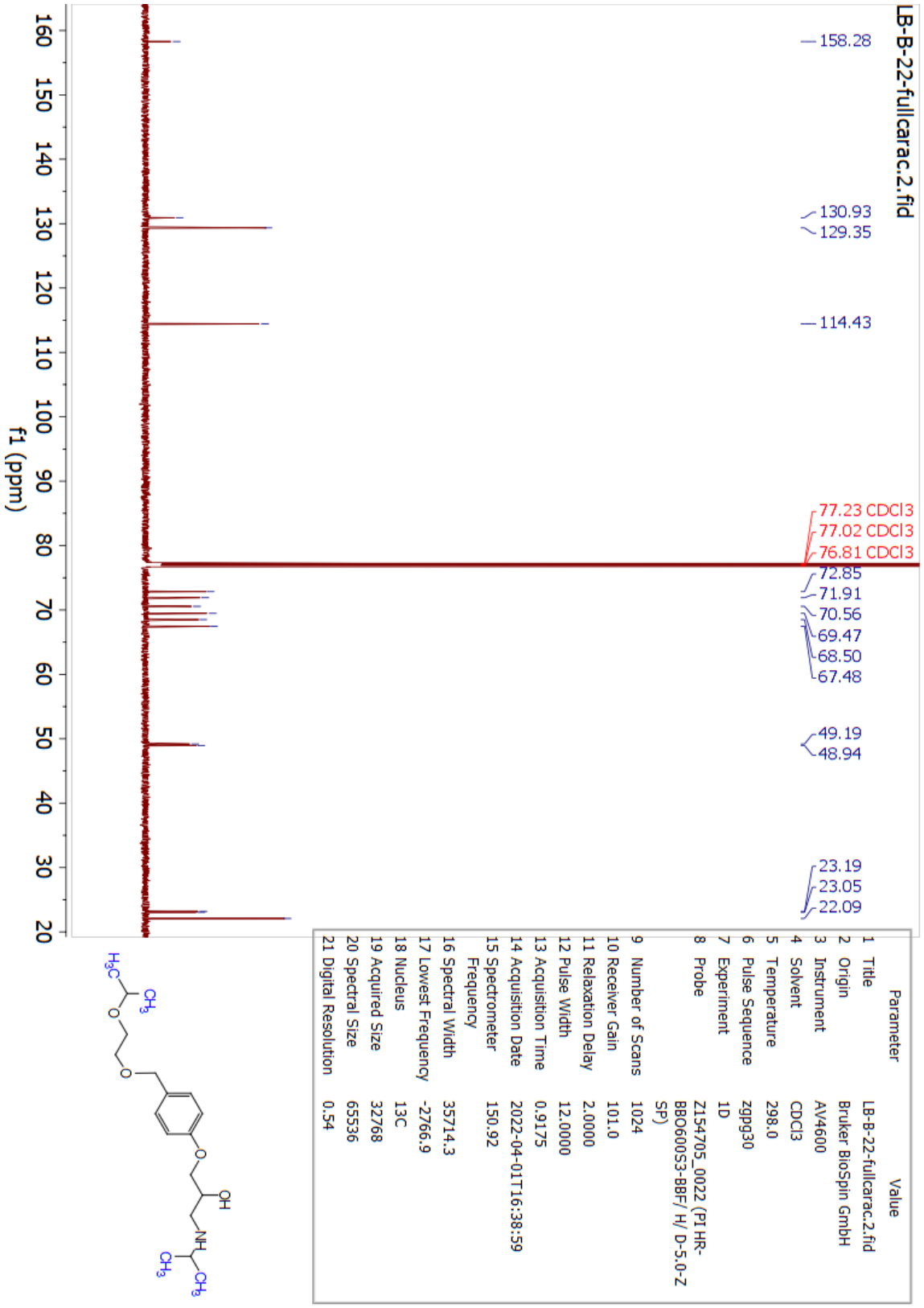

Figure 6.3.17: ^{13}C-NMR spectrum (600 MHz, $CDCl_3$) of bisoprolol (**17**).

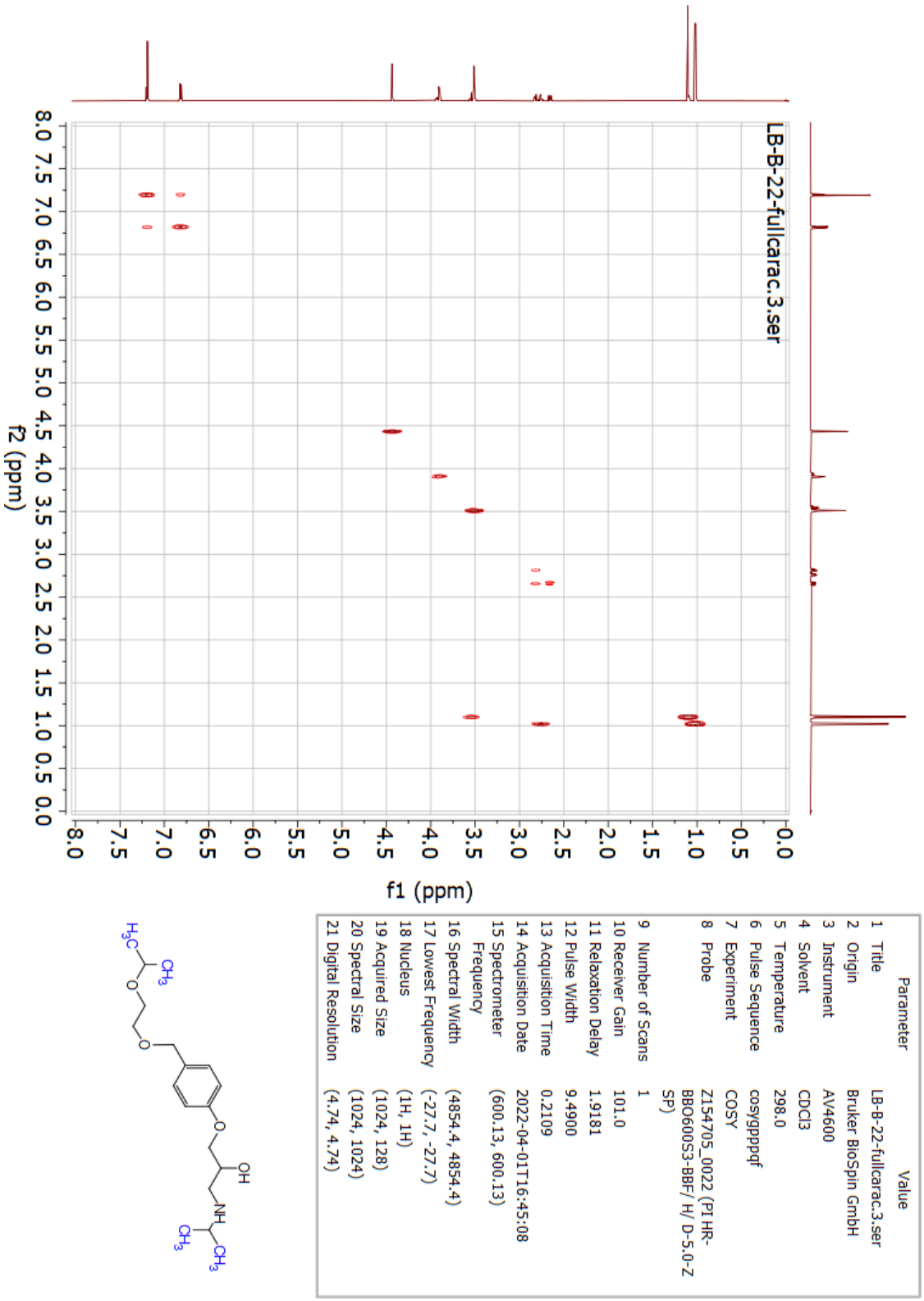

	Parameter	Value
1	Title	LB-B-22-fullcarac.3.ser
2	Origin	Bruker BioSpin GmbH
3	Instrument	AV4600
4	Solvent	CDCl3
5	Temperature	298.0
6	Pulse Sequence	cosygpppqf
7	Experiment	COSY
8	Probe	Z154705_0022 (PI HR-BBO600S3-BBF/ H/ D-5.0-Z SP)
9	Number of Scans	1
10	Receiver Gain	101.0
11	Relaxation Delay	1.9181
12	Pulse Width	9.4900
13	Acquisition Time	0.2109
14	Acquisition Date	2022-04-01T16:45:08
15	Spectrometer Frequency	(600.13, 600.13)
16	Spectral Width	(4854.4, 4854.4)
17	Lowest Frequency	(-27.7, -27.7)
18	Nucleus	(1H, 1H)
19	Acquired Size	(1024, 128)
20	Spectral Size	(1024, 1024)
21	Digital Resolution	(4.74, 4.74)

Figure 6.3.18: H,H-COSY-NMR spectrum (600 MHz, $CDCl_3$) of bisoprolol (**17**).

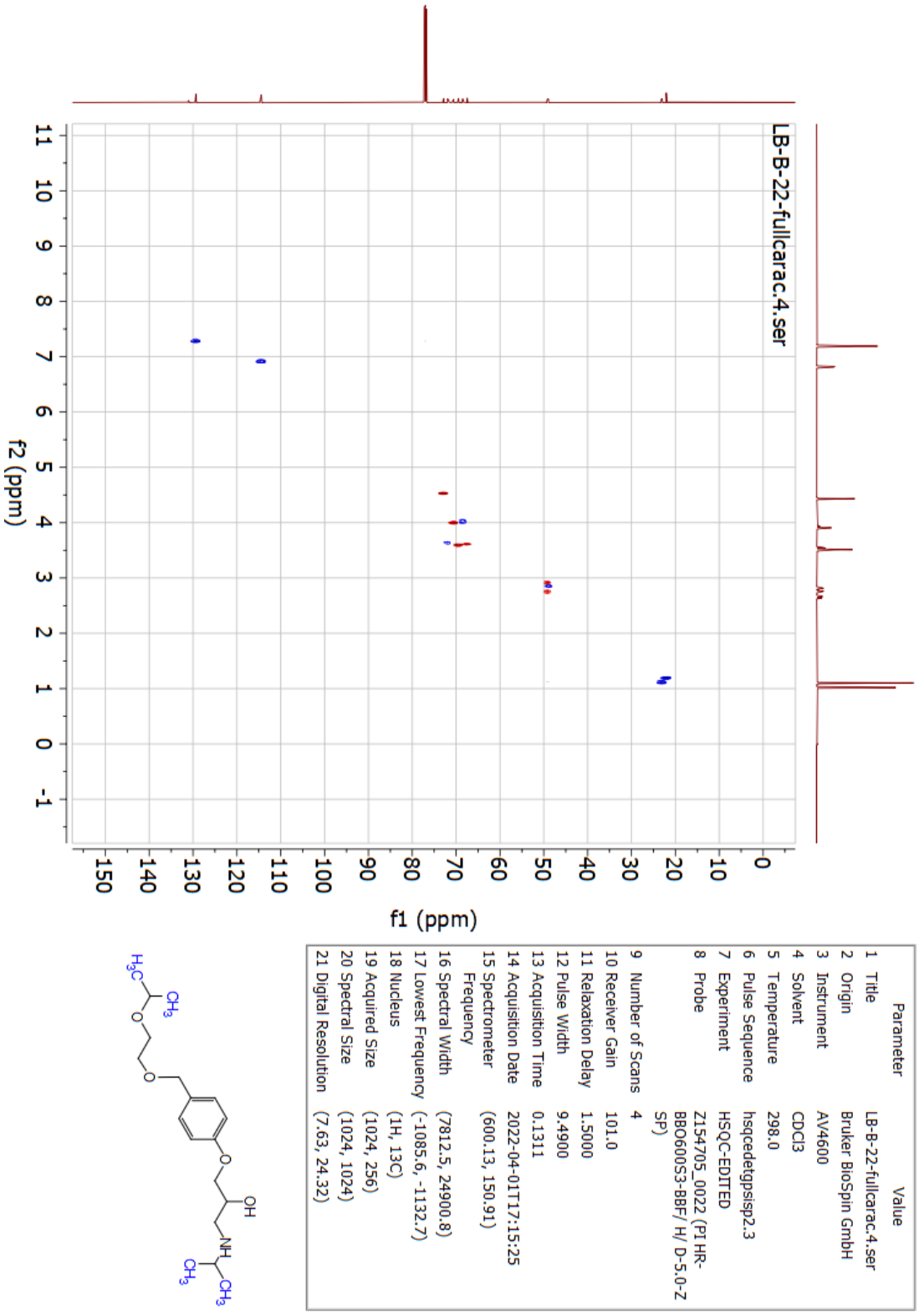

Figure 6.3.19: HSQC-NMR spectrum (600 MHz, $CDCl_3$) of bisoprolol (**17**).

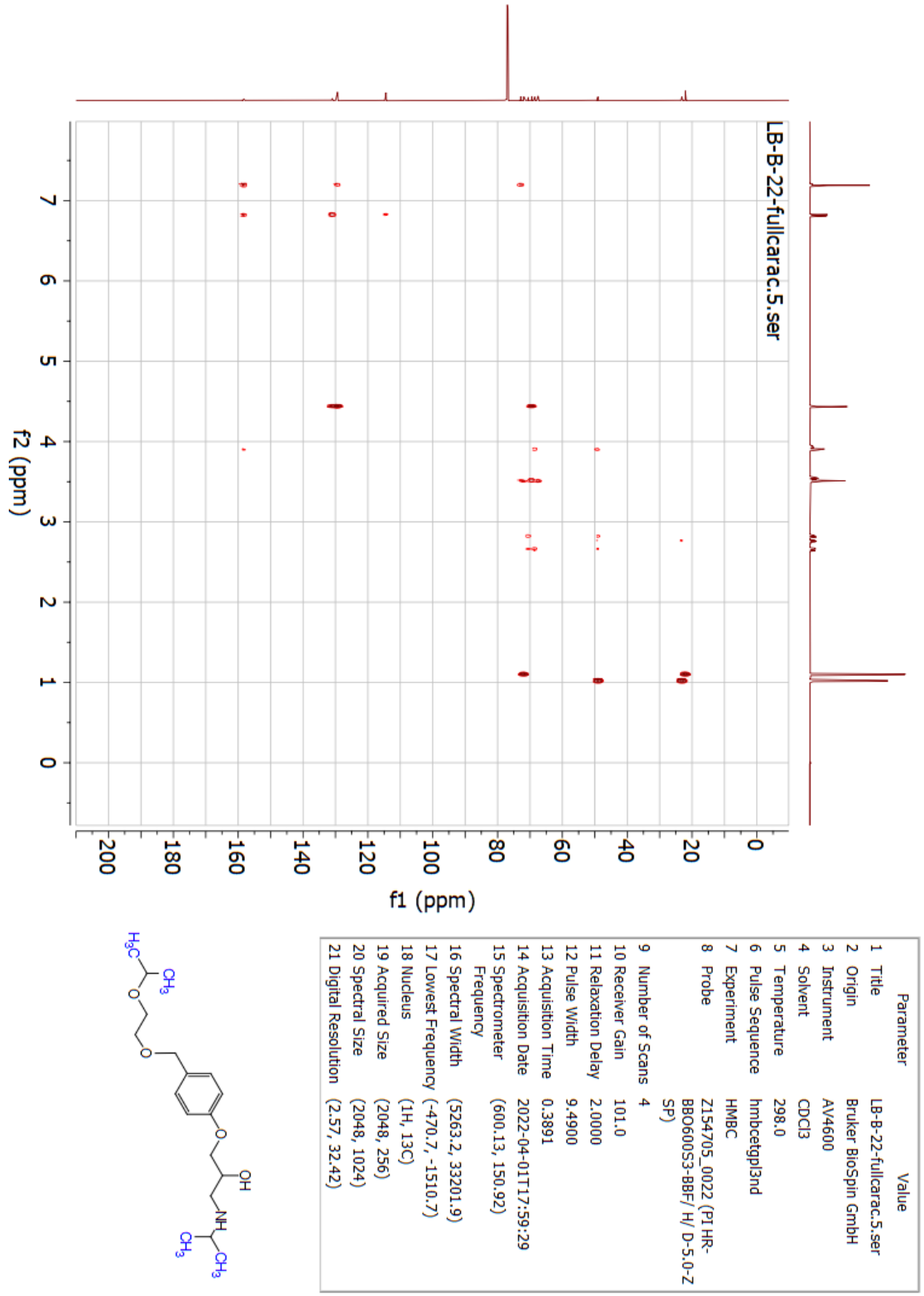

	Parameter	Value
1	Title	LB-B-22-fullcarac.5.ser
2	Origin	Bruker BioSpin GmbH
3	Instrument	AV4600
4	Solvent	CDCl3
5	Temperature	298.0
6	Pulse Sequence	hmbcetgpl3nd
7	Experiment	HMBC
8	Probe	Z154705_0022 (PI HR-BBO600S3-BBF/ H/ D-5.0-Z SP)
9	Number of Scans	4
10	Receiver Gain	101.0
11	Relaxation Delay	2.0000
12	Pulse Width	9.4900
13	Acquisition Time	0.3891
14	Acquisition Date	2022-04-01T17:59:29
15	Spectrometer Frequency	(600.13, 150.92)
16	Spectral Width	(5263.2, 33201.9)
17	Lowest Frequency	(-470.7, -1510.7)
18	Nucleus	(1H, 13C)
19	Acquired Size	(2048, 256)
20	Spectral Size	(2048, 1024)
21	Digital Resolution	(2.57, 32.42)

Figure 6.3.20: HMBC-NMR spectrum (600 MHz, $CDCl_3$) of bisoprolol (**17**).

6.3.5 Bisoprolol hemifumarate (17salt)

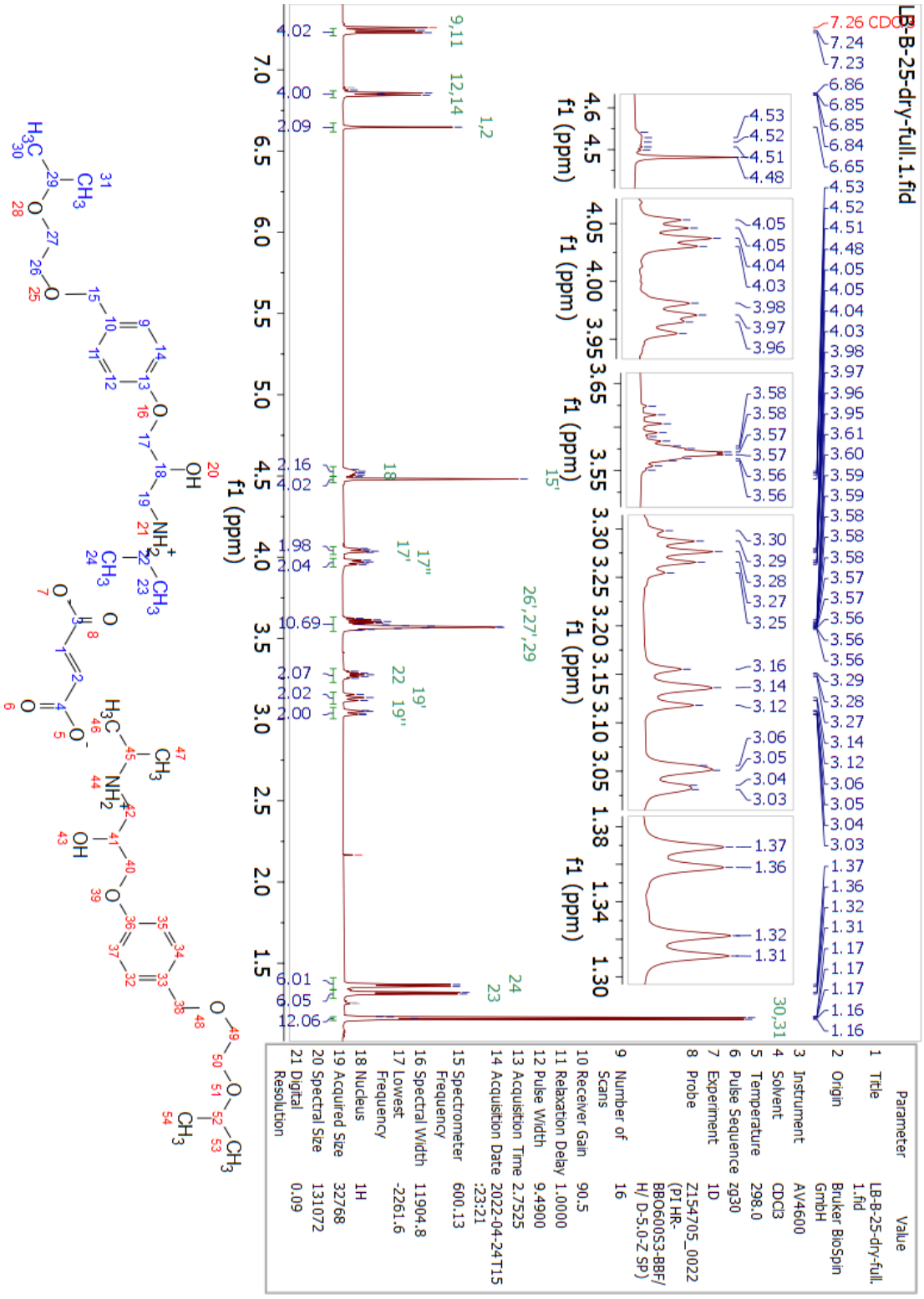

Figure 6.3.21: ^{1}H-NMR spectrum (600 MHz, $CDCl_3$) of bisoprolol hemifumarate (**17salt**).

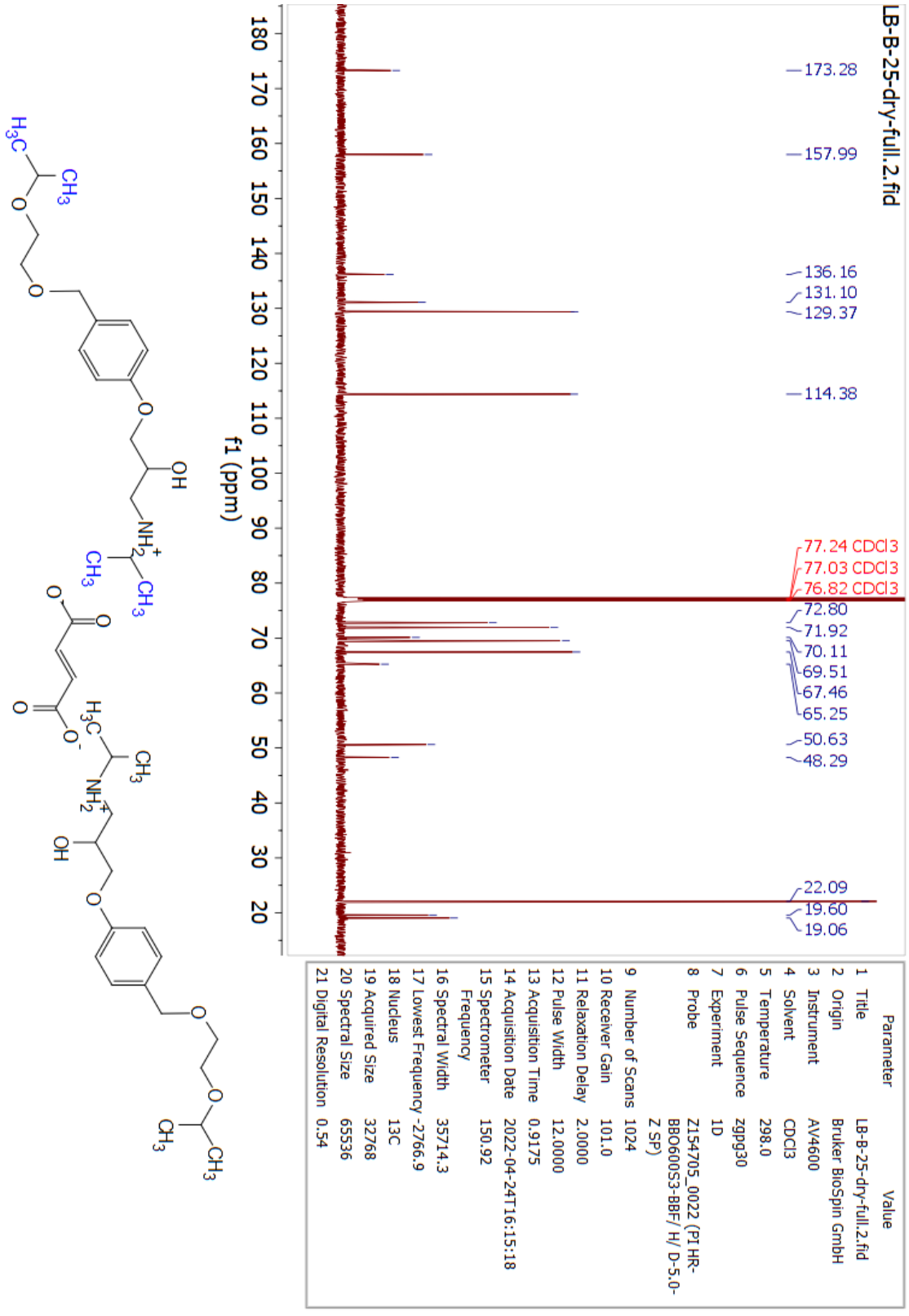

Figure 6.3.22: ^{13}C-NMR spectrum (600 MHz, $CDCl_3$) of bisoprolol hemifumarate (**17salt**).

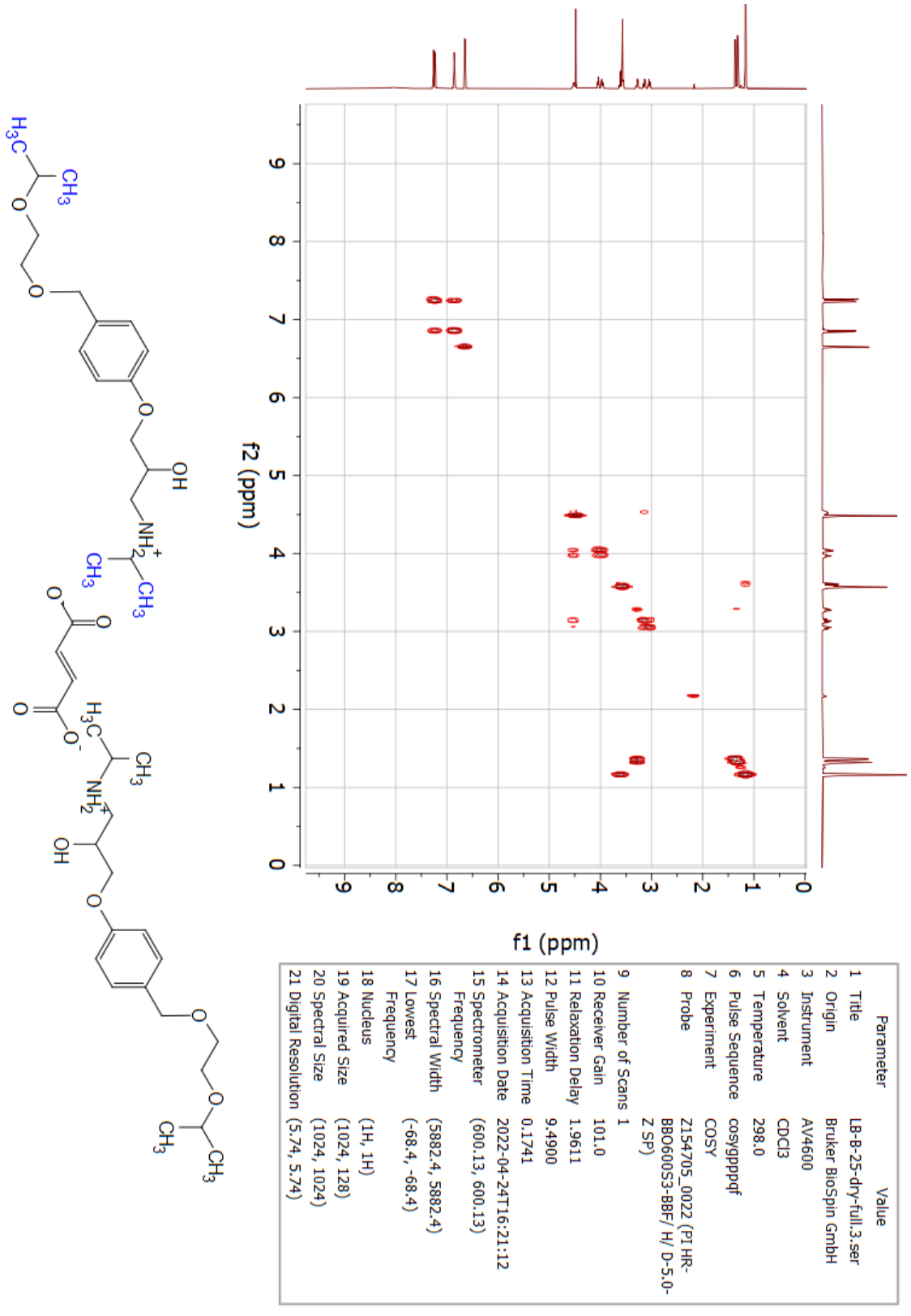

Figure 6.3.23: H,H-COSY-NMR spectrum (600 MHz, $CDCl_3$) of bisoprolol hemifumarate (**17salt**).

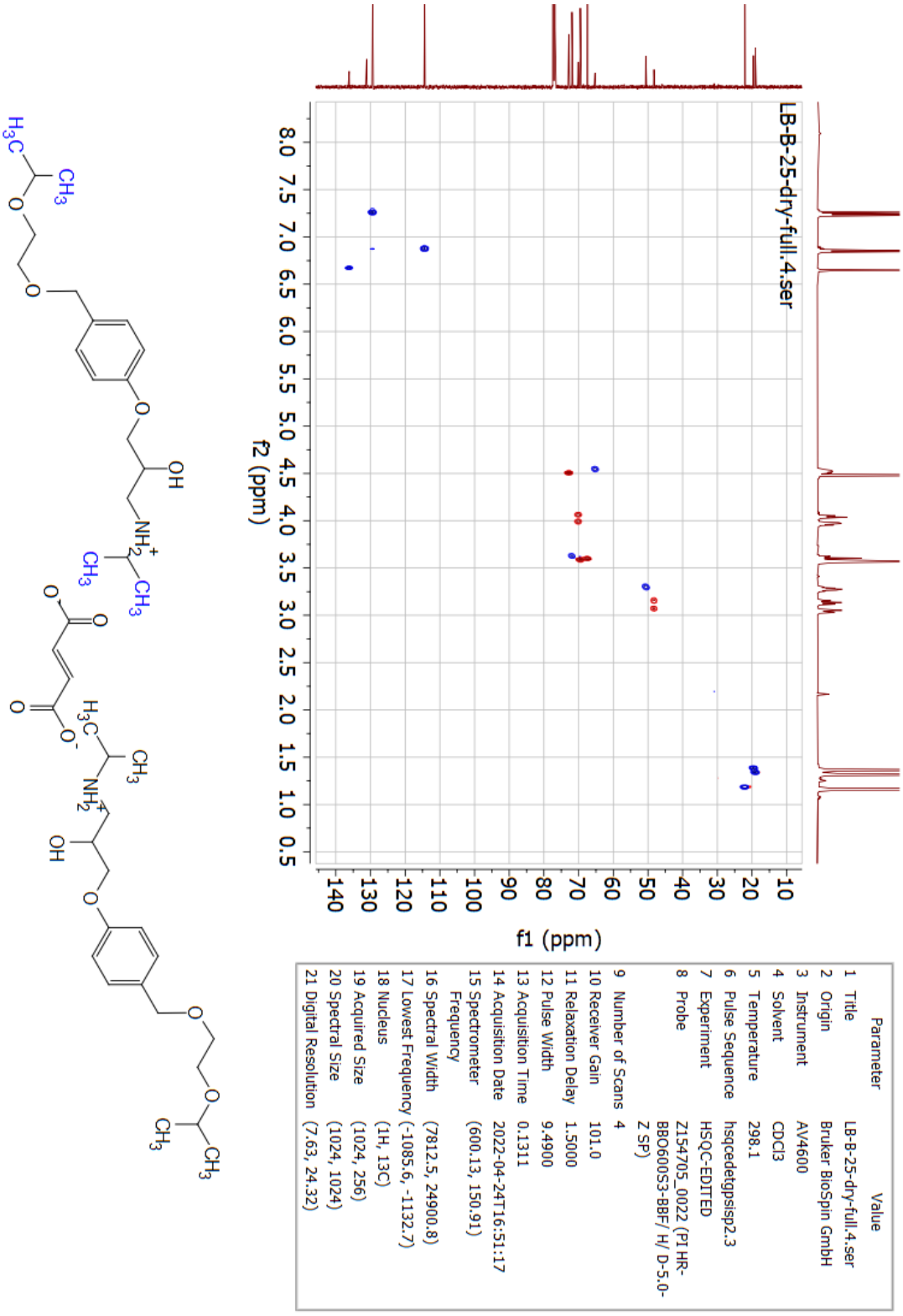

Figure 6.3.24: HSQC-NMR spectrum (600 MHz, $CDCl_3$) of bisoprolol hemifumarate (**17salt**).

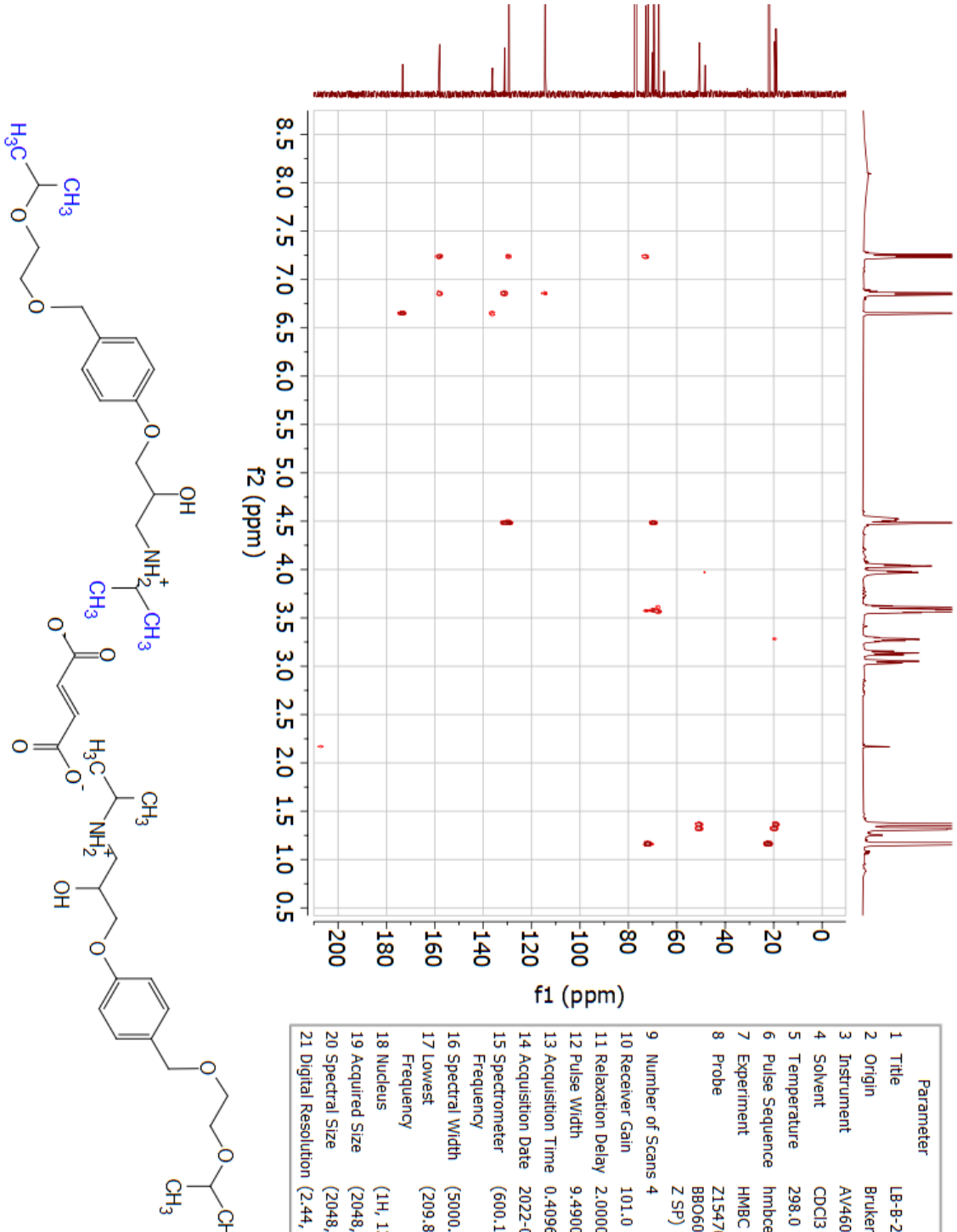

Figure 6.3.25: HMBC-NMR spectrum (600 MHz, $CDCl_3$) of bisoprolol hemifumarate (**17salt**).

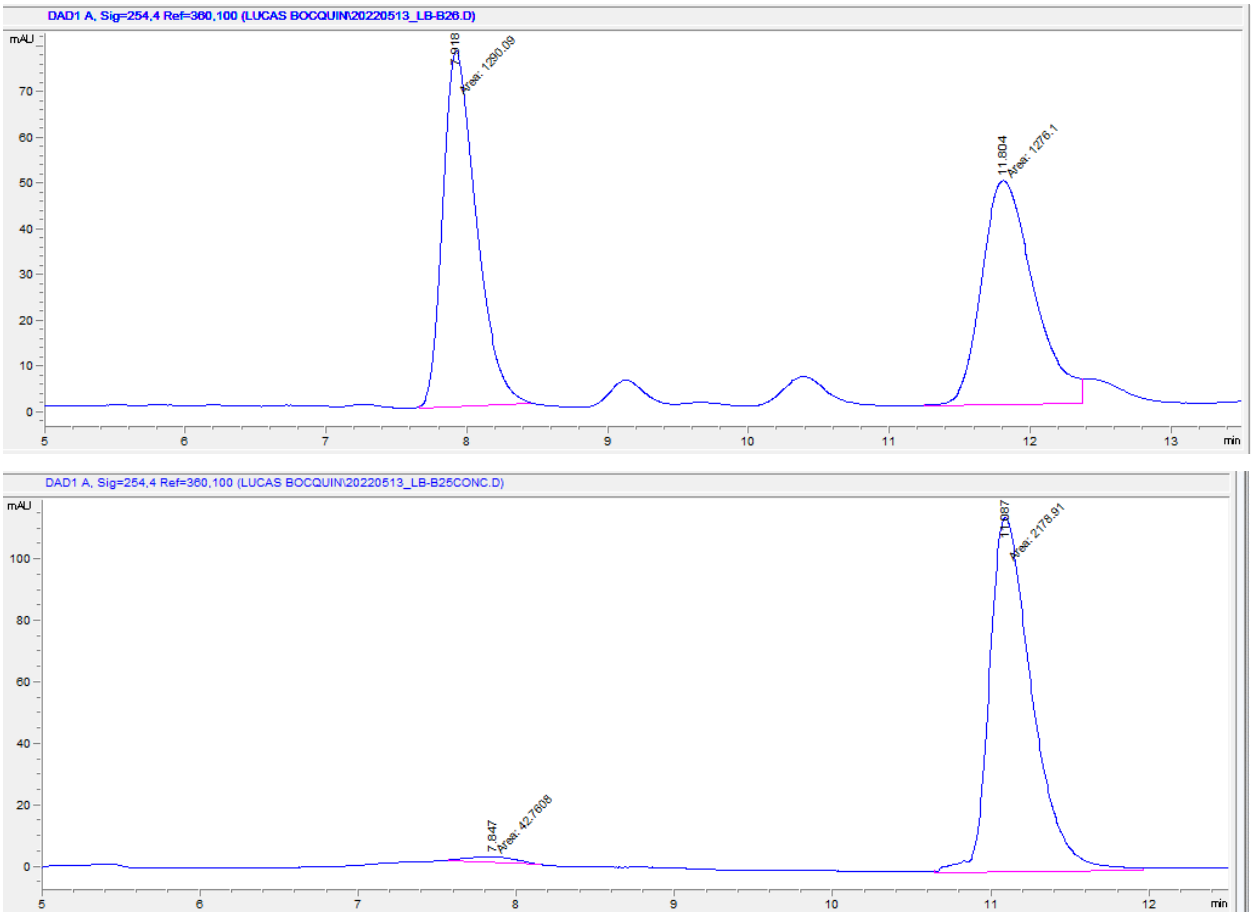

Figure 6.3.26: Chiral HPLC chromatogram of racemic bisoprolol hemifumarate (**17salt**) (upper chromatogram) and enantiopure (*R*)-**17*salt*** (bottom chromatogram). The analysis was performed on a Chiralcel OD-H column with hexane (90%) and 2-propanol containing 2% diethanolamine (10%) as eluent and 1 mL/min flow, and with a detection wavelength of 254.4 nm. The retention times obtained are t_R((R)-**17*salt***) = 7.92 min and t_R((S)-**17*salt***) = 11.8 min (upper chromatogram). The resolution factor in the upper chromatogram is R_S((S)/(R)-**17*salt***) = 7.02.

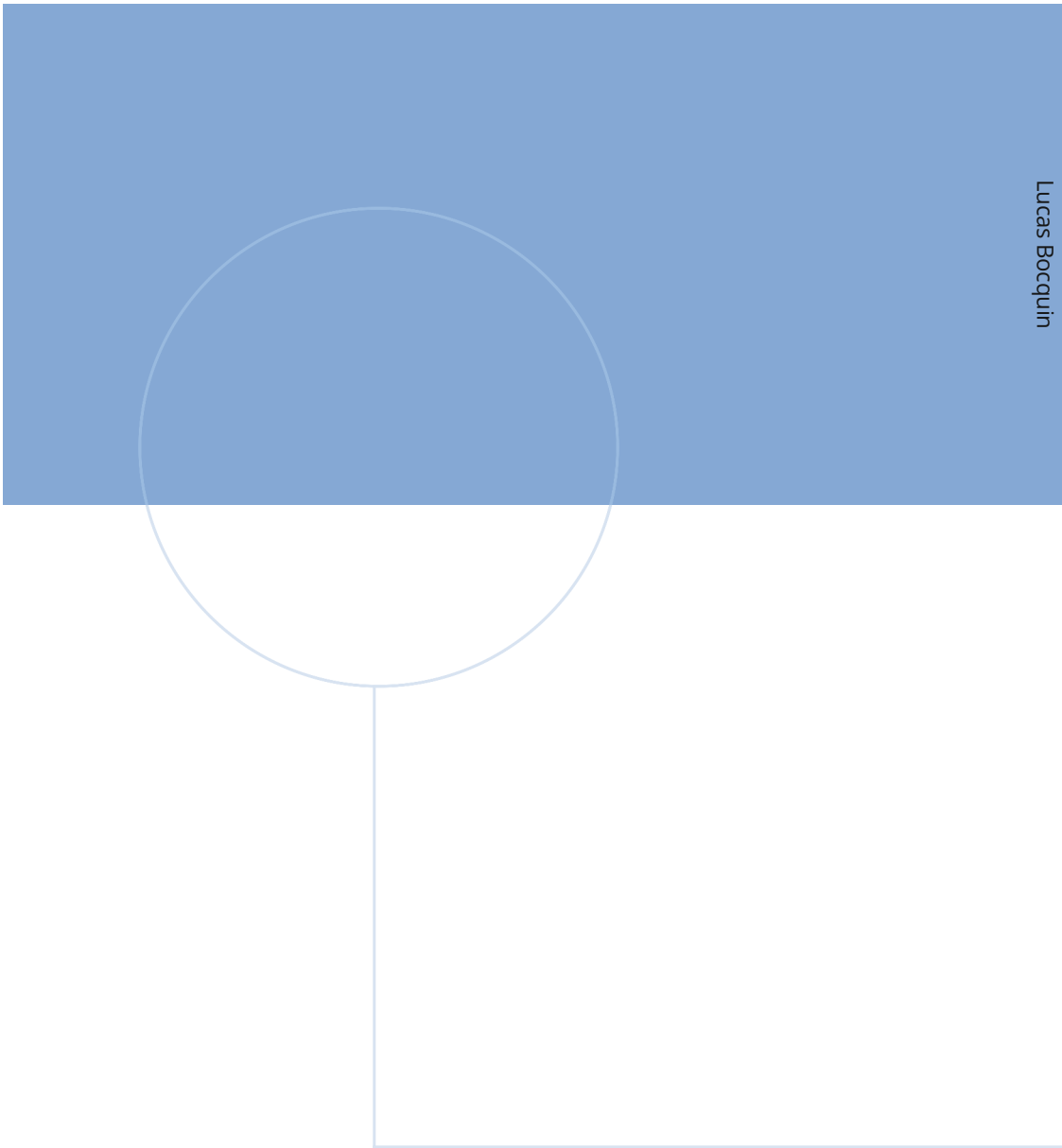

Lucas Bocquin

NTNU
Norwegian University of
Science and Technology